ECONMICAL DESALINATION PROCESSES IN QATAR

FALEH N AL-THANI

A thesis submitted in partial fulfillment of the requirements

of the University of Hertfordshire for the degree of Doctor of Philosophy

The programme of research was carried out in the

Department of Aerospace, Civil and Mechanical Engineering,

University of Hertfordshire

February 2002

ABSTRACT

The limited underground water resources and the dramatic increase of fresh water consumption in Qatar forced the government to seek alternative ways to compensate for the lack of fresh water resources. Unfortunately, most of the currently available alternatives are costly in terms of excessive fuel consumption; also they require large capital investment and high maintenance cost. Such plants currently produce over 98% of the total fresh water in Qatar. This ratio may increase to 100% in the next few years. The main aim of this work is to investigate the most viable water desalination processes, which can produce sufficient, and a continuous supply of fresh water with low operation and construction costs.

Climatic conditions and solar radiation in Qatar have been studied and analysed to determine the performance of any potential solar system applicable to this country. A technical and economical investigation into the current and common desalination methods with particular emphasis on the three main desalination systems including multistage flash, multiple effect distillation and reverse osmosis were conducted and included. A comprehensive literature survey on various water desalination methods was undertaken.

The current experimental program was confined mainly to one novel type of tilted tray solar still system, namely pyramid tilted tray solar still, which was developed to increase productivity by increasing the receiving surface area of the still (the absorber) in order to collect the optimum amount of solar radiation. Two types of cover have also been selected and tested in this work, namely pyramid and dome shapes. These tilted tray solar stills were designed and constructed on a small scale and have been tested under controlled laboratory conditions at the University of Hertfordshire. Various parameters, which are likely to effect the still performance have been investigated. These include water flow rate, spacing between cover and tray surface, glass thickness, insulation layer, and inlet water temperature. Finally, a comparison of the stills performance characteristics of the two shapes has been carried out. The laboratory experimental results of hourly production revealed that pyramid type solar still yield higher distilled water output results than the dome type. However, the use of the pyramid shape with tilted tray solar can lead to further

increase in the still productivity by optimising the orientation and surface area of the still absorber.

The field experimental results of pyramid solar still, which were conducted under local climate conditions of Qatar, indicated clearly that solar desalination can be a suitable economical option, particularly for remote areas, where the fresh water demand is low and water transport is expensive. Moreover, a theoretical model was employed to predict the effects on solar still performance under three various parameters under typical climatic conditions of Qatar; These include the thermal insulation layer, the water depth and wind speed. Due to the economical reasons the dual-purpose multistage flash process will remain for the foreseeable future the preferred process, when fresh water and electricity demands are growing concurrently and rapidly.

ACKNOWLEDGEMENT

First of all, I thank the God for his guidance and his blessings to complete this work.

I would also like to take this opportunity to express my deepest gratitude particularly to my supervisors Prof. A.A.M.Sayigh and Dr. Sami Nasser, for their support, guidance, and encouragement, which contributed to this research.

Special gratitude and thanks to Dr. A.Hamid Marafi, from Qatar University, for his assistances and supervision, which helped to complete the work field part of this research in proper way.

Finally, I'm so grateful to my dear parents, my wife and children for their help, support and patience.

CONTENTS

APPENDICES:

[a]

- Auto CAD Dome solar still. 3D.
- Auto CAD Pyramid solar still. 3D.

[b]

- Computer Programme.

[c]

- Calculation of the glass cover transmittance and the thin water film.

LIST OF FIGURES

Chapter One

Chapter Two

Chapter Three

Chapter Six

LIST OF PLATES

LIST OF TABLES

NOMENCLATURE

C_g Heat capacity of glass cover. J/kg/°C

C_p Specific heat capacity of humid air, J/kg/°C.

C_w Heat capacity of water, and basin. J/kg/°C

D Day

d_f Average spacing between water surface and glass cover, mm.

F Shape factor.

h_c Convective heat transfer coefficient. kw/ m^2. °C

h_e Evaporation heat transfer coefficient. kw/ m^2. °C

h_r Radiative heat transfer coefficient. kw/ m^2. °C

H_s Solar radiation on horizontal surface. MJ/m^2

IR Infrared.

L Water depth in the basin. mm

$M.m^3$ Million cubic meters.

MED Multiple stage Distillation.

MSF Multistage Flash.

MW Megawatt,hour.

M_w Water content of the basin, kg.

P_g The saturation vapor pressure of water at glass temperature, (N/m^2)

PPM Part per million.

P_w The saturation vapor pressure of water at water temperature, (N/m^2).

q_b Conductive heat loss from water basin to the ground. kw/ m^2

q_c Convective heat loss from water to the cover. kw/ m^2

q_{ca} Heat loss by convection from cover to atmosphere . kw /m^2

q_{cw} Convective heat transfer rate from water to glass surface, kw/ m^2

q_{ew} Evaporative heat loss from water to the cover. kw/ m^2

q_{ga} Heat loss from cover to atmosphere. kw/ m^2

q_r Radiative heat loss from water to the cover. kw/ m^2

q_{ra} Heat loss by radiation from cover to atmosphere. kw/ m^2

RO Reverse osmosis.

SD Solar Desalination.

t Time, second.

T_a	Ambient temperature, °C.
TDS	Total dissolved solids, mg/ litre.
T_g	Glass temperature, K.
T_s	Radiant sky temperature, K.
T_w	Water temperature, K.
U_p	Overall heat transfer coefficient.
V	Wind speed, m/s.
Y	Total distillation yield of the still, litre/h.

GREEK LETTERS

β	Still cover slope.
ϕ	Latitude.
$\propto_w$	Absortivity of water basin liner.
$\propto_g$	Absorptivity of glass cover.
ℓ	Latent heat of water (J/kg).
ε	Emmissivity
ε_g	Emmissivity of glass cover.
ε_w	Emmissivity of water.
η	Still efficiency %.
ρ	Water density (kg/m^3).
σ	Standard deviation of a sample.
l	Covariant.

CHAPTER ONE

INTRODUCTION

1.1 Problem Definition

Global resources of fresh water are limited, unevenly distributed and, in many cases, may require some from of treatment and handling. These scarce water resources resulted in water shortages in 88 developing countries across the world containing 50 % of the world's population. Water supplies in theses countries cannot meet urban and industrial development needs as well as associated changes in lifestyle. In Qatar, the economical progress that occurred as a direct result of the discovery of oil has changed many things. Like other Gulf States, Qatar has passed through social, economical, and industrial changes. Consequently, the population has increased three to six times over few decades; therefore the government was forced to consider obtaining water supplies from underground resources. Consequently, most of these resources either dried up or become salty. Moreover, as a result of the dramatic population increase there was an increase in the number of farms needed for more food production. As a result, the limited underground water that accumulated over centuries by a short seasonal rainfall, was dramatically consumed in few years. This fact is clearly demonstrated in Fig 1.1.

This situation has been aggravated by the poor fresh water resources and limited subterranean supplies, particularly in areas where people are totally dependent on such sources for their fresh water. Like any arid region of the world Qatar lacks reliable alternative sources of fresh water such as rivers or lakes. Therefore, the government has been forced to seek alternative ways to fulfill the nations need for fresh water, mainly from desalination plants. This expedient is used in many other countries with similar conditions to those found in the Gulf.

Although, desalination plants such as multi-stage flash [MSF] produce adequate amounts of fresh water in reasonable time, their initial and operation costs are very high. Moreover, their operations require energy in the form of heat to raise the brine water temperature. This is provided normally in the form of natural gas or crude oil by means of exhaust heat from gas turbines or by gas/oil fired boilers. In addition, desalination plants require considerable care as they always suffer from an accumulation of scale and corrosion. Hence, such plants are expensive to operate and maintain. According to Soteris, (a) (1997) "*The production capacity of the desalinated water system in 1990 reached 13 million m^3/day which, by the year 2000,*

is expected to double. It has been estimated that production of 13 million m^3/day requires 130 million tons of oil per year".

In addition, desalination plants can affect the environment by outpouring large amount of blow down (rejected brine). This brine has a different temperature, chemical composition, alkalinity (pH) than the sea, and dissolved substances such as heavy metals. All this can destroy, some times for ever, marine life. Also the long-term effects of pretreatment chemicals like polyphosphate and acid based additives on health are unknown. (Rajka, 1996). In recent years, there has been increasing public awareness of the limited lifetime of the fossil fuels and the harmful effects of using the fuels on the environment. Technology was able to reduce some of the emissions of sulphur dioxide and nitrous dioxides, but carbon dioxide emissions continued to cause environmental damage through its contribution to global warming. Moreover, natural gas, which is relatively cleaner form of fuel, is still expensive for those countries that are unable to produce it locally. In addition, nuclear energy is not likely to be an option for most developing countries, mainly due to cost and its hazardous impact on life and the environment.

In Qatar, the high instillation and operational costs, expensive maintenance, environmental problems, and limited fossil fuel reserves rendered the development of alternative water desalination plants and processes very necessary. Since Qatar currently detains 98% of its total fresh water supply from desalination plants and is situated within the high solar radiation belt, production of potable (fresh) water using solar desalination process constitutes a very viable and attractive proposition. Solar radiation can provide a renewable, clean, safe, free, and low-maintenance source of energy for desalination process. This energy source is only limited by the initial plant cost and the fluctuation in solar radiation. (Qatar General Electricity & Water Corporation, 2001).

This research was aimed at investigating and determining the most important factors that affect various water desalination plants performance and cost. The conceptual designs of existing water desalination plants in Qatar and solar desalination plants were discussed technically and economically.

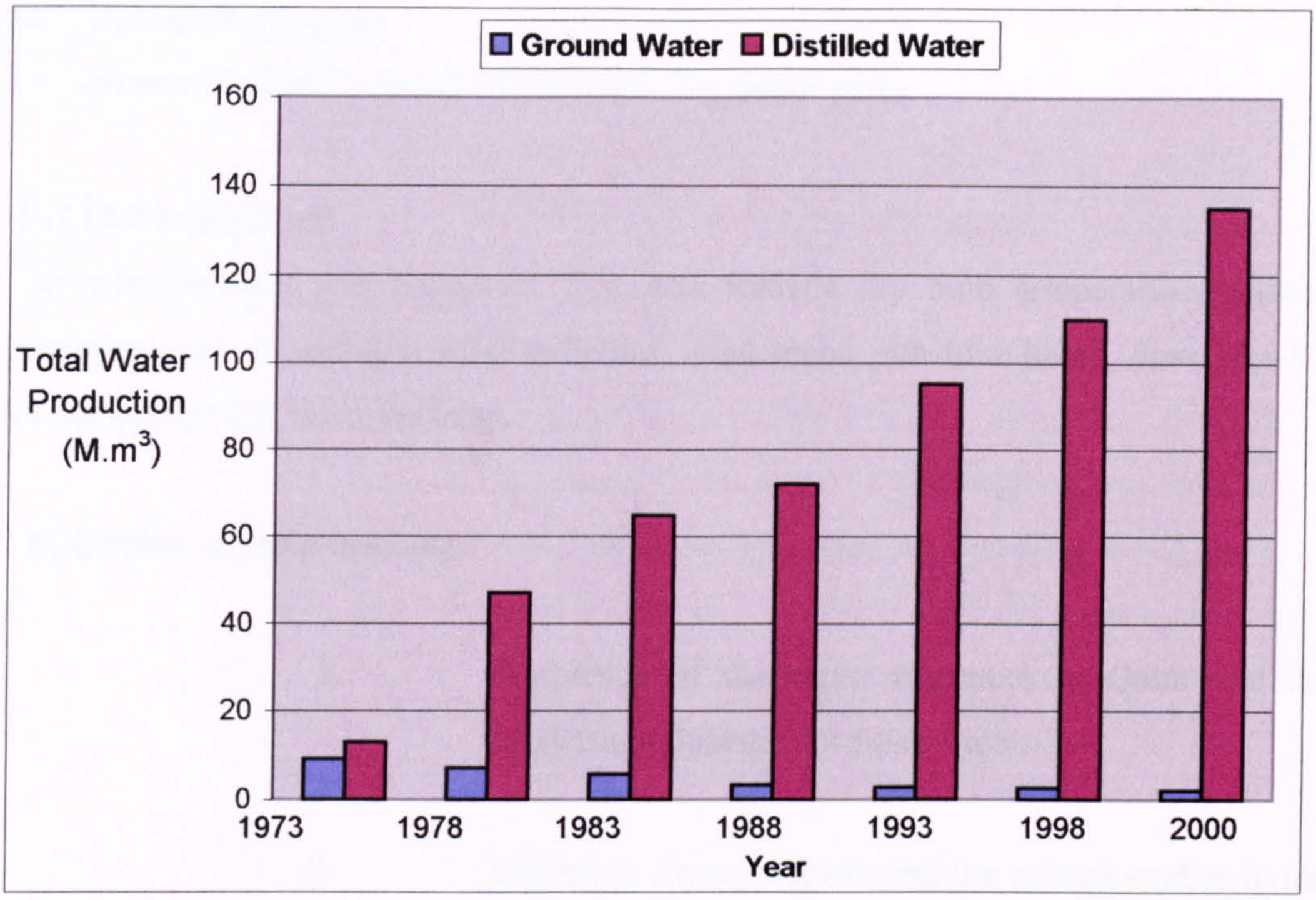

Fig 1.1 The total water production in Qatar by ground water & desalination plant (Qatar General Electricity & Water Corporation, 2001)

1.2 Research Objectives

As has been indicated in the previous section of this chapter, continuing long-term development in Qatar and limited natural fresh water resource forced the government to seek alternative ways of obtaining the nation needs of fresh water from desalination plant, which is still considered most expensive method of producing fresh water.

The objectives of this research project were:-

- Investigate the fresh water resources and the general climatic conditions in Qatar during the last three decades.
- Investigate the most viable water desalination processes that can reduce the costs of water desalination in Qatar.
- Studying both technical and economic characteristics of various desalination processes.
- Investigate the currently available solar stills designs to determine the important parameters that affect their performance (material, dimension, orientation, insulation).
- Developing a typical absorber of tilted try solar still to a pyramid shape absorber to receive an optimal amount of solar radiation.

1.3 Research Method

The research method consists of the following major parts:

[A] Data collection:

The climatic data was collected. This data include dry bulb temperature, relative humidity, vapour pressure, solar radiation, wind speed, sunshine hours, dust, cloud… etc during the last three-decades.

[B] Review of information: -

I. Definition of the water resources in Qatar and the increase in demand for fresh water.

II. Literature survey: Reviewing the related studies to the subject in general and covering the currently available solar still plant designs.

[C] Analysis and evaluation: -

I. Climatic data analysis and estimation of a year model.

II. Evaluation of the cost of distilled water production.

III. Identification of the most suitable method of producing fresh water in Qatar.

IV. Economical study of various desalination processes.

V. A comparison of the performance and efficiency of the other current desalination plants in Qatar.

VI. Design and fabrication of solar stills.

[D] Experimental:

The experimental work is divided into four parts:

I. Testing the performance of the two prototype designs of solar still [model 1 (Dome and Pyramid)] under controlled laboratory conditions.

II. A comparative study of the performance of the two still types using identical operation technique was followed. Here, various operation parameters were also tested including inlet water flow rate, inlet water temperature, and the cavity volume.

III. The outdoor testing was carried out with selected prototype design, the large size of pyramid tilted tray solar still (model 2) has been constructed and tested in the University of Qatar under local climatic conditions during May-June 2000.

IV. As part of the field work, a comprehensive study of the desalination process in a main desalination plants in Qatar was undertaken. The aim of this study was to observe and investigate the various parts of the desalination plant processes, in order to estimate the exact distilled water cost. This study conducted during the months of February to July 2000.

[E] Theoretical:

A specially designed computer programme was written in Visual Basic Version (5) and has been employed to predict the yield, climatic conditions and other parameters of solar still over 24 hours period throughout the year. This programme was subsequently tested for the following: -

I. The sensitivity of the programme to varying climatic conditions in Qatar (temperature, radiation, sunshine…etc).

II. Estimation of suitable design parameters for developing the solar desalination efficiency for a specific application under certain environmental conditions.

III. The analysis and determination of the solar stills potentiality as an alternative method of producing sufficient fresh water in Qatar during the whole year.

CHAPTER TWO

CLIMATIC ANALYSIS OF QATAR

2.1 Introduction

The state of Qatar is situated on the western coast of the Arabian Gulf. It is a peninsula covering an area of 11,437 square kilometers that extends northwards into the Gulf. It lies between 24° 48″ and 26° 17″ N and between 50° 75″ and 51° 66″ E. Almost the whole state is covered by desert and is dominated by identical climatic conditions. The climate of Qatar is basically hot and humid, with a daily temperature that routinely exceed 30°C. The winter months are somewhat cooler, with temperatures often around 20°C.

The climate of Qatar is characterized by being part of the central Arabian anti-cyclone. The air mass is polar continental flowing in a SE direction over the dry land mass to the north, thus there is very little cloud cover and rainfall, the sun shines intensely and continuously, and the intensely hot air flows over the arid land in north direction. The combination of clear sky and dry land produces high mid-day air temperature; during the night high radiation to the clear sky from the dry land produces low night-time temperatures. The wind is generally fairly steady from the north-west. During the summer about 25% of nights are defined as calm, with wind speeds of 4.4 m/s or less.

2.2 Climate

2.2.1 Relative humidity

Humidity is somewhat higher than in Central Arabia, due to the proximity of the sea, and there is a less marked seasonal variation, although the lowest humidity figures were recorded in the summer months and the highest figures in the winter months, as shown in Fig 2.1. The relative humidity varies with the season and also with the time of day, i.e. with the diurnal fluctuation in temperature. Figure 2.2 shows that the mean monthly maximum and minimum relative humidities exhibit the same trend through the year. The mean monthly maximum relative humidity ranges from 66% in June to 88% in January and February, while the mean monthly minimum ranges from 20% in June to 48% in December to February.

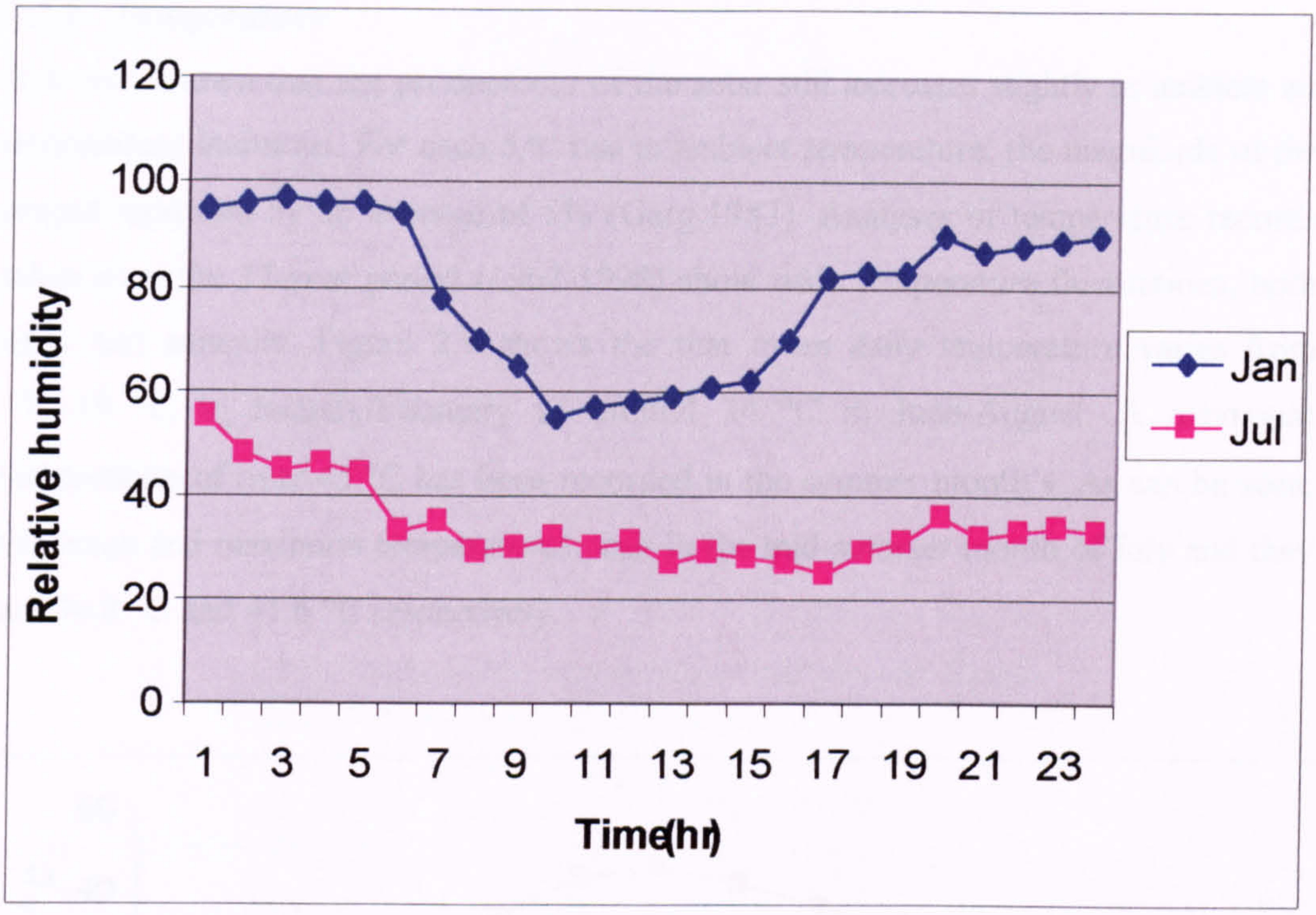

Fig 2.1. Hourly mean relative humidity in Qatar (Ministry of Communication & Transport 1962-1998).

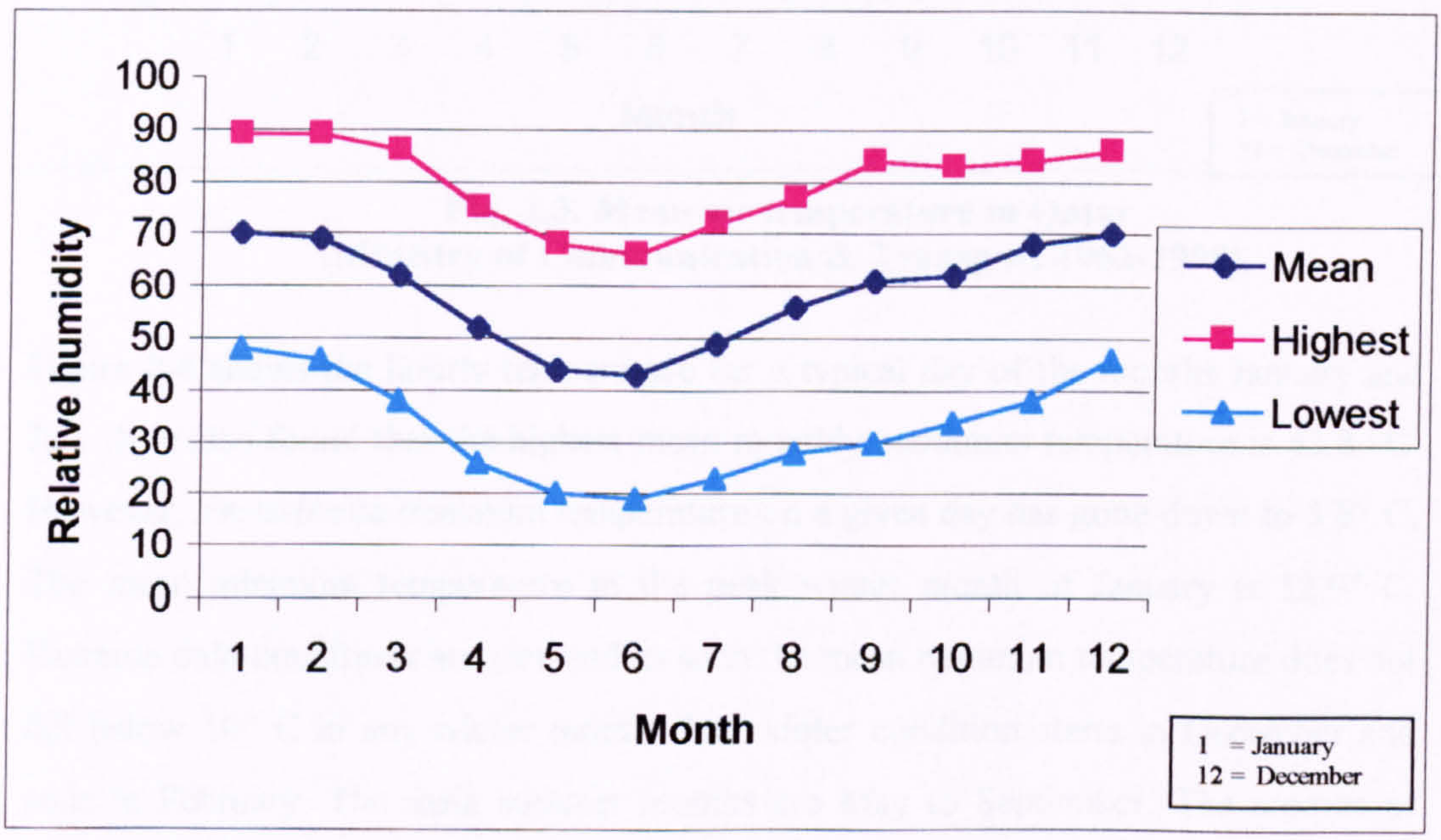

Fig 2.2. Mean monthly relative humidity in Qatar (Ministry of Communication & Transport 1962-1998).

2.2.2 Temperature

It is well known that the productivity of the solar still increases slightly as ambient air temperature increases. For each 5 °C rise in ambient temperature, the magnitude of the output increases by an average of 5% (Garg,1987). Analyses of temperature records taken over the 37-year period (1962-1998) show wide temperature fluctuations, both daily and annually. Figure 2.3 shows the that mean daily temperature varies from 17 -19 °C in January/February to around 34 °C in June-August. A maximum temperature of over 45 °C has been recorded in the summer month's .As can be seen, the mean and maximum temperatures peak in the mid-summer month of July and they are 34.8 °C and 41.6 °C respectively.

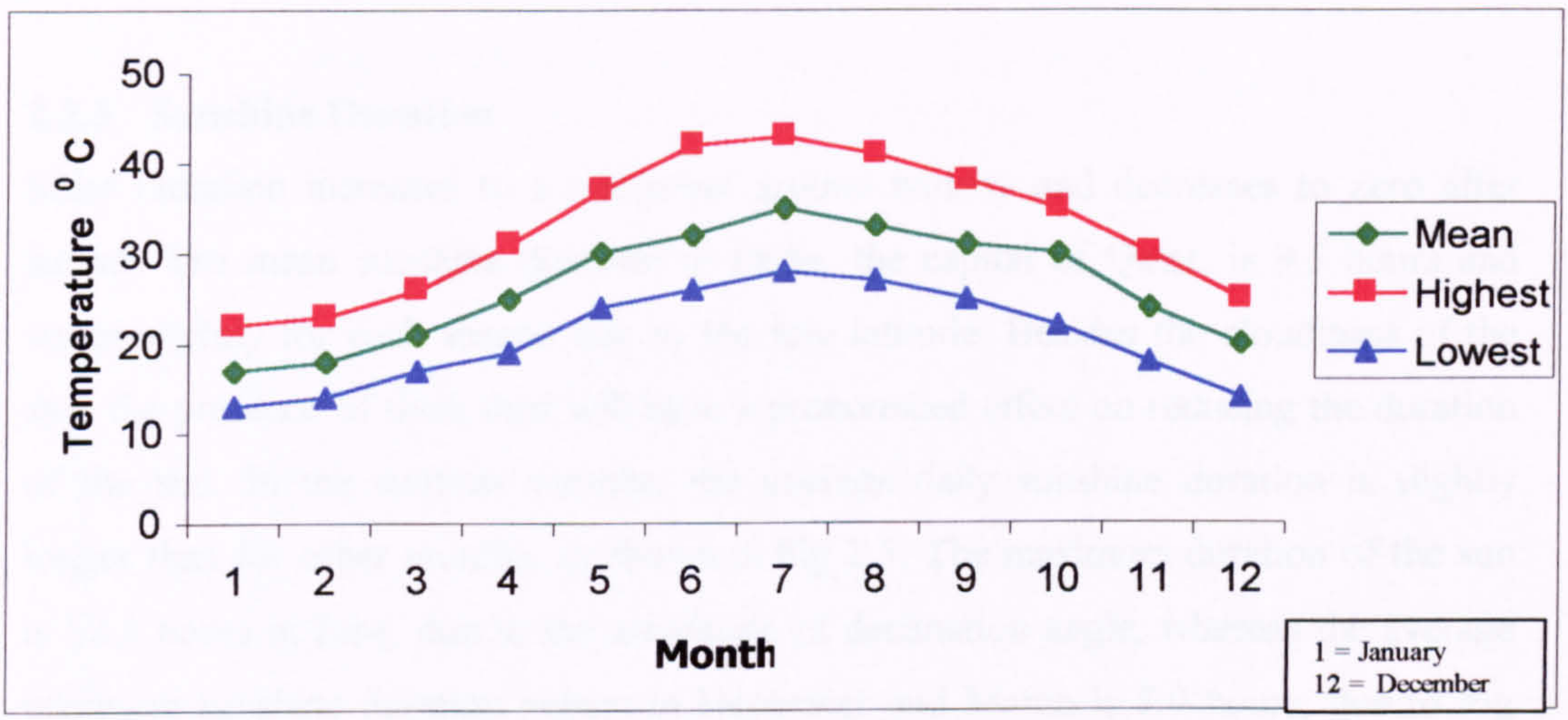

Fig. 2.3. Mean air temperature in Qatar (Ministry of Communication & Transport 1962-1998).

Figure 2.4 shows the hourly temperature for a typical day of the months January and July. It is also found that the highest mean monthly maximum temperature is 43.8 °C. However, the extreme minimum temperature on a given day has gone down to 3.8° C. The mean minimum temperature in the peak winter month of January is 12.9° C. Extreme cold conditions are rare and as such the mean minimum temperature does not fall below 10° C in any winter month. The winter condition starts in December and ends in February. The main summer months are May to September. The months of March to April and October to November may be regarded as transitional months from winter to summer and summer to winter respectively.

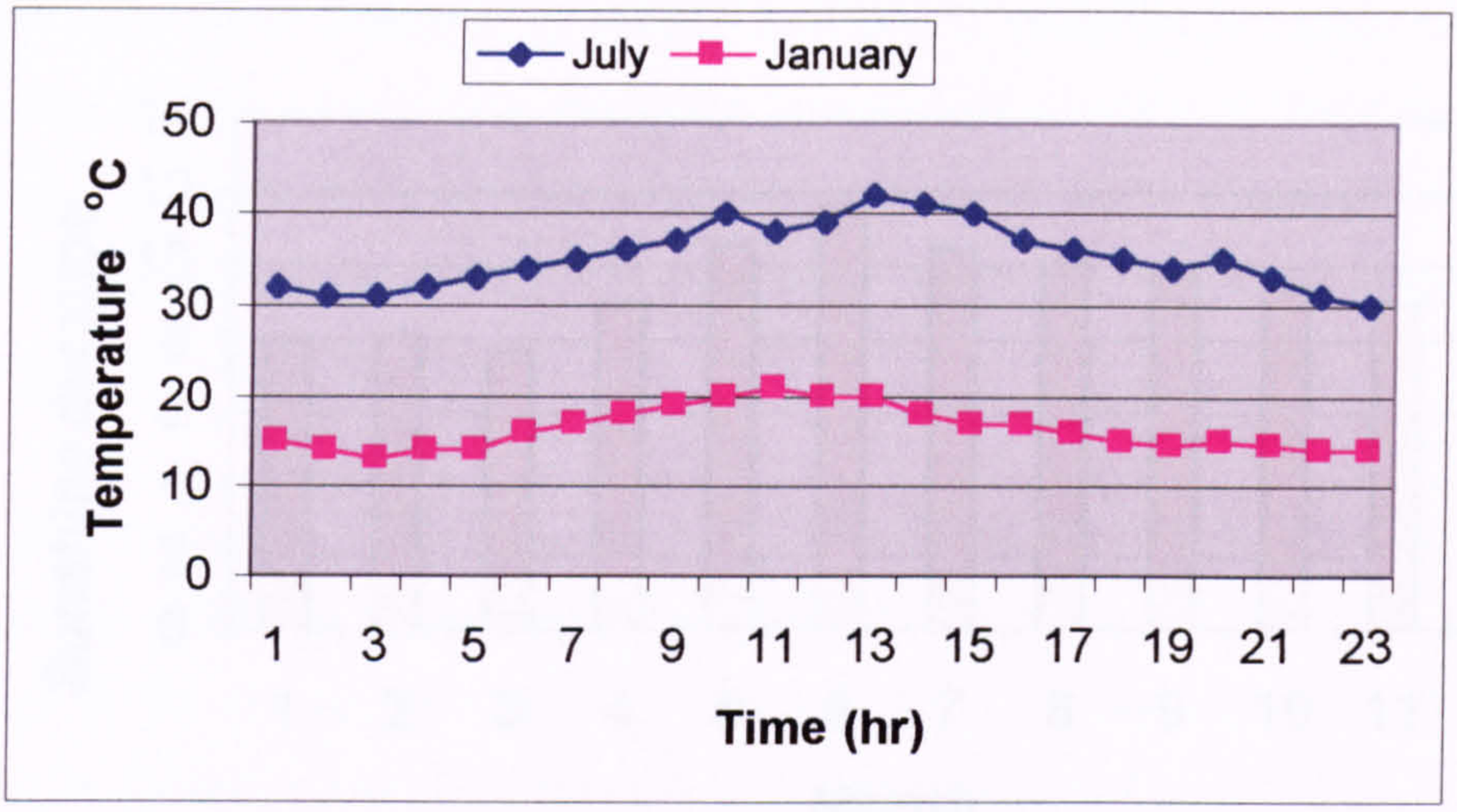

Fig 2.4. Hourly temperature variation in Qatar (Ministry of Communication & Transport 1976-1998).

2.2.3 Sunshine Duration

Solar radiation increases to a maximum around midday and decreases to zero after sunset. The mean sunshine duration in Doha, the capital of Qatar, is 9.5 hours and varies slightly for each season due to the low latitude. Besides the cloudiness of the sky, the presence of thick dust will have a pronounced effect on reducing the duration of the sun. In the summer months, the average daily sunshine duration is slightly longer than for other months, as shown in Fig 2.5. The maximum duration of the sun is 12.3 hours in June, due to the amplitude of declination angle, whereas the average minimum sunshine duration occurs in December and March is 7.9 hours, due to fog and clouds respectively.

2.2.4 Rainfall

The month-wise rainfall along with monthly mean rainfall for different months, rainy days (rainfall equal to or more than 1mm) during a period of 37 years 1962-1998, is shown in Fig 2.6. Significant amount of rainfall generally occurs in winter months, the total annual rainfall in Doha is 213.6mm. It may be noted that rainfall is mainly confined to the period of December-April, with peak rainfall in the months of February and March, having an average rainfall of 17.8mm and 22.3mm respectively. Rain is absent in the summer months of June-September. The highest annual rainfall of 302.8mm was recorded at Doha in 1964.

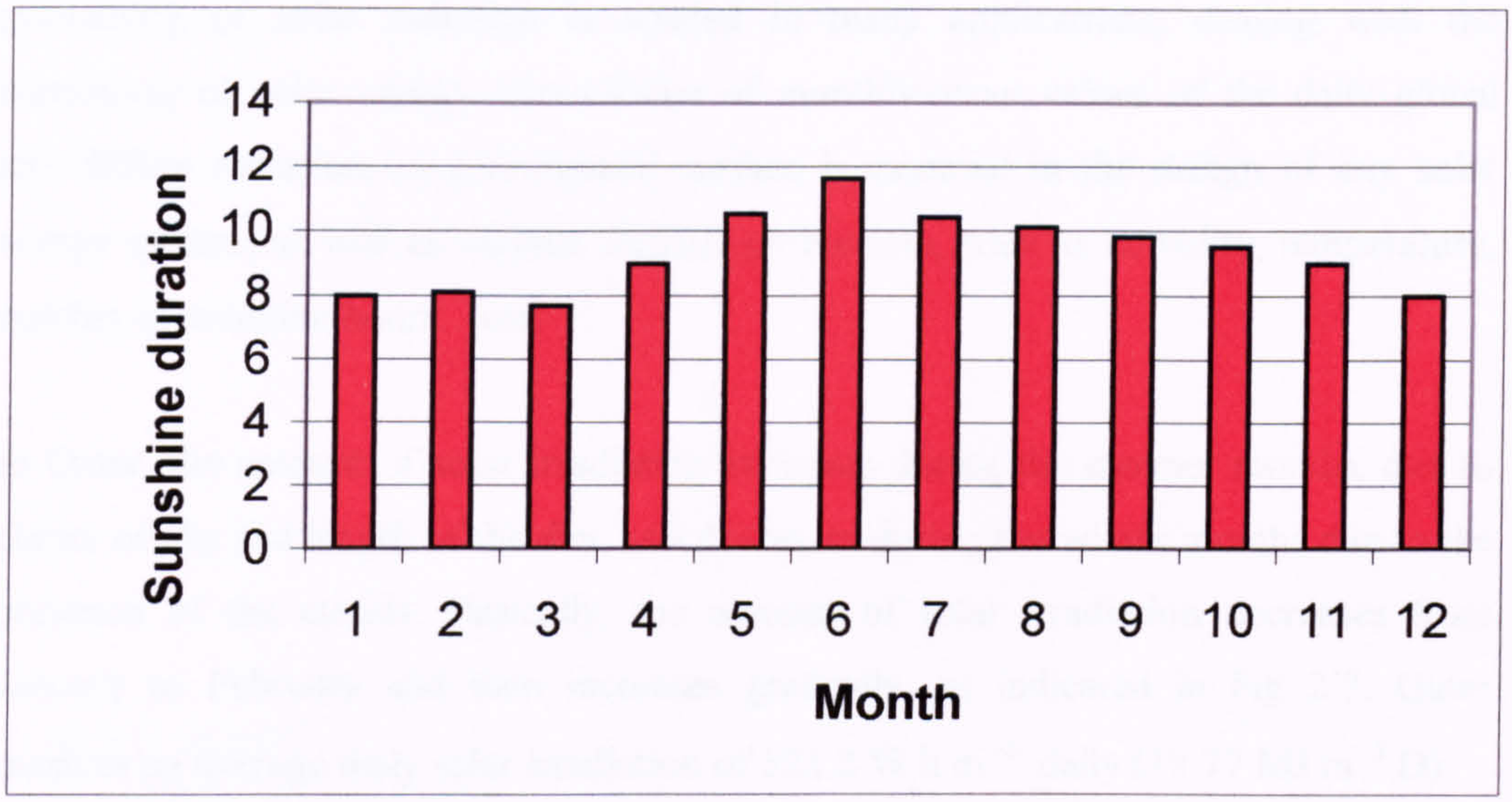

Fig 2.5. Mean monthly sunshine duration in Qatar (Ministry of Communication & Transport 1962-1998).

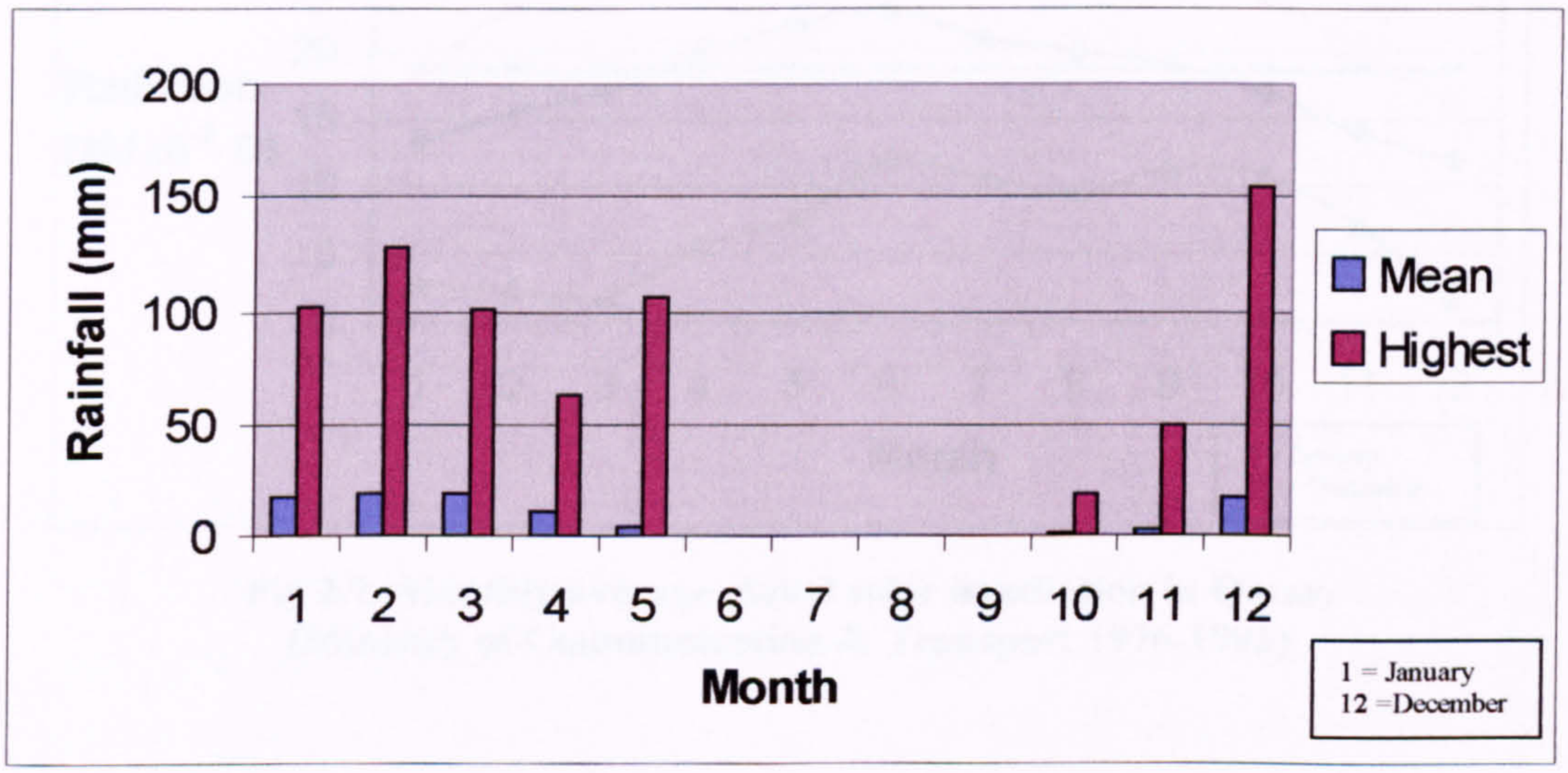

Fig 2.6. Monthly average rainfall in Qatar. (Ministry of Communication & Transport 1962-1998)

2.2.5 Solar Irradiation

The solar desalination process is very sensitive to the intensity of the solar radiation. Water production is proportional to the radiation intensity. The former can vary from zero at night, to full production during the day. Solar radiation reaching the earth's surface depends on the local climatic conditions and the latitude. Information on the

availability of solar radiation is needed in many applications, dealing with the harnessing of solar energy. Knowledge of monthly-mean values of the daily global and diffuse radiation on a horizontal surface is essential in the design of any solar energy system, as well as various climatic parameters, such as humidity, temperature, number of sunshine hours…etc.

In Qatar, the amount of solar irradiation increases during the summer months, due to clarity of sky and length of the day, and decreases during the winter months due to the presence of the clouds. Basically, the amount of solar irradiation decreases from January to February and then increases gradually, as indicated in Fig 2.7. Qatar receives an average daily solar irradiation of 521.2 $W.h.m^{-2}$ daily (18.77.$MJ.m^{-2}$ D).

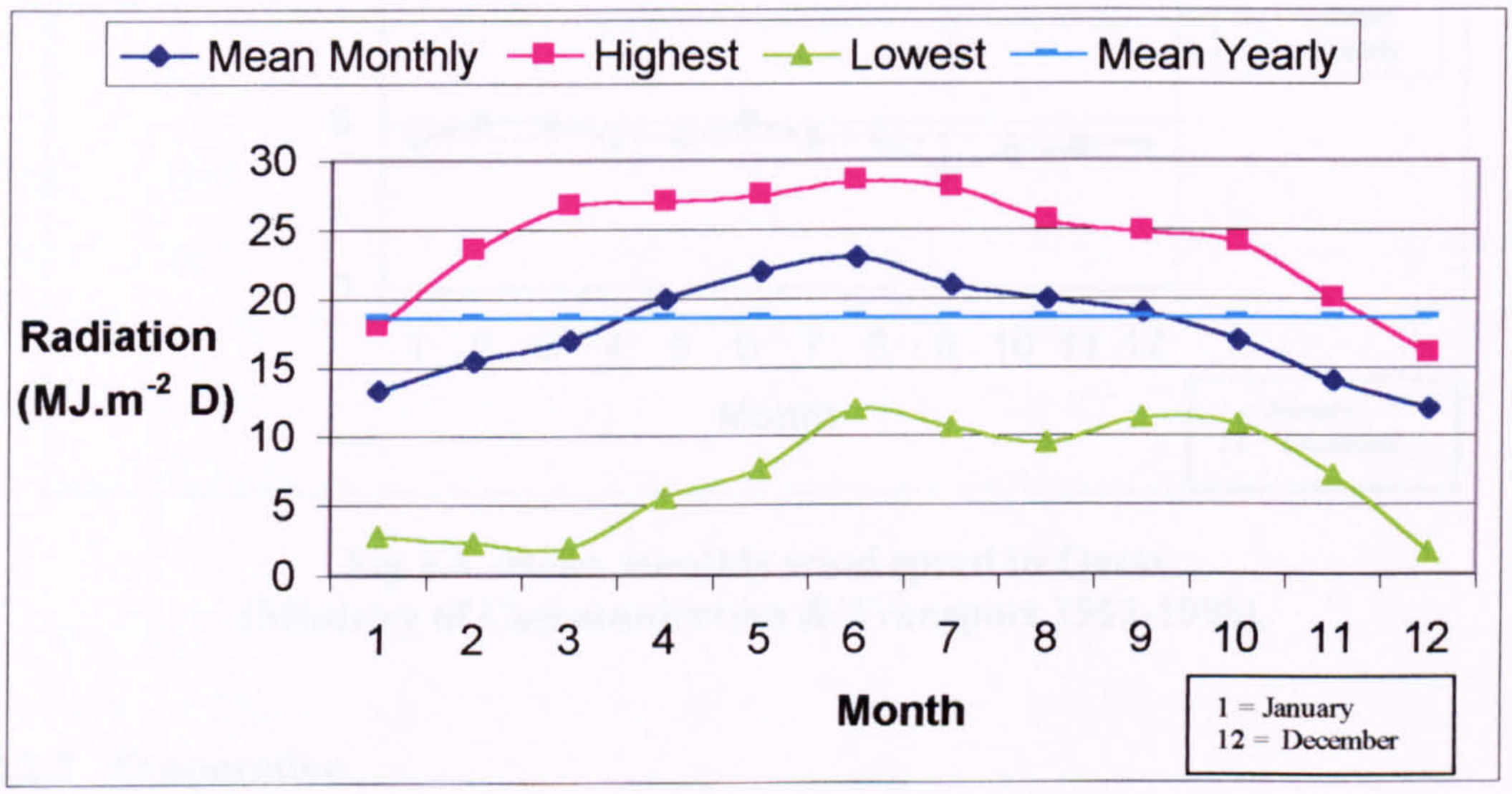

Fig 2.7. Monthly average global solar irradiation in Qatar. (Ministry of Communication & Transport 1976-1993)

2.2.6 Wind

Wind is considered as the main controlling factor of the atmosphere as it affects all atmospheric phenomena. The mean annual wind speed in Qatar is 4.4 m/s, at 10 m above the ground, as shown in Fig 2.8. During winter months the wind direction is variable, with the predominant direction in December being north to north westerly (NNW) while in February the predominant direction is south to south easterly (SSE). For the rest of the year the predominant direction is north to north westerly (NNW). Mean wind speed in summer and winter is around 4.4 m/s. The period from March to

end of June is characterized by sandstorms coming from the northern part of Saudi Arabia which lower visibility to less than 1 km. Calm winds with changing direction from northerly to north easterly are dominant during the autumn months.

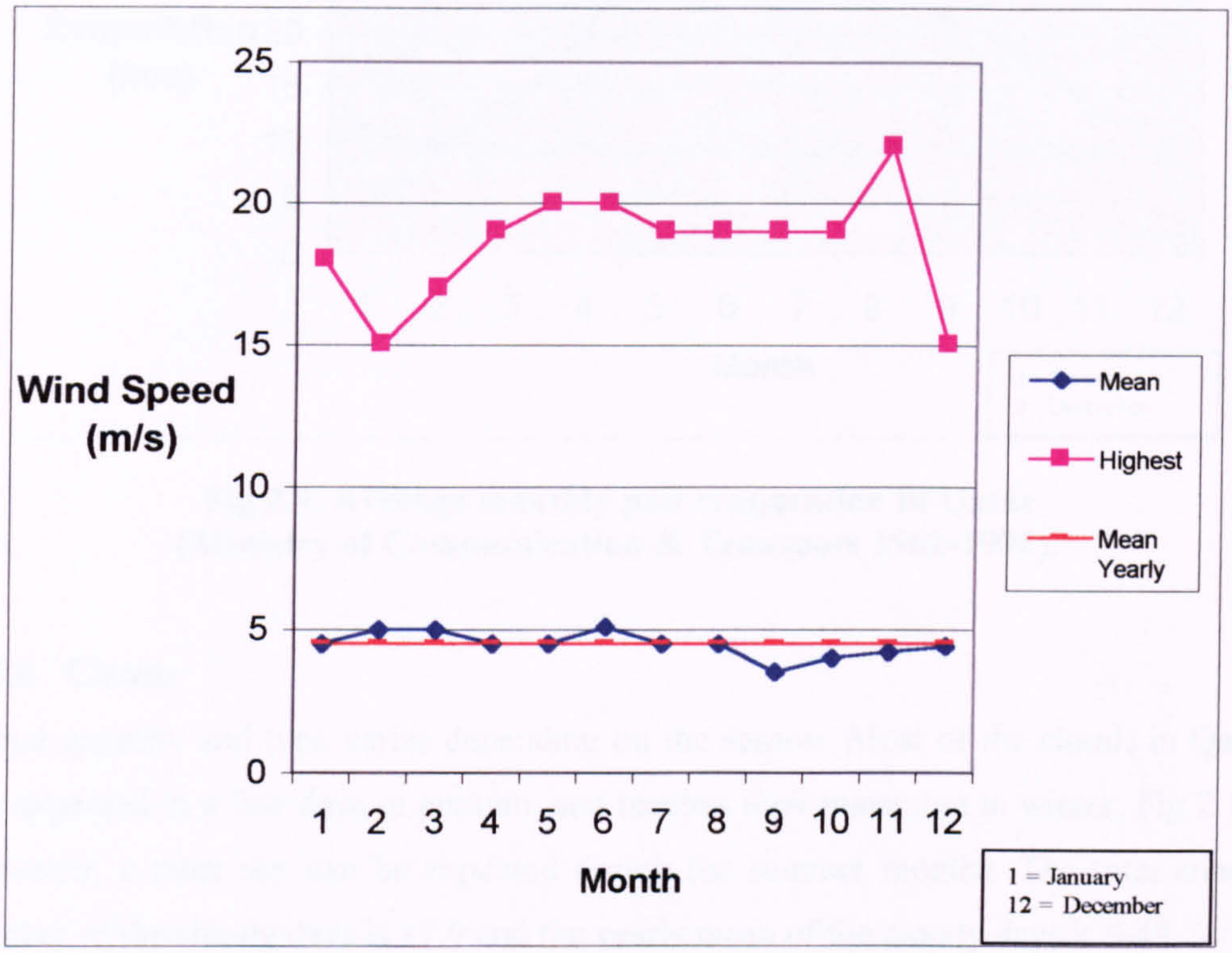

Fig 2.8. Mean monthly wind speed in Qatar (Ministry of Communication & Transport 1962-1998).

2.2.7 Evaporation

Water vapour is an important constituent of the atmosphere. In Qatar, two common metrological instruments, Pan evaporation and Piche evaporation, were employed to measure evaporation. Pan evaporation from an open tank is more widely used as an index of evaporation and evapotranspiration. These two instruments calculate the evaporation rate through a shallow and graduated water container. The annual mean Pan evaporation calculated from meteorological data is 8.6 mm/, month. Figure 2.9 illustrates that the highest evaporation is extending from the period May to August and is at a level higher than 25mm/month followed by a slight decrease in September. In winter months it decreases to a low level. The data indicates that it stays at a level of 20 mm/month for six months per annum.

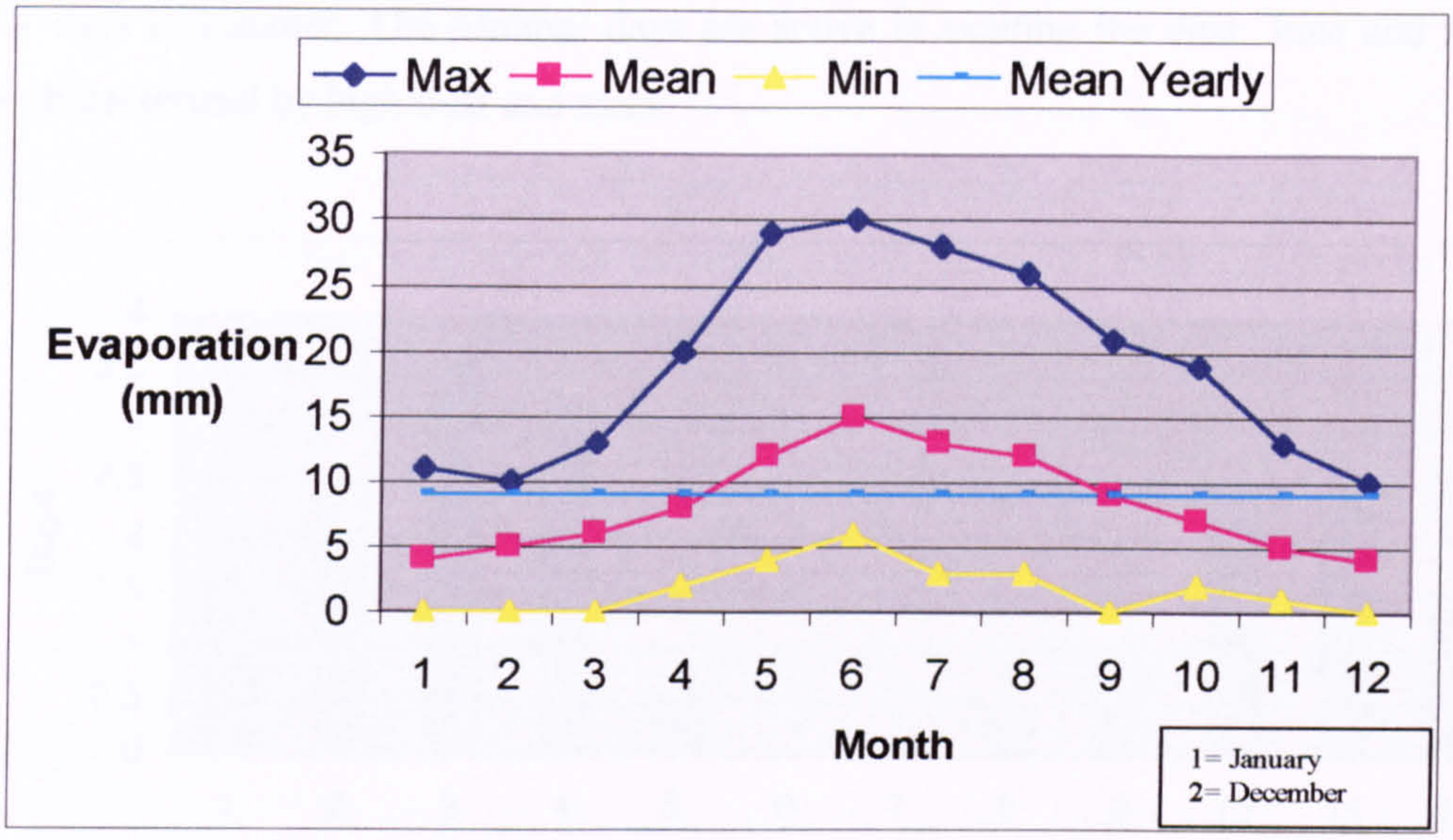

Fig 2.9. Average monthly pan evaporation in Qatar (Ministry of Communication & Transport 1962-1998).

2.2.8 Clouds

Cloud quantity and type varies depending on the season. Most of the clouds in Qatar are expected in a few days in autumn, and reaches their maximum in winter, Fig 2.10. However, a clear sky can be expected during the summer months. The total annual number of the cloudy days is 17.9 and the yearly mean of the cloudy days is 9.49.

2.2.9 Fog

The fog in Qatar is mostly caused by radiation. On clear nights fog occurs in Qatar as a result of high water vapour, little cloud, slight wind and stable weather conditions. It can be seen from Fig 2.11, that most of the foggy days founds in autumn and winter than the other seasons. This may be the result of the water vapour blown by the sea breeze and low temperature at night. The total annual number of foggy days in Qatar is 19.8 days of which 9.6 is in winter.

2.2.10 Dust and Sand

The solar still productivity is significantly affected by the quantity of solar radiation; therefore any dust or sand layer on the cover surface can minimize the absorbed radiation. Figure 2.11 illustrates dust, mist, haze, and sand throughout the year. The total number of days with visibility of 1 km to less than 5 km is 90.4 days of which

47.1 days in summer. The summer days are active in exciting the dust. June and July are characterized by high dust and sand.

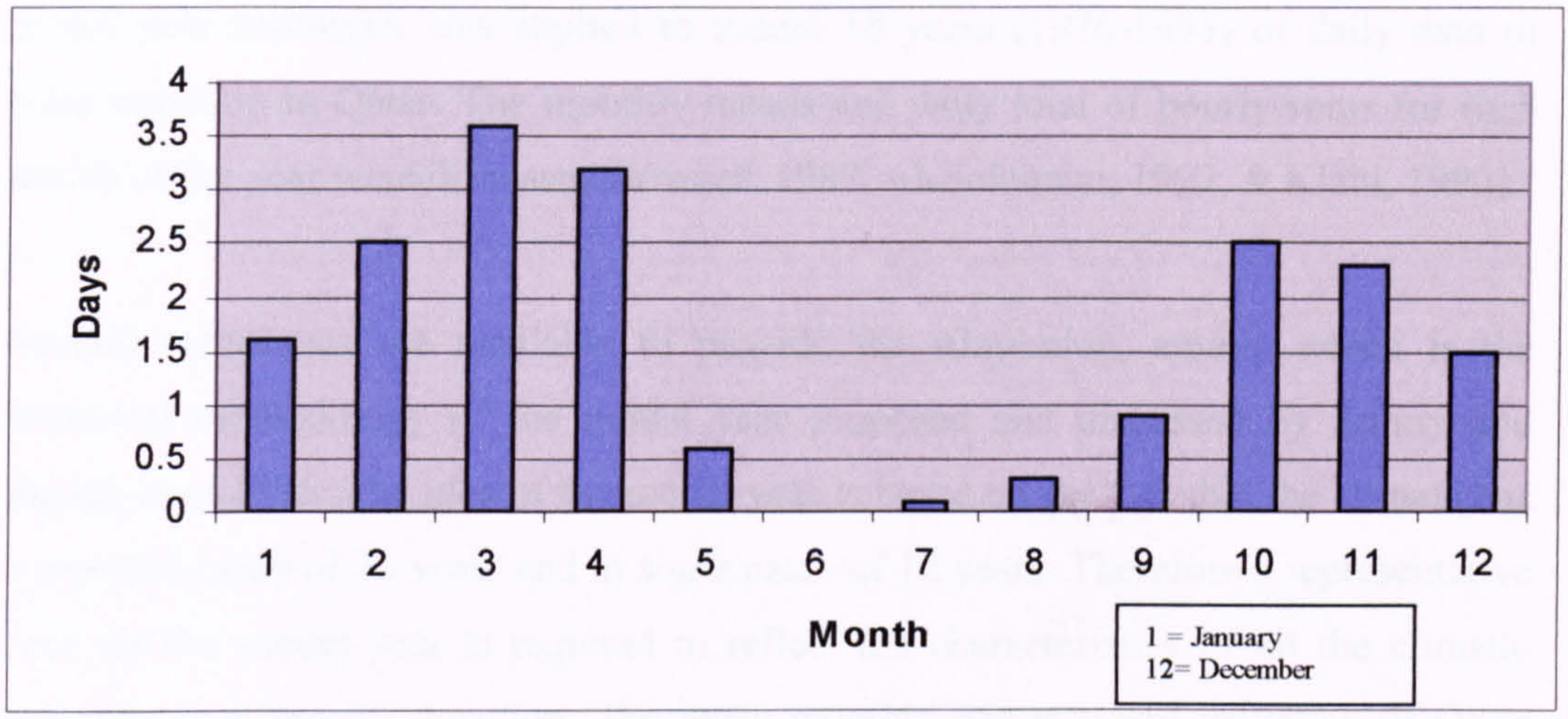

Fig 2.10. Monthly average cloud cover in Qatar (Ministry of Communication & Transport 1962-1998)

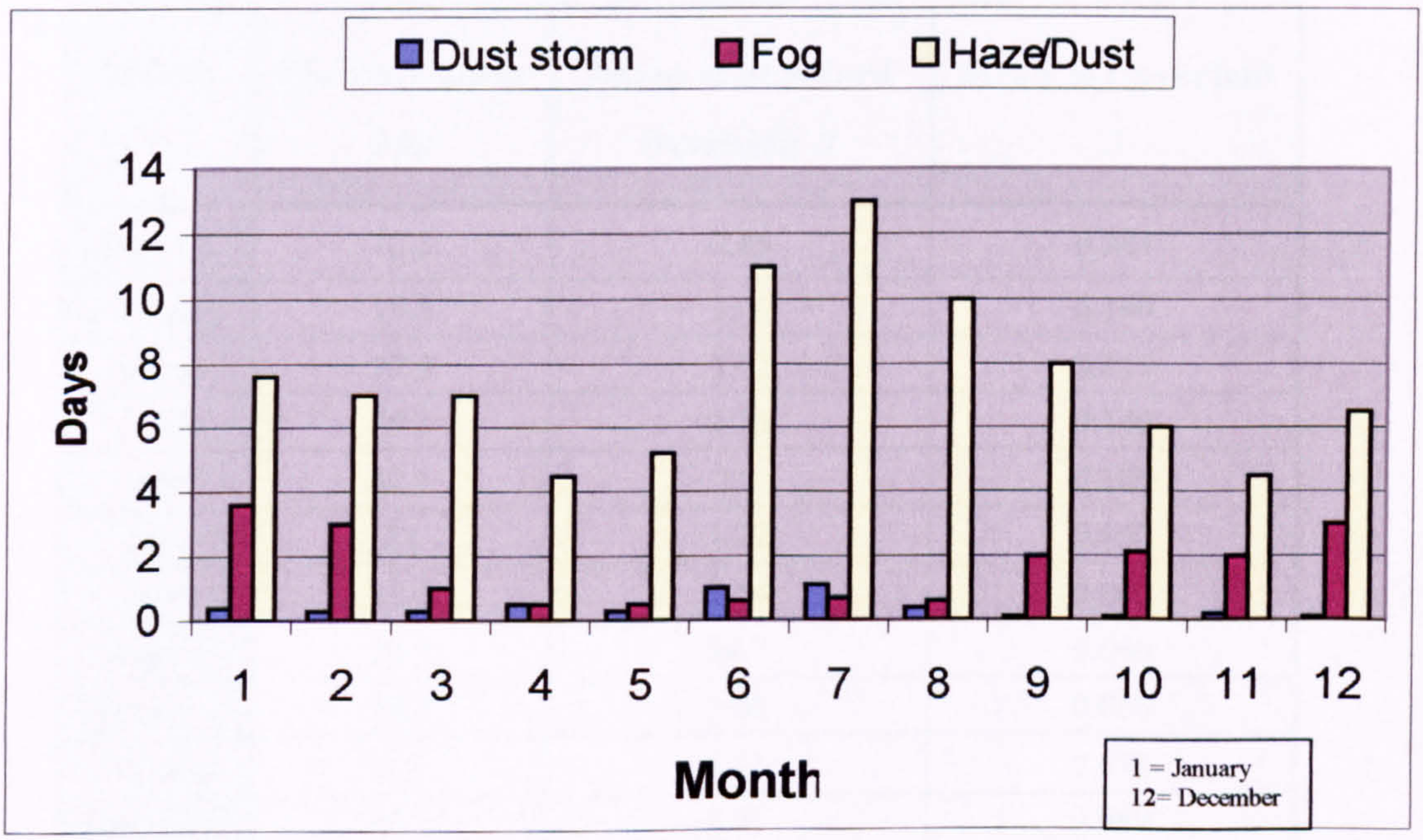

Fig 2.11. Mean number of days with fog (visibility less than 1 km) in Qatar (Ministry of Communication & Transport 1962-1998).

2.3 The Radiation Model Year

The investigation and estimation of the amount of solar radiation at any area is an important factor for any design or system utilizing solar energy applications. The model year technique was applied to model 18 years (1976-1993) of daily data of solar radiation in Qatar. The monthly means and daily total of hourly sums for each month of the year were discussed (Yousef, 1987, Al-Sulaiman, 1997, & Klabi, 1990).

Several techniques are available to provide the simulation, among which is the statistical methodology of the model year proposed and discussed by Zuhiry and Sayigh *et al* 1995. The idea of the model year is based on the fact that the climate has a repeated cycle of 30 years and in some cases of 12 years. Therefore a representative year for the model year is required to reflect the characteristics of all the climatic variables in a specific location. The mean monthly and standard deviation of Qatar have been calculated and displayed in Table 2.1.

Month	**Monthly mean** $\bar{Mm}$	**Mean of Standard Deviation** $\bar{S}$	**Mean of Covariant** $\bar{\lambda}$
January	13.3	2.86	0.201
February	15.5	3.06	0.199
March	17.5	3.72	0.217
April	20.3	2.76	0.140
May	22.1	2.2	0.100
June	23	1.22	0.053
July	21.6	1.44	0.068
August	20.7	34.7	0.060
September	19.3	1.08	0.056
October	17	1.21	0.072
November	14.7	1.31	0.089
December	12.4	2.14	0.176

Table 2.1 Calculated of Monthly, Standard Deviation and Covariant Mean Global Radiation ($MJ/m^{2)}$ State of Qatar (1976-1993).

2.4 The Model Year Technique

The model year for hourly total solar radiation on horizontal surface, H, can be established, based on the year in which the data for each month are real data. Each month is represented by the month for which both the mean and the standard deviation are closest to the long-term standard deviation for that specific month. The radiation model year of Qatar has been estimated and displayed in Table 2.2. Figures 2. 12 and 2.13 shows an isoradiation maps for the Arabian Peninsula calculated by applying the proposed formula of Sabbagh, Sayigh, and El-Salam. 1977.

2.4.1 The Daily Mean [$\bar{D}$]

The following formula for the calculation of the daily mean values of the hourly data is proposed:

$$\bar{D} = \frac{\sum_{1}^{24} h}{24} \qquad (2.1)$$

where $\bar{D}$ = daily mean of hourly values, h = hourly values of solar radiation.

2.4.2 The Monthly Mean [$\bar{M}$]

The calculation of the monthly mean for each month of each year is shown in equation 2.2.

$$\bar{M} = \frac{\sum_{1}^{N} \bar{D}}{N} \qquad (2.2)$$

where $\bar{M}$ = monthly mean of daily sums for a specific month in a specific year.

N = number of days for that specific month. $\bar{D}$ daily mean of hourly values.

2.4.3 The Standard Deviation and The Variant [S & S^2]

Calculation of the standard deviation and variant for each month of the year in all the years by comparing the daily means with the monthly means as revealed in equation 2.3.

$$S^2 = \frac{\sum_{1}^{N} (\bar{D} - \bar{M})^2}{N} \qquad (2.3)$$

2.4.4 The Covariant (λ)

The covariant (λ) can be calculated from the following equation:

$$\lambda = \frac{S}{\bar{M}} \qquad (2.4)$$

where λ = covariant, which is to be calculated for all the months in all the considered years, S = standard deviation and $\bar{M}$ = monthly mean.

2.4.5 The Monthly Mean for Each Specific Month [$\bar{M}m$]

Equation 2.5 is used to calculate the mean for each specific month from the monthly means of that month in the whole period can be calculated as:

$$\bar{Mm} = \frac{\sum^{X} \bar{M}}{X} \qquad (2.5)$$

where $\bar{Mm}$ = mean of the monthly means of each specific month, X = number of years.

2.4.6 The Mean Of The Standard Deviation [$\bar{S}$] and The Mean Covariant [$\bar{\lambda}$].

The calculation of both the means of the standard deviation and the covariant is shown below:

The mean standard deviation, $\bar{S} = \frac{\sum^{X} S}{X}$ (2.6)

The mean covariant, $\bar{\lambda} = (\frac{\bar{S}}{\bar{Mm}})^2$ (2.7)

Month	Year	The closest values of (λ- $\bar{\lambda}$)
January	1981	0.000952572
February	1991	0.004351462
March	1979	0.000577496
April	1988	0.003674197
May	1977	0.004351462
June	1984	0.0000681745
July	1993	0.000883701
August	1993	0.0000865985
September	1986	0.0012338
October	1991	0.00643062
November	1980	0.000298248
December	1982	0.003974058

Table 2.2. Calculated Radiation Model Year for Qatar. 1976-1993.

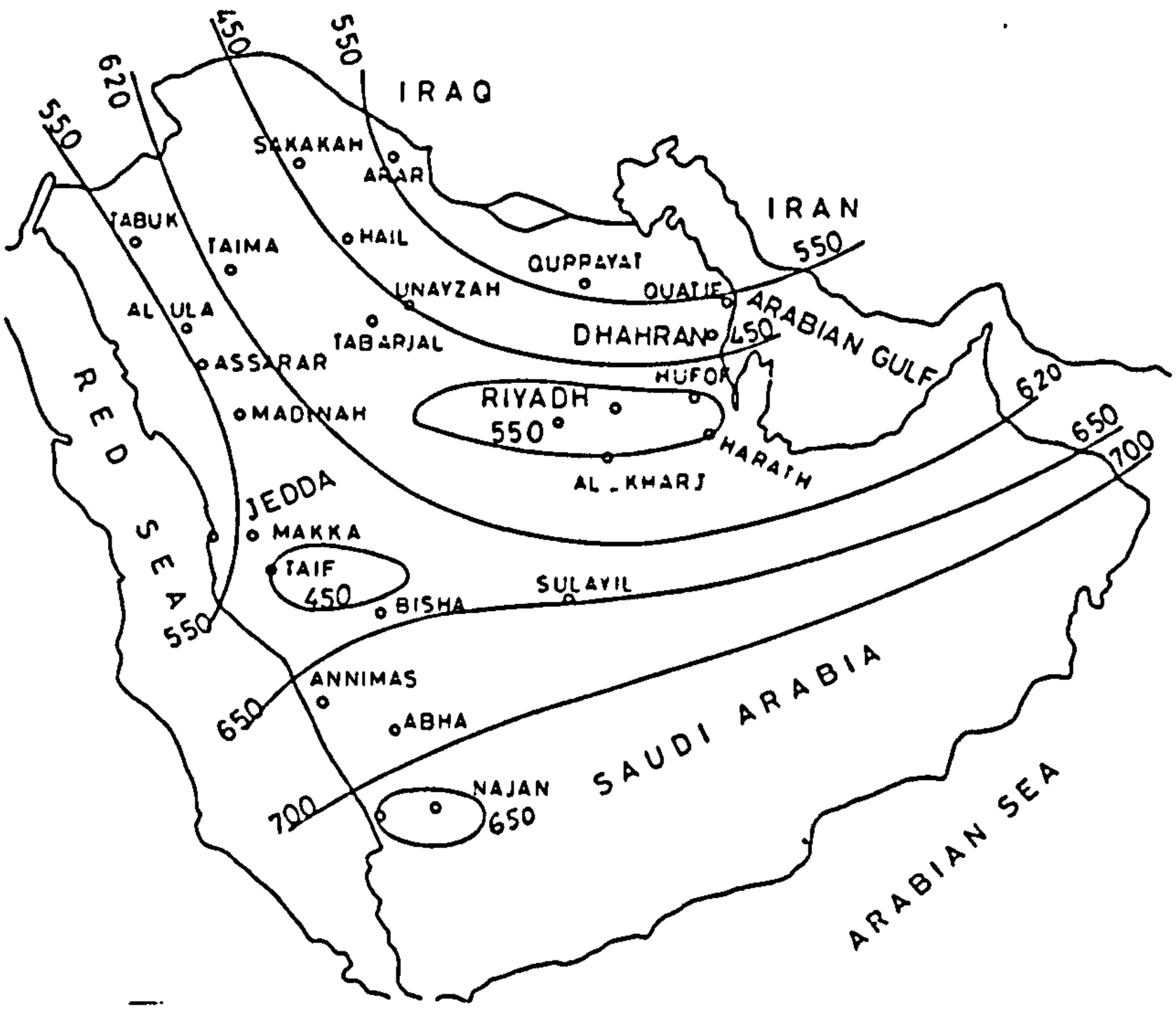

Fig 2.12. Iso-Radiation map for the Arabian Peninsula for the months-4, 5, 6,7, 8, & 9 (Sabbagh, Sayigh & El-Salam, 1973)

Fig 2.13. Iso-Radiation map for the Arabian Peninsula for the months-1, 2, 3,11, 10, & 12 (Sabbagh, Sayigh & El-Salam,1973).

2.5 Methods of Predictions

Knowledge of global solar radiation at any country is vital for designing solar energy conversion systems. The essential need for measurement of solar radiation and its analysis for domestic and industrial applications led to an increased need for detailed information on distribution of solar energy, particularly the global solar radiation. The correlation between the ratio of global irradiation to the extraterrestrial solar radiation (H/Ho) on a horizontal surface in Qatar at latitude 24° 48" and 26° 17" N is investigated in an attempt to establish the best accurate model that takes into consideration of all these factors. The daily long-term data (from the Ministry of Communication & Transport, Annual Meteorological Report) as well as average data for the past 37 years is employed in this work.

Solar radiation at normal incidence received at the surface of the earth is subject to variations due to changes in the extraterrestrial radiation. The radiation emitted by the sun looses its intensity in space only due to distance traversed. However, as the sun's rays enter the earth's atmosphere they continue to suffer additional depletions due to absorption and scattering. Hence detailed studies of solar radiation under local climatic conditions have been carried out at various places (Al-Sulaiman and Ismail, 1997). Many attempts have been made to predict the amount of solar radiation at a given location from few known parameters (Yousef, 1987).

One of the models, which is used for prediction of global solar radiation, is Angstrom correlation, (Angstrom, 1956). The global solar radiation was calculated from the empirical relation given by the following equation:

$$H/H_o = A + B\,(S/S_o) \tag{2.8}$$

where H is the monthly average of the daily global radiation on a horizontal surface, H_o is the extraterrestrial solar radiation of the mean data for the month, S is the monthly average of daily hours for bright sunshine, S_o is the maximum daily hours of sunshine, A and B are regression constants. The study of the latitudinal variation of the coefficients in the linear regression equation give the estimated values of H from known values of S. The values of A and B were obtained in terms of latitude ϕ. This is shown in Table 2.3 where A and B have the forms given in equations 2.9 and 2.10.

$$A = f\,\phi + g \tag{2.9}$$

$$B = p\,\phi + q \tag{2.10}$$

where ϕ is the latitude, and *f*, g, p, and q are termed as conversion or geometric factors for diffuse, global, direct and beam radiation for Qatar, respectively.

Values of S_o and H_o are computed from the following relations:

$$S_o = \frac{2}{15}\cos^{-1}(-\tan\phi\tan\delta) \tag{2.11}$$

$$H_o = \frac{24}{\pi} Io\,(1 + 0.033 \cos \frac{360\ Ds}{365})\,(\cos \Phi \cos \delta \sin \omega + \frac{24\pi}{360} \omega \sin \Phi \sin \delta) \quad (2.12)$$

Where the solar constant $Io = 48.8\ MJ/m^2$, Ds is the day number starting from 1st January, δ is the solar declination, ω is the hour angle.

The values of mean monthly hours of sunshine S and the total solar radiation H are given in Table 2.4. The monthly variation of H/H_o, and the fraction of diffuse solar radiation of sunshine hours S/S_o are shown in Fig 2.14. Also this graph illustrate that these climatic prediction formulas are consistent with the real collected data.

Month	***f***	**g**	**p**	**q**
January	-0.00301	0.34507	0.00495	0.44572
February	-0.00255	0.33459	0.00457	0.35533
March	-0.00303	0.36690	0.00466	0.36377
April	-0.00334	0.38557	0.00456	0.35802
May	-0.00245	0.35057	0.00485	0.33550
June	-0.00327	0.39890	0.00578	0.27292
July	-0.00369	0.41234	0.00568	0.27004
August	-0.00269	0.36243	0.00412	0.33162
September	-0.00338	0.39467	0.00564	0.27125
October	-0.00317	0.36213	0.00504	0.31790
November	-0.00350	0.36680	0.00623	0.31467
December	-0.00350	0.36262	0.00559	0.30676
Year	-0.00290	0.36239	0.00491	0.31876
Means	-0.00313	0.37022	0.00606	0.32029

Table 2.3. Values of *f*, g, p, and q in terms of latitude and month of Qatar (Angstrom, 1956).

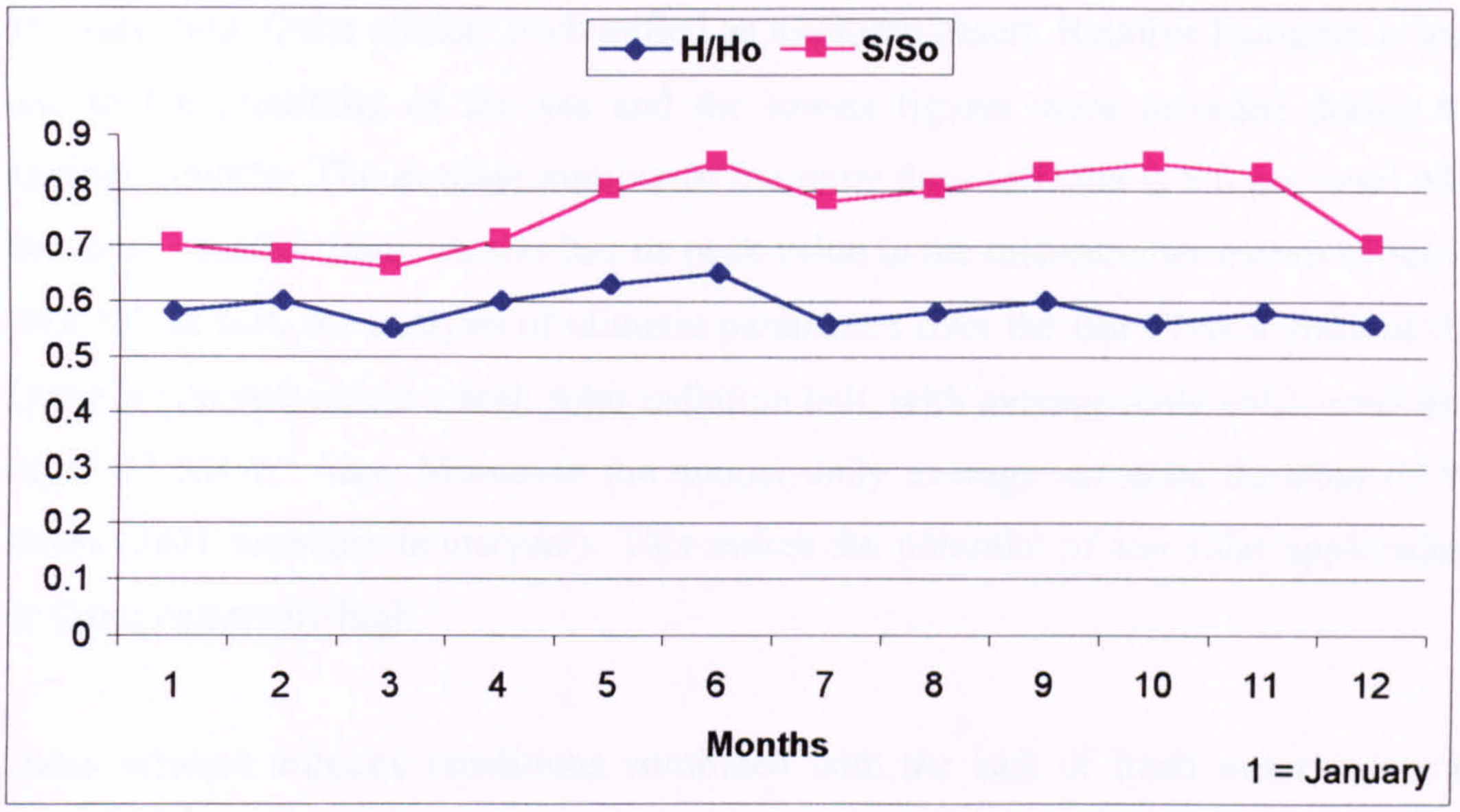

Fig 2.14. The monthly variations of S/So and H/Ho for Qatar.

Month	H (Solar radiation MJ/m^2)	S (Daily average sunshine hours)
January	13.75	7.3
February	16.30	8.0
March	18.00	7.8
April	21.60	9.0
May	23.47	10.5
June	24.37	11.4
July	22.81	10.4
August	22.56	10.5
September	20.74	10.1
October	17.58	9.7
November	14.92	9.0
December	12.85	7.5
Means	18.78	9.3

Table 2.4. Values of mean monthly hours of sunshine (S) and the total solar radiation (H) for Qatar (1976-1998) (Yousef, 1987).

2.6 Conclusion

In conclusion, Qatar climate is classified as maritime desert. Relative humidity is high due to the proximity of the sea and the lowest figures were recorded during the summer months. The average number of the rainy days in Doha is 9.6 per year. Also the mean monthly temperatures has its peak value in the mid-summer month of July is 34.8 °C. In fact, the analysis of climatic parameters over the last 37-year showed that Qatar is situated within a high solar radiation belt, with average daily solar irradiation of 18.77 $MJ.m^{-2}$ /day. Moreover the annual daily average sunshine duration of 9.5 hours (3431 sunshine hours/year). This makes the potential of any solar applications in Qatar extremely high.

Qatar extreme climatic conditions combined with the lack of fresh water resources made solar desalination in Qatar a high necessity. The result of the study of the model year for hourly total solar radiation on horizontal surface, H, can be used to estimate solar radiation for Qatar and for evaluating the daily global solar radiation.

A comparison was made between recorded and calculated data. It was found that monthly global solar irradiance could be estimated with approximately 5 % relative error with the model year formulae.

CHAPTER THREE

WATER DESALINATION PROCESSES

3.1 Introduction

The rational behind all water desalination technologies relies on the provision of water with salinity level below 500 PPM, the upper limit of dissolved salt in fresh water. The water desalination process is one such methods of converting seawater into potable water. Multi Stage Flash [MSF], Multi Effect desalination [MED], and Reverse Osmosis [RO] are three desalination processes, which have an advanced commercial operation. The selection of any type for particular application is based on the size of the unit to be built and the experience gained by the client. In Qatar, all these desalination processes have been employed and over 98% of the total water produced in Qatar relies on the MSF technique. This chapter investigates and evaluates the characteristics of the most common desalination processes, particularly, their inherent problems and specific performance. The solar desalination methods [SD] were also reviewed with emphasis being placed on desalination plants built in Qatar.

3.2 Desalination Plants and Wells Production In Qatar

3.2.1 Ground Water

Ground water constitutes one of the most important water resources worldwide and it is evident that there are three main reasons. Initially, it must be remembered that, 95% of the earth's water is contained in the oceans. It is salty and in the main considered useless for plants, animals, or human consumption. Fresh water, which people can utilise for drinking or for agriculture, is located either on the earth's surface in the form of lakes and rivers, or in underground resources such as wells. Surface water constitutes 0.05%, while underground water is 4% of the earth's water. Consequently, groundwater provides 95% of the available fresh water on the earth. Secondly, groundwater is vital not only because of the quantity of the supply, but also because of its dependability. It is always available, since it does not depend on seasonal rain or snow. The final consideration relies on the assumption that, until recently, groundwater was clean. It was not necessary to purify it prior to its use as drinking water, (Sosna, 1984).

In Qatar, people have been using groundwater for many years as the only exclusive source of fresh water. However, in the last five decades, like the other Gulf States, Qatar has undergone many social, economic, and industrial changes. The catalyst for

these changes was the discovery of numerous, substantial oil reserves. The population of the state of Qatar has increased from 80 thousand in 1940s to 550 thousand in 1998, Fig 3.1. In 1989, the birth rate in 1989 was 3.18% and death was 0.25%, which means natural increase was 2.93%. Unfortunately, with this expansion in population comes an escalation in the demand for water. Consequently, most of the available underground water resources have gradually diminished or, have become undrinkable. Currently, ground water production has curtailed to less than 2% of total fresh water used in Qatar. The balance is produced from desalination plants (Ministry of Water & Electricity, 1998).

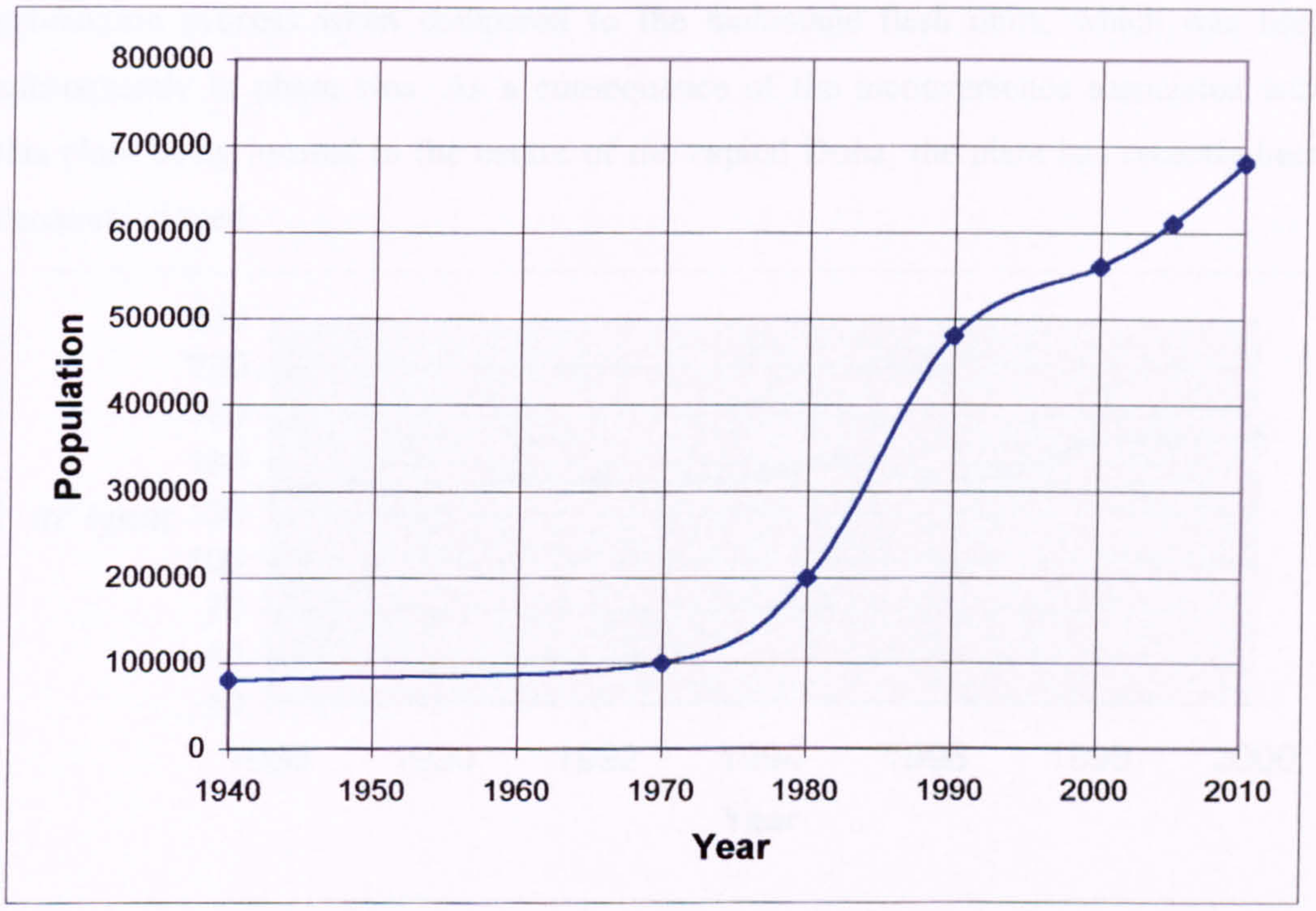

Fig 3.1. Qatar population since 1940-2000, and future forecast based on 2.93% of natural increase of population (Qatar Electricity & Water Co, 2000).

3.2.2 Power & Water Desalination Plants

Limited fresh water resources and high water consumption has forced many countries to identify alternative methods of obtaining their fresh water requirements from desalination plants. Seawater desalination plants have been constructed in many countries of the world, particularly in the arid Middle East, primarily because there were no alternative sources of fresh water available.

Desalination plants were launched in Qatar in 1953 with the plant having a capacity of 248,200 cubic meters per year. Plant size and location have altered considerably during the last few years and there are now three principle desalination plants; Ras Abu Abboud, Ras Abu Fontas [A] and Ras Abu Fontas [B] with a total nominal capacity of 144 millions m^3/year which is over 98% of the total fresh water produced in Qatar. As can be seen from Fig 3.2, water desalination plants first emerged in Qatar in 1953; the first desalination plant for Central Doha was installed, with a total capacity of 248,200 m^3/year. This plant uses two different processes of water desalination. The initial phase incorporated the Submerged Coil concept, which has superseded the multi-effect process which is considered somewhat old with a limited production process when compared to the multistage flash units, which was used subsequently in phase two. As a consequence of the inconvenience associated with this plant being located in the centre of the capital Doha, the plant has recently been decommissioned.

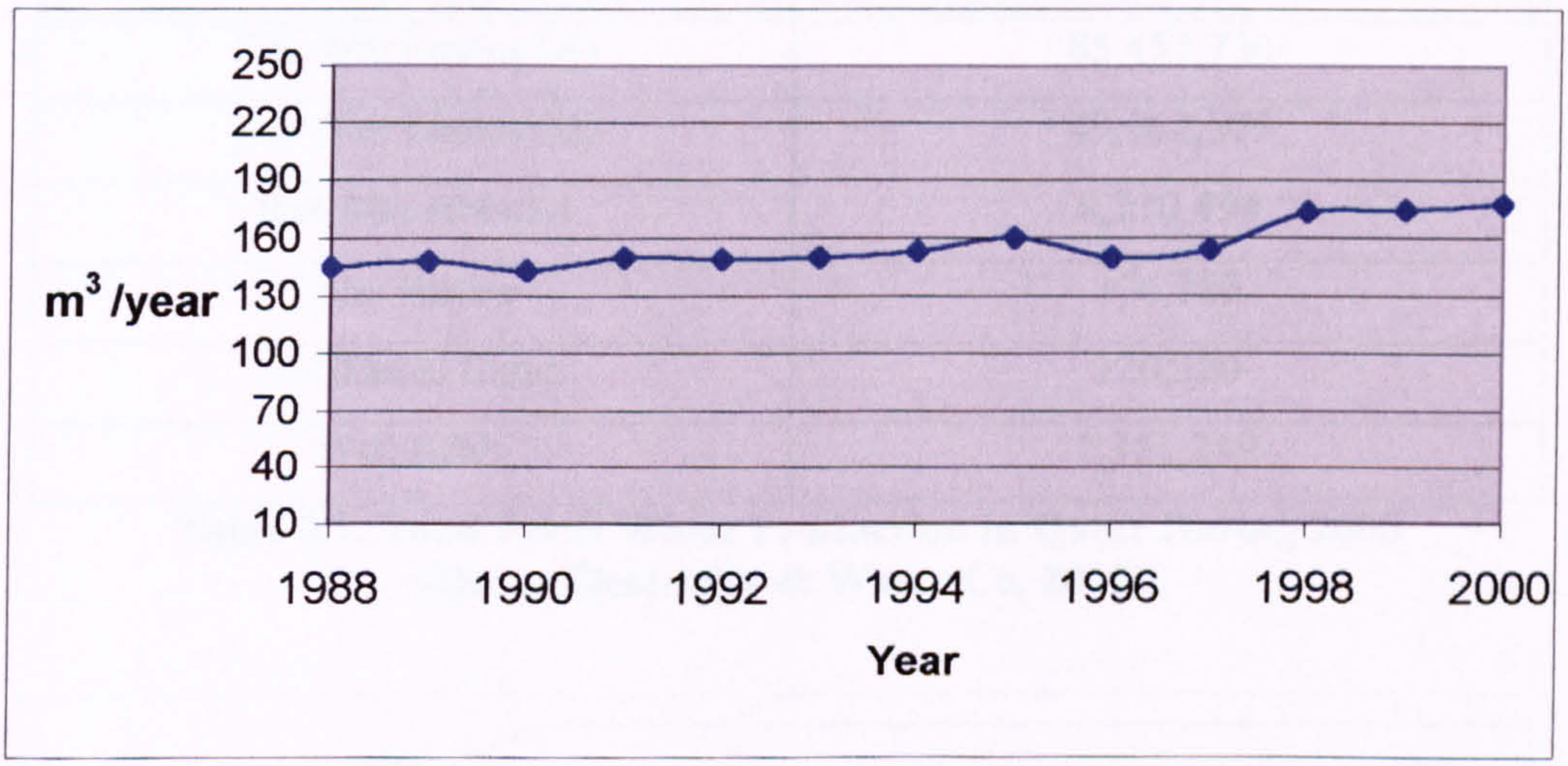

Fig 3.2. Water consumption per capita in Qatar.
(Qatar Electricity & Water Co, 2000)

Ras Abu-Abboud is the second Power and desalination plant, which was commissioned at the time in 1963, at a more appropriate distance from the city of Doha. However, due to the capital expansion it is presently considered to be located in part of Doha city. The community of Doha is very critical and worried of effect of the gas emissions and rejected water on the environment and human health. This plant was designed to produced 10 million m^3/year and 210 MW. However, in these days

the total production of this plant is about 8.2 million m^3/year, also see Table 3.1. The multistage flash system adopted in this plant was used for all the forth phase. In 1977, the third desalination plant Ras Abu Fontas (A) was installed. This has a total capacity of water production of 86.9 million m^3/year and 620 MW electricity power. This plant consisted of five phases using a multistage flash system. Due to the constant high volume fresh water consumption, Ras Abu Fontas (B) was brought into service in 1998, which forms the latest desalination plant with a total design capacity of 49 million m^3/year and a power output of 610 MW. The growth of national demand for electicity power in Qatar is likely to be around 10% per annum over the next ten years and the corresponding figure for water is 6%. Here, the total power consumption in Qatar is shown in Fig 3.3. This plant also employs a multistage flash system, and consists of a dual commissioning phase (Qatar Electricity & Water Co, 2000).

Station	Total Water Production (m^3)
Ras Abu Fontas (A)	85,457,750
Ras Abu Fontas (B)	49,062,509
Ras Abu Abboud	8,210,494
Abu Samra	106,765
Al-Shamal Camp	120,320
Well fields	2,351,249

Table 3.1. Total Fresh Water Production in Qatar During 2000 (Qatar Electricity & Water Co, 2000).

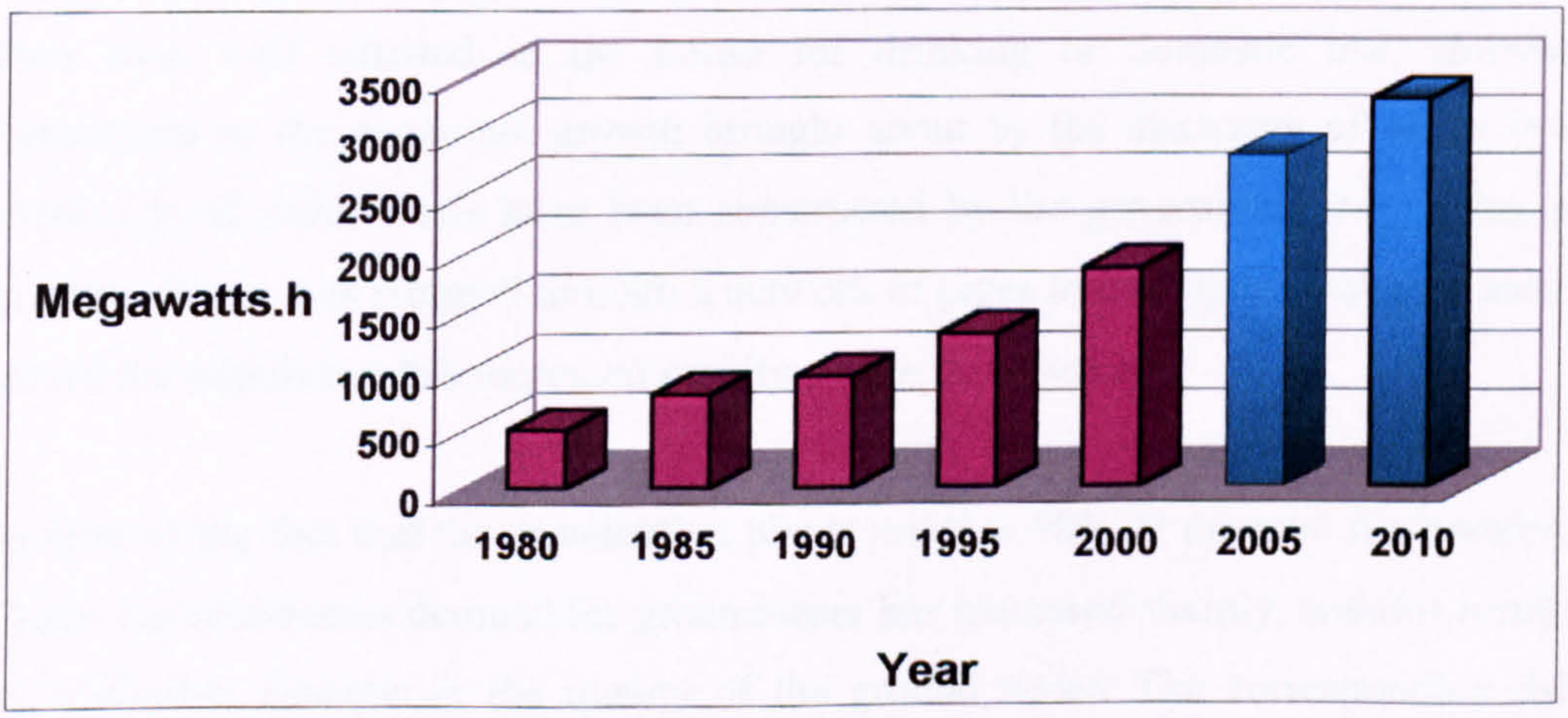

Fig 3.3. Qatar total electricity production and future requirements based on 10% increase in national demand for electricity (Qatar Electricity & Water Co, 2000).

In addition, two plants employing the reverse osmosis process were commissioned to those remote geographical locations such as Abu-Samra and Al-Shamal. The output of these plants are 106,765 m^3/year and 120,320 m^3/year, respectively. Furthermore, three sub-stations power plants were constructed in 1983 and have been subject to gradual up grading and expansion. They include the Al-Wajba, the Al-Sailya, and the South Doha Station. Total capacity of theses sup-stations averages at 501 MW. (Qatar Electricity & Water Co, 2000).

3.3 Other Water Desalination Plants

More limited number of small-sized desalination plants exist almost exclusively for the industrial sector. A good example is provided by the Dukhan Power and Desalination Station, which utilizes the multiple effect desalination and generates water at the rate of 9000 m^3/day. Qatar Petroleum operates this plant for Dukhan industrial city, which contains the primary oil fields in Qatar. Another example is giving by the Am-Bab Desalination Plant, which also utilizes a multiple effect desalination system. The principle purpose of this plant is to produce low salinity water for use by the adjacent Cement factory. This plant uses the wells brackish water instead of seawater due to its location being too far away from the coast.

3.4 Water Demand

For many years up until 1953, Qatar was totally dependent on the ground water form wells. Historically, the population was distributed in small communities, usually situated in close proximity to the fresh water wells, with often every family having their own well situated in the house for drinking or domestic use. However, subsequent to the economic growth brought about by the discovery of oil in 1949, thousands of water wells have been constructed by the government throughout the country. Water was pumped through a network of pipes to the capital Doha, an area in which the population has increased rapidly over a short period.

In spite of the fact that the desalination plants produce 98% of the total fresh water in Qatar, the continuous demand for groundwater has increased sharply, and this resulted in noticeable changes in the quality of the ground water. The corresponding daily average groundwater consumption in Qatar was around 40,000 m^3/year in the 1960s

for domestic and agriculture purposes, this has rapidly risen to 2.35 million m^3/year in 2000. Many studies have predicted that the water demand will continue to increase dramatically in the future. Calculations based on the average rate of annual water consumption of 2.7 m^3 per person show that the total water demand will increase up to 150 million m^3/year until the year 2003, therefore a shortfall of a proximately 5-10% is forecast. In response to this, the government have decided to install a forth-main power and water desalination plant in Ras Laffan Industrial Area over the forthcoming years. This is expected to reduce the continuing fresh water deficit. This project is scheduled to be completed and fully operational by the summer 2003, phase one has a projected power producing capacity of 750 MWs and 182,000 m^3 of water daily. The second phase will probably be operational at the end of 2007, which is expected to double water and power the total production, see Fig 3.4. (Qatar Electricity & Water Co, 2000).

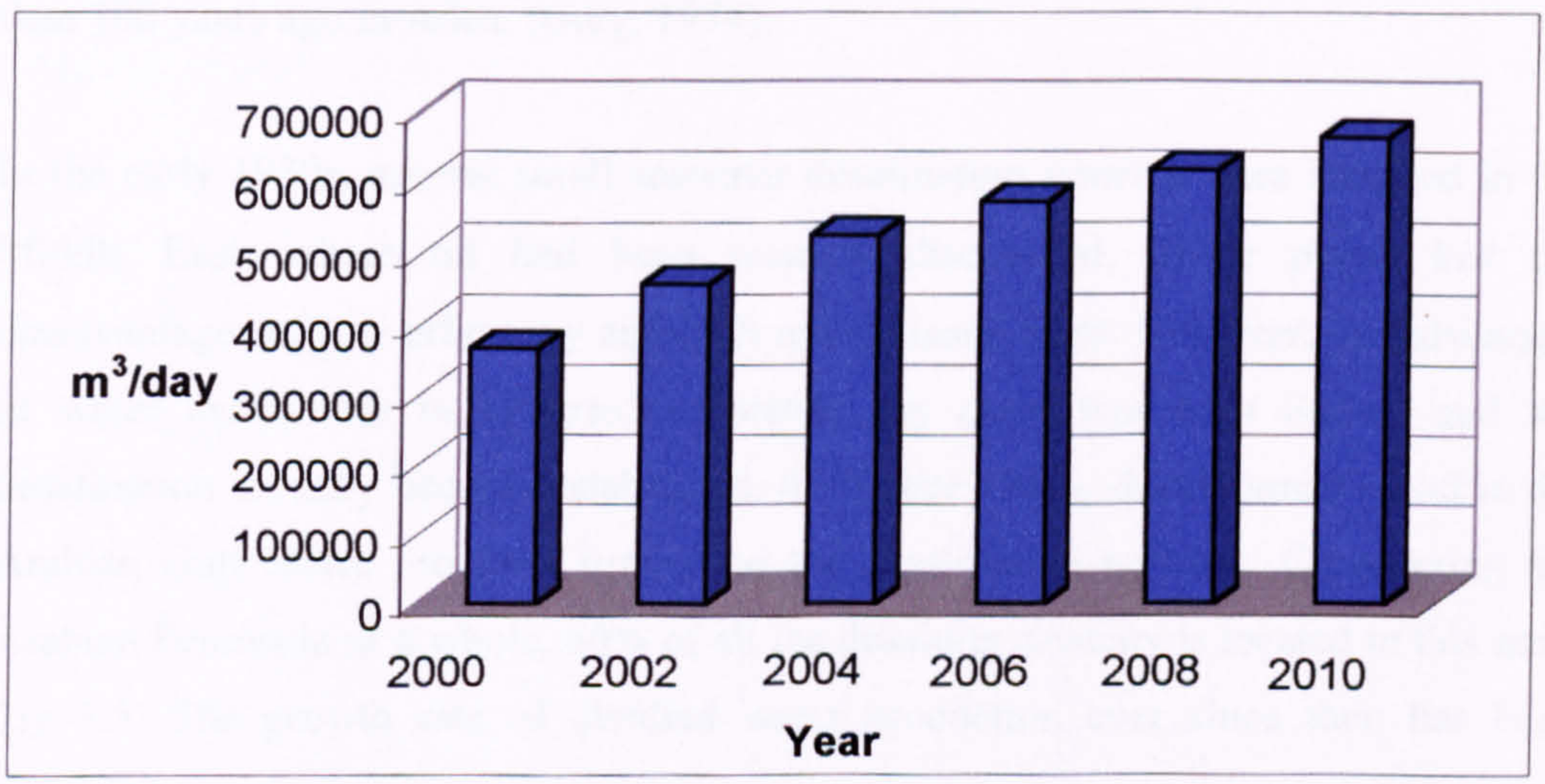

Fig 3.4. Anticipated Qatar's future water demand based on 5-8% increase in national water requirements (Qatar Electricity & Water Co, 2000).

3.5 Water Distributions

The number of consumers benefiting from a piped water supply has increased with the development of the water network. In 1971 there were 9,500 and by the end of 1994 this number had inflated to 75,000, most of whom live in the capital Doha. This pipe network distribution was developed continuously and has expanded from a total of 390 kilometres in 1971 to 2,540 kilometres at the end of 1994. The water distribution system is controlled from the telemetry control centre in Doha. Part of it

is controlled locally by the operations personnel at reservoirs. Production, pumping, storage, and flow rates are controlled from the centre through radio links and lines. The growth of the distribution system has resulted in a reduction in the need for water to be delivered by tanker, particularly to the rural areas.

3.6 History of Desalination

The principle of obtaining fresh water from seawater has been known to mankind for thousands of years. Desalination is one of the oldest known methods of separating fresh water from a salt solution. The first current desalination systems were draughted into service over 200 years ago to provide fresh water from the sea by desalination on board ships. Many of the various commercial distillation processes have been developed only during the last 100 years. All these technologies were based on the thermal desalination process. The most popular was the submerged tube design. Land based plants have also gradually gained popularity. The first one was installed more than 100 years ago in Aden. (Garg, 1974).

In the early 1930s, several small seawater desalination systems were installed in the Middle East, where oil had been recently discovered. These plants had the disadvantages of low efficiency and high maintenance costs. However, the advantage of water availability in hitherto completely dry areas was high lighted and the desalination industry become established. In the late 1940s, development of oil in the Arabian Gulf States provided support to the desalination industry. Considering the Arabian Peninsula as a whole, 60% of all the desalting capacity is located in this area, Fig 3.5. The growth rate of distilled water production ever since then has been spectacular.

Until the 1950's, the largest desalination unit ever built had an output of less than 2,283 m^3 per day. The overall worldwide capacity was 10,045 m^3 per day. In 1960, the production from all the land-based desalination plants in the world had risen meteorically to one million m^3 per day. In 1977, this value had escalated to of 3.8 million m^3 per day. By the 1980's, worldwide desalination capacity was a phenomenal 7.3 million m^3 per day. A study made by Flour, 1985 for the office of water Research and Technology, which determined that the anticipated minimum United State desalted water demand in the year 2000 to be approximately 132.5

million m^3 per day and the overseas demand in the region of 25 million m^3 per day, Fig 3.6. This represents an average growth rate of 18% (Khan, 1986; Porteus, 1988).

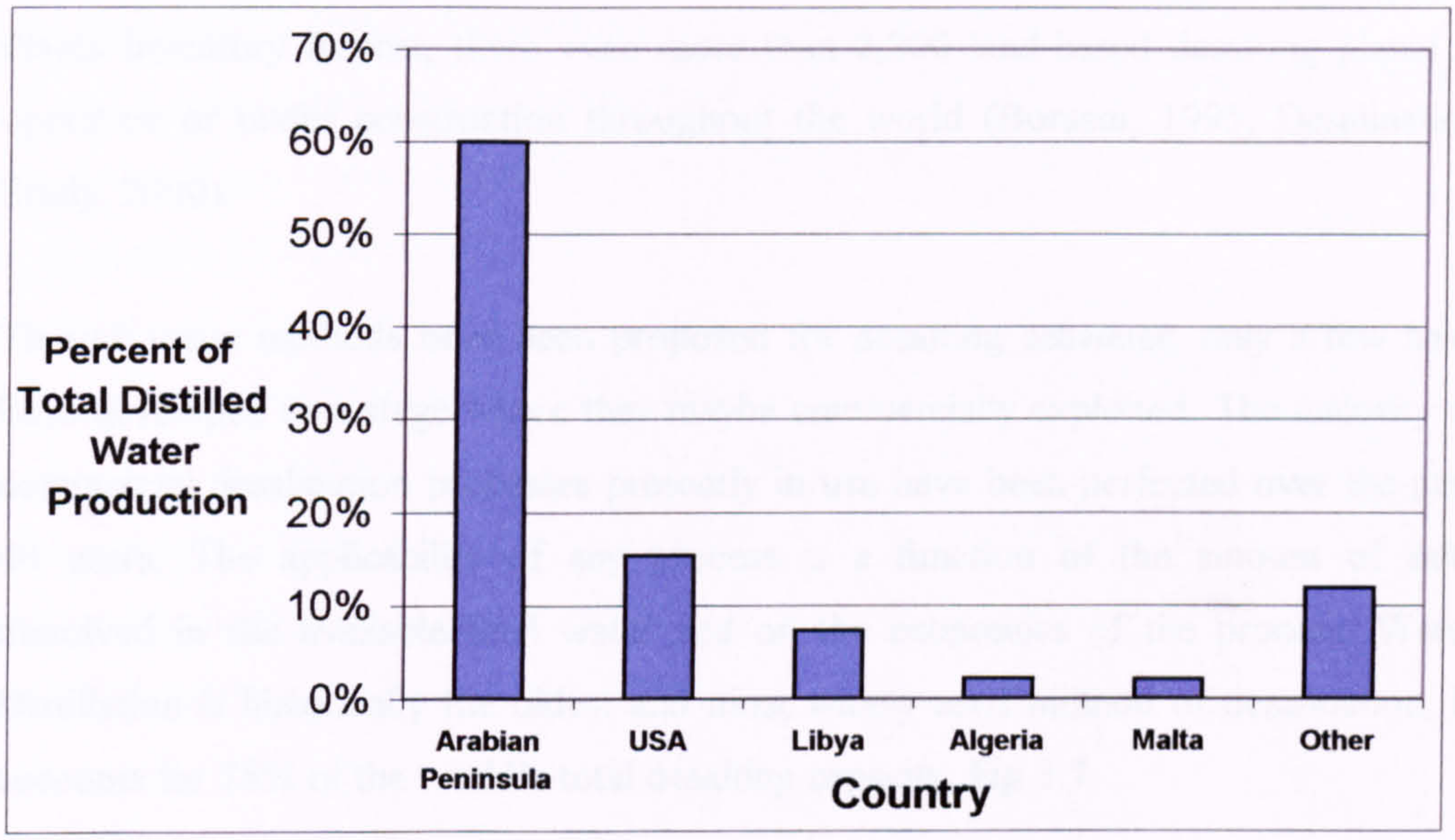

Fig 3.5. Percent share of the total distilled water production in the worldwide (Khan,1986).

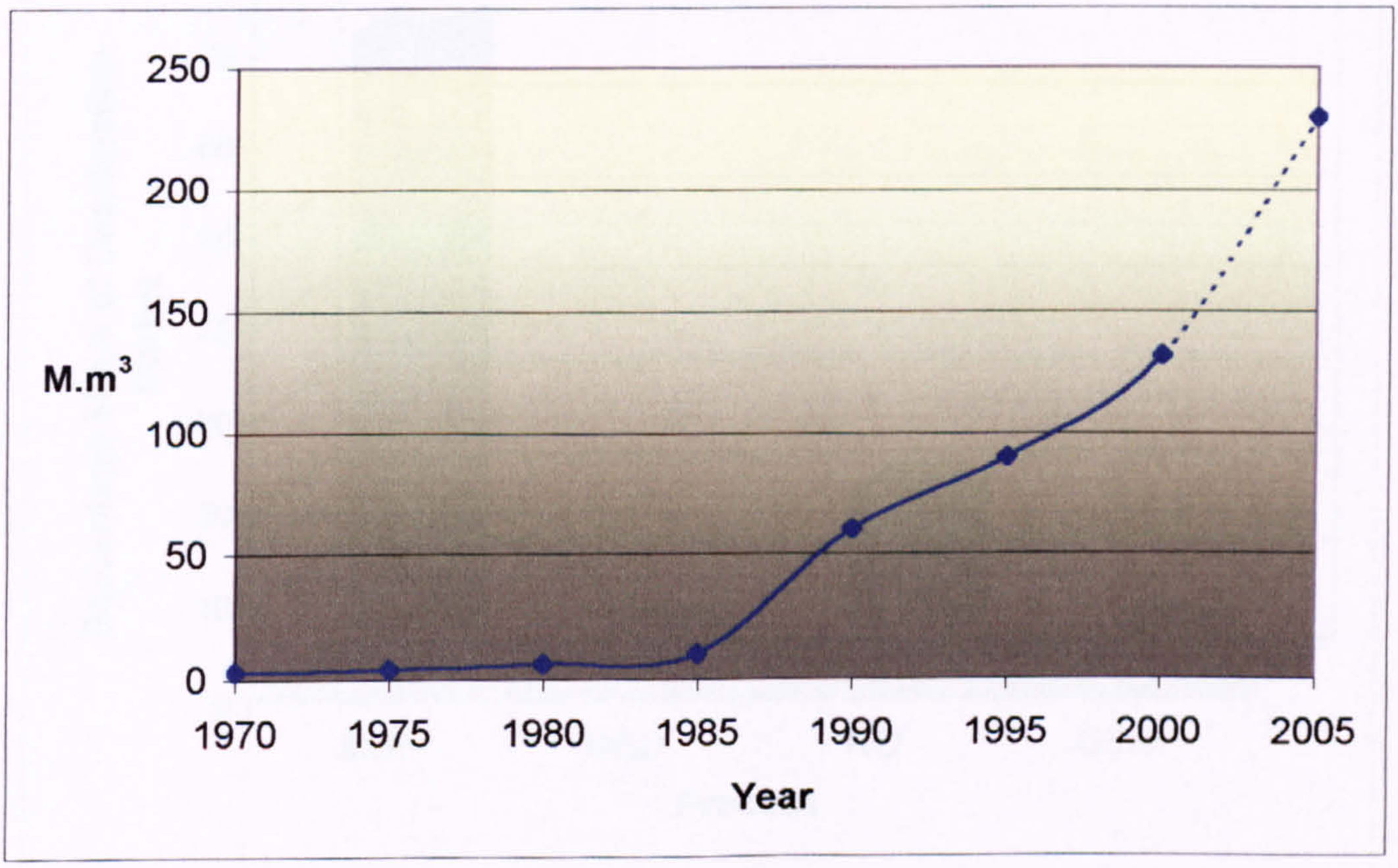

Fig 3.6. Increase of global water desalination requirements (Porteus, 1988).

Unit sizes have also been increasing. In the early sixties, a 4,566 m^3 /day unit size was regarded as being quite large. More recently, most of the unit sizes are in

22,830 m^3/day. The size of the largest multistage flash unit is 36,528 m^3 / day. The huge Al Juabil 2 complex in Saudi Arabia constitutes the largest multistage flash plant ever built. It has capacity of 0.95 million m^3/day. According to the 7th Desalting Plants Inventory Report, there were more than 2,200 land-based desalting plants in operation or under construction throughout the world (Borsani, 1995; Desalination Study, 2000).

Though many methods have been proposed for desalting seawater, only a few have been developed to a stage where they maybe commercially exploited. The majority of commercial desalination processes presently in use have been perfected over the past 40 years. The applicability of any process is a function of the amount of salts dissolved in the available feed water and on the economics of the process. Water Distillation is historically the oldest and most widely used method of desalination. It accounts for 75% of the world's total desalting capacity, Fig 3.7.

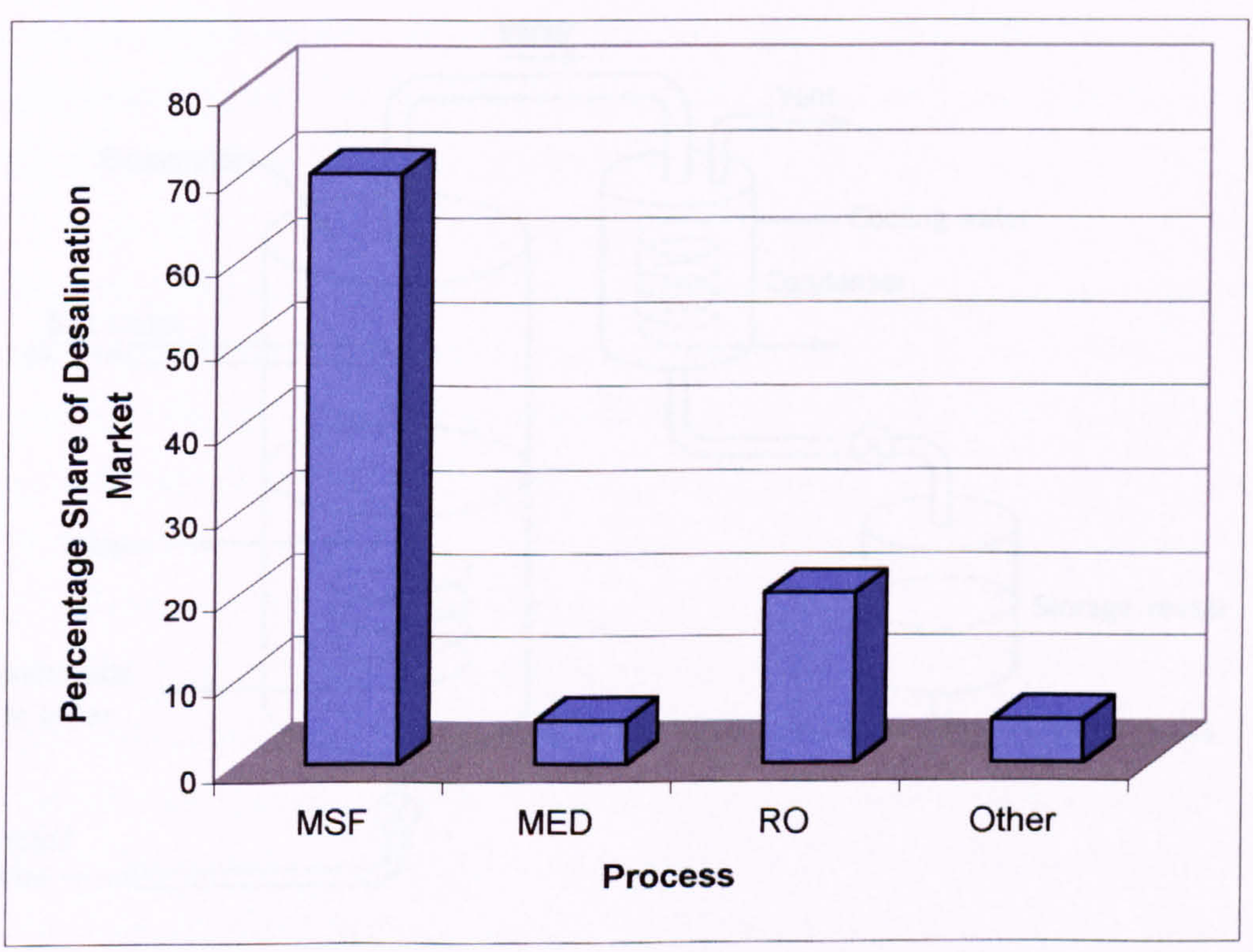

Fig 3.7. Percentage share of all Water Desalination Processes (Khan, 1986).

3.7 Principles of Desalination Processes

The phase change of water, transforming into vapour from liquid, is the basis of the most forms of distillation. The principle, which is illustrated in Fig 3.8, is quite simple. Seawater is boiled in the evaporator by passing hot steam through the steam chest, and it is here that the steam condenses on the inside of the chest and is returned to the boiler. The vapours rising from the seawater are cooled in the condenser and thus converted into pure water, which is collected in a storage tank. The system is vented through an ejector and thus the amount and pressure of the air within it can be regulated. The brine concentrate is continuously or intermittently withdrawn from the evaporator. In distillation, the salinity of the raw feed water is not an important factor in the overall efficiency of the process. However, increased feed water salinity increases the boiling point of the solution and the allowable concentration ratio. This ratio is reduced to avoid any expected scaling.

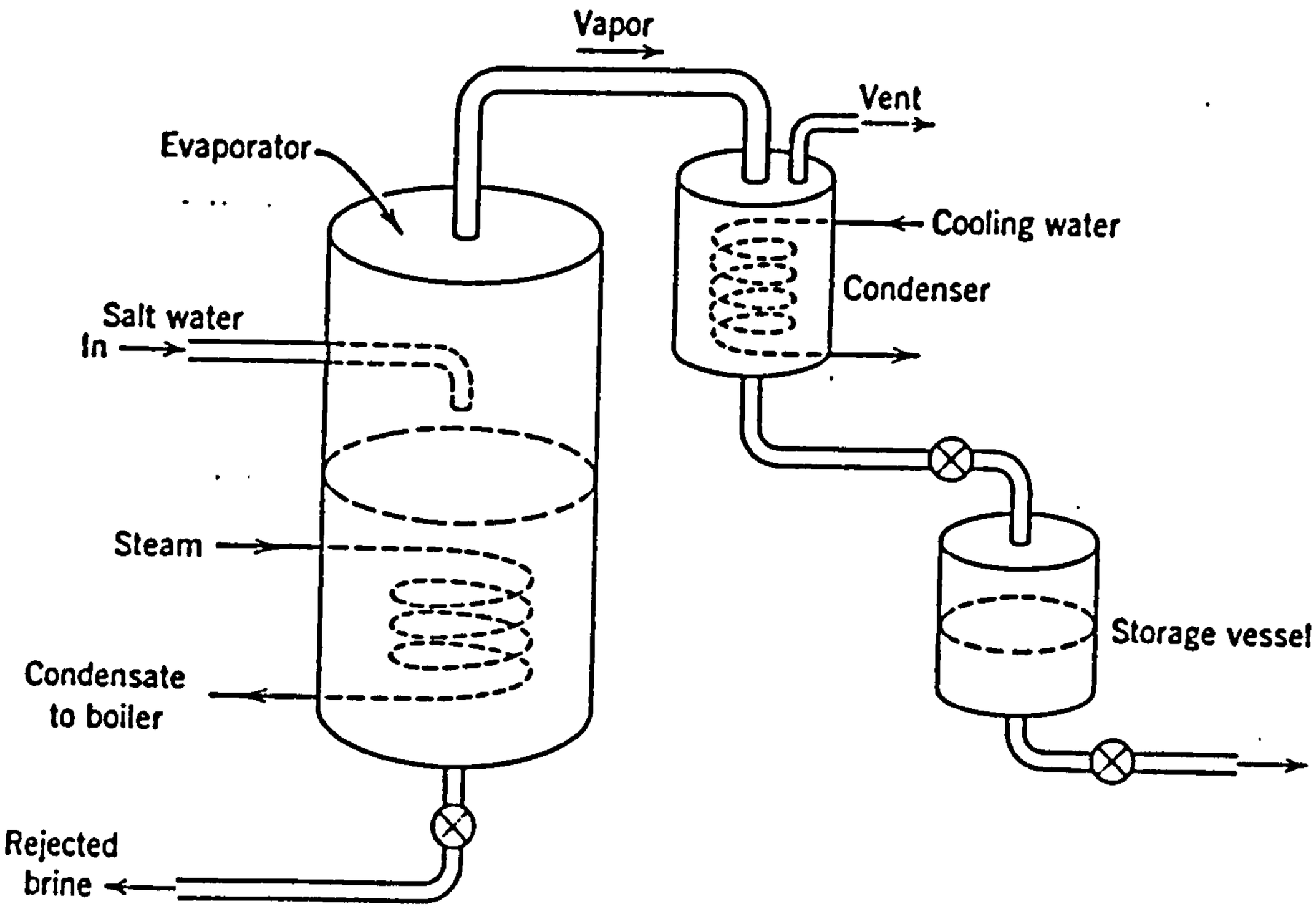

Fig 3.8. Principle of desalination process (Spiegler,1981).

3.8 Water Desalination Methods

Desalination of seawater involves dividing a body of salty water into two different components, one of which is salt-free and the other of which may contain a range of salt concentration. Although in theory this process requires very little power, in practice it requires considerably more with regard to real efficiency of the thermodynamic cycle and rotary machines. Among many methods that have been proposed for desalting seawater, only a few have actually progressed away from the drawing board. On the market, there are two main techniques for desalination seawater: Membrane Filtration (Reverse Osmosis) and heat processes (MED, MSF). Seawater accounts for 70% of desalinated water world wide, i.e., a total of 14 million m^3/day and the remaining 30% being supplied from of brackish water. Of this, 15% is treated by membrane filtration processes and 85% by MED and MSF. *One of the main advantages of the desalination process is that it required heat only up to 120 °C, which can be supplied from solar energy or any other cheap fuels.* (Grag, 1987). Moreover, water obtained by desalination is very pure; it is used in industrial processes or for human consumption after remineralization and the addition of low concentration of chlorine in order to preserve its quality as it is conveyed through the distribution network right up to the consumer tap.

In the following sections the four types of seawater desalination processes; multistage flash, multi-effect distillation, reverse osmosis, and solar desalination were investigated in detail, with the emphasis being placed on solar desalination system as a novel technique to be adopted in Qatar.

3.9 Multiple- Effect Distillation

The Multiple-Effect Distillation process has a fairly long history. Thousands of MED plants were constructed in the past hundred year by the chemical industry. They were primarily used for the recovery of brine. Horizontal and Vertical tube evaporators were widely adopted for the production of sugar. The MED process was the first used to produce significant amounts of fresh water from the sea. Although they have been replaced by the MSF system as the most important and dominant process, they still accounted for a substantial amount of desalination water. The MED processes comprise of about 5% of the global desalting capacity.

The most important MED type is the (VTE) process. The main feature of this process is that saline water falls through vertical tubes. These tubes are heated by steam on the outside. Steam is condensed while part of the saline water is vaporized and transported to the next stage. This is repeated in several stages, which are performed at progressively lower pressures. This ensures that boiling occurs in successive stages at lower temperatures. All external steam provided to the first stage is utilized. The greater the number of stages or effects, the less is the energy is required for a given input. Another variation of the ME process is the horizontal tube process (HTE), which is similar to the (VTE) process, but the tubes are orientated in a horizontal rather than vertical configuration. At present, the largest MED unit is 22,830 m^3/day, which is equal to the MSF unit size employed in Ras Abu Fontas [A] and Ras Abu Fontas [B].

3.9.1 The Principle of MED

In this process, vapours are produced by two means. The first is by pressure reduction (flashing) and the second is by heat input (boiling). In the single stage distillation, approximately 1 kg of distillate is produced for each kg of input steam. The performance ratio in this case is one. Despite preheating of the feed water, a large part of the enthalpy of vapours produced in the single stage evaporator are lost in the condenser. MED distillation was conceived in order to recycle the lost heat energy and increase the yield of distilled water for the same heat input. In the MED process, the evaporators are arranged in a series. Assuming that three evaporators are capable of producing a heat input of approximately 1 MJ, the amount of water vaporized in this initial stage is half kg. The generated vapours would be utilized in the subsequent stages where they function as the heating medium, whereby they vaporize half kg of brine in each stage. The vapours produced in the second stage are condensed in the third after producing an additional half kg of vapour. Therefore as a consequence of the three stages, approximately 1.5 kg of water are produced for an input of 1 MJ. (Khan, 1986).

3.9.2 Multiple-effect General Operation Process

In the MED process, two or more evaporator stages are employed. Each stage operates at a successively lower temperature and pressure. The first, which functions at the highest temperature, is heated by low-pressure steam. The heat sources are

often prime steam, gas turbine exhaust steam, or extraction steam. Vapours are generated from feed water in the initial stage tubes. These vapours are transported to the second lower temperature and lower pressure effect. Thus, vapours from one stage are used as the heat source for the next to facilitate the evaporation of the brine, as shown in Fig 3.9.

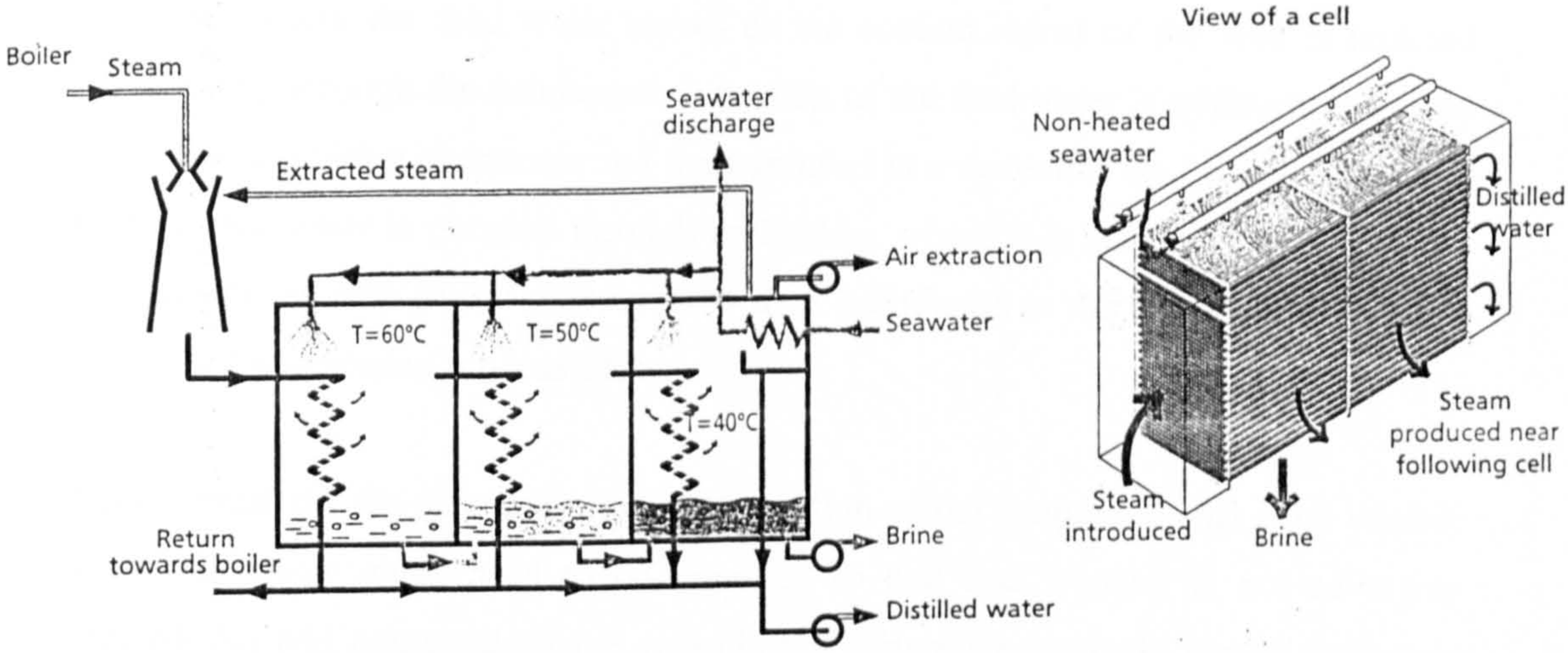

Fig 3.9. The principle of Multieffect Desalination Process (Memotechnique, 1999).

Vapours produced in the first stage are channelled through demisters prior to being passed to the tube bundle of the second stage, some of the vapours produced in each stage delivered to the associated preheated (boiler), where they heat incoming feed water and are condensed. The remaining vapours pass to the next stage. If preheaters were not used, a substantial fraction of steam would be required in order to raise the temperature of incoming feed to its saturation temperature. In each stage, steam is condensed on one side of the tubes. On the other side, brine receives the heat of condensation and is evaporated. Unevaporated brine is pumped to the next stage on the process for further vaporization. The repetition of this process several times, ameliorate the effectiveness of the original low pressure steam in the first stage, gives the process its concept. This is only feasible so long as the temperature differential between the condensing vapours and brine solution remains high enough to act as the driving force for the evaporation process. (Helal, 1986).

It is only by reducing the pressure in each stage, relative to the one preceding it, that the heats of vaporization and condensation can be used repeatedly. As can be seen from Table 3.2, lowering the pressure of the stage allows the brine to boil at progressively lower temperatures, as it moves from stage to stage. Brine from the last stage is rejected as blowdown. Vapours from the last stage are condensed in a final condenser where the feed water serves as the coolant. Most of the feed is rejected after passing through the condenser. A portion of the feed water is withdrawn, treated with scale inhibiting chemicals and then sprayed in a deaerator next to the last stage. Treated feed water is pumped through preheaters, where it is heated by vapours from each associated step in the process. It is then introduced at the top of the first stage where the vaporization process starts.

It is essential for the safe and effective operation of the evaporator that it be vented. Non-condensable gases need to be removed so that heat transfer is not adversely affected. Air and non-condensable gases in the system are typically vented from step to step. They are collected and removed from the system by an air ejector system. Theoretically, the plant performance ratio is equal to the number of steps in the process because an additional one kg of distillate can be produced in each consecutive step. In practice, however, this is not likely the case.

The latent heat increases as the pressure decrease, which means that the amount of vapours formed in each successive step will be less than that formed in the previous one. Insulation is not perfect and heat is lost to the atmosphere. Some of the heat supplied by condensing steam is absorbed due to heating cold feed water from the low supply temperature to its boiling temperature. Losses can be traced to design features and to the differences in temperature used as the driving force. A practical figure for the system is about 0.8-0.85 kg of water per stage for each kg of steam supplied from outside (Darwish, 1987). To increase the performance ratio, the number of stages has to be increased. By doing this, the intereffect temperature difference is reduced. Eventually, a limiting temperature difference is reached, depending on the boiling point elevation and certain heat transfer considerations (Khan,1986).

Pressure (bar)	**Boiling Temperature** (°C)
3	140
2	120
1	100
0.5	80
0.25	65
0.10	45

Table 3.2. Temperature at which Water Boils When the Pressure Varies (Memotechnique, 1999).

3.9.3 Heat Transfer in Multiple-effect Distillation

In earlier plants, it was not possible to use more than 6 or 7 effects. This was due to the fall off in the heat transfer rate, which occurred with reduced boiling temperatures and reduced temperature differentials throughout the effects. Generally, performance ratios higher than 6 were not obtainable. Khan, 1986 has proposed a useful define of the gain output ratio (GOR). The GOR is used to specify that steam economy is equal to:

$$\mathbf{GOR} = \frac{\textbf{The amount of distillate produced - kg}}{\textbf{The amount of heating steam supplied to the first effect - kg}} \qquad (3.1)$$

The performance ratio is slightly less than the number of effect. The steam economy is also expressed in terms of the performance ratio, which is the number of kilograms of distillate produced per 1 MJ of heat input. The performance ratio of a multi-effect plant can be calculated from the following equation:

$$\frac{1}{R} = \frac{1}{n} + \frac{Cp.\Delta T}{\ell . Rc} \qquad \text{Khan, 1986} \quad (3.2)$$

where, R = performance ratio, n = number of effects, Cp = specific heat of brine, ΔT = temperature difference between brine leaving the top preheater and brine in the

top effect, ℓ = latent heat of the evaporating brine, and Rc = recovery ratio of the plant.

Basically, the performance ratio is slightly greater than the GOR. This is attributed to the fact that the heating steam is supplied at near atmospheric pressure. In such a condition, the latent heat is less than 1 MJ. To maximize the performance ratio of the earlier MED submerged tub plants, a large number of stages with low temperature differentials were used. Typical temperature differentials were approximately 3 °C for polyphosphate plants and 7 °C for acid dosed plants. The low temperature differentials caused poor heat transfer. Loss of temperature differential in large plants was also considerable due to the hydrostatic head (Spielger, 1981; Khan, 1986).

In 1967, Chambers investigated a simple solution, to overcome this problem. Brine was sprayed onto the outside of the vertical tubes through nozzles or distributors. It then fell as a fine film from which the name vertical tube evaporator' falling film' is derived. The other method by which brine is distributed is the 'climbing film' process. In this method, brine is introduced at the bottom of the tubes. It then rises up the tubes in the form of a thin film. In the horizontal tube MED process, the tube configuration is horizontal. Spraying carries the advantage that the fluid to be evaporated is efficiently distributed over the evaporator tube bundle surface. In each stage, there are several spray nozzles. They distribute the feed water over the evaporator tubes in a shower of fine droplets. The high velocity of the droplets ensures even brine distribution in a thin liquid film. This allows for a high heat transfer rate.

The overall heat transfer coefficients are very high in this process compared to the MSF process. In the VTE process, the heat transfer coefficients are about ten times greater than in the MSF. As a consequence, less heat transfer surface is required. Also, fewer and smaller tube sheets, much smaller pumps and drivers, as well as simpler instruments and controls are necessary. However, there are two problems associated with the MED plants. They tend to be more complex and have limited capacity. The MED plants do not employ recycling. They are based on the single-once through principle. As a result, the lowest salinity occurs at the highest temperature, while the highest salinity occurs at the lowest temperature. This reduces

scaling and makes plant operation easier. Also, pumping requirements are reduced to 40-50% of that required for the MSF system (Mawer, 1966; Silver, 1967).

3.9.4 Optimum Number of Stages

In principle, many stages can be obtained in this process. The condensation temperature of the heating steam always has to be slightly higher than the boiling salty feed. However, since the boiling point reduces by lowering the pressure of the stages, the temperature difference between boiling seawater and fresh water, respectively, are also reduced. Figure 3.10 illustrates the difference in boiling temperature of sea and fresh water. In practice, however, it is necessary to maintain a temperature difference considerably larger than 0.7 °C across the heat transfer surfaces for each stage, in order that the heat flows at a reasonable distillate production rate. Thus, an ideal MED process operates between the temperature of 100 °C and 27 °C in the first and last stage, respectively.

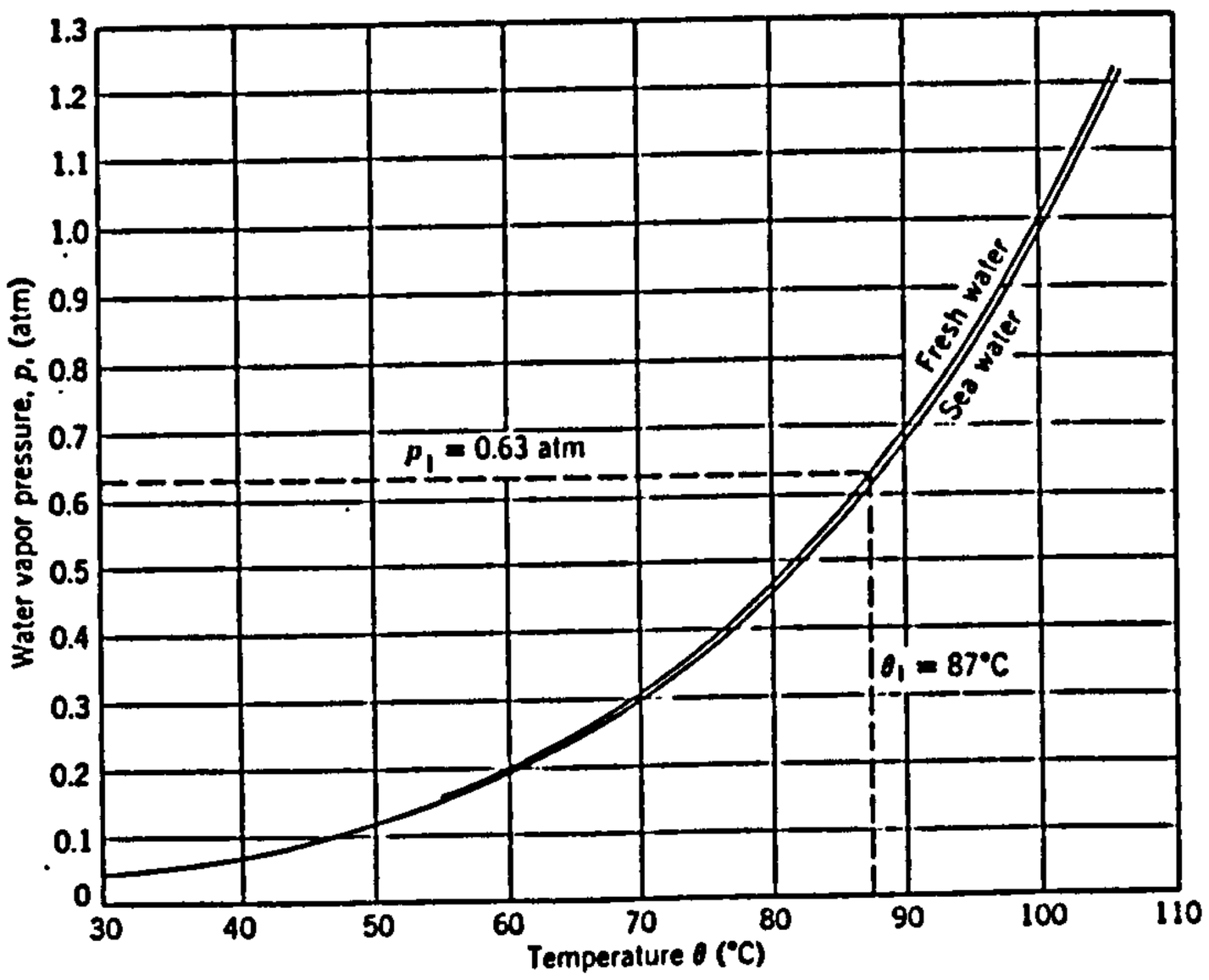

Fig 3.10. Relationship between temperature and pressure at the boiling point (Spiegler, 1986).

3.9.5 Submerged Tube Evaporator Process

A submerged tube evaporator is shown in Fig 3.11. Steam is introduced through the tubes in the first evaporator. These tubes are submerged in brine. Steam is condensed

after giving up its latent heat to the brine. The heat gained by brine causes it to boil and the vapours are released. These vapours from the first stage serve as the heating source for the second stage. The second stage supplies vapours to the third stage in the same way. This continues till the last stage, where the temperature of the vapours released is too low to permit any productive heating. Vapours from the last stage are condensed separately in a condenser cooled by cold seawater.

The submerged tube distillation suffers from two major problems. The first is the brine pool cannot be vaporized as efficiently as in other systems because of the relatively smaller surface area exposed. The second is the lack of positive circulation of the saline water. Therefore, scale forms on the tube surfaces, which reduces the thermal efficiency.

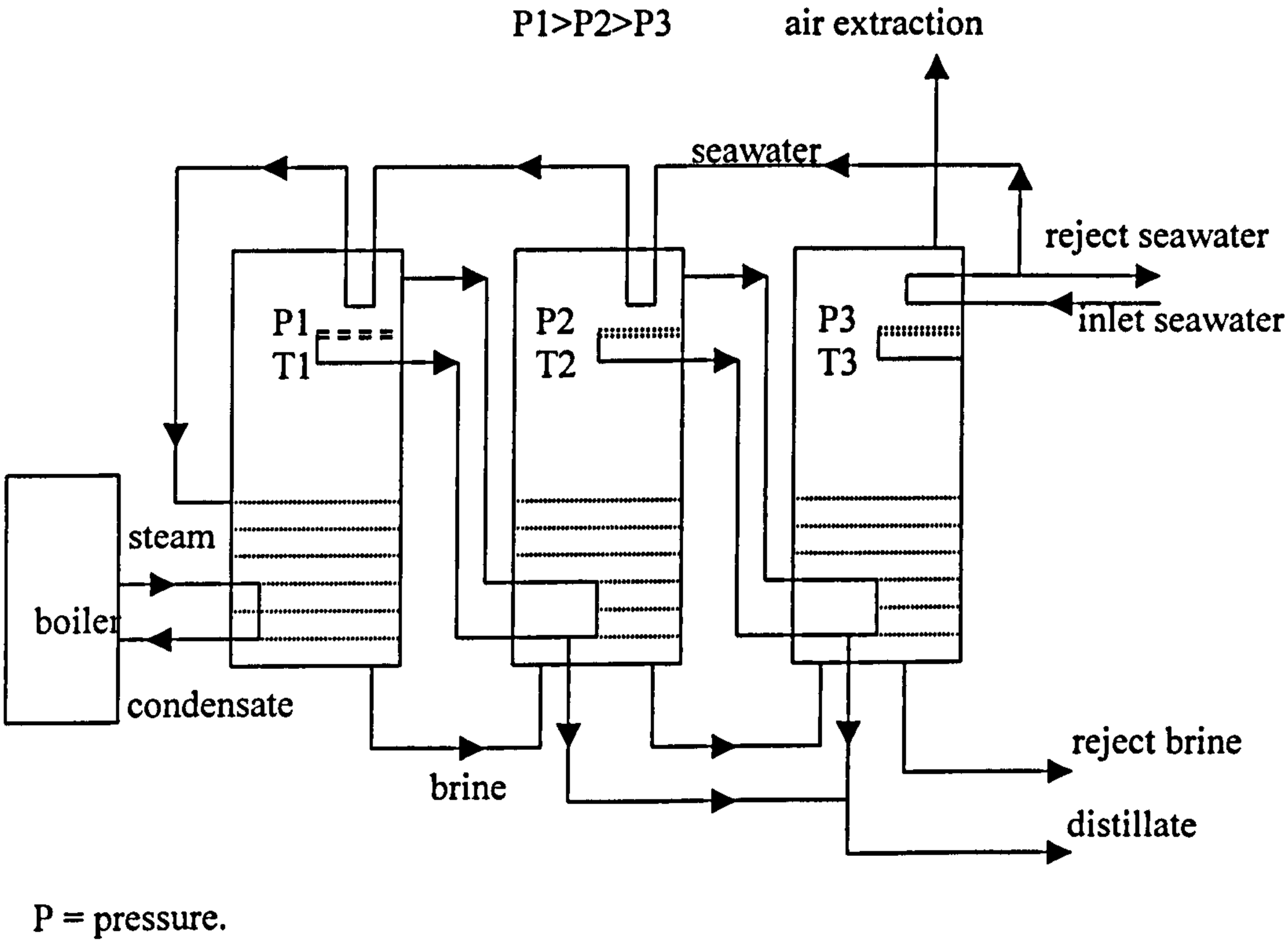

P = pressure.
T = Temperature.

Fig 3.11. Submerged Tubes desalination process (Khan, 1986).

Scale formation dictates the upper limit of the maximum brine temperature in the plant. Scale is very hard to remove. In earlier plants, it was removed either by

mechanical or by thermal shock. Polyphosphates have been used to inhibit scaling but they restrict the upper temperature to 90 °C. This temperature restriction limits the plants thermal efficiency. Sulphuric acid can also be used for the pretreatment of seawater to prevent carbonate and hydroxide scale formation. One of the earliest plants in which acid was used commercially is the 9460 m^3/day plant in Aruba, Antilles, which was constructed in 1958.

The heat transfer coefficient of a natural circulation, submerged tube evaporator drops appreciably relative to the operating temperature. Temperature differentials should be satisfactory as heat transfer falls considerably with low temperature differentials. Loss of the temperature differential attributable to the hydrostatic head can become very significant in such process. In spite of these disadvantages, submerged tube evaporators present a potential economic choice in a low cost fuel situation. Even with a low performance ratio, it may still yield water at an overall acceptable cost.

3.9.6 Vertical Tube Evaporator Process

As a means of overcoming the lack of circulation in the submerged tube process, the vertical tube evaporator configuration was designed. In this process the temperature differential loss due to the hydrostatic head has been decreased. However, the VTE plants are more complex. They require far more external piping and pumps than the submerged tube plants due to the necessity of pumping brine between the stages. In the VTE process, brine falls down inside vertically oriented tubes. There exists only a thin film of condensate on the outside and a thin film of brine on the inside. The remainder of the space is filled with vapours. To ensure even distribution of brine around the circumference of the tube, a distributor cap is fitted on each tube. Blockage of the cap can cause scale to build up in localized areas. Not withstanding scaling, a drop in performance ratio can be expected in such a situation. Snamprogtti of Italy has built the largest VTE plant for a refinery in Italy. Its capacity is 1640 m^3/day. Water produced by this process represents 3 % of the total worldwide desalting capacity (Dickson, 1997).

This type of plant operates on the principle that seawater boils at progressively lower temperatures when introduced into the stages, which are maintained at successively lower pressures. Each stage has an associated feed heater, which uses product vapours

as the heating source. The feed water passing through the final heat rejection effects to condensate the vapours and require heat before passing to the first stage. Feed then flows into the first stage, where steam from a boiler is introduced outside the tubes. Brine evaporates while being heated by steam flowing around the tubes.

Steam condenses and returns to the boiler. Heating steam at saturation temperature exist at approximately 1 to 3.013×10^5 Pa. Vapours formed from brine in the first stage are directed to the second stage. These vapours assume the role of the heating source for evaporation in the second stage.

The second stage occurs at a lower pressure than the first. This allows vaporization to occur at lower temperatures. The brine cools down after flashing and becomes slightly concentrated. The slightly concentrated brine in the first effect sump is pumped under automatic level control to the top water box of the second stage, where it is distributed to the tubes. As can be seen in Fig 3.12, in the falling film process, brine has to be pumped from the bottom to the top from the second or third stage onwards.

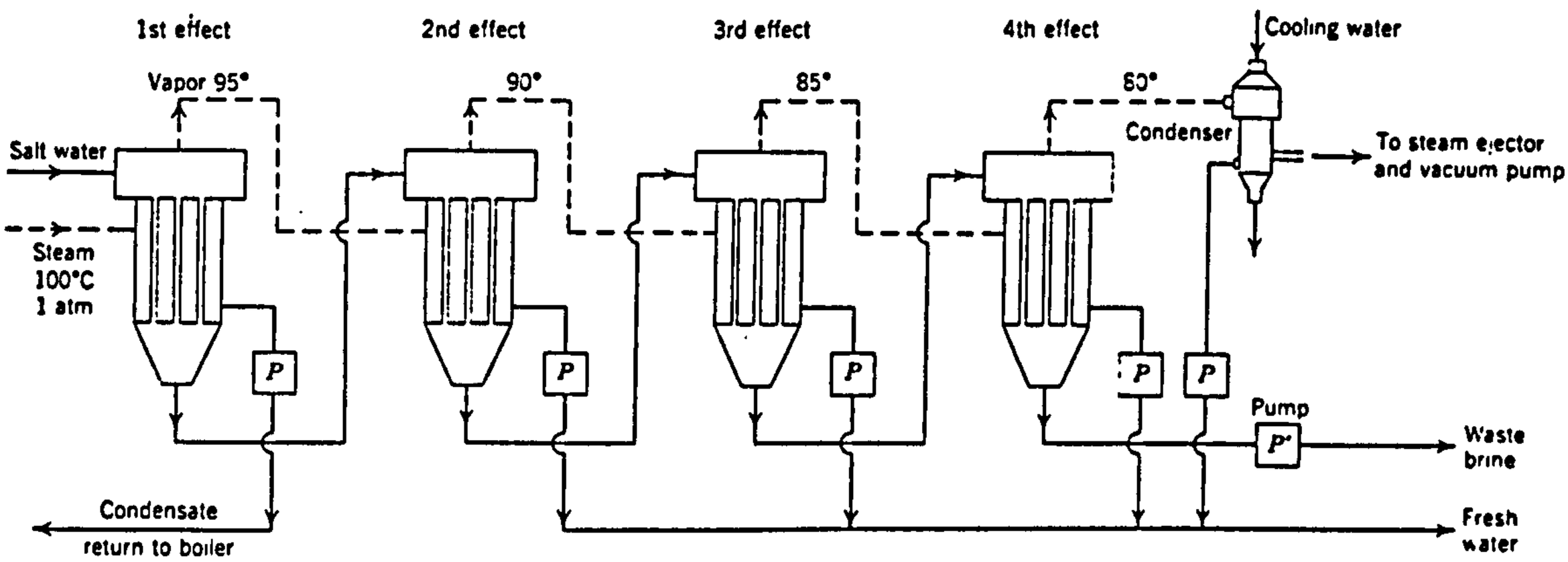

Fig 3.12. Process flow diagram for a Miltieffect Vertical Tube Evaporator (Spiegler, 1981).

The boiling process continues till the last stage is reached. A vacuum in the final stage is maintained by an ejector. Most of the vapours are condensed while heating the circulating brine. The vapours generated in the steps are partly used for preheating

raw seawater in the preheaters. The combined stream flows through a sealing orifice into the next stage. It cools down to the saturation temperature and the vapours from product flashing are joined by those from the next stage. Only vapours in last stage are cooled by cooling seawater in a separate condenser and brine water from the last stage is either rejected or sent for by-product recovery.

3.9.7 Horizontal Tube Evaporator Process

A significant portion of the maintenance and initial costs of a VTE plant is associated with the pumps. These pumps are required to move brine from the bottom of one stage to the top of the next. The HTME process was proposed as a solution to overcome this restriction. In this process, the tube arrangement is horizontal, Fig 3.13. The evaporator is of the MED type, in which the effects or stages are stacked vertically on top of each other.

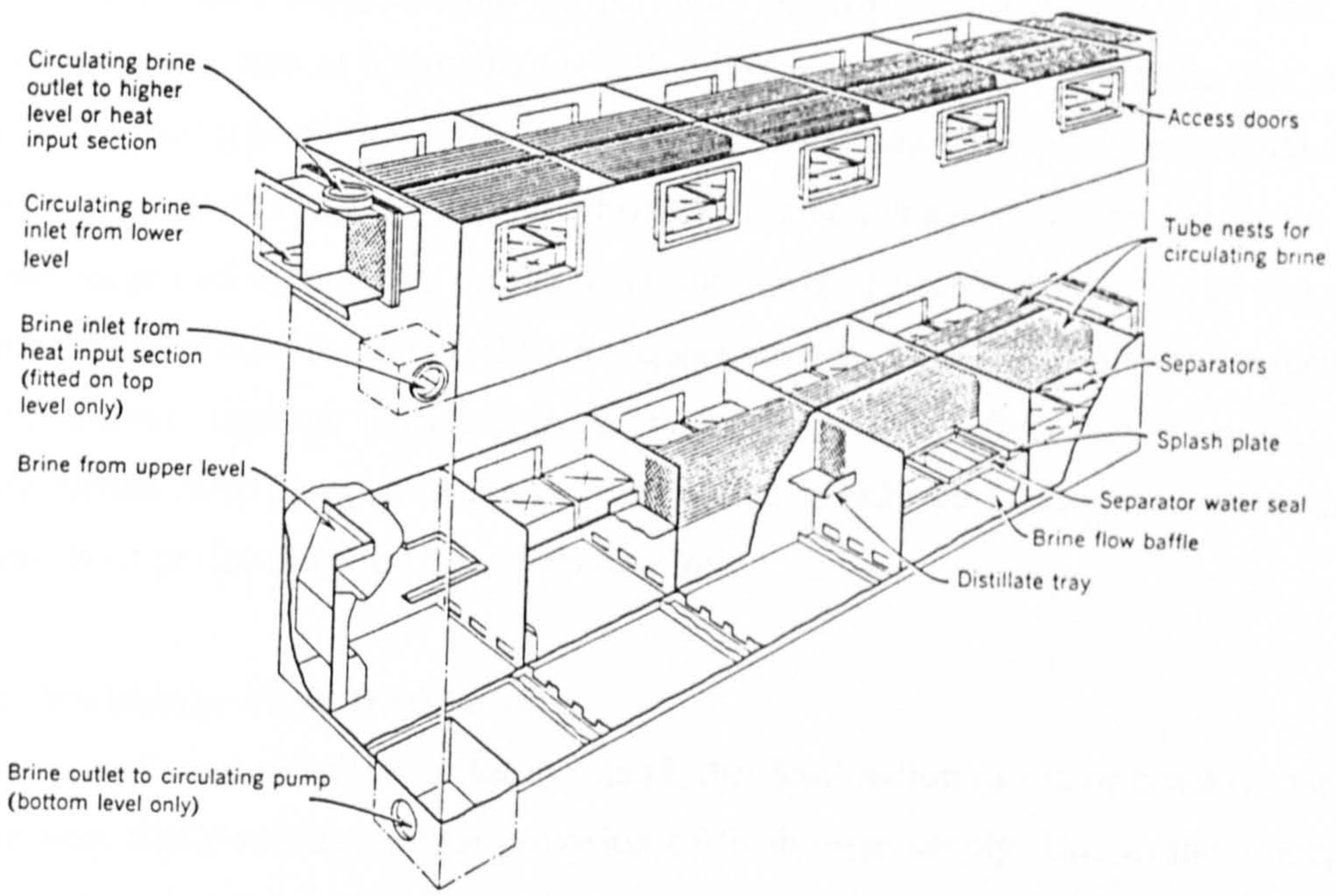

Fig 3.13. Process flow diagram for a Miltieffect Horizontal Tube Evaporator (Hanbury, 1992).

The largest unit size installed so far is 5400 m^3/day in the US Virgin Islands. This process contributes about 1% of the total worldwide desalting capacity. In this set up, only the first effect receives low pressure steam from a boiler. The second and

subsequent effects (stages) use steam produced by the previous effects. Inside each stage, the tubes are arranged horizontally (Chmbers, 1967).

Vapours condenses inside the tubes while boiling brine flows on the outside. Brine flows down through the nozzles from the hot top effect to the colder one below, as a function of gravity and pressure differences. The principle of operation is quite simple. Seawater supplied by feed pump is preheated in each stage. It is then sprayed on the outer surface of the evaporating tubes of the first stage. Steam is fed into the first stage tubes.

A portion of the feed evaporates. The vapours quantity produced in this stage is only slightly less than the amount of steam supplied. Heating steam condenses inside the tubes and is returned to the boiler. Vapours from the first stage are fed into the tubes of the second. There condense subsequent to divesting themselves of their latent heat to the colder brine being sprayed on the tubes. Spraying is accompanied by flashing. Condensation occurs at a temperature a few degrees lower than that in the first stage due to the successively lower pressure in each effect down the plant, the condensate becomes the products. Unevaporated brine in the first stage flows by gravity to the second stage and then sprays on the outer surface of the tubes in the second stage. It then flows in similar fashion to the subsequent effects. As well as the vapours formed in the second stage are delivered to the tubes of the third effect and so on. As the steam passes from stage, to stage its temperature is reduced to the point where it is incapable of performing any brine vaporisation.

3.10 Multistage Flash Distillation

In many arid areas, whether costal or inland, the desalination of sea or brackish water is the only likely solution to the provision of freshwater supply. Due to the strategic nature of the product, many countries tend to decide upon the relatively expensive desalination process, which has been proved to provide a sustainable source. Among the distillation techniques, MSF is the most widely used process. The multistage flash evaporation process MSF, which by its development and instigation halved the cost of building and operating plants for producing fresh water from sea, was developed and patented in 1957 by a team led by Professor. R. S. Silver, then the Research Director of the Weir Group in Glasgow, Scotland. Multistage flash distillation was practiced in

the Gulf States in the 1970s and still account for 90% of the desalination units, which have been set up in the region. The adoption of the desalination process by the Gulf Sates, as well as by number of industrial countries, has resulted in a rapid growth in the industry since its inception in 1950s. Since then, the number of operating units has increased from a handful to more than 11,000 in 1996. This increase in the production volume has been associated with a decrease in the power consumption from 100-250 kW per 4.5 m^3 in 1955 to 15-40 kW per 4.5 m^3 recently (Hanbury, 1992).

Similar progress has transpired in the MSF process, where the unit capacity has been dramatically increased from the modest capacity of 2283 m^3/ day during the 1950's and 1960's to a current unit capacity varying from 31963 to 57077 m^3/day (Bednarski, 1997).

3.10.1 The Principle of Multistage Flash Distillation

The MSF operates on the principle that water boils at progressively lower temperatures, when it is subjected to progressively lower pressures. While input seawater is introduced into the MSF evaporator, which is maintained under sufficiently low pressure, it boils or flashes. The vapours produced are condensed to obtain a pure distillate. An MSF evaporator consists of a series of stages or chambers, usually 18 or more, each operating at a lower pressure than the its predecessor, as illustrated in Fig 3.14. These stages improve the efficiency of the heat transfer process. The process operates from a low vacuum in the first stage to a high vacuum in the final stage. The differential in pressure between stages is the key to repeated flashing. The pressure is released in small steps thereby ensuring a high degree of internal heat recovery. For each 1 MJ of heat input, typically a yielded of 3-10 kg of water are produced (Hanbury, 1992).

As it passes through each chamber, the seawater successively releases the quantity of vapour needed to restore the equilibrium with the prevailing pressure. Whereas the initial temperature of the vapour is recorded at about 110 °C, it falls to 40 °C in the final stage. In the upper part of each chamber, the released vapour is transformed by condensation into distilled water as it comes into contact with a bundle of tubes in which pre-treated cold seawater circulates. Warming up as it goes through the system from the coldest to the warmest stage, it is this cold water, which is used in the first

distillation chamber, accompanied by a supplementary input of power to elevate its temperature to 110 °C.

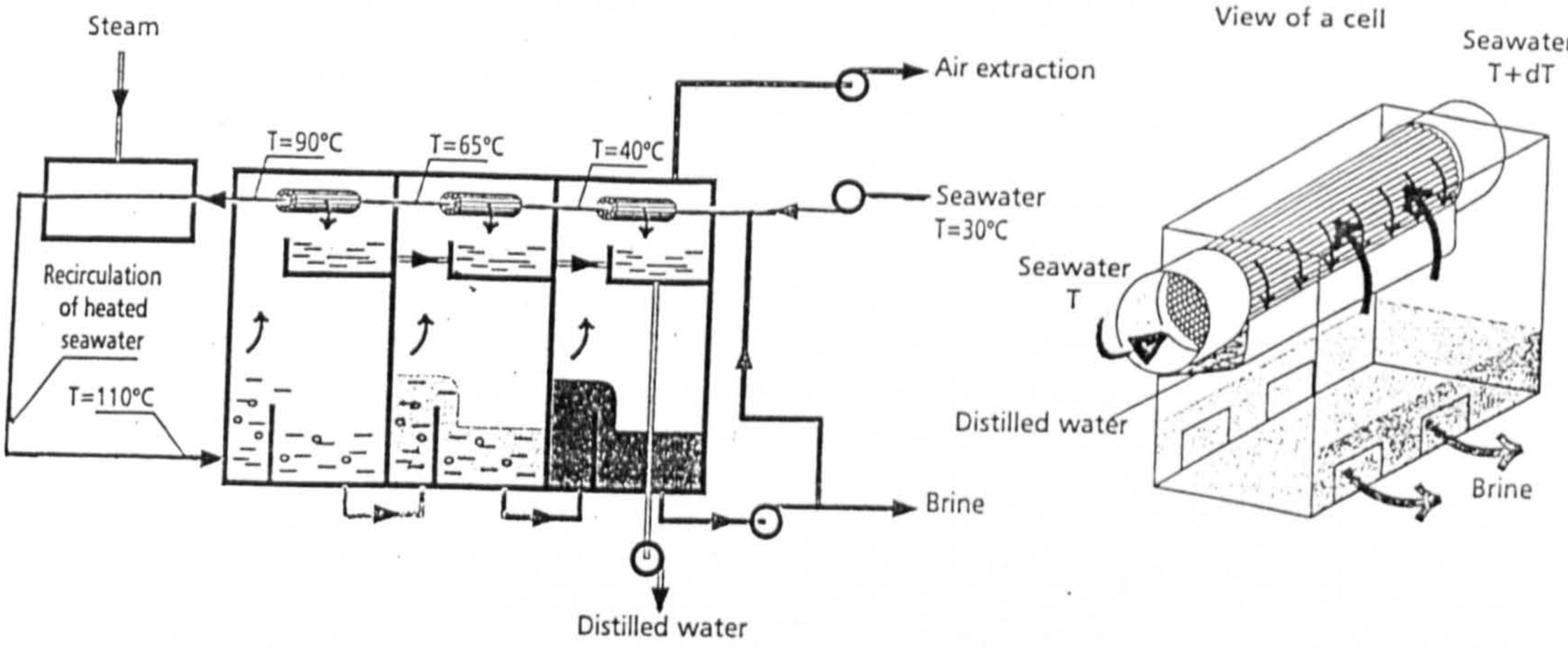

Fig 3.14. Principle of Multistage Flash Desalination Process (Memotechnique, 1999).

The distilled water is recovered in tray located beneath the tube bundles and extracted from the last chamber by pumping. Meanwhile, the brine concentrated in the lower part is also pumped out, and then discharged back into sea. In this type of system, it is necessary to add scale- and foam-inhibiting products in the water circulation network. Furthermore, the inside surfaces of the tubes are kept constantly clean by the use of small sponge balls, which are recovered at the outlet.

The MSF process is a well tried and reliable technique, which makes it possible to construct large-scale facilities producing up to 50,000 m^3 of water per unit per day, and to have several units operate in parallel. On the other hand, the MSF technology experiences energy breakdowns, which are not really optimised. The largest MSF plant is the Al Jubail. It has a capacity of 946,000 m^3/day (Desalination Study,2000).

3.10.2 Multistage Flash General Operation Process

A schematic diagram of the MSF system is illustrated in Fig 3.15. The system involves six main streams: intake seawater, rejected cooling seawater, distillate

product, rejected brine, brine recycle and heating steam. The system contains flashing stages, a brine heater, pumping units, venting system, and a cooling water control loop. The flashing stages are divided into two sections: heat recovery and heat rejection. The number of flashing stages in the heat rejection section is commonly limited to three. On the other hand, the number of flashing stages in the heat recovery section varies between 15 and 40.

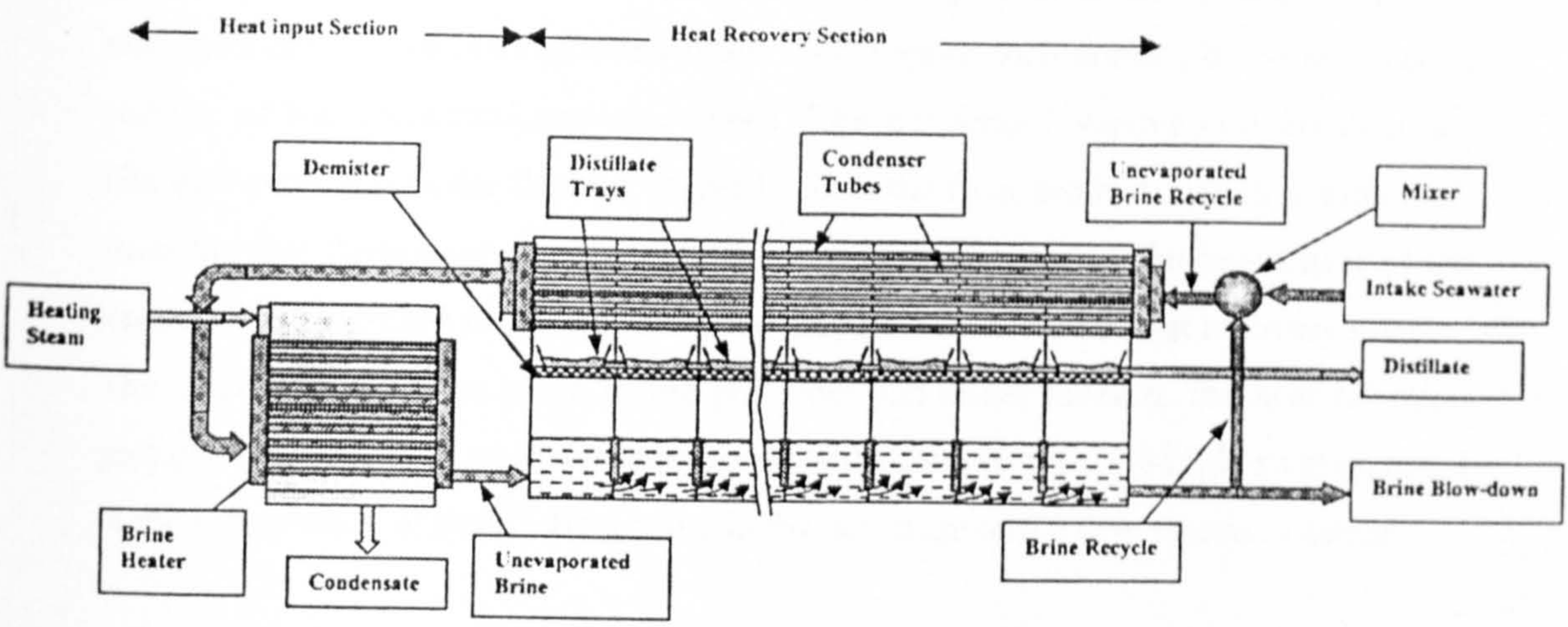

Fig 3.15. Multistage Flash Desalination Process (Silver, 1967).

The intake seawater is introduced into the inside of the preheater/condenser tubes of the last flashing stage in the heat rejection section. Similarly, the brine recycle stream is introduced into the inside of the preheater/condenser tubes of the last flashing stage in the heat recovery section. The flashing brine flows in a counter direction to that of the recycled brine from the first to the last flashing stage. The saturated heating steam with a temperature range of 97-118 °C drives the flashing process. The heating steam flows along the outside of the brine heater tubes and the brine stream flows on the inside of tubes. As the heating steam condenses, the brine stream gains the latent heat of condensation, the brine stream gains the latent heat of condensation and its temperature reaches the desired top brine temperature. This parameter, together with the flashing temperature in the last stage, defines the total flashing range.

The hot brine enters the first flashing stage, where a small amount of product vapour is formed. The flashing process reduces the temperature of the unevaporated brine. The temperature reduction across the flashing stages is associated with a drop in the stage pressure, where the highest stage pressure is found in the first stage after the brine heater and the lowest pressure is that of the last stage. The pressure drop across the stages allows for brine flow without the use of interstage pumping unit. (Silver, 1967).

In each stage, the flashed off vapour flows through the demister, which removes entrained droplets of unevaporated brine. This vapour then condenses on the outside surface of the preheater/condenser tubes. The condensed vapour collects over the distillate trays across the flashing stages to form the final product, which is drawn off from the last flashing stage. The condensation process releases the latent heat of the vapour, which is used to preheat the brine recycle stream in the heat recovery section. The same process takes place in the preheater/condenser tubes in the heat rejection section. This results in an increase in the seawater temperature to a higher value, equal to the temperature of the flashing brine in the last stage of the heat rejection section.

The seawater intake stream leaves the heat rejection section, where it is divided into two streams. The first stream is the cooling seawater stream, which is rejected back to the sea, and the second is the feed seawater stream, which is mixed in the brine pool in the last flashing stage in the heat rejection section. Prior to the mixing location of the feed seawater stream, the rejected brine stream is withdrawn from the brine pool. On the other hand, the brine recycle is withdrawn from a location subsequent to the mixing point. The brine blowdown is rejected into to the sea and the brine recycle is channelled into the last stage of the heat recovery section.

Additional units in the desalination plant include pretreatment of the feed and intake seawater streams. Treatment of the intake seawater is limited to simple screening and filtration. On the other hand, treatment of the feed seawater is more extensive and includes deaeration and addition of antiscalant and foaming inhibitors. Other basic units in the system include pumping units for the feed seawater, brine recycle and brine blowdown. The release of non-condensable gases occurs simultaneously with the flashing process. The presence of non-condensable gases reduces the efficiency of the vapour condensation process. This is caused by the low thermal conductivity of

the non-condensable gases, which act as an insulating layer around the preheater/condenser tubes. In addition, the presence of non-condensable gases reduces the saturation pressure of the flashing vapour, which results in a lower condensation temperature. Consequently, the driving force for condensation is reduced, as the overall thermal efficiency of the process.

To prevent the accumulation of non-condensable gases and their harmful effects on the condensation process, an external deaerator is installed to reduce the dissolved oxygen content in the feedstock to approximately 0.05 mg/l prior to introduction into the evaporator, and gas-venting units are employed to withdraw the non-condensable gases such as carbon dioxide from a number of flashing stages (El-Dessuky, 1998). Steam or air ejectors are adopted to generate sufficient vacuum to withdraw the gases from collection points near the preheater/condenser tubes. The selection of these locations is necessary to minimize undesirable losses of the flashing vapour.

3.10.3 Configuration and Stages Numbers

One of the major factors determining the size of distillation unit is the rate of heat transfer across the heating tubes between the condensing steam and the water. This is given by Spiegler's (1981) equation.

$$L_Q/t = U \times A \times \Delta T \qquad (3.3)$$

where L_Q = amount of heat flowing from steam to water side to tube in J, A = area through which heat flows inside and out side areas of the tube in m^2, ΔT = temperature difference between steam and water side of tube in °C, t = time of heat flow in second, and U overall heat-transfer coefficient across the wall of the tubes.

The larger the overall heat-transfer coefficient, the faster the heat flow and hence the smaller the installation necessary to distil a given quantity of water. The overall resistance to the flow of heat encountered in distillation practice is the composite of several layers as shown in Fig 3.16. To effect distillation the heat condensation must pass through all these layers whose heat flow resistance increases with their thickness.

The thermal conductivities of the materials in these various layers are varies and widely, as shown in Table 3.3.

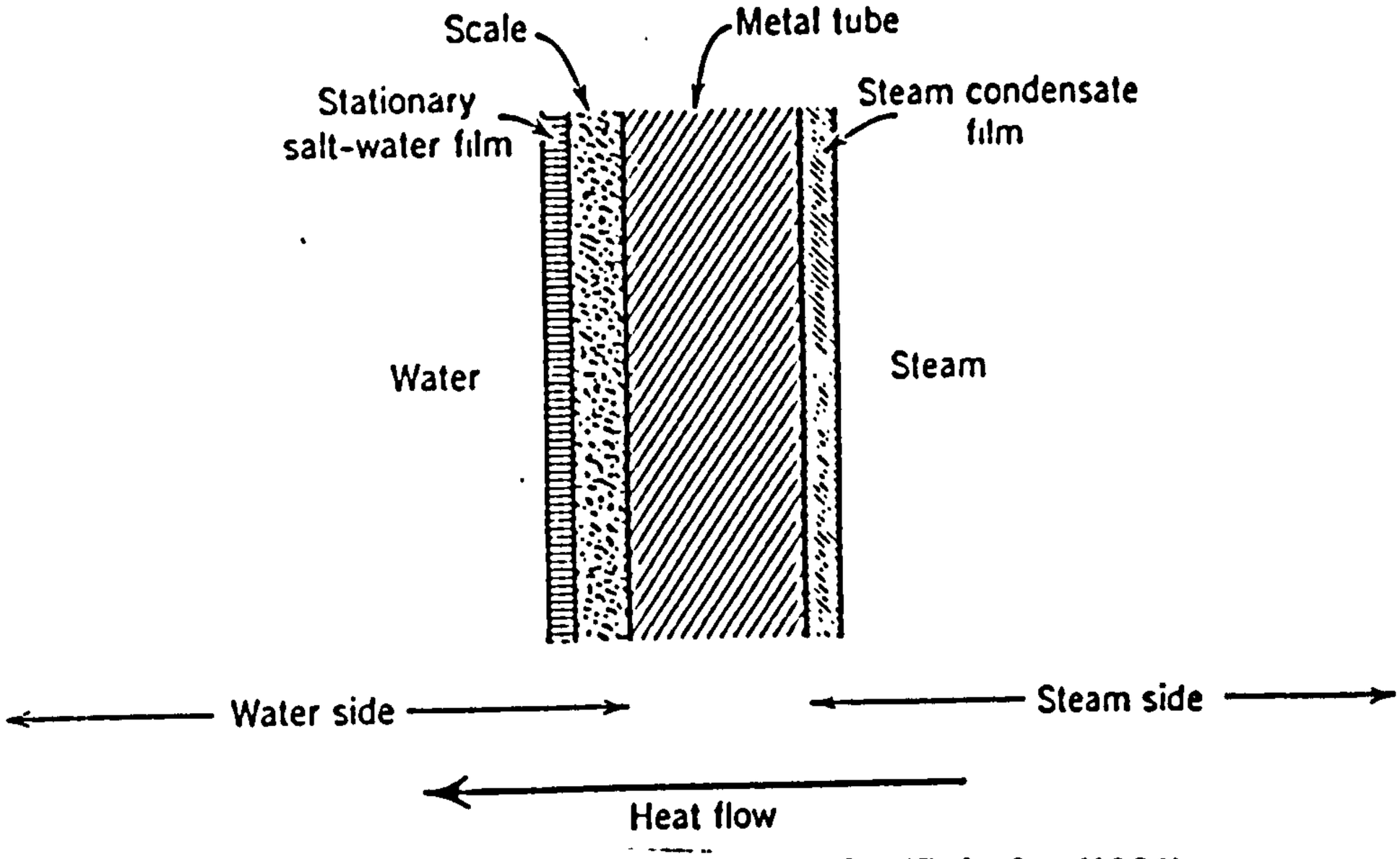

Fig 3.16. Heat flow a cross evaporator tube (Spiegler (1981).

Material	Temperature (°C)	Thermal Conductivity W/m. °C
Copper	100	380.6
Aluminium	100	204.7
Nickel	100	57.6
Steel	100	44.8
Water	40-60	0.64
Steam	100	0.67
Calcium carbonate	25	2.97
Calcium sulphate	100	6.28
Magnesium oxide	50 -1130	1.15 - 3

Table 3.3. Thermal conductivities of different materials (Spiegler, 1981).

To obtain the overall resistance to the flow of heat R_o, the resistances to heat flow on the steam side, in the metal, and on the water side R_S, R_M, and R_W, respectively, must be added.

$$R_o = R_S + R_M + R_W \qquad (3.4)$$

The MSF distiller comprises a number of stages or chambers in series. It is, therefore, of prime importance that the layout or geometry of these stages should reflect both technical and economic considerations. The elements comprising a stage are the condenser bundle, the demister and the brine transfer device. The designer's objective is to arrange these elements within the stage in such a way that the final design reflects the economy of materials and results in a good technical performance.

For effective design, however, the stage dimension should be compared with that required for demister and tube bundle layout. In the situation where the latter consideration results in a smaller stage length, the designer must compromise between the provision of additional structural material to minimize the equilibration loss or, the provision of additional heat transfer surfaces to circumvent the reduction in vapour condensation temperature resulting from non-equilibration.

Current practice in plant design is to assign equilibration dimension a secondary consideration and allow for the fact that the brine will flow into successive chambers before an equilibrium is reached, by combining this loss with other temperature losses. The two geometrical types of stage wieldy adopted are cross tube and long tube.

An important advantage of the MSF process when compared to the other desalination processes is that the number of stages is not strictly tied to the performance ratio of the plant. The minimum number of stages is greater than the performance ratio. The boiling point elevation restricts the maximum number of stages. The minimum interstage drop must be greater than the boiling point elevation for flashing to occur. The number of stages can be varied within this restriction. Increasing the number of stages improves the efficiency of heat recovery during flashing in each stage. The temperature difference over heat exchanger is decreased and a heat loss transfer surface is required. This means less cost for heat exchangers.

However, this results in an increase in the partitioning/chamber costs. Due to a more efficient heat recovery, the amount of heat required in the brine heater is reduced. The actual number of stages varies from 16-40, spanning a total temperature range of approximately 50 °C with polyphosphate treatment, and 70-80 °C for acid treatment.

In the following section, two main types of MSF were investigated and studied (Khan, 1986).

3.10.4 Once-through Multistage Flash

In this process, as shown in Fig 3.17, the seawater is fed to the last stage of the evaporator by the seawater pump. It flows through the condenser tubes of all the stages up to the brine heater. In each stage, it receives a preheating treatment. On leaving the first stage condenser tubes, the seawater is heated up to the top temperature in the brine heater by low pressure steam. The hot feed is then introduced into the first stage flash chamber. It flashes and the vapours produced are condensed on the condenser tubes. Unflashed brine is sent to the next flash chamber, where it again flashes due to the lower pressure maintained there. This process is repeated until the last stage. The vapours produced are salt free. Any entrained brine droplets are removed with the help of knitted wire mist separators (demister).

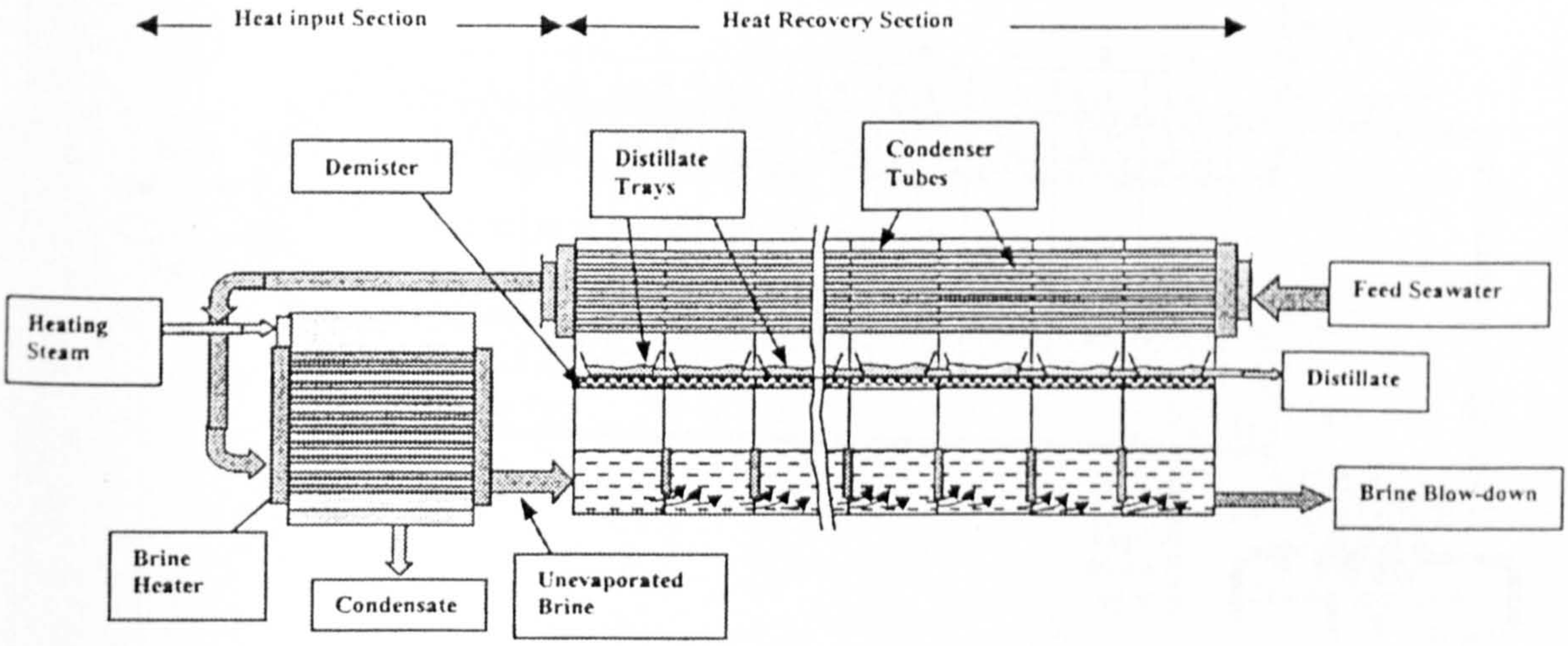

Fig 3.17. Once-through Multistage Flash Desalination Process (El-Dessouky, 1999).

Unevaporated brine in the last stage is returned back to the sea. It is extracted by the brine blowdown pump. The amount of blowdown is equal to approximately 10% of the feed recovered as distillate (El-Desouky, 1999). Due to the relatively low percentage of distillate recovery and greater amount of chemicals required, once-trough plants are not widely used. Their advantage is that operation is relatively

simple, especially during startup. Moreover, balancing flows through all the stages is easier than in a recirculation type plant, which will be discussed later. This type of plant is routinely exposed to low brine concentration because brine is not recirculated. Hence, scaling problem is limited.

3.10.5 Recirculation Multistage Flash

This is a modification of the Once-through MSF process which has been constructed in Ras Abu-Fontas (A) and (B). This process, the latent heat required for flashing is supplied by the sensible heat change of the liquid. This is assuming a brine temperature of 100 °C in the first stage and 30 °C in the last stage. This is equivalent to a loss of 293 KJ/kg. This is approximately $1/8^{th}$ the energy required to vaporize 1 kg of water. Hence, production is only $1/8^{th}$ of the recirculating flow. To reduce the amount of fresh feed required and to have better heat recovery, part of the brine coming out of the last stage is recycled as shown in Fig 3.18.

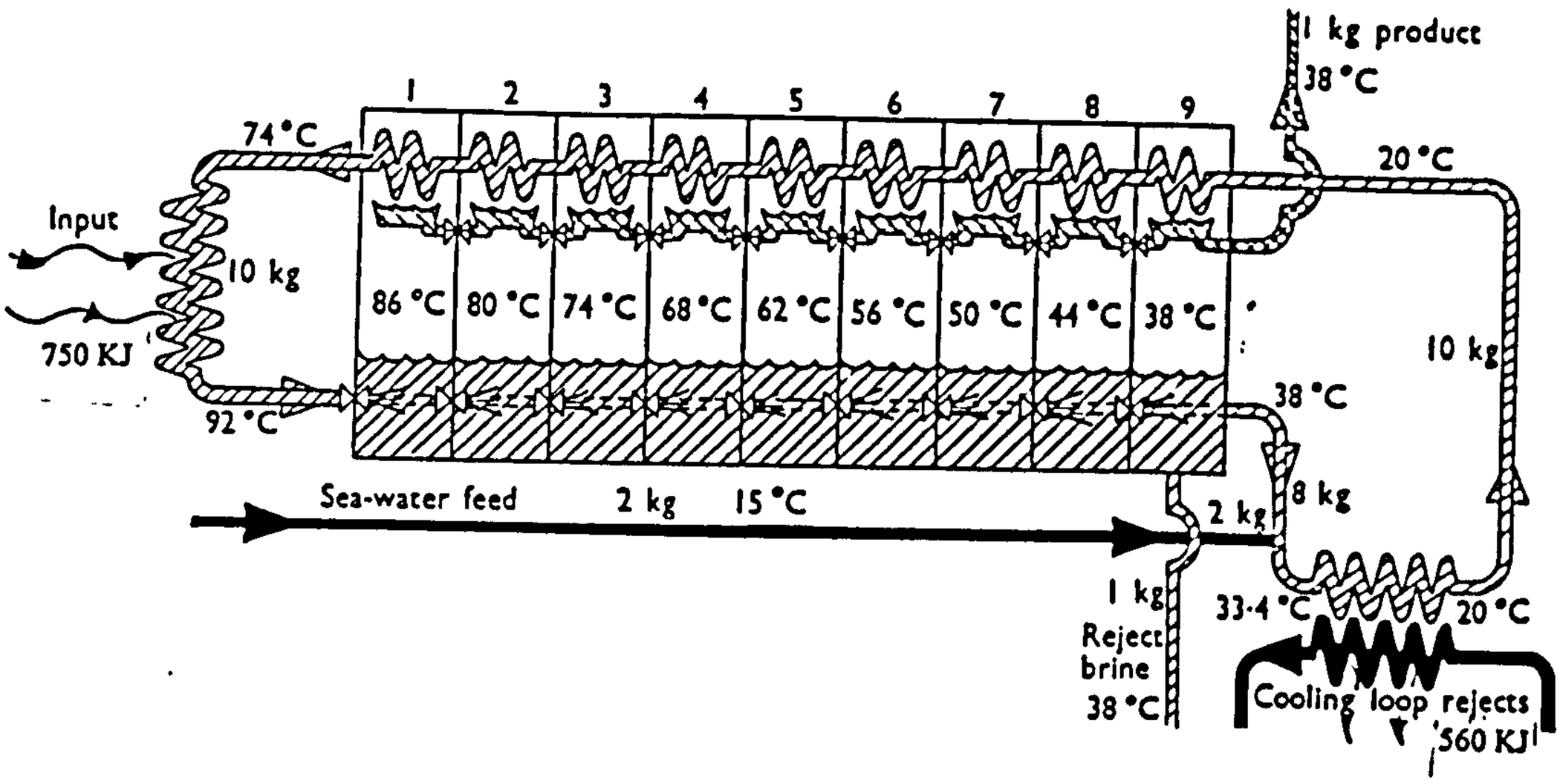

Fig 3.18. Recirculation Multistage Flash Desalination Process (El-Dessouky, 1999).

Recycling permits selection of a desired feed to product ratio, which is directly related to the concentration ratio. Usually, 50-75% of brine from the last stage is mixed with fresh feed seawater and recirculated through the brine heater. The balance is rejected as blowdown. Makeup flow is equal to the sum of the distillate and blowdown flows.

The ratio of makeup to blowdown is called the concentration ratio and usually varies in the 1.3 to 2 range. It is effected by the raw seawater salinity and the maximum temperature selected for flashing brine. The scale deposition process is dependent on the concentration ratio. In general, a value of 1.7 should not be exceeded. To keep the concentration ratio within safe limits, seawater makeup is continuously added to brine in the last stage (Clelland, 1967; Darwish, 1987).

3.11 MSF and MED Steam Requirements

Steam generation can be achieved via two routes, either fuel is used as an energetic source in a conventional fired boiler; or as sensible heat by hot flue gas, wasted by gas turbines, can be recovered in recovery boilers. Several cogeneration cycles are thus possible, among which the most significant for this application can be summarized as follows, with respect to power/steam production:

3.11.1 Gas Turbine - Heat Recovery Steam Generation Cycles

Configuration 1 considered as a conventional configuration, which comprises a high efficiency gas turbine, normally powered by natural gas, in conjunction with a heat recovery steam generator for steam production. In the simplest configuration 1.A, steam is produced at a relatively low-pressure e.g.20 bar, at saturation temperature. It is then fed to the desalination plant brine heater and ejector system after undergoing a pressure reduction, which infers a superheating effect. An auxiliary boiler is normally employed, to integrate steam production and to guarantee steam flow to the desalination plant, particularly in winter, when the load of electricity is low and also during gas turbine assembly trip/ maintenance.

This configuration generates a great deal of power per unit desalinated water produced. However, it is slightly less flexible than other configurations, because of non-optimum operation of gas turbines, when operated at part load. Alternative cycles can be defined, when either higher or lower values of power/water production ratios are required, Fig 3.19. (a, b, c). In the first case, when a higher power production is required, defined as 1.B, steam can be produced by heat recovery steam generation at higher pressures and temperatures, to be expanded in a back pressure turbine, before being delivered to the desalination plant (Borsani, Superina and Sommariva, 1995).

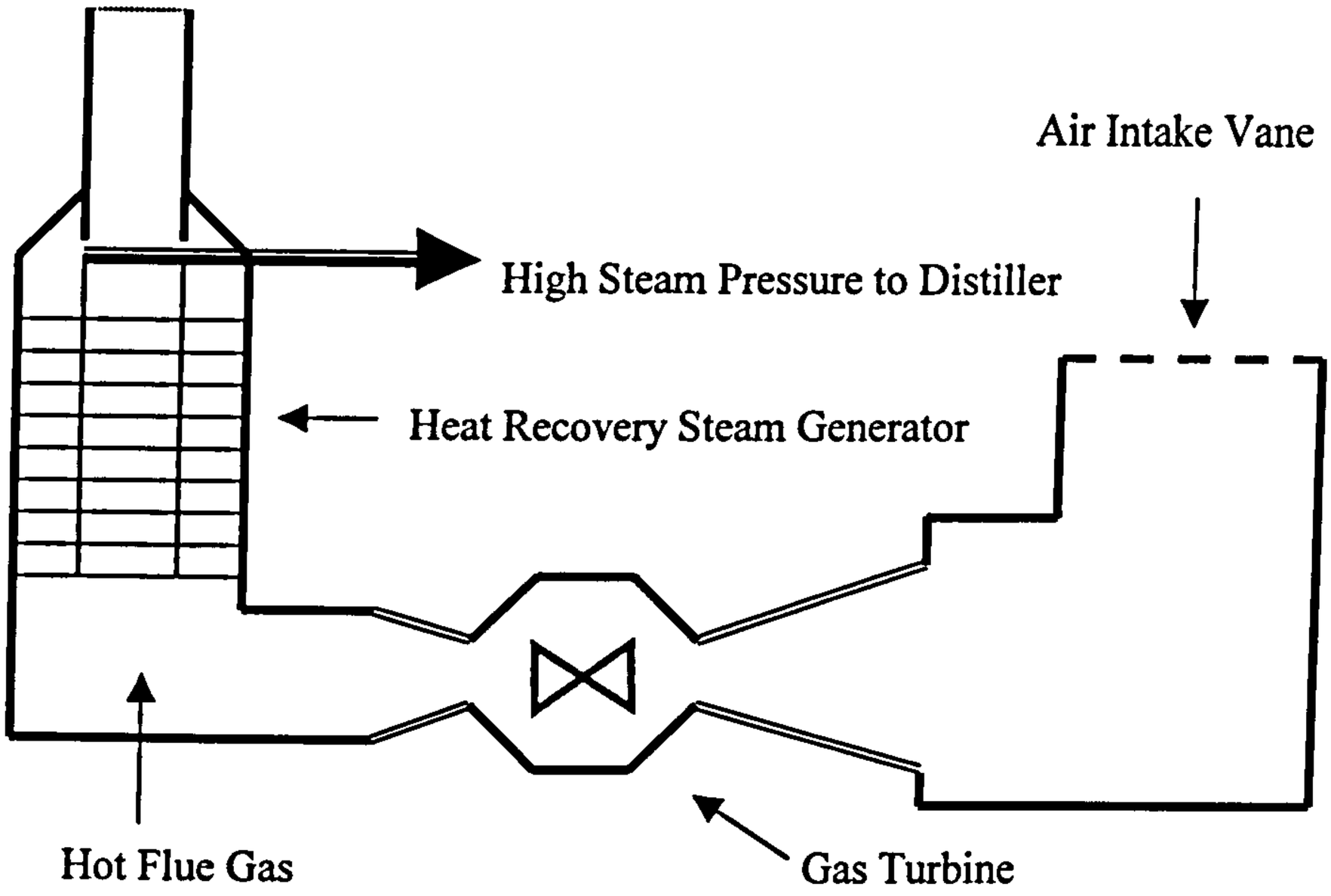

Fig 3.19.a, Gas turbine with heat recovery steam generator type 1.A.

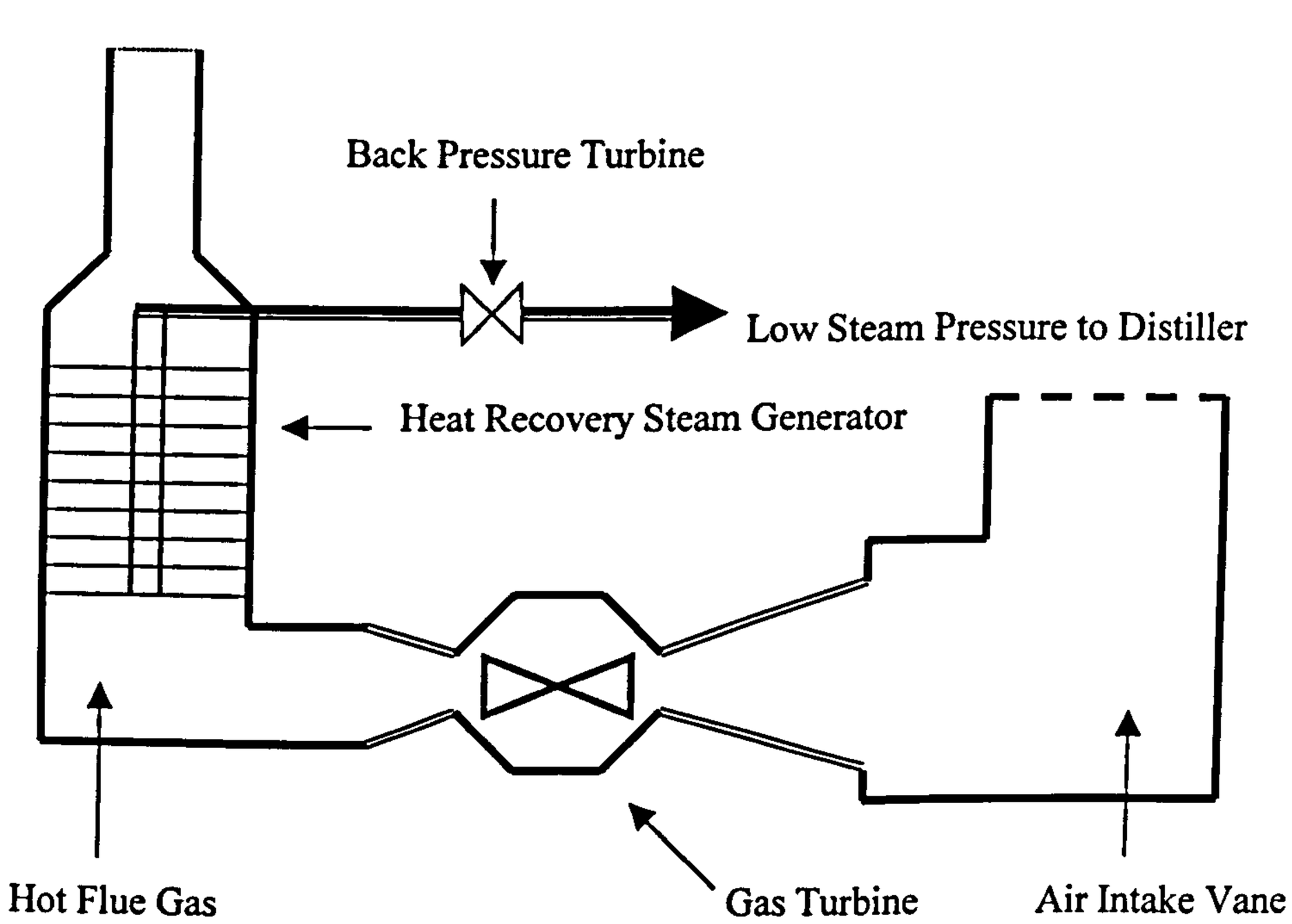

Fig 3.19.b, Gas Turbine With Heat Recovery Steam Generator Type 1.B

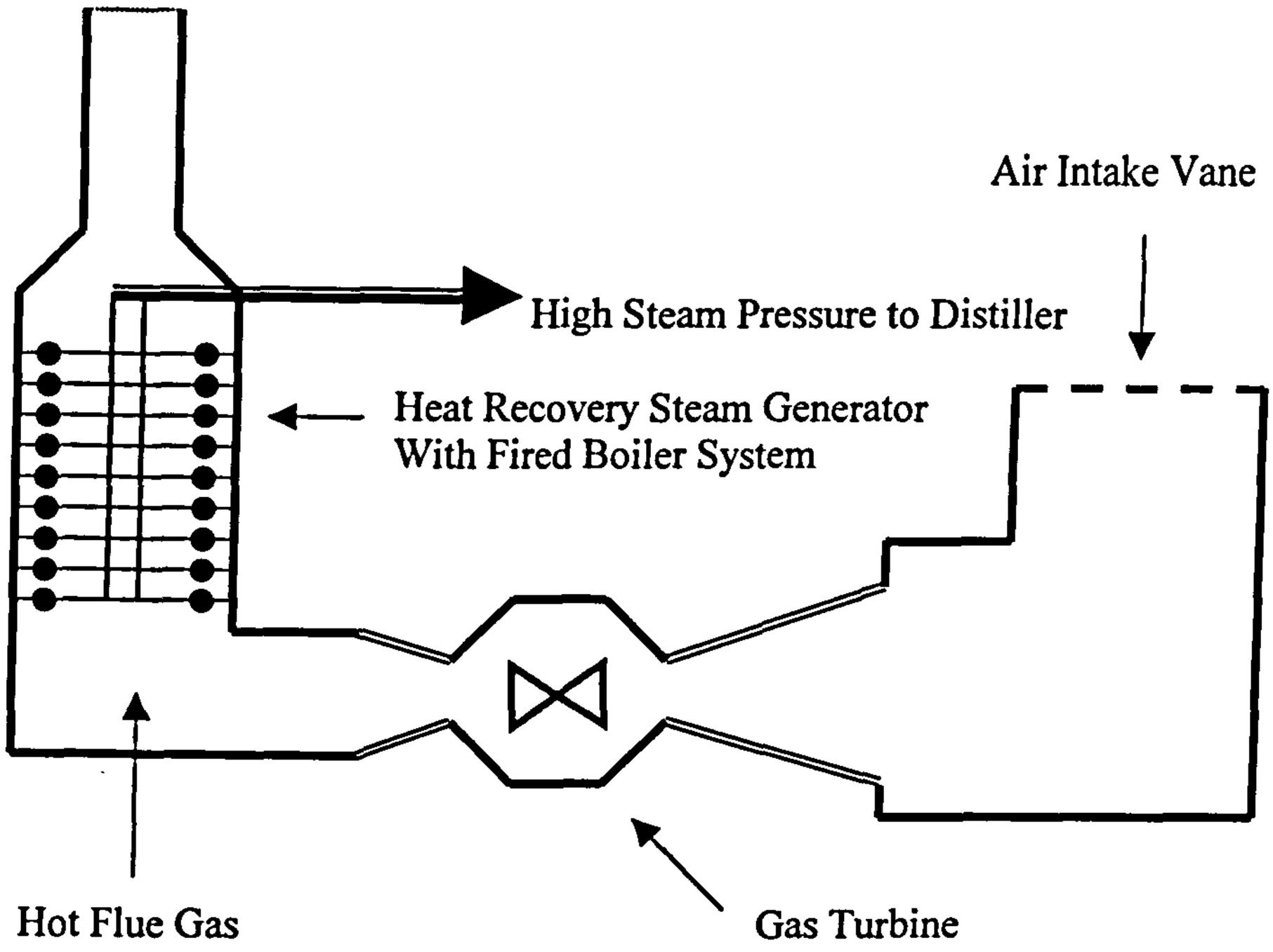

Fig 3.19.c, Gas Turbine With Heat Recovery Steam Generator Type 1.C

In this configuration it can be noticed that the boiler design should be modified and additional section, named the back pressure turbine, should be added which can considerably increase the capital cost of the plant. However, the balance between additional costs and the resultant additional power production normally make these additional costs economically viable. Compared with the first cycle type 1.A, the results revealed that, in the second cycle type 1.B has more power production, when the same gas turbine employed. However, the steam production was lower in cycle 1.B, as shown in Table 3.4. In case of higher water production is required than power, the third cycle of type 1.C is likely a proper configuration. In this configuration, case 1.C, a set of natural gas burners can be situated in the waste gas stream, in order to elevate the temperature and thus the recovery steam. In this technique, a maximum steam/water production increased approximating 30%. Higher recovery rate would require higher gas temperatures, which would necessitate a change in boiler materials and design criteria, and as a consequence this is not recommended.

However, in Qatar this configuration 1.C is employed in Ras-Abu Fontas-A power and desalination plant, were the water demand is very high. This configuration has some disadvantages that any defect in the heat recovery boiler such as tube leakage may trip the gas turbine.

Configuration 1

	Type 1.A	Type 1.B	Type 1.C
Steam Characteristics (ton/h – bar- °C)	270; 20; 215	217; 12.5; 135	346; 110; 540
Back pressure turbine electric power, MW	0	35	0
Overall cycle electric power generation	120	155	120
Overall cycle steam production, ton/h	284	231	360

Table 3.4. Comparison Between Type 1A, 1B, and 1C. Data are referred to cogeneration plant with one gas turbine 120 MW (Borsani, Superina and Sommariva, 1995).

3.11.2 Fired Boiler - Back Pressure Turbine

Configuration 2 is the cycle which represents an advance over of the simple electric power production. It comprises a fired boiler, which supplies steam only to the desalination plant. As a consequence, high pressure and temperature steam can be utilized to produce an additional electric power by the supplied steam through a back pressure turbine, Fig 3.20. The distiller ejector system in this configuration obtains the steam either from an extraction on turbine or from a pressure reducing station fed on high-pressure steam. In this type the combination of steam pressure and temperature must be selected in order to ensure that the back pressure steam still maintains some amount of superheating.

It is apparent that a range of power generation values prevails, for the same steam production, depending on the steam characteristics. However, the thermal cycle

operating with very high characteristics steam becomes excessively complex to be justified for an application, which produce a relatively low power production. The reference value of the ratio of electric/water generation for cycles with configuration 2 is much lower than that of cycles 1. The actual ratio during plant operation can be altered from this reference value down to zero, by partially by-passing the back pressure turbine. This action can effectively be employed to compensate for the reduction in electric demand, while water demand is not decreasing in the same way. Therefore, this infers deterioration in the efficiency of the steam production.

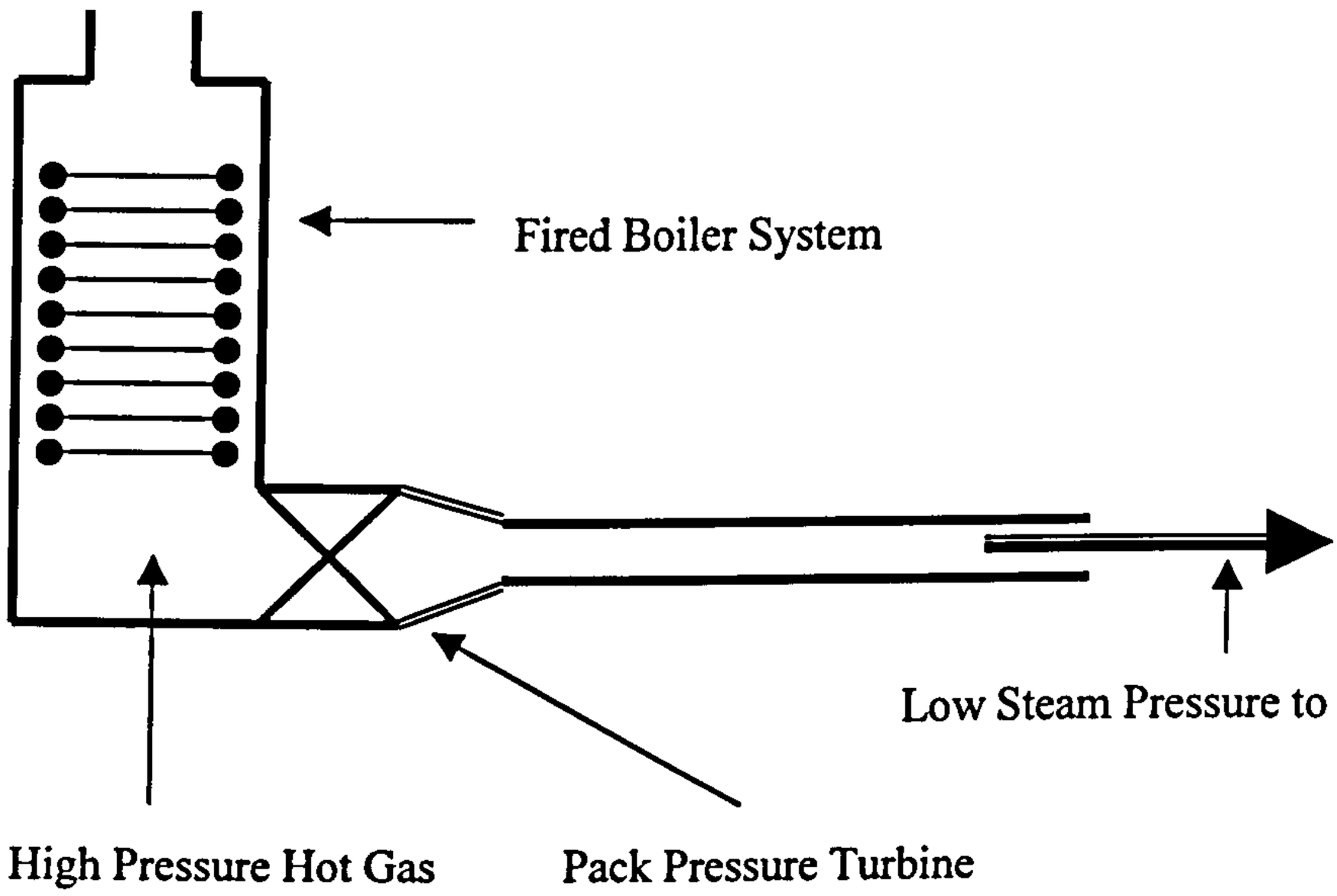

Fig 3.20. Fired Boiler With Back Pressure Turbine Configuration 2.

3.11.3 Fired Boiler – Condensation Turbine

In contrast to the cycles of configuration 2, a condensing or steam turbine-based cycle can be constructed. In configuration 3, the steam from the condensing turbine is extracted for the requirements of the desalination plant, Fig 3.21. Compared with cycle of configuration 2, higher power production levels are produced for the same feed steam characteristics to the turbine and the same water production level. Due to a minimum steam requirement to the low pressure section of the turbine, the extraction steam can be represent only as a fraction of the total steam produced. Theses plants are inherently more complicated with respect to cycles of configuration 2, and the steam characteristics are higher. Conventionally, these are selected when a power

station, with desalinated water as by-product, are required. The ratio of electric/water production can be varied between a minimum and a maximum, which theoretically has no limits, and can in reality also be very substantial for large-scale power stations coupled with small desalination plants.

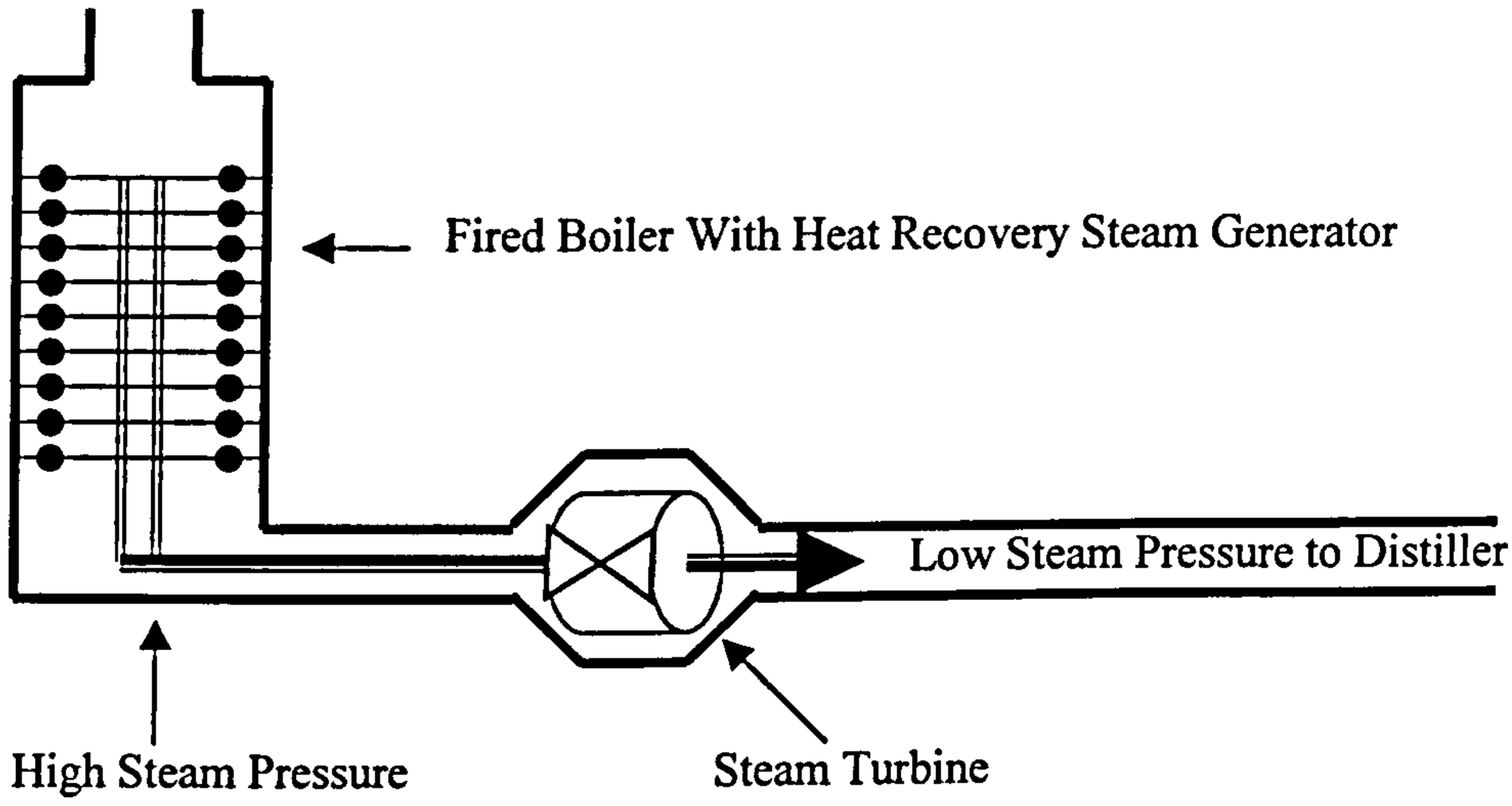

Fig 3.21. Fired Boiler With Steam Turbine Configuration 3.

It was found that back pressure turbine applications are generally limited to lower power production levels, both as absolute values and in relation to desalinated water requirements. For bigger power stations, the choice between cycles of configuration 1 and 3 depends on the specific requirements to be met. As a general consideration, it can be noticed that gas turbine cogeneration cycles are cheaper and energetically more efficient; while condensation cycles can be more flexible and can sustain a larger unit size.

However, the operation hours and lifetime of a condensate turbine exceeds that of a gas turbine. The characteristic low maintenance requirements for condensing turbine probably reflect the fact that it is operated by clean steam, which exert a significant influence on the long-term cost of the plant operation. However, it must be recognized that the greater flexibility associated with condensate turbines is intended as capacity to produce higher electric power/water ratios, while the minimum value is comparable to that of the cycle 1.C, with after-burners. Furthermore, not only the electric

efficiency, but also the unit size of gas turbines are rapidly growing; and this confers a general advantage to this type of system (Gunzbourg,1998).

3.12 Comparison of MED with MSF

Compared to the very low recovery in an MSF plant, the MED process performs satisfactorily. It is able to recover 40-65% of the feed. A high temperature in the MSF plant can result in the recovery of about 25-50%. The MSF process utilized sensible heating. This significantly reduces the effective utilization of the available heat transfer temperature difference. In the MED process, concurrent condensation opposite evaporation creates a constant temperature difference down the tube. This increases the utilization of the available temperature difference (Mockler, 1987; Memotechnique, 1999)

Moreover, the MED process, has many advantages, such as, simplicity and compact construction, operation without recirculation, low pumping power, high performance ratio/unit of installed heat transfer surface area and stable operation. The temperature of the heat source supplied by the solar collector (60-75 °C) matches that required for low temperature MED desalination plants operating at a top brine temperature of 50-60 °C. On the other hand, the MSF system has some disadvantages namely; the performance ratio is limited, there are low heat transfer coefficients, and any leaks in the tubes can result in serious product contamination. However, the MSF process can be constructed to produce very large capacities, the performance ratio is not directly related to the number of stages, and it is less effected by fouling compared to the MED process.

3.13 Materials for Desalination Plant

Many factors can be important in dictating the choice of materials for specific purposes. In general, when considering the design and construction of desalination plant, the major factors governing the choice of materials for the various components are cost, corrosion resistance, and mechanical strength. It is clear that material practice has been largely founded upon economic considerations. In fact, under the intense pressure of competition, the tendency has been to utilize the cheapest materials. It is convenient to consider desalination materials under the following:

(i) Flash Chambers

The conventional material for these applications has been ordinary structural Carbon Steel. Selection of material is strongly recommended on economic, mechanical property and fabricability grounds. However, it has poor corrosion resistance. Thus, in large plants economic considerations necessitate the retention of carbon steel. A cladding of stainless steel 316L layer is, typically 3 mm thickness, of the first few high temperature flash chambers. The remainder of the plant is normally fabricated of carbon steel, which painted with epoxy paint.

(ii) Heat Exchanger Tubes

In thermal desalination processes, a copper-nickel alloy was often employed for the brine heater and heat rejection section. Some researches have recommended that titanium tubes should be used, but the economic arguments generally indicate that a 70/30 copper-nickel is ratio adequate. Regarding the heat transfer surface, the general practise since the inception of multistage flash evaporation, has been to utilize those tube materials generally available in the market. This has led to an almost exclusive use of aluminium brass particularly in heat recovery section. The major advantages of this set-up in lower heat transfer resistance combined with the already established means of manufacturing quality control.

(iii) Tubeplate Materials

Although considerable debate has taken place concerning the performance and durability of the tubes, there has been relatively little debate concerning tubeplate materials, steel tubeplates clad with copper-nickel, which offer strength advantages similar those of aluminium bronze. However, doubt exists concerning the thickness of cladding necessary to secure a seal at the tube expansion.

(iv) Waterboxes

Waterboxes functions under onerous flow conditions involving velocity changes, abrasion, and water-hummer risks. Moreover, the risk of galvanic stage between the predominantly copper alloy tube/tubeplate region and the steel of the waterbox makes a protective coating or lining mandatory. Basically, the load-bearing material of a given waterbox is carbon steel with either a copper-nickel or monel lining where severe conditions are frequently forecast.

3.14 Chemical Treatment Requirements

The requirements for chemical additions to the various fluids involved in the MED and MSF distillation are very essential to improve the system performance. In this section, the general chemicals required during the various distillation processes are discussed.

(i) Chlorination

The pre-treatment of the typical seawater by chlorination prior to processing in a distillation plant is practiced for the purpose of preventing the growth of marine animal and plant life within the intake cooling seawater. The presence of chlorine in the seawater retained during a shutdown will result in the production undesirable hydrogen sulphide (H_2S). The required dosing rate is of 1 mg/l, which frequently leaves a noticeable residue at the intake seawater exit. The majority of desalination plants produced the required of chlorine by seawater ion exchange process in cells.

(ii) Acid Addition

The use of acid, either sulphuric or hydrochloric, allows higher heat transfer values to be obtained by reducing the alkaline depositions on the heat transfer surfaces. However, it can also accelerate corrosion in the evaporator tubes once the pH control is not strictly adhered to. The upper limits on temperature and brine concentration using acid are about 120 °C and 65g/l.

(iii) Polyphosphates

Feed water treatment with polyphosphates such as 'Hagerap' or 'Calgon' precipitate in the form of a non-adhesive sludge and is deposited on the evaporator/condenser tubes. There, the maximum temperature is restricted to 91 °C.

(iv) Anti-Scale

'Belgared' or 'Flocon' scale prevention is widely used in desalination plant. These allow the plant to be operated at higher temperatures giving flash ranges comparable with those obtainable with acid-dosed plants. These comkgs inhibit scale formation and produce crystal distortion, which prevents individually precipitated particles from sticking to each other or to metal surfaces.

(v) Anti-foam

The use of surface-active agents or anti-foams has become a more widely accepted practice, as their use enables lower disengagement heights to be used in the flash chambers. The release of carbon dioxide within the flash chamber when an additive treatment is used tends to create a foam, which can result in overloading of the vapour separators with a consequent unacceptable purity of the water produced. Anti-foaming agents such as alcoholic comkgs with rate of 0.1-0.5 mg/l of feed quantity can successfully suppress this tendency.

3.15 Reverse Osmosis Distillation

Reverse osmosis has been developed in direct competition to the other desalination processes. This process appeal lies in the fact that it requires no heat. It needs electrical energy only and can be operated at ambient temperature. In general, other distillation processes require that the saline water be heated up to the 90-120 °C range. Seawater is vaporized and the vapours condensed to obtain the distillate. RO, operates with low energy requirements in one phase only.

Reverse osmosis plant maybe split into two major categories depending on the type of feed water used; seawater plants and brackish water plant. The design philosophy tends to be different for each situation. Seawater plants generally operate on a feed supply of somewhere between 39-50 g/l TDS and are usually located near the cost. Hence there is no problem with brine disposal and so it is possible to operate the plants at a relatively low recovery ratio. Brackish water plants on the other hand tend to be using feed water between 2-10 g/l TDS and may also be located inland where there maybe a serious problem with the disposal of concentrated brine reject without polluting local water sources (Glueckstern, 1999).

3.15.1 Principal of Reverse Osmosis

The reverse osmosis process operates on the opposite principle to osmosis. Osmosis is a natural process, whereby pure water flows through a membrane from a less concentrated to a more concentrated solution. If a saline solution in contact with a semi-permeable membrane is placed under pressure, which is in excess of its osmotic pressure, water from the solution will flow through the membrane. Water flow will continue till the pressure created by the osmotic head equals the osmotic pressure of

the salt solution. The energy required to operate the process varies with the osmotic pressure of the solution, which increases with an increase in salinity. This fact imposes constraints on the membrane life and performance.

The principal of the process is illustrated in Fig 3.22. Once a semi-permeable membrane is placed between seawater and fresh water, both are kept at the same pressure, diffusion of seawater into fresh water will occur because of nature's tendency to equalize concentrations. This process, called osmosis, is exactly the reverse of the desired action, namely, the transfer of water from the salt solution into the fresh water section. To persuade the process/stage to proceed in the desired direction, pressure (c) must be exerted on the seawater.

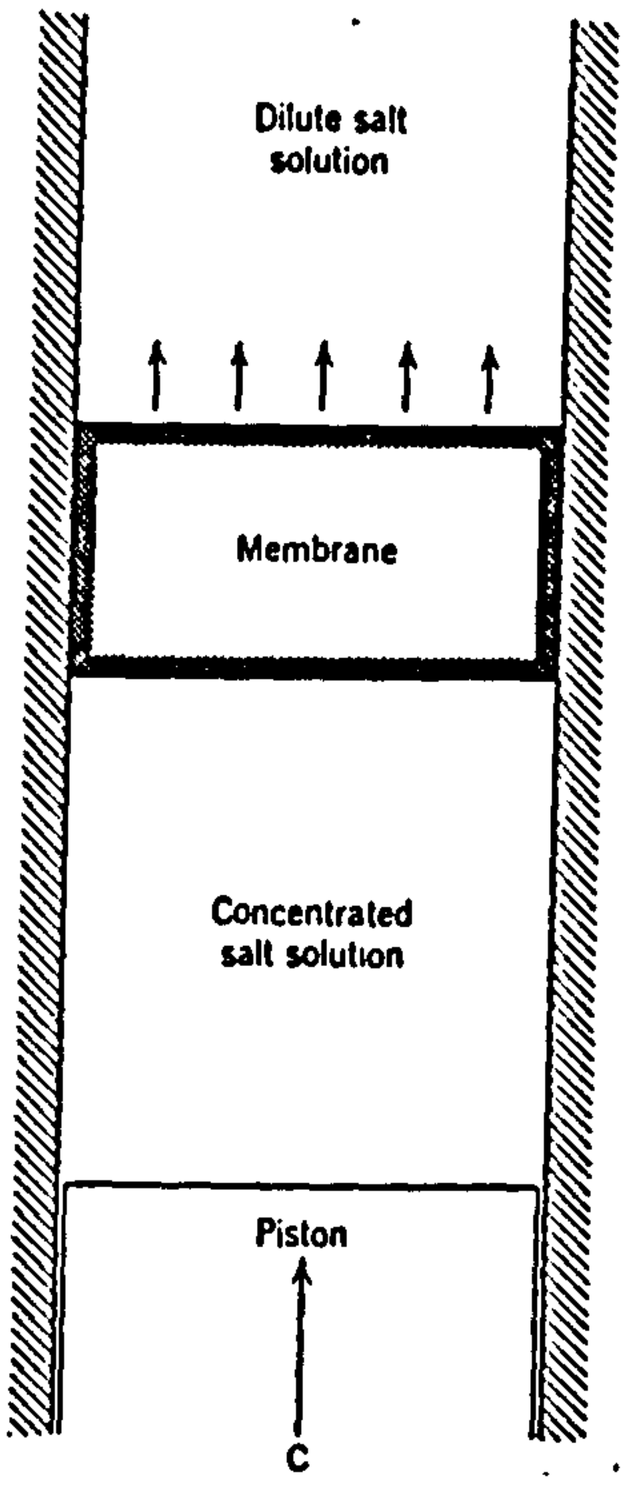

Fig 3.22. Principle of Reverse Osmosis Theory (Spiegler, 1981).

This is the principle membrane reliant process, which employed in water desalination. Osmosis membranes act as a filter, which retain all particles bigger than 1 Angstrom as well as any monovalent and bivalent ions. For water to pass through the semi-permeable membranes, pressure greater than the osmotic pressure, which is 32 bars for seawater of 40 g/l salt content, has to be applied. The reverse osmosis process is sensitive to qualitative variations in inlet water. Whereas this process is ideally suited to brackish water, its use is considered less appropriate in the case of seawater, which

is a living, changing, and complex medium. Furthermore, to avoid problems linked to clogging of the membranes, an efficient pretreatment system upstream of the reverse osmosis process is required. This means that the water is routinely chlorinated, filtered, and then dechlorinated, before actually being desalinated. The first commercial seawater RO plants were commissioned in the late 70's and presently account for 25% of the worldwide desalting capacity. The largest seawater reverse osmosis plant built so far is the one in Ghar-Lapsi, Malta. It become fully operational in February 1983. Its production capacity of 22500 m^3 a day for a feed with a total concentration of 38,9 g/l dissolved salts (Hasnain, 1998).

3.15.2 Reverse Osmosis General Operation Process

Seawater is pretreated, filtered, and then pumped using a high pressure feed pump through modules containing semi-permeable membranes as shown in Fig 3.23. The required pressure is 25-40 bars more than the osmotic pressure to generate the additional driving force required. At the membranes, separation of most of the salts occurs. The feed water is separated by the module into two streams. The permeate passes through the membranes due to the high pressure, while the concentrated brine is continuously rejected through a flow control valve. This ensures that there is no precipitation of supersaturated constituents in the brine, these can cause plugging of the membranes and reduce the flux rate through it.

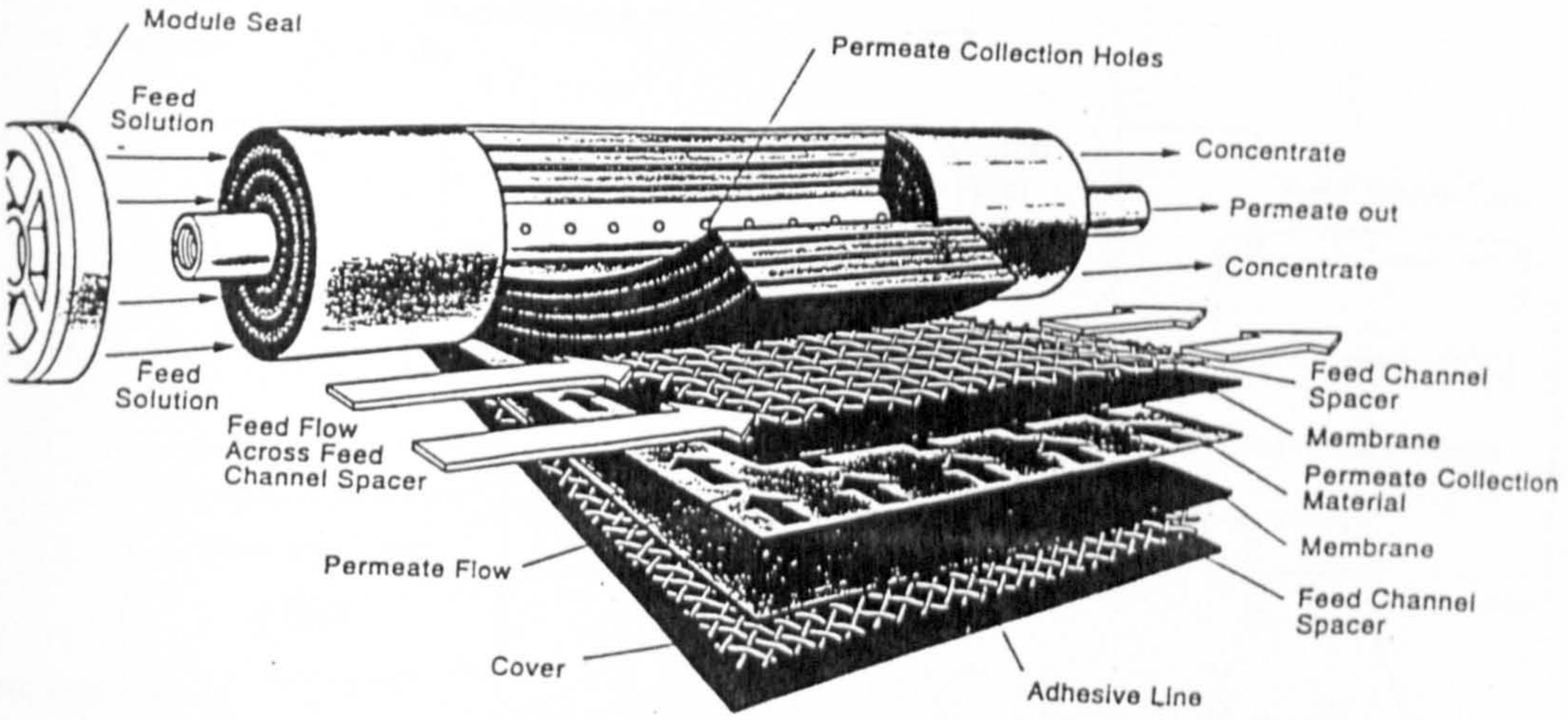

Fig 3.23. Reverse Osmosis Membrane Element (Herold,1998).

Moreover, if there is no blowdown, the progressively increasing concentration of dissolved salts would require the intervention of a pump to generate increased energy to overcome the increased natural osmotic pressure. The brine is pumped into the sea. To facilitate a satisfactory flow of fresh water, the applied pressure has to substantially exceed the osmotic pressure. The major energy consumed by the RO process is that utilized to pressurizing the feed water through the membranes (Gocht, 1998).

3.15.3 System Description

As illustrated in Fig 3.24, the reverse osmosis plant cane be divided into the following components: -

3.15.4 Raw Water Intake

The raw water intake system usually incorporate a well field adjacent to the beach, whereby 5 to 6 individual wells are required to supply a medium-size plant (capacity of 9,000 m^3/day) operation, plus the insurance of two standby wells. The required raw water flow from the well field during maximum plant operation is approximately 986 m^3/hour.

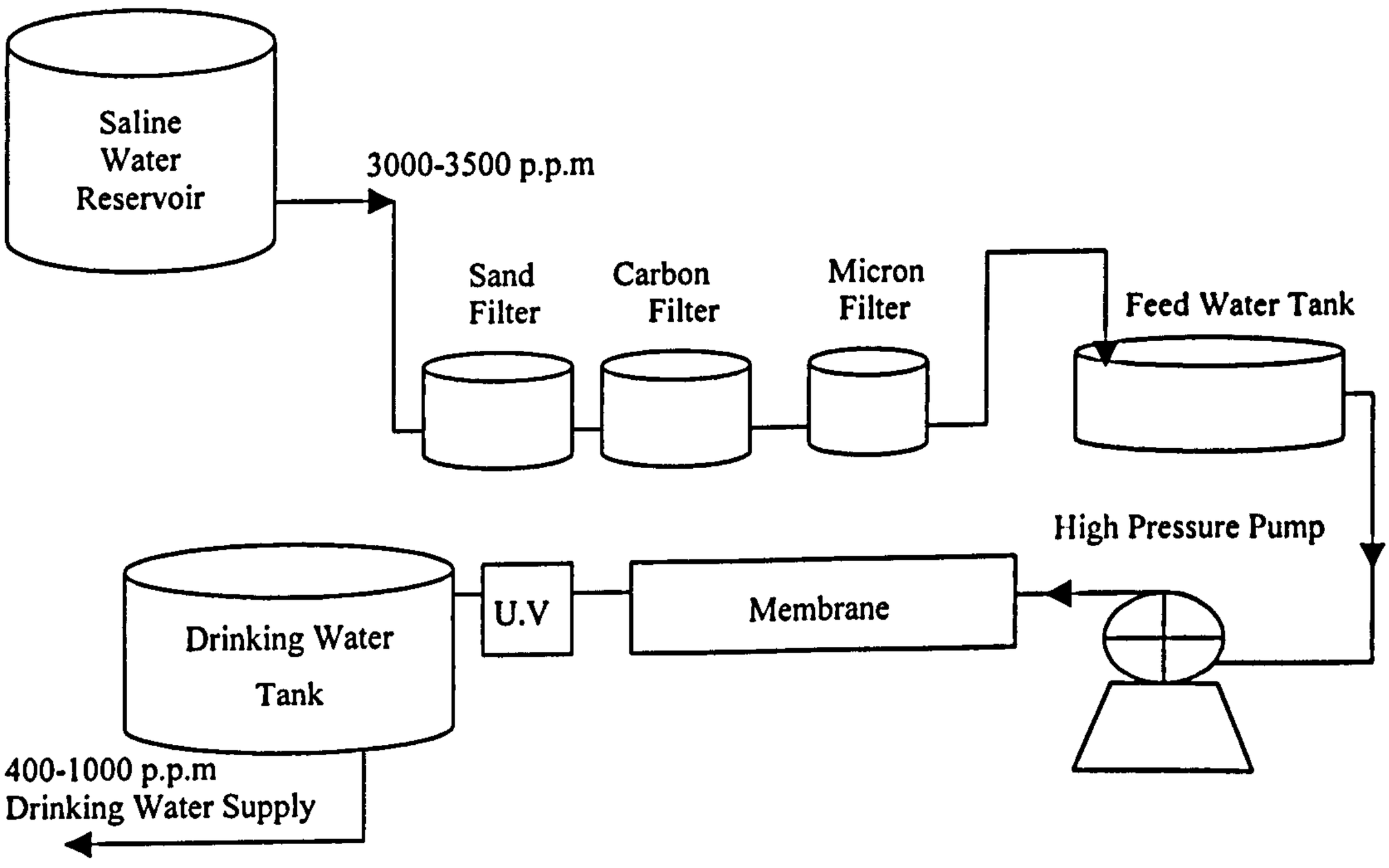

Fig 3.24. Simplified diagram of typical reverse osmosis plant (Glueckstren, 1999).

3.15.5 Pre-treatment

3.15.6 Chlorination and Flocculation

In advance of the water inlet to the sand-filter station at the plant, the raw water is chlorinated to avoid marine life and biological growth in the membranes, which result in to heavy biofouling and is a major recognized problem of plant operation. The chlorination is achieved with chlorine gas, which is introduced through duplicate chlorinators in the booster line, which transfers the chlorine solution to the raw water line. The required residual chlorine in the raw water for a plant operation is minimum 1 mg/l. Another additive is used to prevent of oxidation of the raw feed water, this is achieved by adding the flocculation agent $FeCl_3$ at the dosing station.

(ii) Filtration and Filter Water Storage Tank

Prior to the beginning of the mechanical pre-filtration of the raw water sufficient numbers of pressure sandfilters are installed which are filled with two layers of filtersand. The filters are usually made out of steel, internally lined with hard rubber with a nozzle shape floor, the filter diameter is 3-5 microns which is sufficiently small enough to prevent any solid substances occurring at the feed water, which may damage the membranes. The raw water velocity through the filters is adjusted to approximately 13 m/hour. Provided that all filters are on stream, filter backwash of one filter can be performed during operation without effecting the overall operation of the plant when the differential pressure across the inlet and outlet of the sandfilter exceeds 1.5 bar. After filtration the filtered water is transferred to the filtered water tank, which consists of a bolted steel tank. Prior to the sandfilter station the following raw water parameters are measured: flow, temperature, pH-value, conductivity, and free chlorine.

(iii) pH-Adjustment and Reduction of Free Chlorine

In order to reduce the risk of calcium carbonate scaling on the membranes the pH-value has to be reduced to approximately 6 by the addition of sulphuric acid (H_2SO_4). The free chlorine prior to the cartridge filters is reduced by dosing the water with sodium bisulfite ($NaHSO_3$), in order to avoid damage of the membranes by the impact of the chlorine.

(iv) Finefiltration

In this stage, the water is cleaned in cartridge filters, which are loaded with filter cartridges of 10 micron rating. After the finefilters, the water is transferred to the RO-system.

3.15.7 Membranes Process

In the membrane stage the seawater is processed to drinking water through membranes and brine concentrates on the other side. The reverse osmosis plant usually comprises of several membranes depending on the membranes design and plant size. This process can be divided into the following components: -

(i) High Pressure Pump Station

The high pressure pumping station is required to present the required seawater to the membranes with a high pressure to overcome the osmotic pressure of the water, thereby allowing the permeate water to pass through the membranes. In advance of the high-pressure pumps, the raw water is available at a pressure of 2 bar. Subsequently, the high-pressure pump, provides the system with a maximum pressure of 69 bar at the RO-membranes.

(ii) The Membranes

The main aim of utilizing membranes in RO is, which can separate salt from seawater. This separation is caused by an extremely thin dense skin, while the rest of the membrane is quite permeable. These membranes are thin, sheet like materials, which are usually permeable to some species and impermeable to others. These membranes allow water to pass through and 90-99% of all inorganic substances in solution, 95-99% of the organic constituents, and almost 100% of the finely divided colloidal matter are retained. RO membranes have two distinct layers. One is a spongy porous material, which is highly permeable to both salt and water. A second layer, which has the primary role in separating water from a salt solution. Cellulose acetate and polyamide are the most widely adopted membranes in RO plants.

(iii) Cleaning System

The cleaning system is designed to clean individual RO-membranes at a time. The cleaning system incorporates a tank, a cleaning pump, a cartridge filter, and

auxiliaries. The cleaning solution is to be prepared in the cleaning tank and circulated through the module racks.

(iv) Flushing System

After every shutdown of a RO system, the system has to be flushed by permeate water in order to prevent corrosive degradation of the pumps and pipework, as well as biofouling in the system. Flushing is initiated automatically for a period of about five minutes by the flushing pump.

3.15.8 Post-treatment

The post-treatment of the permeated produced in the RO-system is performed according to the following steps, and result in the final production of high quality drinking water to the consumer.

(i) Post-chlorination

The system provided is equivalent to the pre-chlorination system, only the capacity is reduced to the prescribed level, which is usually about 0.5 mg/l.

(ii) Lime Milk Dosing Station

A lime milk dosing system is provided in order to increase the water hardness and to adjust the pH-value of the drinking water. The system consists of a storage silo, a mixing tank, two dosing pumps, two booster pumps to serve the booster line and auxiliaries.

3.15.9 Energy Requirements

Energy is the largest component of any desalination plant's operating costs. The energy requirements of the RO process are due to the requirements of the source water supply and pretreatment system, high-pressure pump, second stage pump and the product distribution pump. The largest load is due to the high-pressure pump feeding the first stage of the membrane. Electricity is used as the primary energy source. However, the RO process can be considered as the most preferred technology for both brackish and seawater for supplying fresh water to remote areas, where fresh water sources are far distant, such AL-Shamal and Abu-Samra RO Plants in Qatar.

3.16 Solar Desalination

One of the most promising options to overcoming the problem of water shortage appears to be desalination. Desalination methods are already mitigating water shortages in parts of the world adjacent to the sea or saline bodies of water by desalination plants. In general, these plants run on fossil fuels, which occur in finite reserves and most importunately, contribute to environmental pollution. Therefore, it seems obvious to identify some other methods of desalination reliant upon renewable sources of energy, such as; solar, wind, and biomass. Solar desalination can be used to purify either seawater or brackish water in areas, which lack potable water and are subject to abundant solar radiation. A good example of such an area is provided by regions in the Middle East, Sayigh (1977).

Solar desalination [SD], shares similarities with the natural hydrologic cycle, which consists of: (i) absorption of solar radiation by the top layers of water in oceans, lakes and rivers, (ii) heating up these layers, (iii) evaporation of the water, (iv) transport of the resulting vapour to cooler regions and (v) condensation of the vapour leading to precipitation as e.g. rain or snow (Menguy, 1980). A simple basin type solar still can illustrate this process, which is schematically shown in Fig 3.25. A shallow, blackened basin of saline water is covered with a sloping transparent roof. Solar radiation that passes through the glass roof heats the water and the blackened basin. Therefore it allows the water to evaporate, which then condenses on the underside of the glass cover and collects in the distillate tray as fresh water. The brine water drains out of the basin via the brine trough as rejected water.

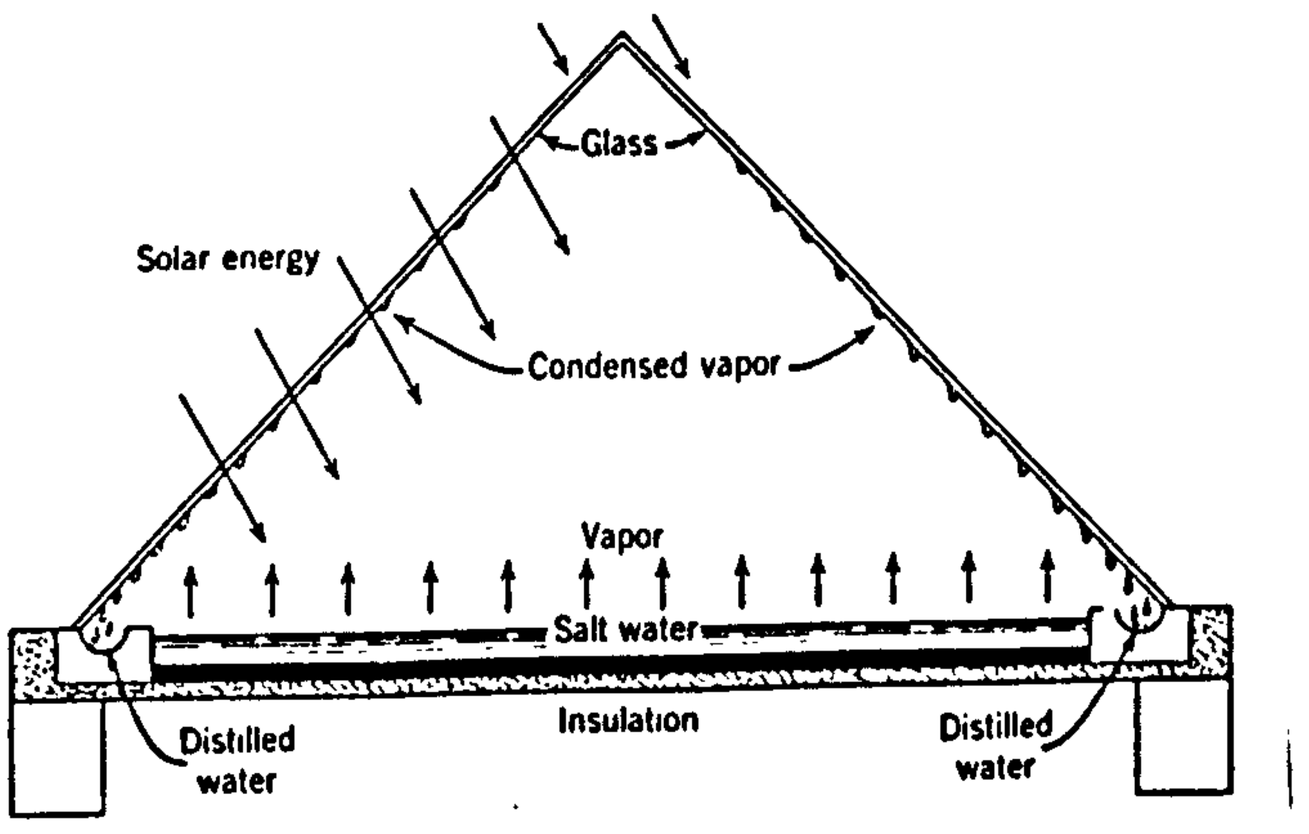

Fig 3.25. Principal of solar still (Spiegler, 1981).

3.16.1 Solar Desalination An Overview:

Solar desalination has been known for a long-time. According to Malik *et al.*, 1982, the first recorded use of solar distillation of seawater, is that of the Arab alchemists in the 15th century reported by Mouchot in 1869. For this venture, some kind of glass vessel was employed to distil the water. It has been utilized particularly for supplying fresh water to small communities, where the natural supplies are inadequate or of poor quality, and where solar radiation is plentiful. The basic approach of distilling saline water using solar energy can be likened to the natural hydrologic cycle. However, in desalination the process can be replicated on a much smaller commercial scale.

The technology of desalination first stated when a Swedish Engineer, who in 1872 designed and built a solar desalination plant in Northern Chile. This 47,00 m^2 total surface area plant consisted of 68 solar still unites. Each unite comprised of a wooden bay of 1.14 m wide and 61 m long, which was covered with ordinary glass. This plant continued to operate for more than 50 years and was producing approximately 340 litres/day of fresh water. The demand for solar desalination increased dramatically during World War II, when the USA army investigated a simple type of solar desalination as depicted in Fig 3.26. The ordinary type of solar still was developed to be more portable, more applicable for use by the USA Navy and Airforce in life raft. The Life Raft consisted of a black felt pad 0.2 m^2 in area which has been saturated in sea water and placed inside a transparent inflatable plastic envelope and a distillate collector connected to the bottom of the plastic envelope. The production rate of this type of solar still is around 1 litre/day of fresh water under clear conditions (Garg, 1987).

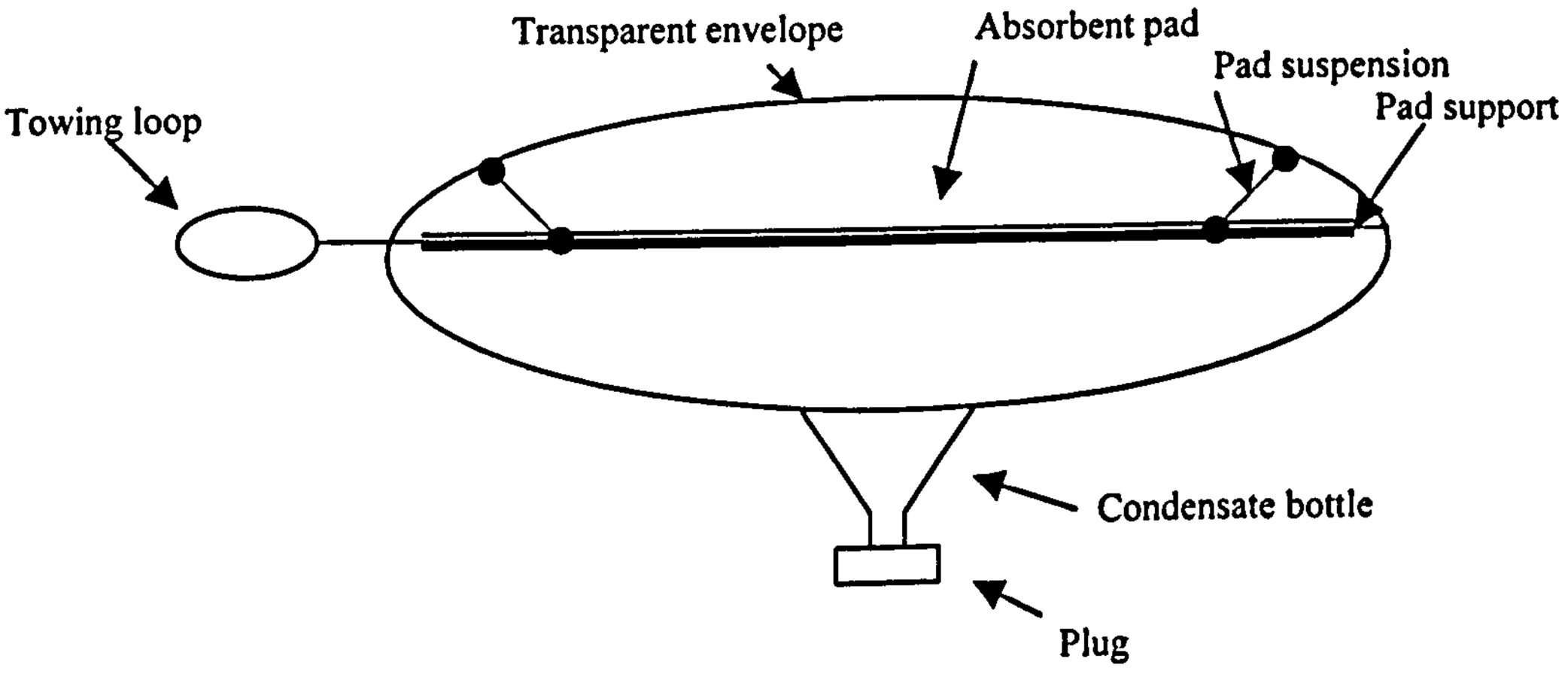

Fig 3.26. The Life Raft solar still (Garg, 1987).

3.16.2 Solar Stills

As a result of the large scale interest in solar desalination, several types of solar stills have evolved. In this work, most of the common types of solar stills have been evaluated, in particular the basin and tilted tray type solar still, with reference to the design parameters that may affect the optimal productivity of the still.

3.16.3 Basin-Type Solar Still

Although many examples have been developed and constructed on large and small scales, Fig 3.27, the conventional type of solar still, as shown in, Fig 3.28 still widely use. It consists of an insulated shallow basin lined or painted with a waterproof black material which can hold a shallow depth (50-200 mm) of saline water that will be distilled. The still is covered with a sloped glass or plastic sheet supported on an appropriate frame and sealed tightly to reduce vapour leakage. A condensing channel runs along the lower edge of the cover, which collects the distillate and transports it to the outside of the still (Hamed, 1986; Kreider, 1985).

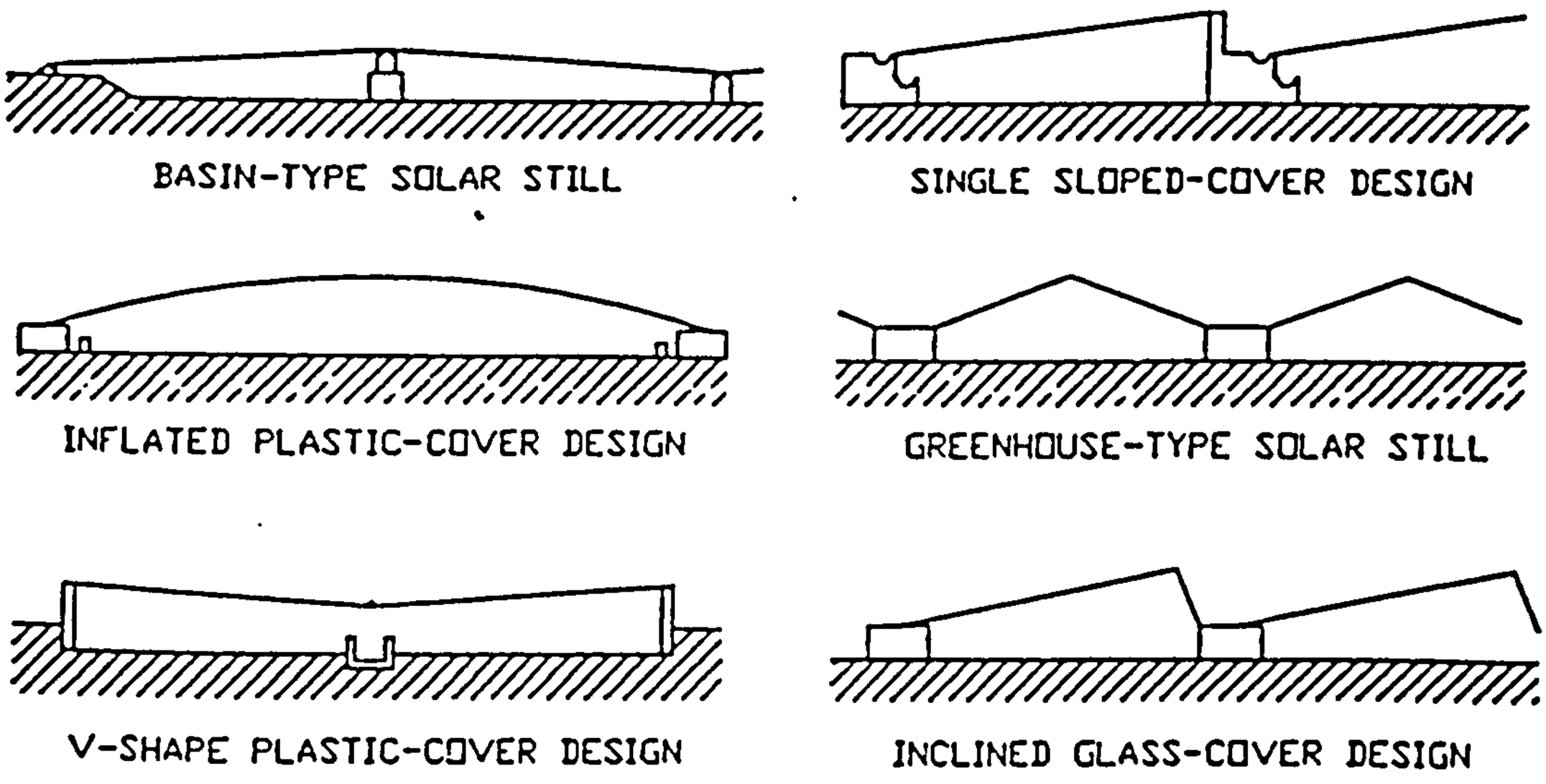

Fig 3.27. Cross-section of some typical basin type solar still (Dunkle,1961).

During operation, the principle concern is the wavelength of the thermal solar radiation range 0.3-3 μm (Lof, 1961). The portion of the spectrum that may include

most of the energy radiated by the sun (Duffie, 1980). This energy is transmitted through the transparent cover and absorbed by the water and lined basin, therefore the water temperature rises in comparison to the cover. The major portion being absorbed in the bottom of the basin, which is usually blackened by a high solar absorption material or lined with a black material. The base of the still radiates energy in the infrared region, which is partially absorbed and re-radiated back into the still by the water and the cover (Cooper, 1972; Gopinathan, 1996).

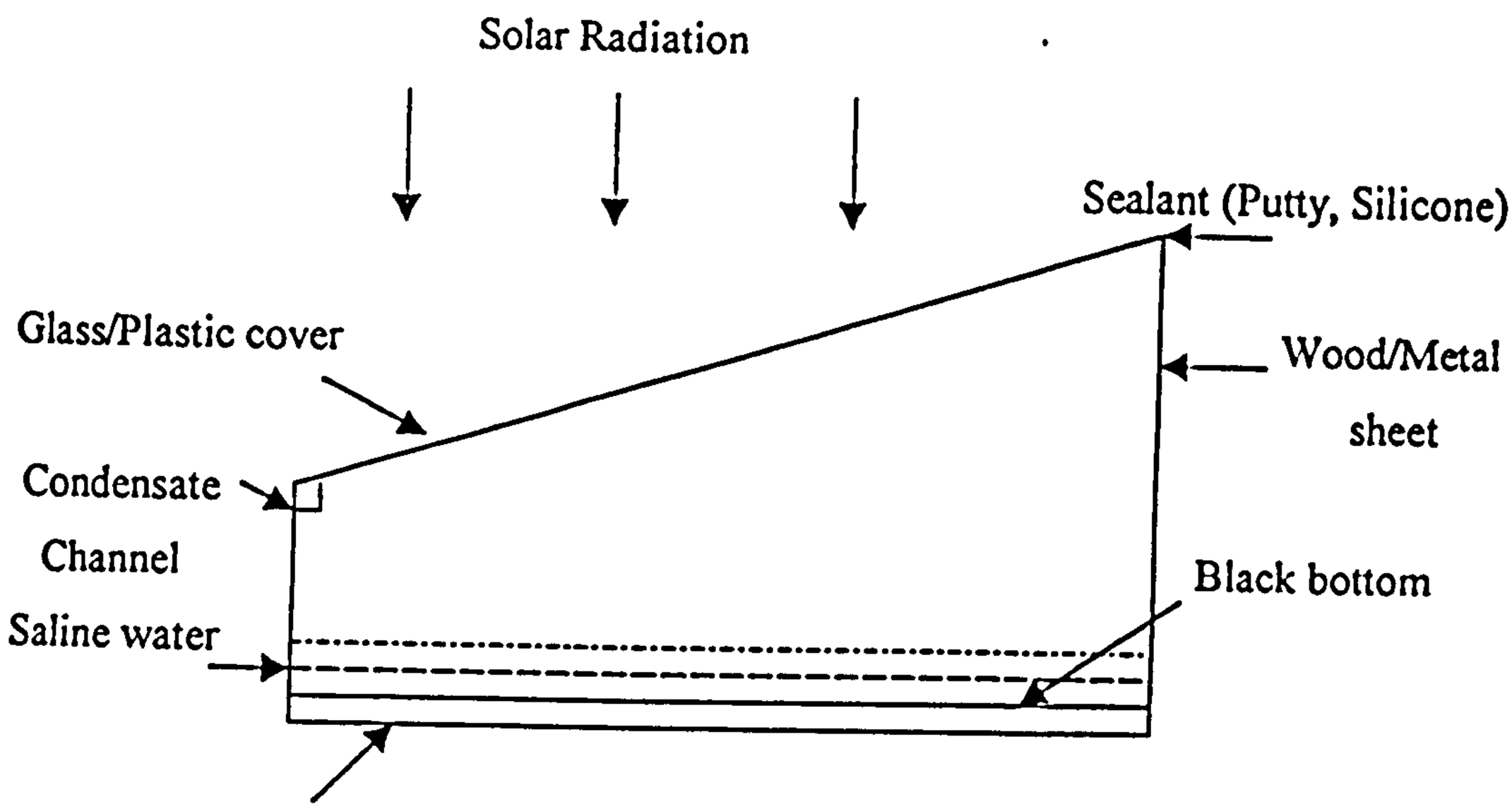

Fig 3.28. Conventional type of solar still.

Heat from the still base is transferred to the water, thereby increasing its temperature. The water now looses heat to the cover by evaporation, convection, and radiation, also by conduction through the base and edges of the still. The evaporated water from the basin increases the air moisture content in the space enclosure and consequently vapour condenses on the inner surface of the cover. The cover is sloped to allow the distillate drops to flow down into the condensation channels and through them, out of the still.

Comprehensive reviews of the theory and application of solar stills have been evaluated by many researchers. One of whom, Dunkle (1961) who analysed the basin

type still whereby the heat and mass transfer relationships were examined, along with the effect of the temperature and pressure on the still performance. Experimentally, Sayigh and El-Salam (1977) tested several single-sloped, concrete basin type solar stills in Riyadh in Saudi Arabia. The still had various thicknesses and slopes of glass cover and the water trays were covered with different solar absorbent materials, like black and red sand, black stones, straw and charcoal. Similarly, Naresh (1990), Tiwari (1994) & Porta (1997) examined the influences of the design parameters and cover tilt angle and the still orientation on the overall still performance and productivity.

Several attempts have been made to improve the efficiency of the basin type solar still, recommendations include the following: -

- Durable materials should be used in it is construction.
- The cover should be thin and have excellent transparency e.g. glass.
- The layer of saline water should be as thin as possible.
- The distance between the cover and the water surface should be as small as possible.
- The whole enclosure should be airtight.

However, the efficiency of the still was insufficient to produce adequate supply of water, which has been improved some of in the other stills, for example the tilted-tray solar stills.

3.16.4 Tilted Tray Solar Still

Tilted-tray or inclined stepped stills, shown in Fig 3.29, have been constructed and studied carefully by Tleimate and Howe in 1966 at the University of California, USA (Howe and Tleimate, 1973; Tanaka *et al*, 1983). The still is sloped at an opportune angle. Usually equal to the latitude of the location, so that direct radiation is received at near normal incidence. The still comprises of a series of steps or trays, with narrow widths and shallow depths of water with insulation on the near side and a glass cover on the exposed side, parallel to the tilted tray. The higher performance characteristic of this type of unit is shown in this comparison with the other basin-type stills.

During operation, the saline or brackish water which is supplied at the top of the tray flows down these inclined surface and finally drains at the bottom of the still. The desalinate water is collected in a trough attached to the glass cover at its lower end. This tilted-tray solar still has produced better results. It can be seen from Fig 3.30 that during sunshine hours, the tilted-tray solar still operates at an average water temperature of about 60°C, while the water temperature in the deep basin solar still is only 40°C (Selcuk, 1964). However, the efficiency of tilted-tray solar stills is reduced during the nighttime, but as a result of the high heat capacity of the deep basin solar still, the water remains warmer and the distilled water is produced while the water in the tilted-tray solar still becomes cooler in the evenings.

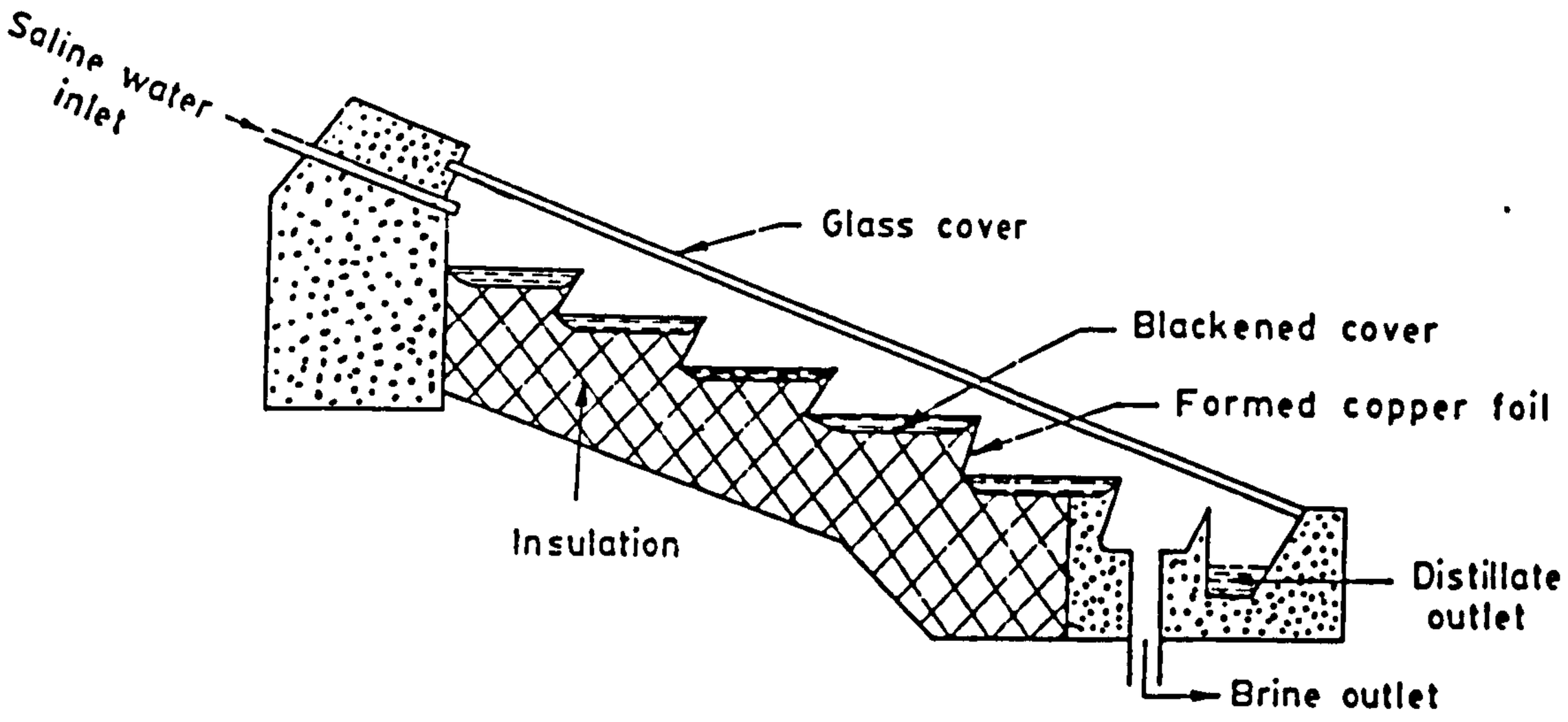

Fig 3.29. Cross-section of tilted tray solar still (Howe, 1973).

In 1973, Achilov conducted an experimental study on a tilted-tray solar still. The aim of this study was to investigate and determine the optimum distance between the evaporation and condensing surfaces, the optimum number of steps and value of step height. Maximum output was recorded in the still when this distance was 90-100 mm, the number of steps or trays was to be 10-12 steps per metre width with a maximum step height of 40mm. The particular still in question has shown high productivity,

with an output range in the order of 5-6 litres/m^2 per day in summer and 1.5 - 2.3 litres/ m^2 per day in winter (Achilov, 1973).

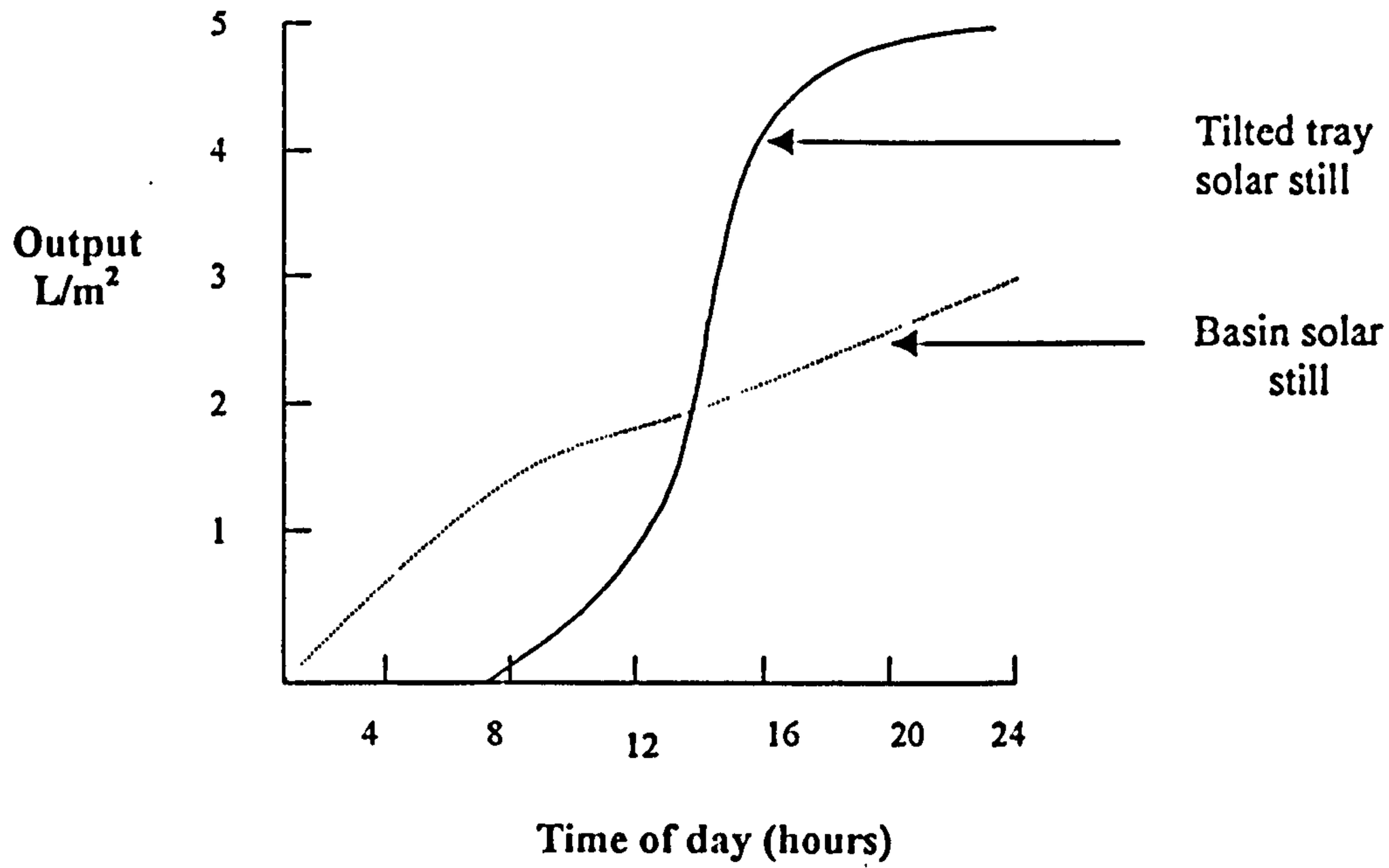

Fig 3.30. Comparison of productivity of tilted tray with basin solar still (Howe, 1973).

3.16.5 Other Types Of Tilted Tray Solar Still

In order to improve the productivity of the tilted tray solar still, many designs have been modified, a point in question is the regenerative inclined-stepped solar still which has been proposed by Akhtamov *et al.* (1978) and Lessley 1977; both added a double glazed cover, Fig 3.31. The idea being, the saline water flowing in between the glass cover is preheated to some extent. However, it has some shortcomings; namely some of the saline water components remain between the two covers, thereby gradually reducing the transmittance of the cover. As a consequence of this fact it requires continuous maintenance to maintain optimum yields.

The inclined wick-type solar still has also been developed, by the addition of a piece of blackened cloth as an absorbent surface, Fig 3.32. The purpose of this, is to provide the still with a low thermal capacity by slowing down the flow rate and ensuring wet conditions at all times. However, this process had many inherent problems, such as

the clogging of the pores of the wick with salt in the course of time, deterioration of the wick cloth, decolouring of wick cloth, and the resulting difficulty in maintaining the water flow (Moustafa, 1979; Cooper, 1987).

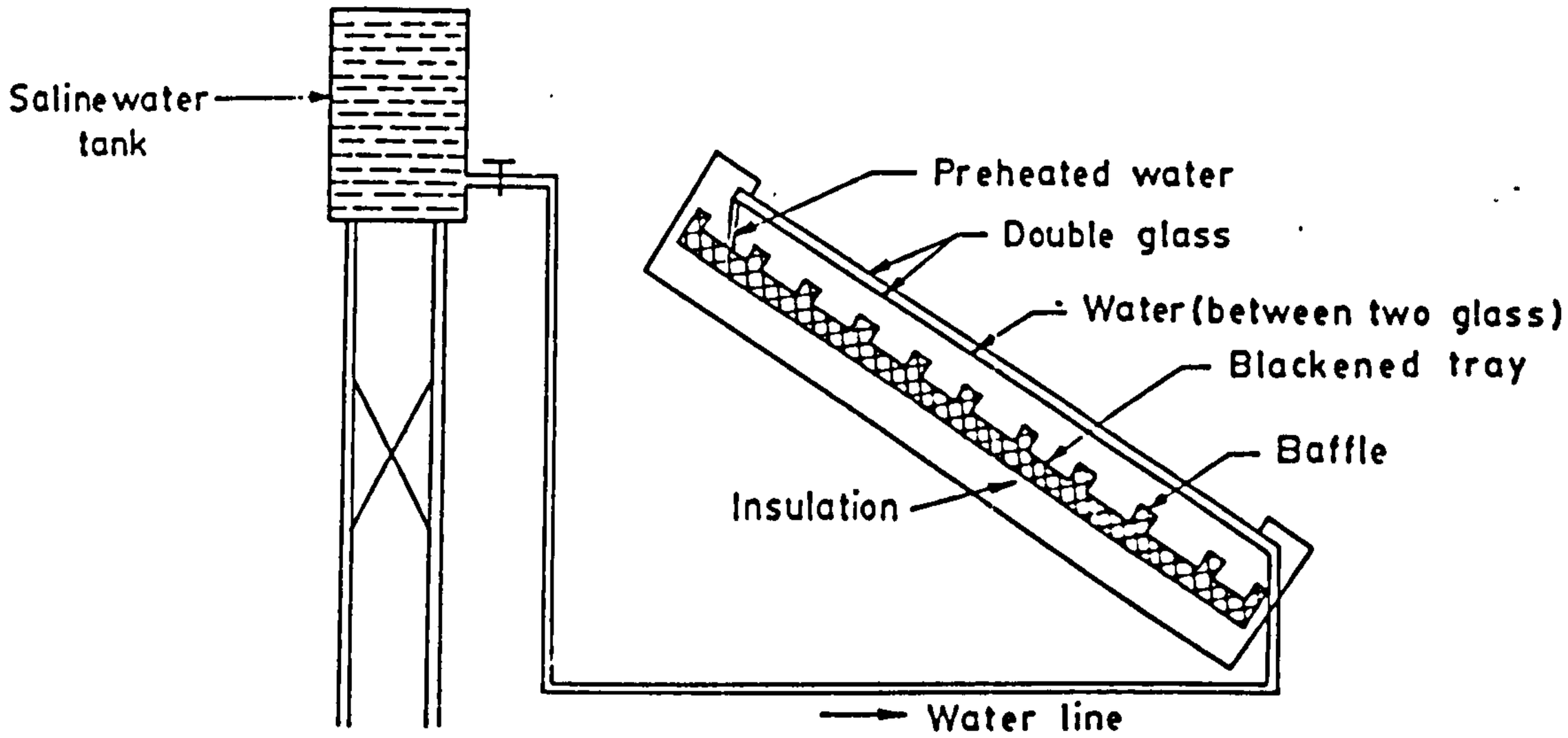

Fig 3.31. Regeneration Inclined Step solar still (Achilov, 1976).

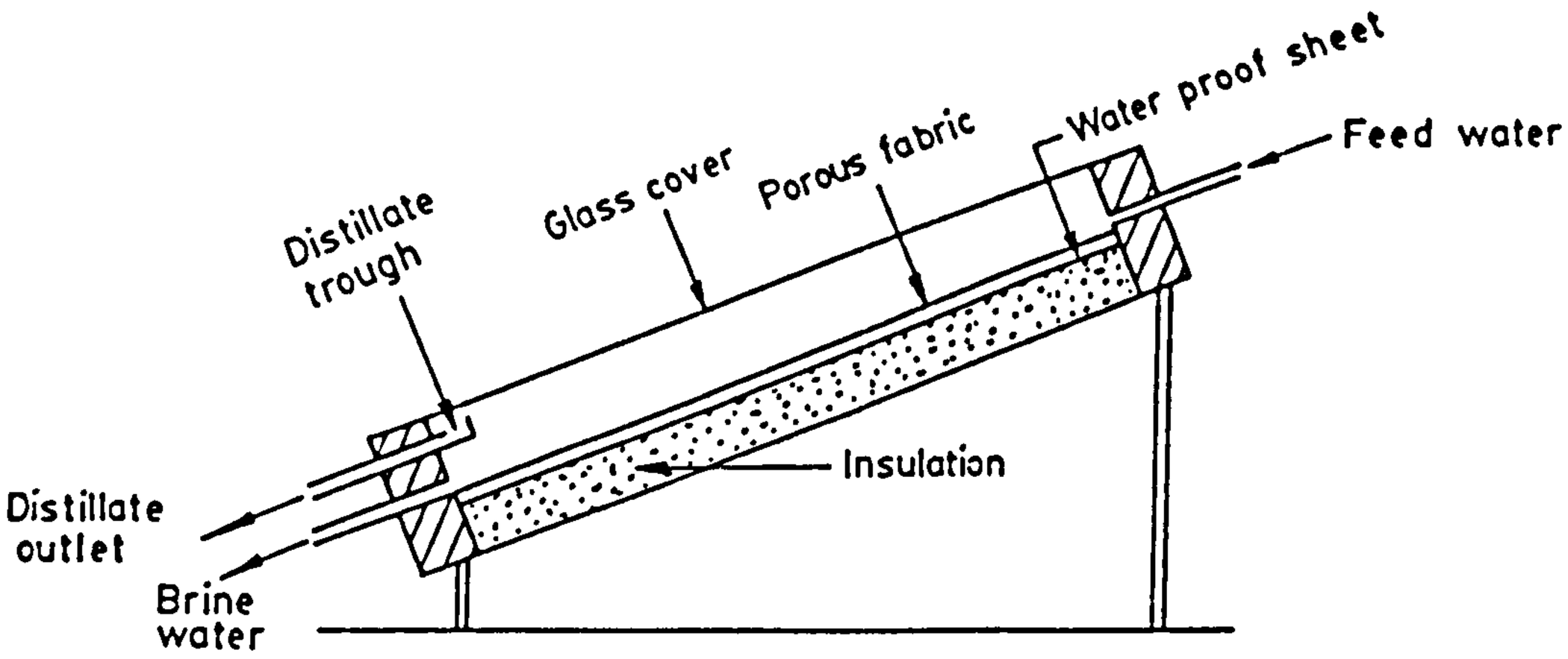

Fig 3.32. Cross-section of Tilted Wick type solar still (Garg, 1987).

3.17 Why Tilted-Tray Solar Still

In the tilted-tray solar still, both the water tray and transparent cover are at an optimum tilt angle approximately equal to the latitude of the region. So that direct radiation is received at near normal incidence, which is not possible in the basin type solar still, due to the glass cover and to water surface being horizontal. Moreover, in the basin-type solar still as water depth reduces, salt depositions can be formed along the basin layer, which dramatically decreases the energy absorption, on contrary, it is easy to approach by the flowing water system in tilted try solar still. Consequently, the heat capacity of the saline water in the tilted try solar still is minimized and the water temperature increases faster resulting in a higher distillate production. The optimum space between the basin water surface and the condensing surface can be attained easily by tilting the tray, which creates a low air thermal capacity in the still enclosure. In addition, water transfer between the tilted-tray increases the water evaporation by mixing the salt solution layers (flushing).

The water flowing system in the tilted-tray solar stills can be operated safely because it helps to decrease any algae growth within the still, which can contaminate the water, and may also affect the performance by covering the blackened absorber material. The water flowing system in the tilted-tray can reduce the salt deposition from the saline water, which increases the radiation reflectance of the trays by depositing a white layer of salt on the tray surface. Finally, the compact nature of the tilted solar still renders it portable, yet it remains simple to operate (Howe, 1973; Harpreet, 1996).

3.18 Investigation of Materials

(i) The Solar Still Absorber.

The absorber of a solar still is one of the most important components influencing its performance, because of its direct effect on the fraction of incident solar radiation mainly absorbed by the absorber metal. Therefore the absorber material should possess a high absorption and good durability. Example of the structural materials used in a solar stills include; wood, galvanized iron, aluminium, asbestos cement, masonry bricks, and concrete. It has been observed that use of wood, aluminium and galvanized iron as absorber materials is not recommended, since it corrodes and

degrades in contact with the saline or ground water. Asbestos cement is a worthwhile material, since it is not effected by the salinity. However, recent research has identified deleterious effect of this material on human health. Masonry bricks and concrete are probably the best materials for use as structural supports and are generally most durable, but its difficult to move or change the still location due to the extreme weight and, the still absorber should be treated by a waterproof layer to protect it from the saline water.

According to the energy transfer mechanism, solar radiation is primarily absorbed by the still basin liner (absorber surface), therefore the material selected should absorb more solar radiation, should be water tight, easily cleanable and should withstand temperatures of around 100°C. Asphalt matt, black butyl rubber, or black polyethylene liners are generally adopted in many solar stills. However, butyl rubber and black polyethylene film can withstand higher temperatures, which may be experienced in case where the still run dry (Matthias, 1982; Cooper, 1974).

(ii) The Solar Still Cover.

The purpose of utilizing one or more transparent covers is to minimize connective and radioactive heat losses from the basin or tray of the solar still to the environment, the object being to perform this function with minimum attenuation of incident solar radiation. The spectral absorbency of a transparent media depends on the fundamental chemical structure of the materials employed, which is due to vibration, stretching and rotational frequencies of the chemical bonds present.

The principle of the transparent cover is to allow the sun's rays to pass through the cover without giving up any significant amount of energy to the cover. Consequently, the saline water absorbs the radiation energy. Moreover, the transparent cover can function as a condenser component in the still. The radiation heats slain water in the still to a temperature higher than that of the glass cover, but lower than water's boiling point. In addition, when the radiation is reradiated form the saline water and still liner bottom at infrared wavelengths, the glass cover prevents it from escaping to the outside of the still enclosure.

Most transparent media transmit selectively; that is, transmission is a function of the wavelength of the incident radiation. Glass, the material most commonly used as a cover material in solar stills, may absorb and reflect portions of the solar spectrum. Although a glass cover is self-supporting and generally has a high long wavelength, infrared absorbency making it opaque to thermal radiation from the plate; also monolithic glass exhibits exceptional resistance to protracted weathering processes. However, a glass cover has some disadvantages in that it is vulnerable to mechanical damage, is inherently heavy, and requires special skills to install over the still.

Polymeric or plastic covers, which provide options for an alternative cover material, may be divided into two types, self-supporting plastic sheet and flexible polymeric films. However, polymeric/plastic materials can be optically distinguished from glass on three accounts; the plastic requires special treatment to make it wettable with water, it is less vulnerable to mechanical damage, light-weight, plastic films may be utilised at thicknesses that significantly reduce fundamental extinction (absorption) at solar wavelengths, thereby also increasing the solar transmittance (Duffie, 1980).

(iii) The Sealant Material

A part of the energy is lost as vapour leakage from the peripheries of the still. To prevent vapour leaks, sealing around the cover is imperative, since leakage can dramatically decrease the production rate. A wide variety of sealant materials are adopted in solar still such as tars, tapes, silicone rubber, etc. One of the major criteria for a good sealant is that it should remain resilient at very low and very high temperatures. However, silicone rubber has the added advantage that it is easily removable when the still needs to be maintained (Garg, 1987).

3.19 Conclusion

Although the increased desalination capacity has reduced the requirements for ground water; the puplic demand for this is still high. Moreover, in Al-Khor city, which is the third biggest city in Qatar, the average brackish water salinity of 2,200 mg/l, the blending with the available desalination water will reach the limit of 1,500 mg/l for drinking water by year 2002-2003 which will necessitate the immediate construction and commissioning of new desalination plants.

It can be concluded from the facts and Figures presented in this study, that by the year 2003, the water demand in Qatar would reach some 182,648 m^3 per day, assuming a successful conservation scheme. Unless additional desalination plants are constructed, the salinity of ground water will reach some 2,500 mg/l in the next few years and this will undoubtedly induce a serious non-recoverable damage to the underground natural resources.

From many techniques have been proposed for desalting seawater, only desalination process has been considered as a viable proposition. The MSF process is still favoured by most contracting authorities for very large-scale facilities (units producing between 30,000 and 50,000 m^3/day) but there has been a gradual tendency to replace it with the MED process which can represent a saving on investment of about 15%, as well as the possibility of higher efficiency levels. Where the MSF is used, between 6 and 8 kg of soft water is produced per kg of vapour; this compares with between 8 to 16 kg for the MED process. As for reverse osmosis, it would appear to be more suited to the treatment of brackish water than to seawater desalination. However, a reverse osmosis plants for medium and large capacity systems, conservation of energy, raw water, and chemicals is usually the optimal solution for both cost effectiveness and minimal impact on the environment.

Solar desalination has the obvious advantage of depending on an energy source, which is available in unlimited quantities and is free. For the isolated location with a small requirement the proper way would appear to lie in building a cheap but well engineered simple basin still. For larger outputs, tilted tray solar stills have yielded competitive outputs when compared to other types of solar still. Solar desalination has been shown to be technically feasible, however, it still require improvement in the economics and production costs. In chapter six, a comparison of those desalination processes is analysed and investigated particularly from economic viewpoint.

CHAPTER FOUR

MATHEMATICAL MODELLING OF SOLAR DESALINATION

4.1 Introduction

This chapter discusses the theoretical principles and modeling of direct solar desalination stills. This principle is involved in all solar distiller designs, which were stated and developed by many authors. Dunkle (1961) analyzed and discussed the heat and mass transfer relationships in a conventional roof type solar still. He indicated the effect of temperature and pressure on the still performance. That work was slightly modified by Morse and Read in 1968, who considered the heat and mass transfer relationships which govern the operation of solar still in the unsteady state and expressed the various heat fluxes as functions of the cover temperature. The analysis was then used to find the effects on output of changes of various parameters such as ambient temperature and heat loss from the still base.

In 1973 Cooper and Read studied both theoretical and experimental operation of the solar still. They showed that successful developments of solar stills, depends upon a design philosophy and involves a working knowledge of solar still operation. The design philosophy led to the establishment of thermal and cost criteria for selection of entrails and design of component parts. Later in 1992 Tiwari and Lawrence made attempt to derive a new formula for the convective heat transfer coefficient in a basin type solar still from the evaporating to condensing surface, including the glass cover and cavity volume.

In general, distilled water productivity from solar still depends on many variables such as climatic parameter, design factors, thermal physical properties of the material used in its construction, and operations parameters such as water depth, mass flow rate of the input saline water, and preheated in let water.

This chapter will cover the general mechanism of energy transfer, which may occur in solar still. The performance prediction of Pyramid solar still has been also investigated in this work.

4.2 Solar Still Operation Process

The principle of the solar still is illustrated in Fig 4.1. Salt water contained in a black pan covered with a sloping glass roof is heated by the sun. Incident solar radiation transmitted through the transparent cover is mainly absorbed by the saline water and

black liner basin. Since solar radiation continues to strike the water and dark receiving surface of the absorber, the water temperature rises gradually and the heat losses increase until a steady stat is reached. At that moment the rate of heat losses and useful recovery is equal to the rate of heat gained.

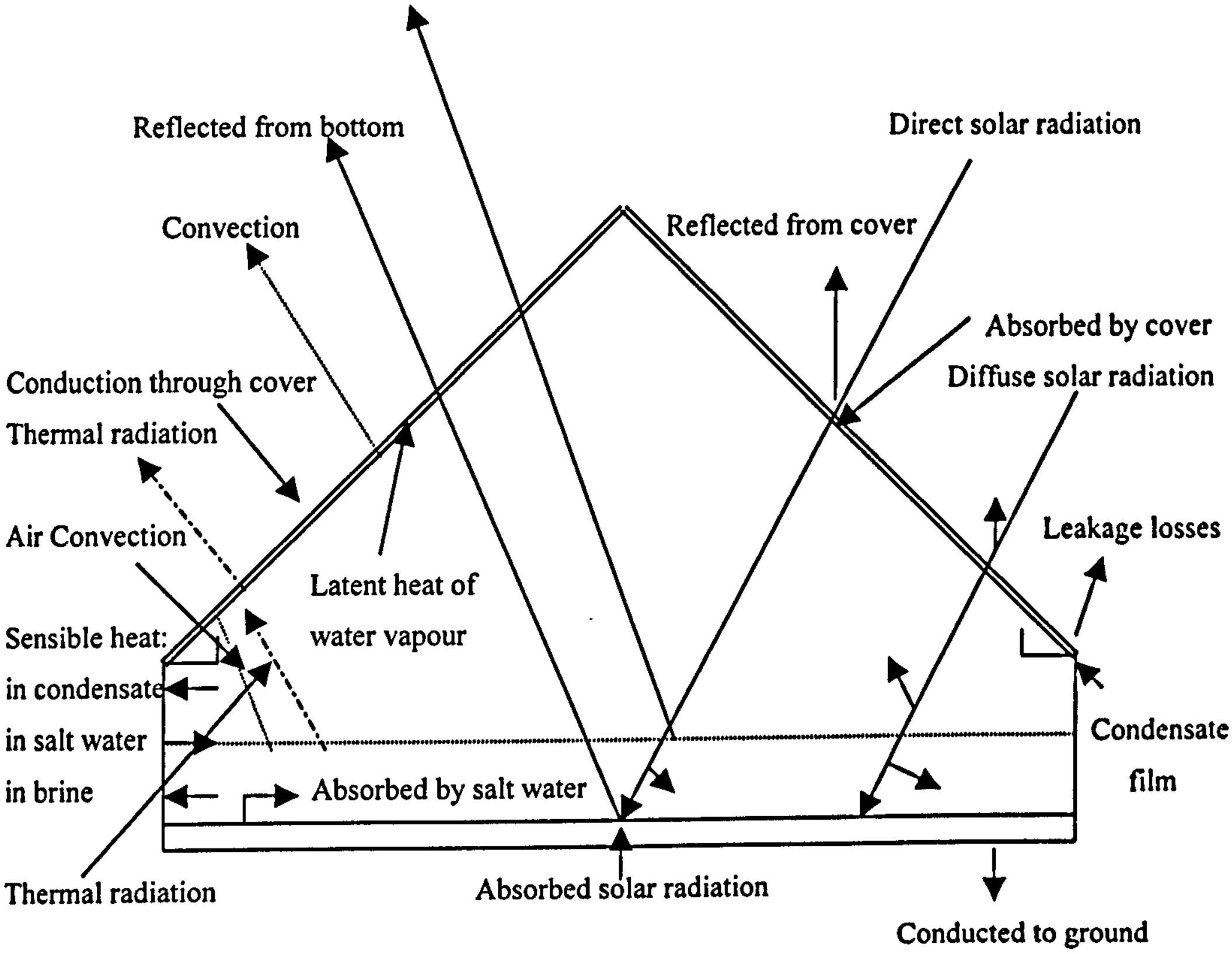

Fig 4.1. Energy transfer in a single basin solar still.

Consequently, the water vapours start forming on the upper saline water surface in the still. The humidity will increases between the water surface and the glass cover in the enclosure which is supposed to be water and vapour tight to prevent any vapour leakages through the still. Finally, the vapour condenses on the inner surface of the glass cover as water drops which slips down into the condensate channel to be collected as a distillate.

In this type of still, water does not boil, but vaporizes slowly, and the vapours reach the cooler glass surface by convection. The rate of evaporation is controlled primarily by the intensity of the incoming solar radiation. If there is no solar radiation, the

saline water in the basin rapidly cools, also its vapour pressure is reduced, and the evaporation process virtually comes to a standstill. In reality, however, the most important factors controlling solar evaporation is the amount of solar heat received per unit surface of the evaporating liquid per unit time (Riffat, 1995). Therefore, it is very important to design solar stills for maximum utilization of the incident energy. It is equally important to estimate the amount of possible yields and the amount of solar radiation intensity as well as the effects of the climatic conditions at the proposed site of the solar still. Some of these conditions have, already, been briefly discussed in chapter 2.

4.3 Heat and Mass Transfer Mechanisms

The total yearly amount of solar radiation received on a horizontal surface in different Gulf States is listed in Table 4.1. These figures include the overall solar radiation which can be divided as; (1) the visible, which comprises somewhat less than 4%; (2) the ultraviolet, which is less than 5% and varies considerably with the humidity of the air because the water vapour absorbs ultraviolet radiation; and (3) the infrared radiation, which, although invisible, contributes 55-60% of the energy needed for the water evaporation. Figure 4.2 shows the heat transfer modes within, and from, the conventional solar still roof type (Morse and Read, 1968)

Country	**Global Radiation Intensity Wh/m^2.day**
UAE	606
Kuwait	599
Qatar	526
Bahrain	523
Oman	541
Saudi Arabia	589

Table 4.1. The yearly average daily global radiation in Gulf States (Al-Sulaiman and Ismail,1997).

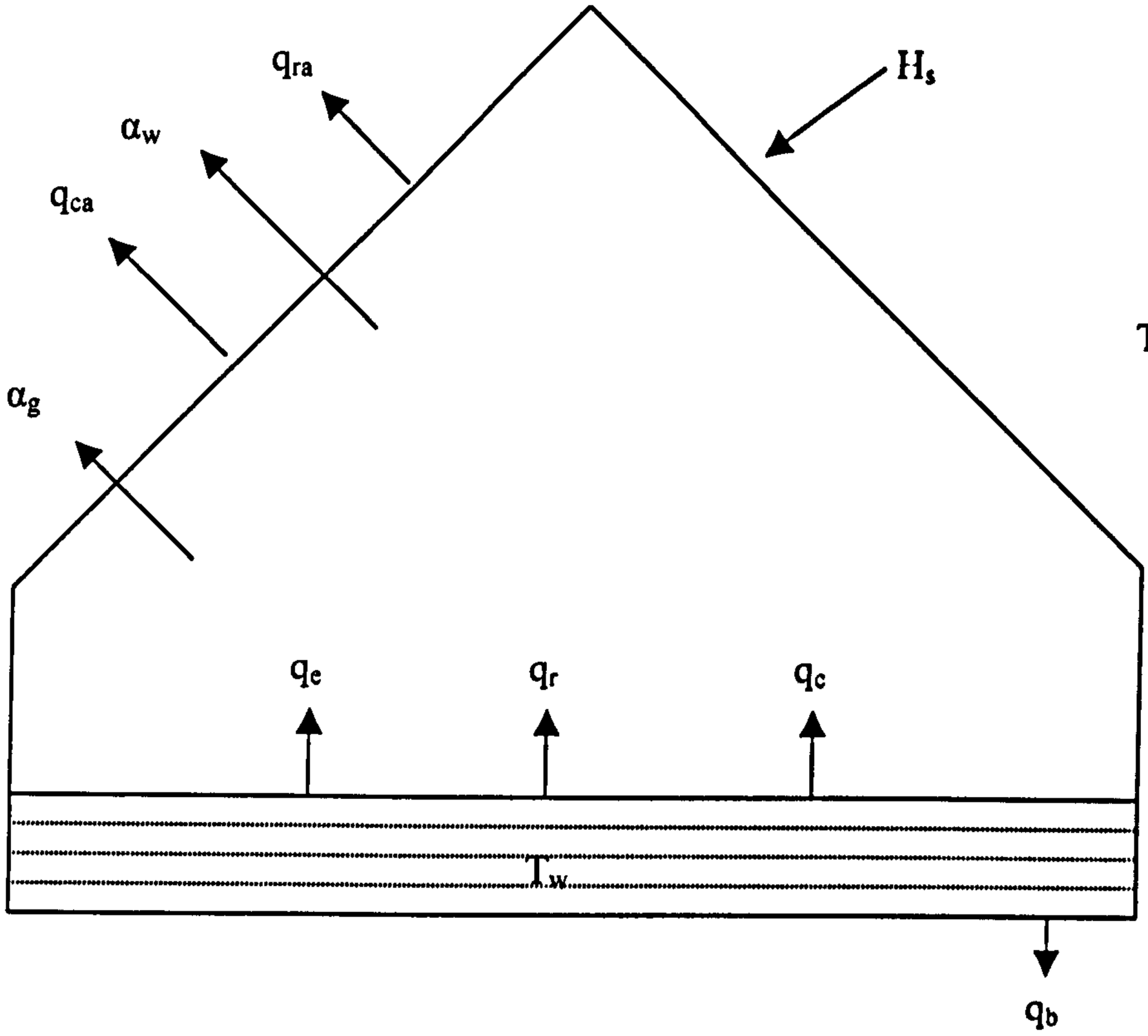

Fig 4.2. Major heat fluxes for a solar still.

Incident solar radiation H is partly absorbed by the glass cover, and some striking the glass cover is reflected to the sky. However, the bulk of the striking radiation goes through the glass to be absorbed by the saline water and the absorbing base. Some of the transmitted energy is also lost through reflection to the cover from the water surface, still walls, and bottom of the basin liner. The saline water heats up and evapourates. The vapour moves towards the cooler glass cover, where it condenses." *Temperature difference between saline water and glass cover required for condensation process of vapours on the glass cover"* (Garg, 1987). The driving force that moves the vapour from near the water surface to the cover is the difference in partial pressure of the saturated vapour near the cover due to difference in temperature. All material objects heat in the form of infrared radiation. The intensity of this radiation depends on the temperature and emissivity of object. A clean polished metal surface with a high reflectivity or transmissivity has an emissivity in the infrared spectrum near zero, being typically $\varepsilon = 0.05$. Most other common materials exhibit high emissivities in the infrared spectrum, including water, glass,

paints, concrete and wood with $\varepsilon = 0.9$ (Idso,1981). Table 4.2 lists the long wave emissivity for some common materials.

Material	**Emissivity (IR)**
Aluminum foil, bright	0.05
Aluminum foil, oxidized	0.12
Aluminum paint	0.5
Red brick	0.9
Glass	0.9
Concrete	0.88 - 0.93
Black paint	0.98
White acrylic	0.9
Sand	0.9
Water	0.96
Vegetation	0.92 - 0.96

Table 4.2. Long wave emissivity of some common materials (Idso,1981).

Heat is then transferred from the water to the glass cover by means of radiation, convection, and evaporation. The vapour loses its latent heat to the glass cover. During a large part of the day, most of the heat gained by the glass cover is lost again to the atmosphere. The glass cover conducts the energy from the inner surface to the outer one and exchange it with the sky. This is then carried a way to the surroundings by convection (q_{ca}) and radiation (q_{ra}). Some heat also can be lost from the sidewall and bottom of the basin by conduction. However, this is greatly minimized by use of insulation layer under the absorber. The cumulative heat balance for a solar still is shown in Table 4.3. Also part of heat can be lost by leakages through the still edges and by convection loss, which is related to the distillation rate, and change of inlet saline water circulation in and out the still.

Energy Transfer	Percent of Solar Radiation
Heat energy for evaporation [q_e]	38.4%
Heat loss by convection in still [q_c]	3.7%
Heat loss by radiation in still [q_r]	12.2%
Heat loss by reflection from glass cover	10%
Heat absorbed by cover	10%
Heat loss by conduction through bottom [q_b]	16%
Unaccounted heat loss such as vapour leakage and side losses	9.7%

Table 4.3 Energy Balance on a Solar Still (Duffie, 1980).

4.4 Determination of Energy Transfer Modes inside and outside the still

4.4.1 Heat and Mass transfer modes inside the still

The modes of heat exchange inside the still between the absorber/evaporator and cover surface are heat radiation and convection accompanied by evaporative heat and mass transfer in the form of water vapour, Sanjay *et al* (1996). Based on the above analysis of energy exchanges within and outside the still, a theoretical model of the still is obtained by taking simple energy balance of water, glass, and the absorb ring base.

Heat balance of the water can be written as:

$$M_w C_w \frac{dT_w}{dt} = \alpha_w \tau_g H_s + q_w - (q_r + q_c + q_e) \qquad (4.1)$$

where M_w is mass of water; C_w is heat capacity of the water and basin; T_w is water temperature; t is time; α_w is absorptivity of water and basin liner; τ_g is transmittance of glass cover; H_s is solar radiation on horizontal surface; q_w is heat transferred from absorber to water; q_r, q_c, and q_e are the radiative, convective and evaporative heat loss from water to the transparent cover respectively.

Heat balance of the glass cover is given in equation 4.2.

$$M_g C_g \frac{dT_g}{dt} = \alpha_g H_s + (q_r + q_e + q_c) - q_{ga} \qquad (4.2)$$

where M_g is energy stored in the glass cover; C_g is heat capacity of glass cover; T_g is glass temperature; t is time: α_g is the absorptivity of glass cover; $q_{ga} = (q_{ca} + q_{ra})$ is the heat loss from cover to atmosphere; and q_{ca}, q_{ra} are the heat loss by convection from cover to atmosphere and heat loss by radiation from cover to atmosphere respectively.

Heat balance of the absorbing base is given in equation 4.3.

$$(\tau_g \tau_w \alpha_b) H_s = q_w + q_b \qquad (4.3)$$

where α_b is energy absorbed by the base and q_b is energy lost from base to ambient.

4.4.2 Convective Heat Transfer Inside the Still

The convective heat loss from hot water surface in the still to the glass cover can be calculated from the following expression:

$$q_c = h_c (T_w - T_g) \qquad (4.4)$$

where h_c is the convective heat transfer coefficient and T_w, T_g are the water temperature and glass cover temperature respectively.

This mode of heat exchange occurs between the absorber/evaporator and inner cover surfaces. It entirely depends on the temperature difference and value of the convective heat transfer coefficient, the value of which depends on many parameters such as temperature of water and glass density, conductivity, specific heat, viscosity expansion coefficient of fluid, and spacing between water surface and glass cover. The convection heat transfer is a function of air vapour mixture properties. It must be obtained from empirical data. Dunkle (1961), has suggested a empirical expression for estimating the value of the convective heat transfer coefficient, which when converted in SI units is given as:

$$h_c = 0.884 \quad [T_w\text{-}T_g + \frac{(P_w - P_g)}{268.9\ 10^{-3} - P_w} T_w]^{1/3} \qquad (4.5)$$

where is P_w and P_g are the saturation partial pressure of water vapour (N/m^2) at water temperature and glass temperature respectively.

4.4.3 Evaporative Mass Transfer Mode

Evaporation accompanies the convective mass transfer in the form of water vapour. The amount of water transferred from the water surface to the condensate film on the cover can be estimated in terms of the analogy between heat and mass flow rate. It is proportional to the heat transfer coefficient and the driving potential. The latter is the difference in partial pressures of material being transferred. (Howe and Tleimat in Sayigh, 1977). The evaporative heat loss q_e from water to the glass cover can be calculated by knowing the mass transfer coefficient, which can be calculated from convective heat transfer coefficient. The algebraic formulation of the corresponding rate of heat flux is:

$$q_e = 16.28\ h_c\ (P_w\text{-}P_g) \qquad (4.6)$$

where $q_e = h_e\ (T_w - T_g)$ (4.7)

and

$$h_e = 16.28\ h_c\ \frac{P_w - P_g}{T_w - T_g} \qquad \text{Tiwari } et\ al(1988) \text{ and } (1986) \qquad (4.8)$$

where h_e is evaporation heat transfer coefficient. This is related to the amount of the condensation on the inner surface of the glass cover by the following expression:

$$M_w = \frac{q_e x\ 3600}{\ell} \qquad (4.9)$$

where ℓ is the latent heat of evaporation of water in J/kg, and M_w is the distillate production rate. Here, ℓ can be expressed as a function of water temperature as:

$$\ell = 10^3 (2501.67 - 2.389\, T_w) \qquad (4.10)$$

where T_w in °C and ℓ is in J/kg.

4.4.4 Radiative Heat Transfer Mode

Radiative heat transfer inside the solar still, between the glass cover and the absorber/evaporator surfaces is considered here as equivalent to that between two infinite parallel plates. With assumptions of diffuse and black surfaces and that the aspect ratio is sufficiently large to neglect edge effects. The heat transfer by radiation q_r from water surface to glass cover can be calculated from the equation:

$$q_r = F\, \sigma\, (T_w^4 - T_g^4) \qquad (4.11)$$

Where F is the shape factor, which depends on the geometry and the emissivities of water and glass cover, σ is the Stefan Boltzmann constant. For the basin type solar still and for low tilt angles of glass cover, assume the basin and glass cover as two parallel infinite plates (Charters, in Sayigh, 1977). Then cover shape factor can be assumed equal to the emissivity of the water surface, which is 0.9. Hence equation (4.11) can be written as:

$$q_r = 0.9\, \sigma\, (T_w^4 - T_g^4) \qquad (4.12)$$

4.5 Heat transfer modes outside the still

Outside solar stills, the heat is transferred to the surrounding by means of radiation and convection from the glass cover, the base and side walls of the solar still. The convective heat loss q_{ca} from glass cover to ambient air can be calculated from the following expression:

$$q_{ca} = h_{ca}\, (T_g - T_a) \qquad (4.13)$$

The convection heat transfer coefficient is assumed to be a function of wind speed only and is expressed by equation 4.14.

$$h_{ca} = 5.7 + 3.8V \qquad \text{Duffie and Bechman, (1980).} \qquad (4.14)$$

where V is the wind speed in m/s.

The radiative heat loss q_{ra} from glass to sky can be determined by the radiant to sky temperature T_s, which depends on atmospheric conditions such as the presence of dust or clouds. Generally for practical purpose when the still is operating, the sky temperature is assumed to be a function of ambient temperature (Duffie and Bechman, 1980).

Therefore, the radiative heat losses can be expressed as:

$$q_{ra} = \varepsilon_g \sigma (T_g^4 - T_s^4) \qquad (4.14)$$

where ε_g is the emmissivity of glass cover. Hence the radiative heat transfer coefficient from the glass cover to the surroundings in the form of long wave radiation can be expressed as:

$$h_{ra} = \frac{\varepsilon_g \sigma (T_g^4 - T_s^4)}{T_g - T_a} \qquad (4.15)$$

Finally, as the soil temperature is unknown, it is difficult to estimate the heat loss from the bottom of the basin to the surrounding air. However, it can be calculated from the following expression:

$$q_b = h_b (T_w - T_a) \qquad (4.16)$$

Where h_b is the overall heat transfer coefficient and can be calculated as:

$$h_b = \frac{1}{h_{ga}} + \frac{X_1}{K_1} + \frac{X_2}{K_2} \qquad (4.17)$$

Where h_{ga}, is heat loss from glass to ambient, and X_1, X_2 are the thickness of the box containing the basin and the insulation material used respectively, and K_1, K_2 are their thermal conductivities (Maaley, 1991; Mowla and Karim 1995). It should be

mentioned here that in the current work, the computer model simplifies some parameters including the effect of water salinity on its properties, the ratio of diffuse to direct radiation, and the variation in absorpativity and transmissivity of glass and water surface with difference angles of incoming radiation. All these parameters were neglected in the current work.

4.6 Energy Balance on The Absorber/Evaporator Surface

Referring to Fig 4.1 "the energy balance on the absorber/evaporator surface," includes the energy transferred to the glass cover by convection, evaporation, and radiation. (Tlimat and Howe, 1986). Thus, the energy input and output from the surface in a given time can be calculated from Dunkle (1961) equation.

$$H_s \alpha_w \tau_g = q_e + q_r + q_c + q_b + C_w \frac{dT_w}{dt} \qquad (4.18)$$

Here,

The Energy Input = Solar radiation absorbed by the absorber and slain water (H_s).

The Energy Output = Energy loss by evaporation of slain water surface (q_e) + Radiant energy loss to the still cover (q_r) + Convection energy loss to the still cover (q_c) + Conduction energy loss to the bottom and wall sides of the still (q_b) + Energy loss by output brine (C_w).

Hence, the energy balance on the absorber/evaporator surface can be written as:

Input energy – Output energy = Increase of energy of the absorber/evaporator

4.7 Energy Balance on The Still Cover

The energy incident on and leaving the glass cover from Fig.4.2 can be written as:

$$q_{ga} + C_g \frac{dT_g}{dt} = H_s \alpha_g + q_e + q_r + q_c \qquad (4.19)$$

Energy input = Solar radiation absorbed by the cover (H_s) + Energy input by [Convection (q_{ca}) + Evaporation (C_g) + Radiation (q_{ra})] from the Absorber/Evaporator surface.

Energy output = Energy loss from the cover by [convection (q_c) + radiation (q_r) to the environment] + Energy loss of distillate (C_w).

Hence, the energy balance equation on the still can be written as:

$$H_s\,\alpha_w\,\tau_g + H_s\;\alpha_g = q_{ca} + q_{ra} + q_b + C_g\,\frac{dT_g}{dt} + C_w\,\frac{dT_w}{dt} \qquad (4.20)$$

4.8 Theoretical Model Predictions

The performance of any solar still can be predicted by writing energy balance equations on various components of the still. In order to use the analytical model described by the equations of the previous sections, a computer program was developed to solve energy balance equations and calculate the water and cover temperature, and the other related parameters after time interval Δt. The computer experiments were performed for Doha (25.25 °N). Reliable models for both the solar radiation and ambient temperature variation during the day are employed. The computer programme was developed by the University of Qatar and written in Visual Basic version 5. The computer programme was run on the university of Qatar at electrical engineering research laboratory. The programme details are listed in Appendix, (B).

The program was run to predict the yield of pyramid solar still over a period of 24 hours. The time interval Δt was considered to be 0.05 hour to avoid unstable solutions. The sequence steps of the computer program are illustrated in a flow chart, which is shown in Fig.4.3. It indicates, briefly, the operations and their functions. By this program, the heat balance equations can be calculated and estimate the heat loses q_r, q_c, and q_e of the solar still (Samboa, 1986).

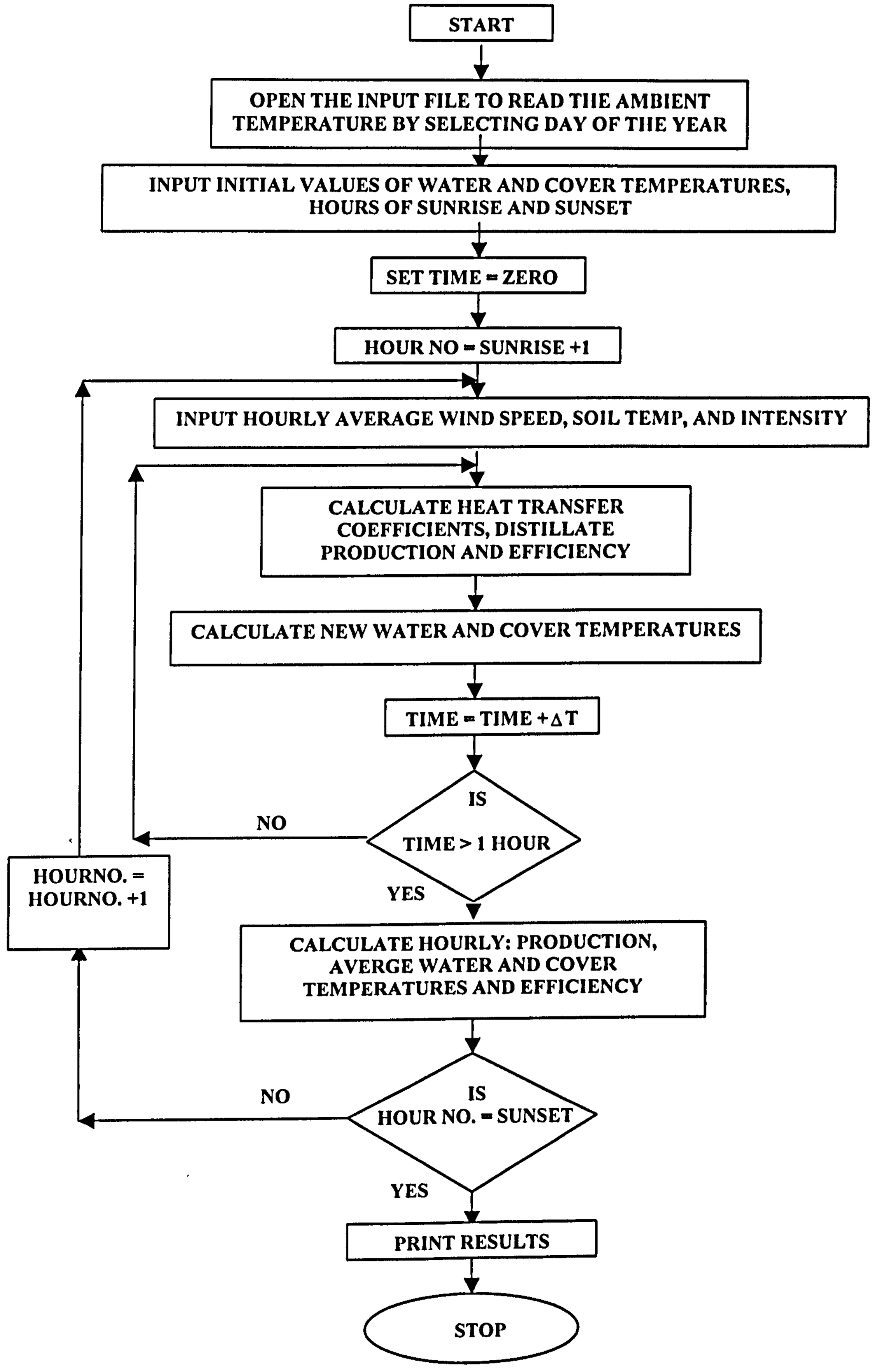

Fig 4.3 The Flowchart of The Computation Program.

Consequently, the hourly rate of water evaporation is given by:

$$M_w = \frac{3600\ q_e}{\ell} \tag{4.20}$$

Where ℓ is the latent heat of water J/kg.

4.9 Predicted Results and Discussion

The theoretical model was employed to predict the effects on solar still performance under three various parameters under typical climatic conditions of Qatar. These include the thermal insulation layer, the water depth and wind speed. The first and second one are design parameters, while the third one is an environmental parameter. Table 4.4 shows the still specifications values, which used in this programme.

Basin area	1 m^2
Glass cover area	1 m^2
Glass cover absorbtivity [α_g]	0.05
Water surface absorbtivity [α_w]	0.80
Basin liner absorbtivity [α_b]	0.80
Latent heat of water [ℓ]	2,450,000 J/kg
Wind velocity [V]	4.00 m/s
Transmittance of glass cover [τ_g]	0.10
Transmittance of water [τ_w]	0.05
Stefan Bollzman constant [σ]	4.87×10^{-8} w/m^2/°C

Table 4.4. Solar Still Specifications.

To make the study of the effect of environmental parameters more adequate, the computer experiments for all three parameters were conducted for a typical summer day [15th of June, i.e. day number = 166] and a typical winter day [15th of Jan, i.e. day number = 15].

Figure 4.4. (a) shows the variation of the ambient temperature, the glass cover temperature, and the saline water temperature over 24 hour, starting at sunrise for a typical summer day. Figure 4.4. (b) shows the hourly variation of the solar insolation,

instantaneous yield for the same day. In Fig 4.5 (a, b) the hourly variation of the same parameters are shown for a typical winter day. It can be found from the theoretical model that Fig 4.4 (a) and 4.5 (a) predicts on average temperature difference of 8-9 °C exists between the water and the glass cover throughout most of the day even over a large part of the night, resulting in nocturnal production. However, it shows that the amount of nocturnal production is relatively negligible, the highest rate of yield occurs around 1 p.m in winter and 12 p.m in the summer. Comparing Fig 4.4. (b) and 4.5. (b) it can be concluded that a solar still nearly doubles its productivity in summer with respect to that of the winter. This can be attributed to that large amount of solar energy and higher temperature can be obtained in the summer.

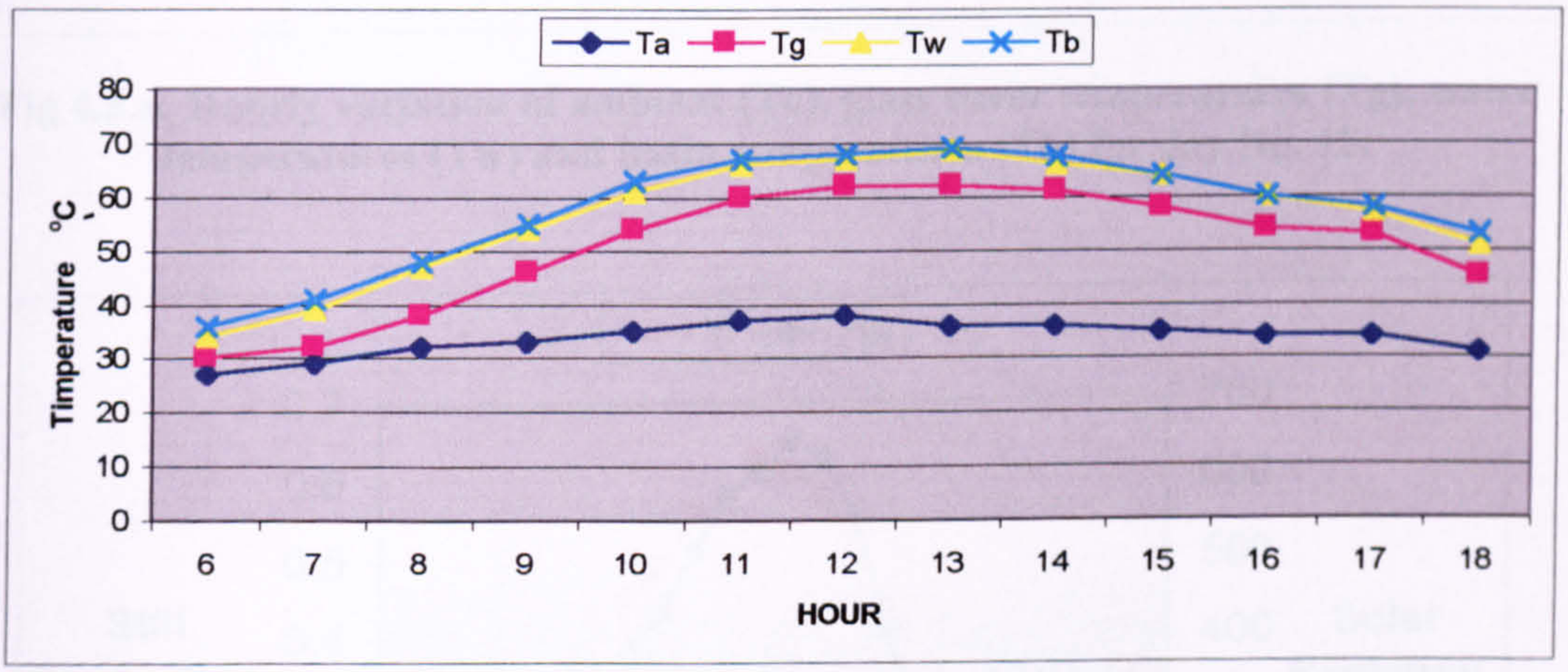

Fig 4.4.a. Hourly variation of ambient (Ta), glass cover temperatures (Tg), water temperatures (Tw) and basin temperatures (Tb) for day No.166

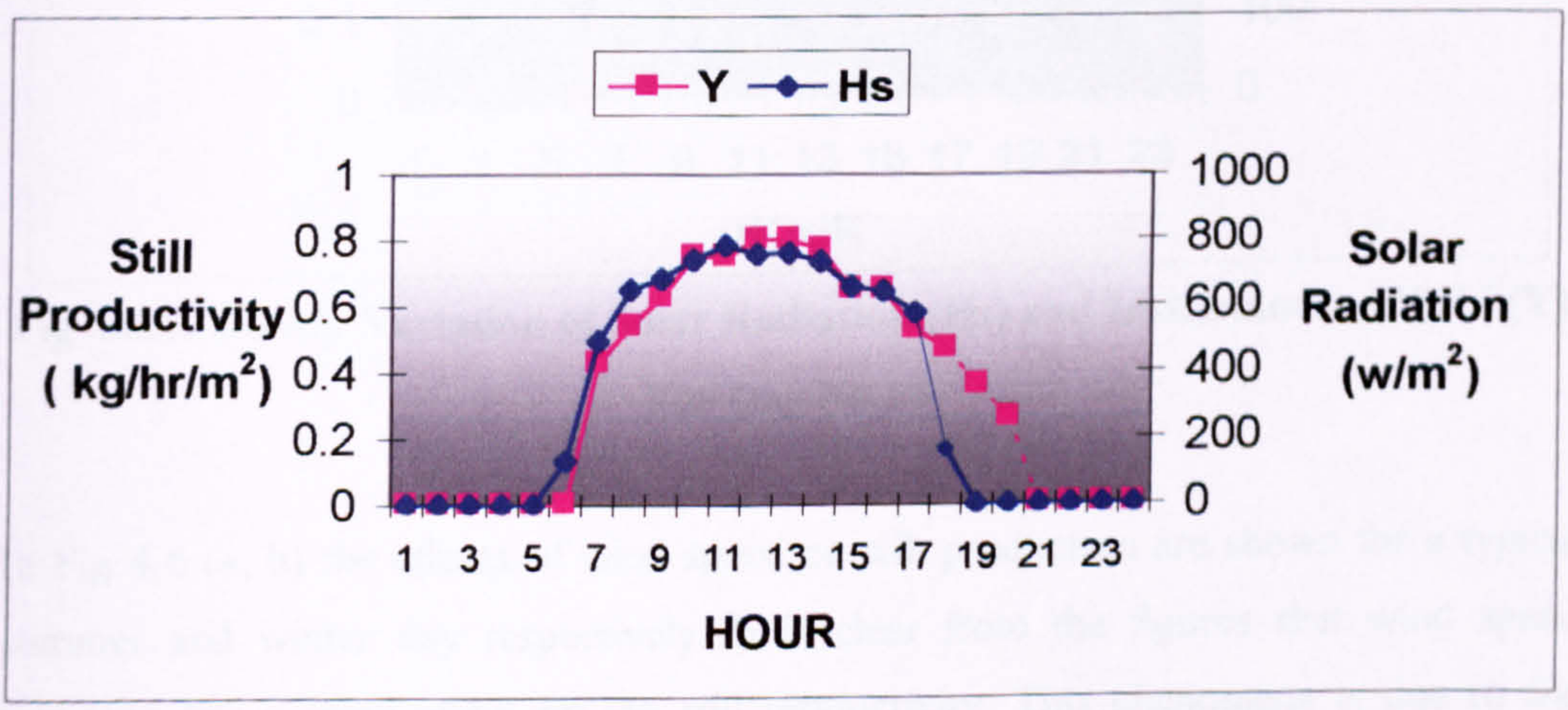

Fig 4.4.b. Hourly variation of solar radiation (Hs) and instantaneous yield (Y) for day No.166.

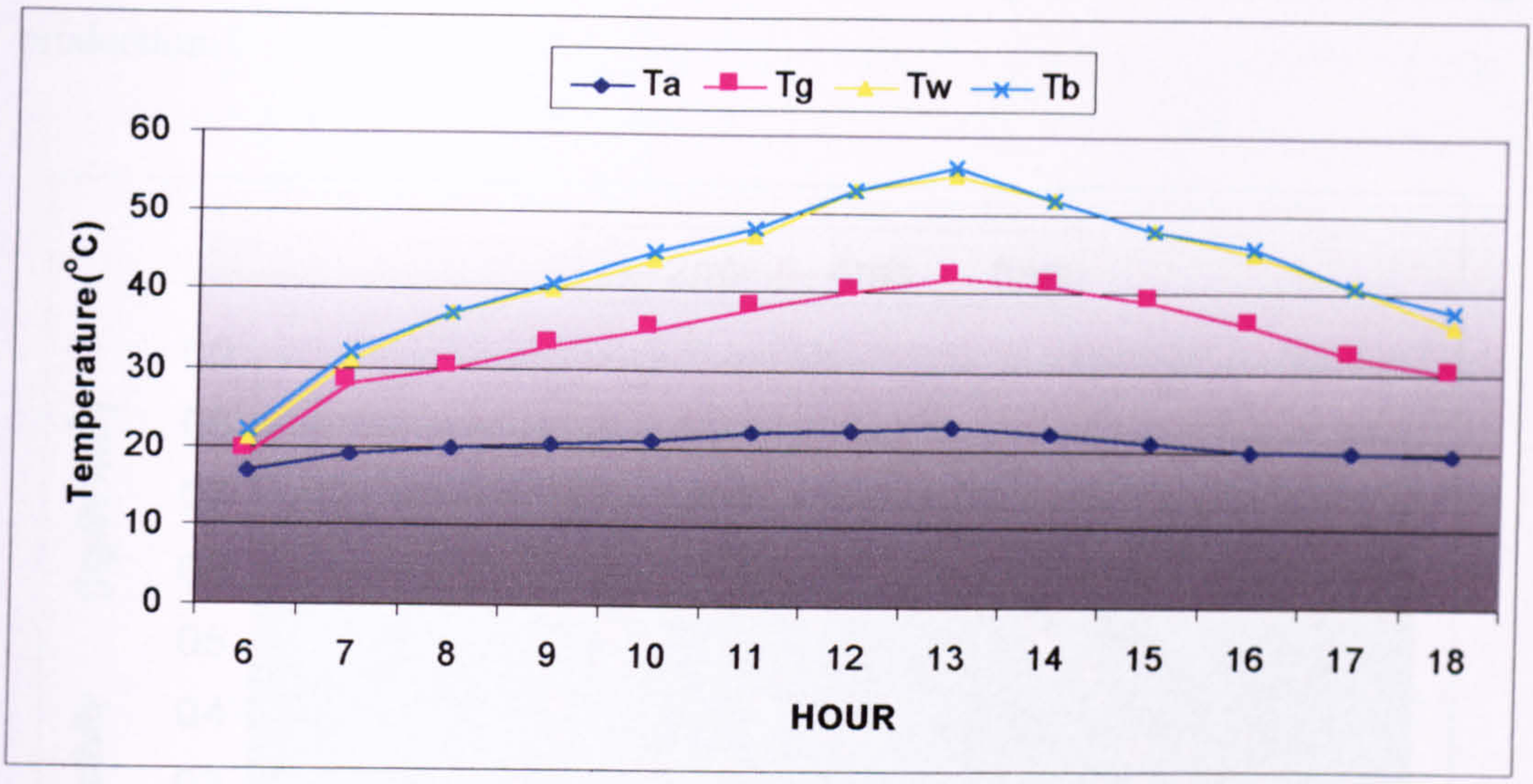

Fig 4.5.a. Hourly variation of ambient (Ta), glass cover temperatures (Tg), water temperatures (Tw) and basin temperatures (Tb) for day No. 15.

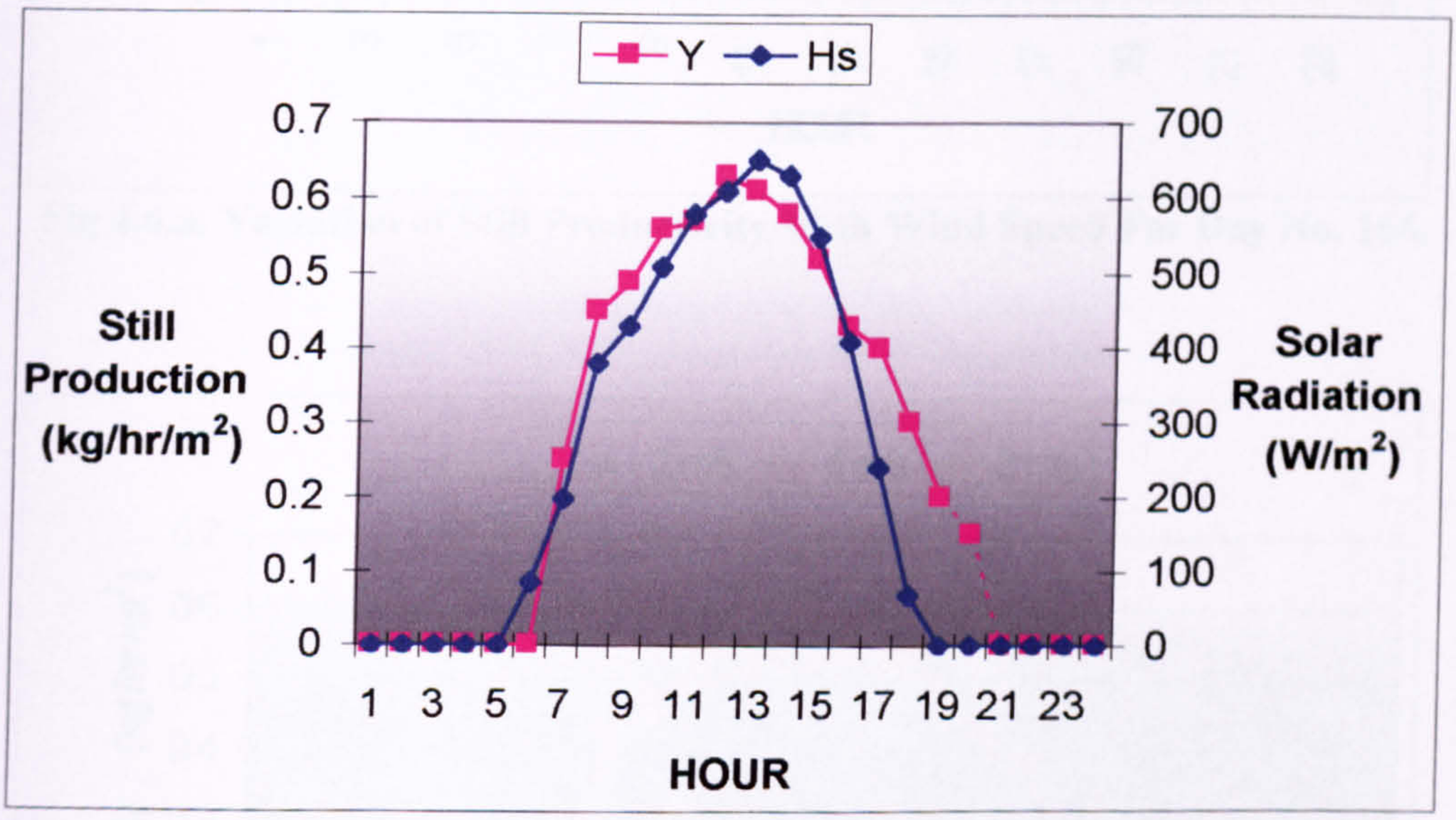

Fig 4.5.b. Hourly Variation of Solar Radiation (Hs) and Instantaneous Yield (Y) For Day No.15.

In Fig 4.6 (a, b) the effects of wind speed on still production are shown for a typical summer and winter day respectively. It is clear from the figures that wind speed variation has a small effect on the still productivity. This phenomena is due to the increase of air leakages through the still which resulting in a very rapid cooling of the

whole system particularly after sunset, thus limiting the amount of nocturnal production.

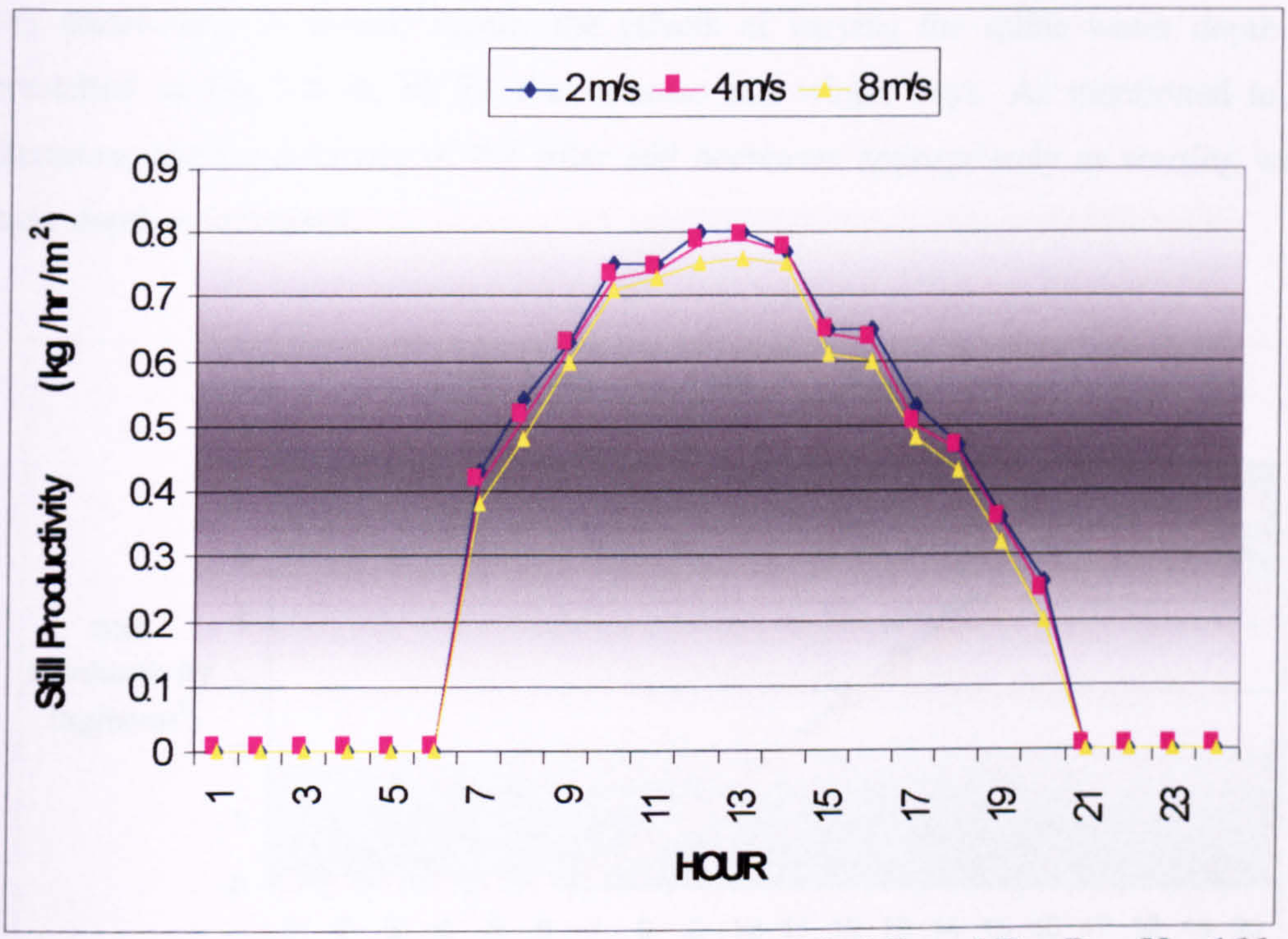

Fig 4.6.a. Variation of Still Productivity With Wind Speed For Day No. 166.

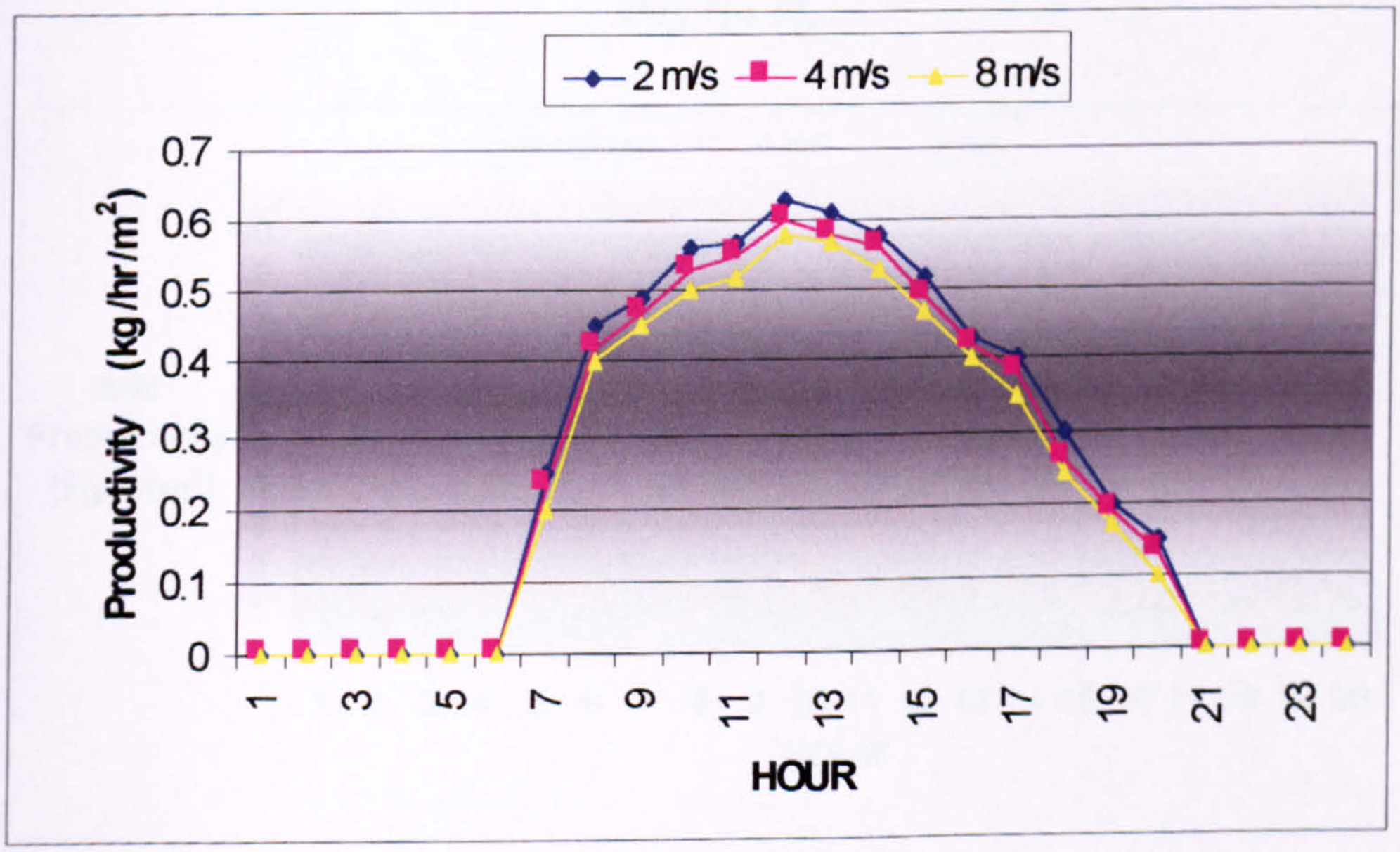

Fig 4.6.b. Variation of Still Productivity With Wind Speed For Day No. 15.

In Fig 5.7 (a, b), the effects of the still bottom insulation on yield, are demonstrated for a typical summer and winter day respectively. As expected when solar still runs with thicker insulation layer, the still production increases noticeably through out the day particularly in winter. Finally the effects of varying the saline water depth are presented in Fig 5.8 (a, b) for the summer and winter days. As mentioned in the literature, the productivity of the solar still decreases appropriately as starting water layer depth is increased.

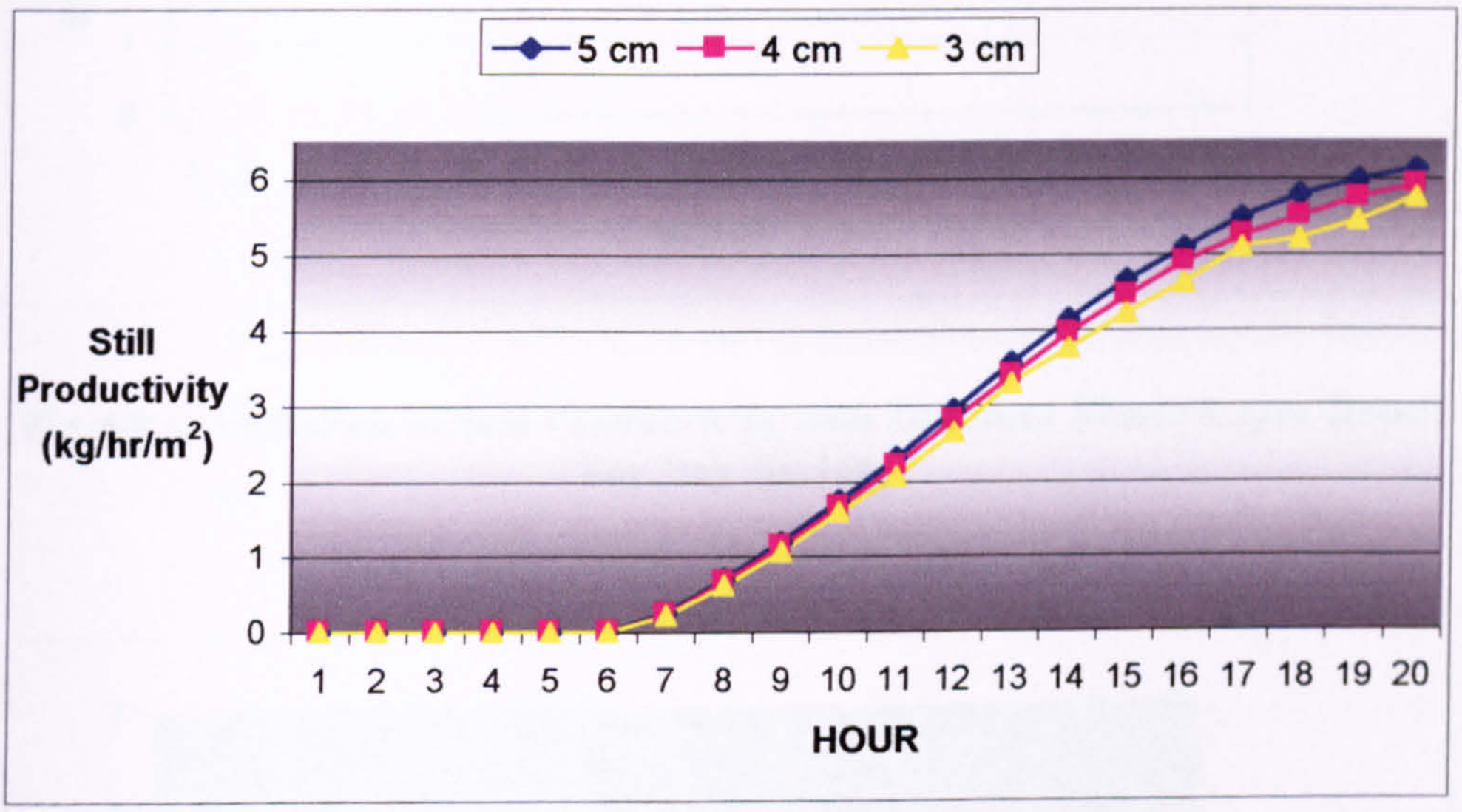

Fig 4.7.a. Variation of Still Productivity With Insulation Thickness For Day No.15.

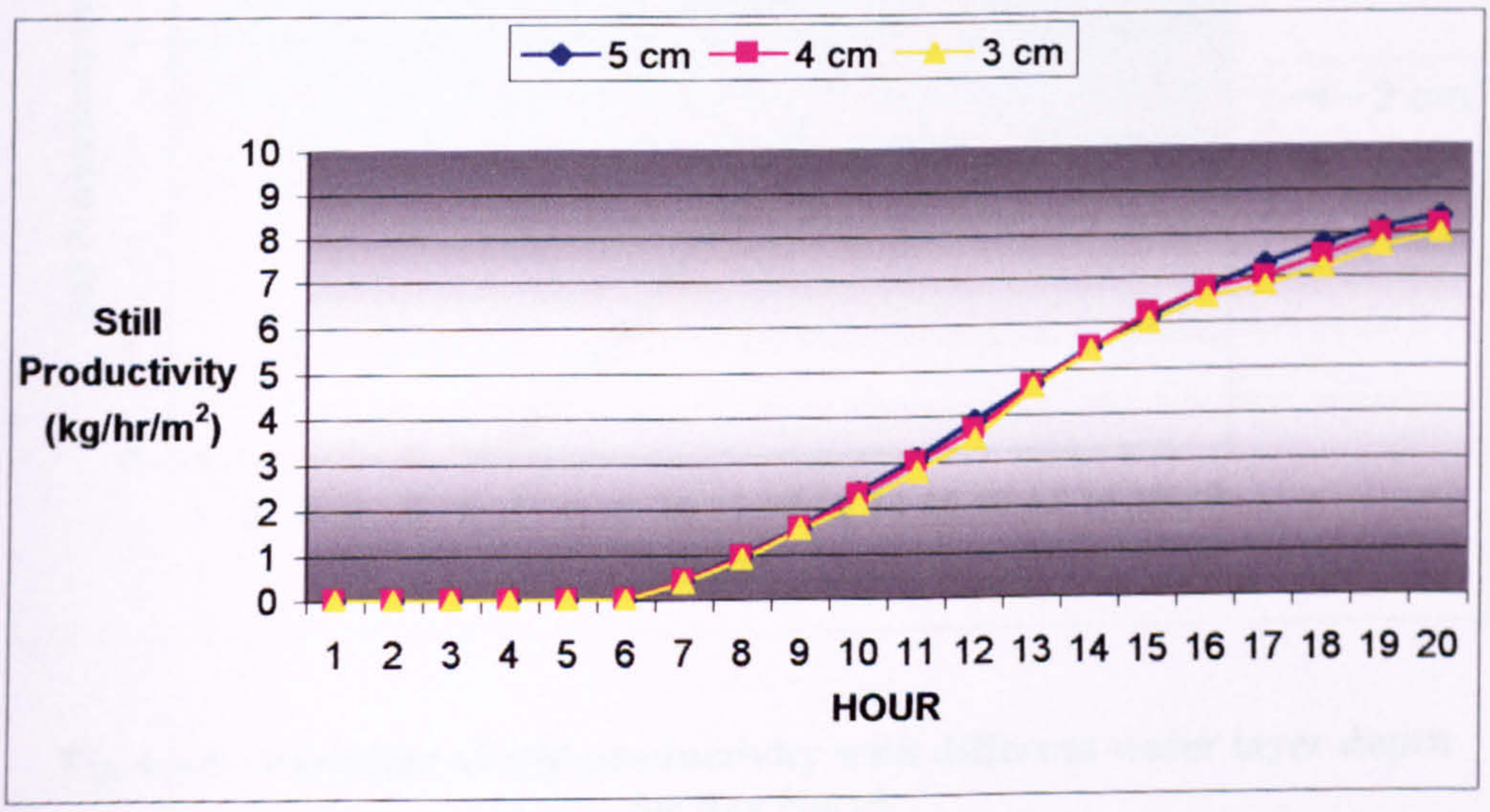

Fig 4.7.b. Variation of Still Productivity With Insulation Thickness For Day No. 166.

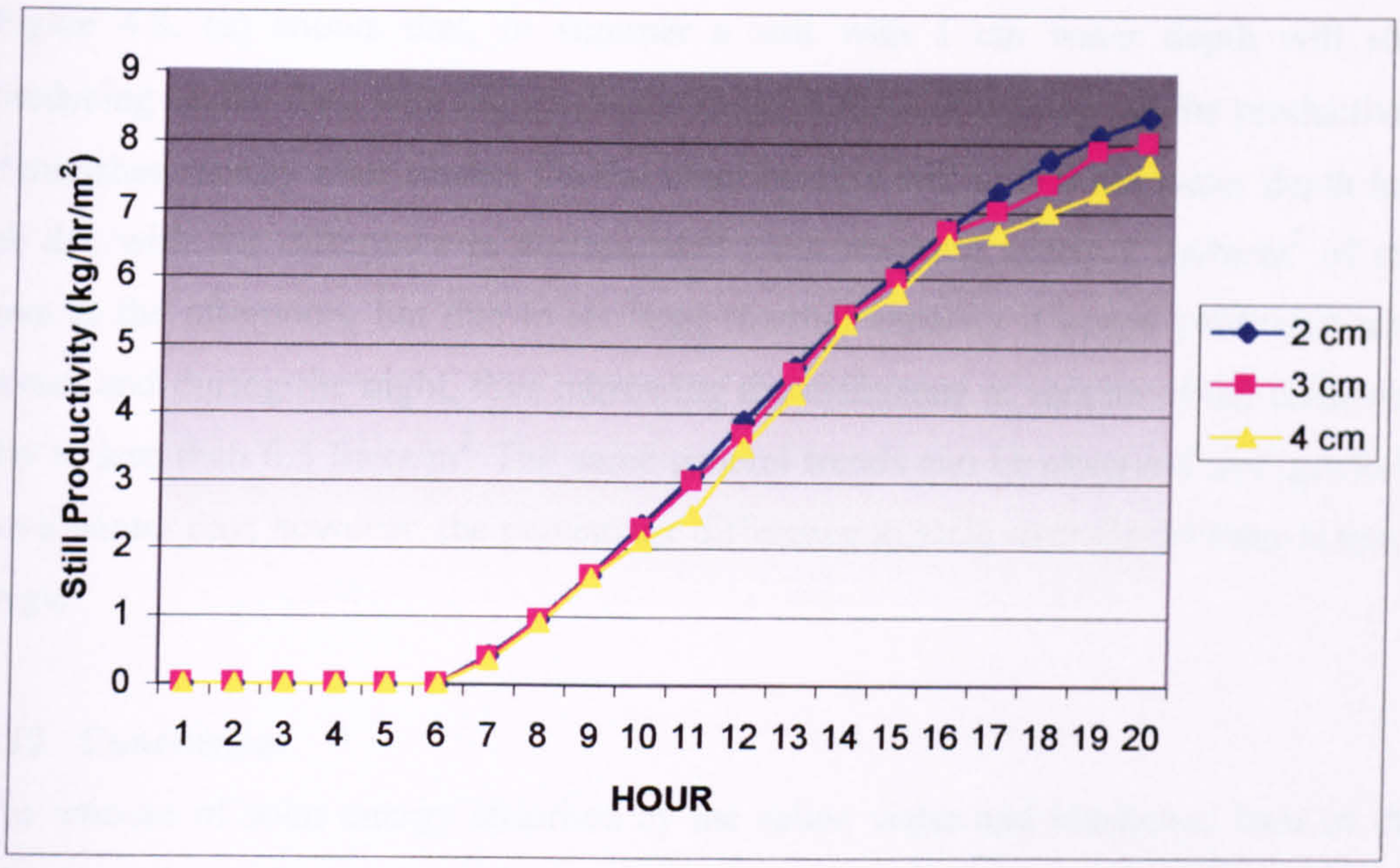

Fig 4.8.a. Variation of Still Productivity with Different Water Layer Depth For Day No.166.

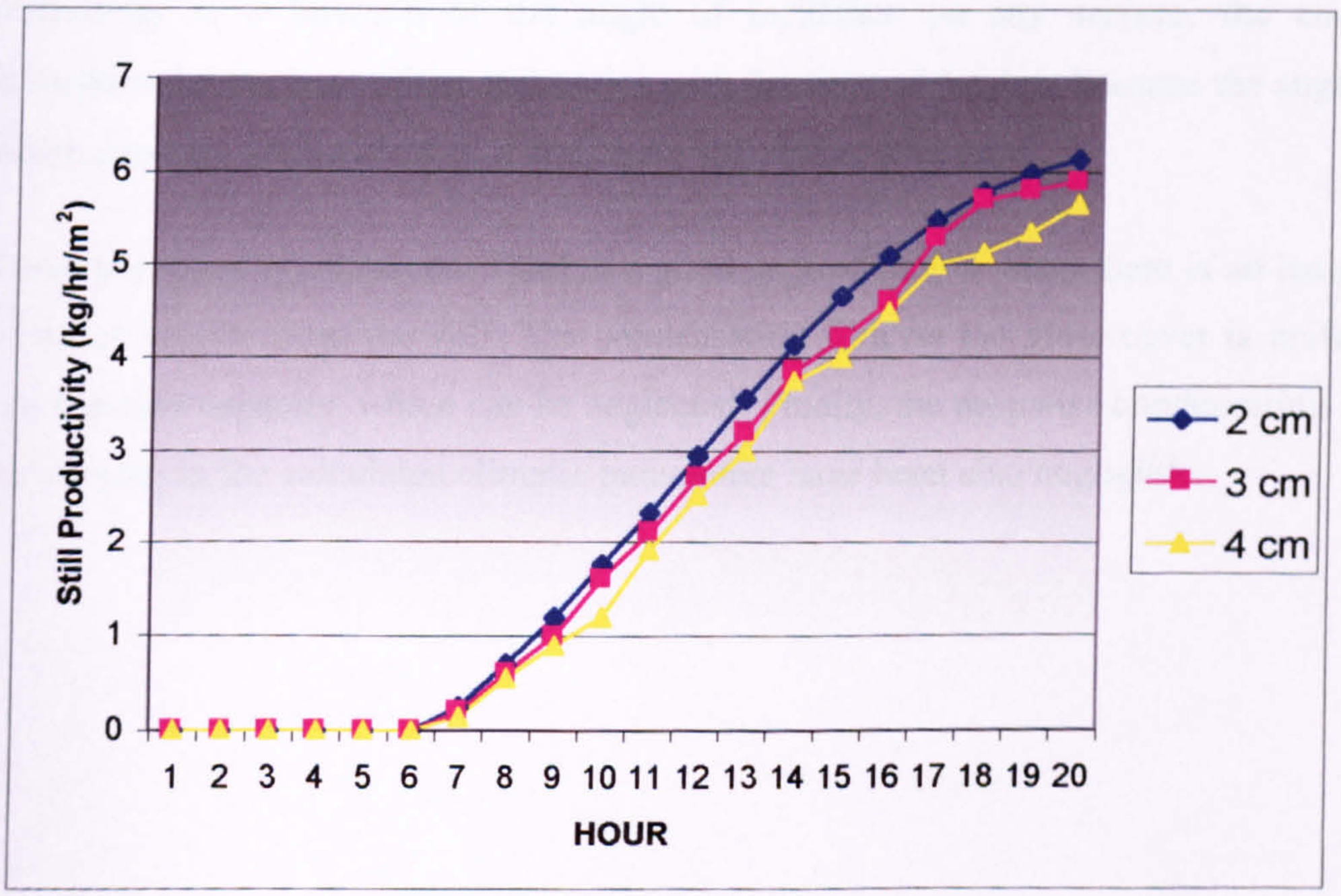

Fig 4.8.b. Variation of still productivity with different water layer depth for day No.15

Figure 4.8. (a) shows that, in summer a still with 1 cm water depth will start producing earlier than with higher depths through most of the day but the productivity diminishes rapidly after sunset. On the other hand, a still with 4 cm water depth lags all day with the difference in accumulated yield reaching nearly 2 kg/hr/m^2 of still area in the afternoon, but due to its large thermal capacity it keeps producing after sunset and during the night, thus narrowing the difference at sunrise of the following day to less than 0.5 liters/m^2. The same general trends can be observed in Fig.4.8.(b) for a winter day; however, the percentage difference in yield over the 24 hour is much larger.

4.12 Conclusion

The amount of solar energy absorbed by the saline water and blackened base of the still depends on the amount of energy reflected and absorbed by the transparent top cover and the amount reflected by the saline water surface and base of the still. The water film (distillate) formed due to the condensation of water vapour on the interior surface of the top cover also contributes to the reflection of solar energy. Since reflectivity is a function of the angle of incidence on any surface, the energy absorption by the base of the still varies with the time of the day, because the angle at which sun rays are incident on a stationary still varies with time.

These proposed equations are valid to a good approximation when there is no leakage of water vapour from the still. The condensation film on the glass cover is uniform and has heat capacity, which can be neglected. Finally, the dropwise condensation and the varying in the calculated climatic parameters have been also negligible.

CHAPTER FIVE

EXPERIMENTAL WORK AND RESULTS

5.1 Introduction

In this chapter, the construction and operation of an experimental pyramid tilted tray solar still is described. The still has been designed and manufactured to facilitate a study on the parameters which may effect the solar still production including shape factor, solar radiation, wind velocity, ambient temperatures...etc. Moreover, the ordinary type of tilted tray solar still had been modified. A pyramid absorber shape with four access surfaces to face sun radiation during the whole day, was tested. Initial laboratory experiments were conducted to investigate the effect of adding four sides to the tilted tray solar still. Furthermore, two different cover shapes were also experimented in this work.

Laboratory experiments were conducted at the University of Hertfordshire, under controlled conditions, to investigate the design parameters that would affect solar still productivity. Two different small models of 4000-mm^2 evaporation surface area were constructed and tested. Dome and pyramid shaped covers have been selected for these experiments, which will be referred later as model 1 (d) and model 1 (p) respectively. Both were made of transparent material and used with pyramidal tilted tray solar still absorber. The pyramid and dome shapes cover were selected as they can provide the four accesses tracking surfaces continuously exposed to the sun radiation. These shapes can, also, provide a surface that is capable of receiving an optimum amount of solar radiation during the movements of the sun throughout the day and seasons.

This laboratory test is useful in studying the various parameters and also in identifying the construction difficulties associated with these types, as a means of adopting them for large-scale model. In the second part of the experimental work, a large-scale pyramid tilted tray solar still which will be referred as model 2 (p), was constructed and tested at the research center of the University of Qatar under local climatic conditions. The model 2 (p), was constructed from galvanized steel with square base dimensions of 980 x 980 x 230 mm and covered with 6 mm thick glass panels. Moreover, in both laboratory and field experiment, the angle of incidence has been minimized by sloping the pyramid sides at angle of 25°, which is equal to the latitude of Qatar. All outdoor experiments were performed during the months of May-June 2000.

5.2 Indoor Experimental Testing Facility

The preliminary indoor experiments were carried out particularly to investigate and study

the reliability of these two novels design. Model 1 (d) and (p) were individually tested under controlled conditions. The features of these two types were carefully observed in this work in order to select the proper design to employing it for outdoor experiment.

5.3 Solar Desalination System

The desalination system consists of four main parts as shown in Fig 5.1. The still (item 1), which is fed by, water from the water bath (item 2), and flow water inducer pump which controls the input flow rate (item 3). Finally, a distillate bottle to collect the distilled water (item 4) was included.

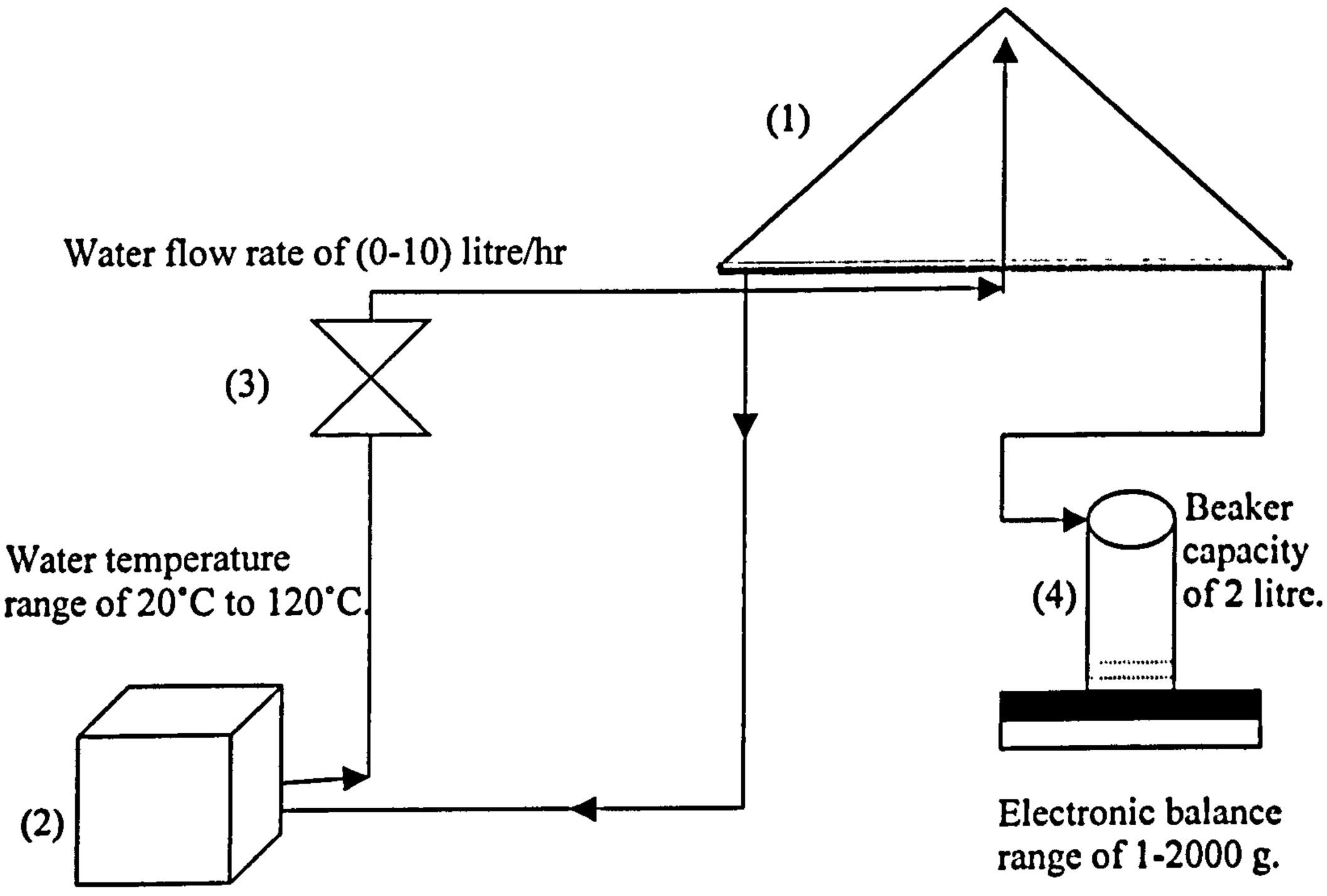

Fig 5.1. Block diagram of the solar still indoor system.

(1) The still, (2) Water bath, (3) Adjustable flow water inducer pump, and (4) Distillate container.

5.4 Design and Construction of Indoor Solar Still

The general schematic diagrams of the indoor experimental stills are shown in Fig 5.2. A sheet of copper with pyramid dimensions of (260 x 260 x 90) mm was divided into six copper trays with width of 20 mm of each tray and depth of 5 mm as a still absorber.

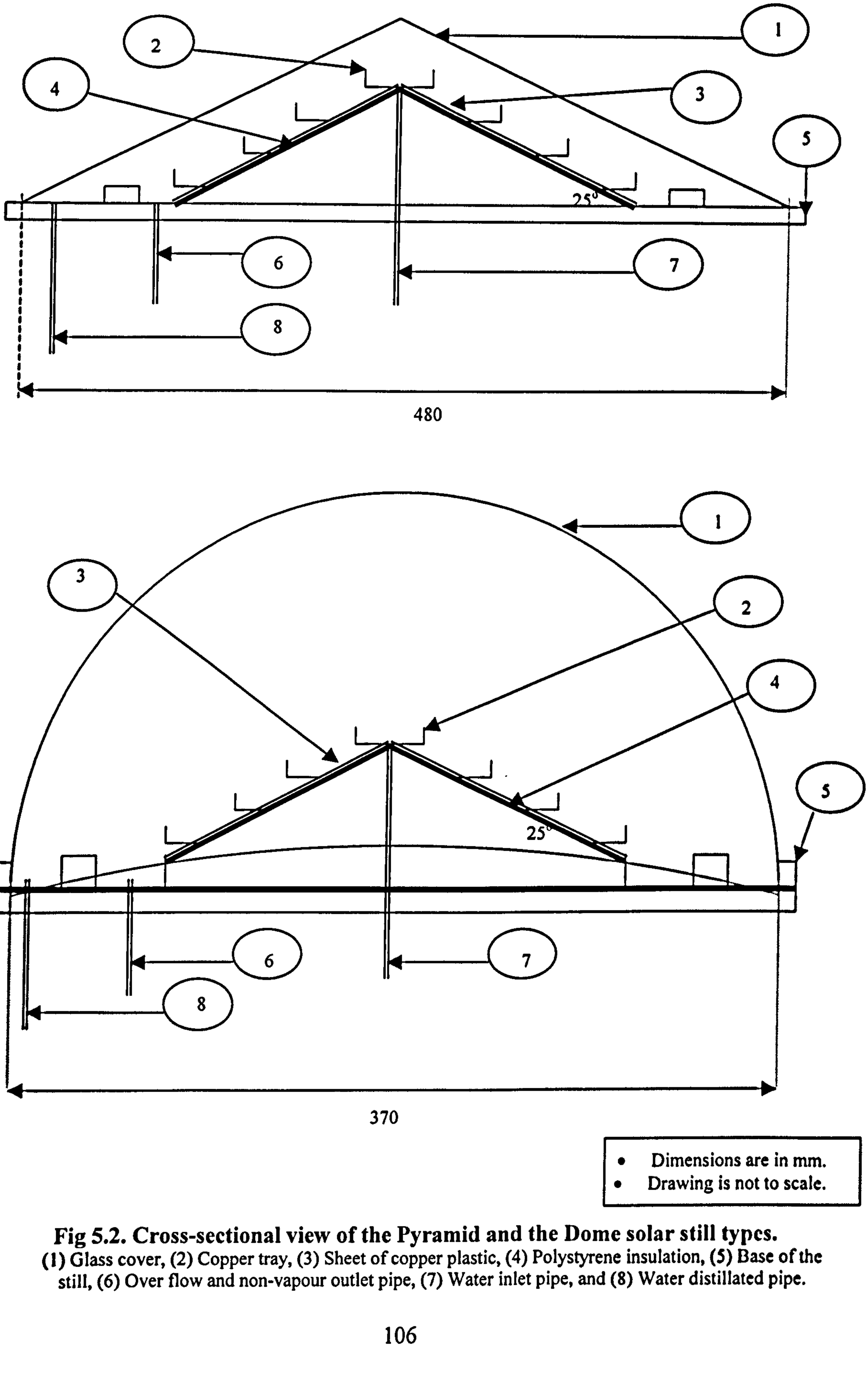

- Dimensions are in mm.
- Drawing is not to scale.

Fig 5.2. Cross-sectional view of the Pyramid and the Dome solar still types.
(1) Glass cover, (2) Copper tray, (3) Sheet of copper plastic, (4) Polystyrene insulation, (5) Base of the still, (6) Over flow and non-vapour outlet pipe, (7) Water inlet pipe, and (8) Water distillated pipe.

The pyramid sides were sloped at angle of 25°. The upper part of the pyramid contains a narrow trough to feed the still by inlet water as shown in Fig 5.3. (a, b). The distillate collection and brine outlet channels were connected to 10 mm diameter outlets through the still base, which was made of a Perspex sheet of a dimension of 500 x 500 x 30 mm. These distillate channels were connected by plastic tubes to the distillate reservoir and water pump respectively.

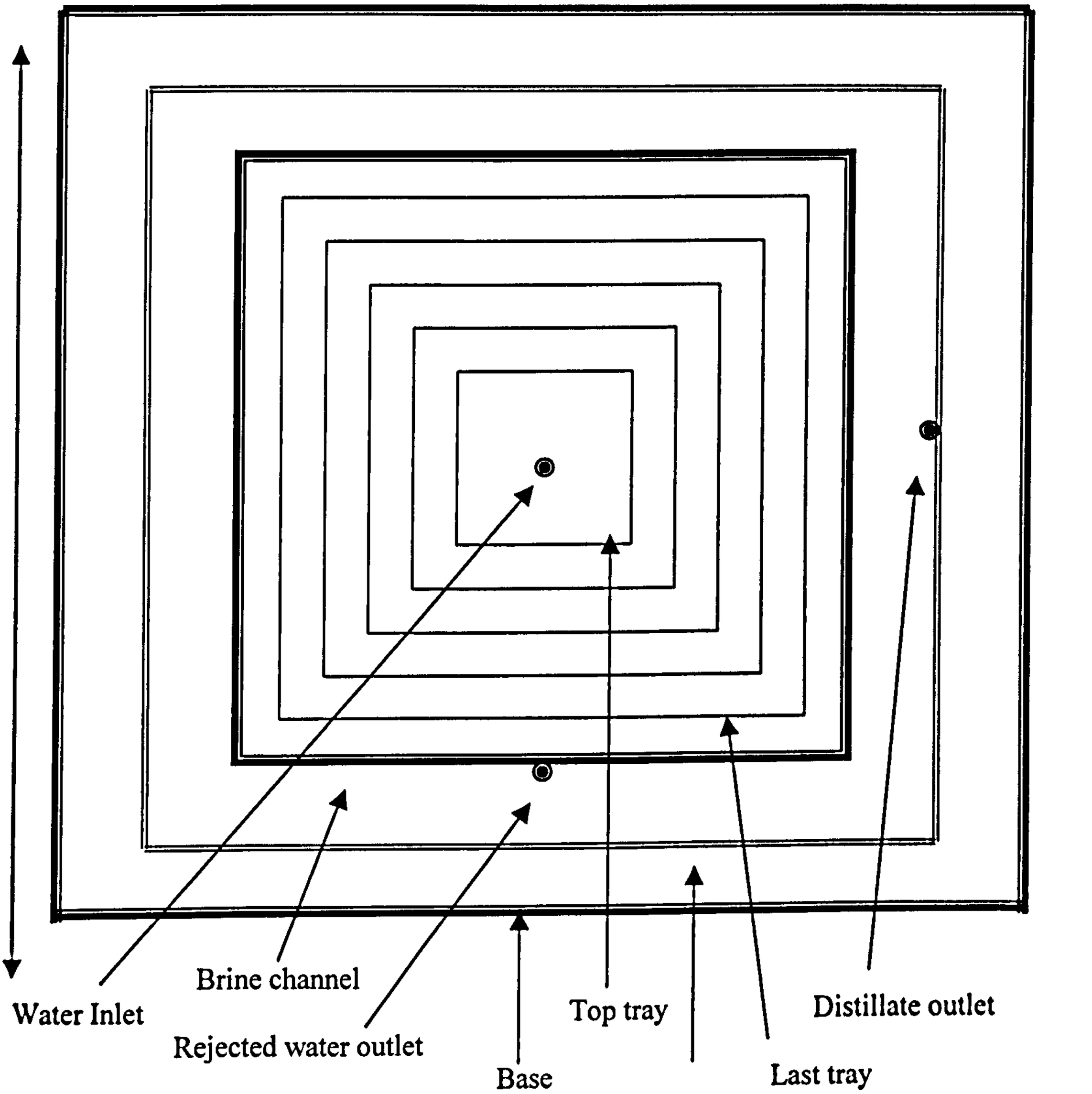

Fig 5.3.a. Plane View of The Pyramid Solar Still

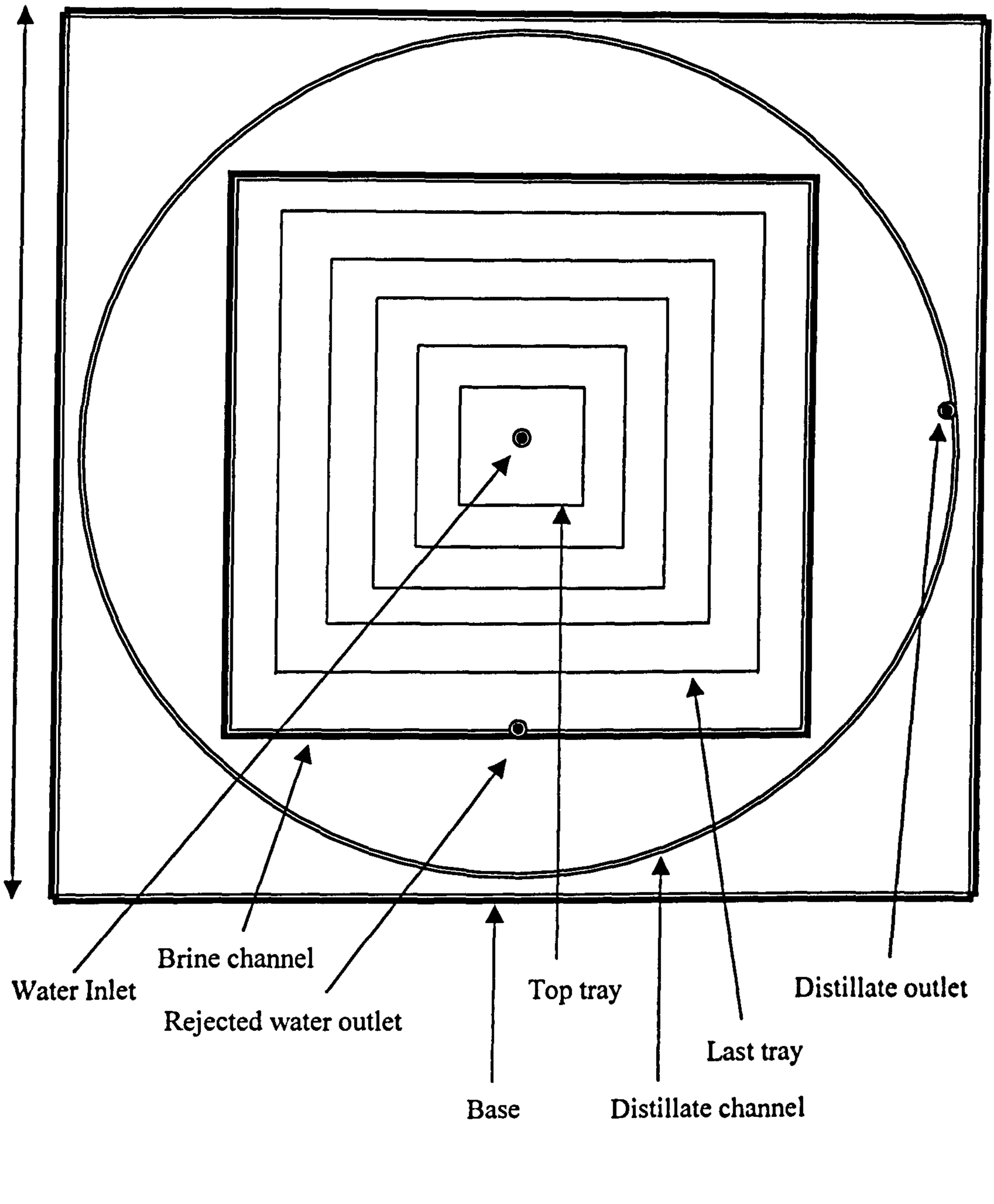

Fig 5.3.b. Plane View of The Dome Solar Still.

As it is shown in Fig 5.4. (a, b), the pyramid absorber was covered by 4mm thick glass for the both types. In the model 1 (d) case, a half spherical shape made of glass diameter of 370mm and height of 185mm was employed. The model 1 (p) was formed by jointing four triangular glass together by silicon glue. The pyramid base was 480mm and the height was 110mm. The cover was held about 115mm and 40mm above the saline water surfaces for the model 1 (d) and (p) respectively..

The lower edges of both covers are fixed tightly to the special channel on the upper surfaces of the still base. A sponge rubber gasket is located between the cover and the still base arranged so that there are no gaps between the cover edge and the still base. Plats [1- 6] illustrate both stills.

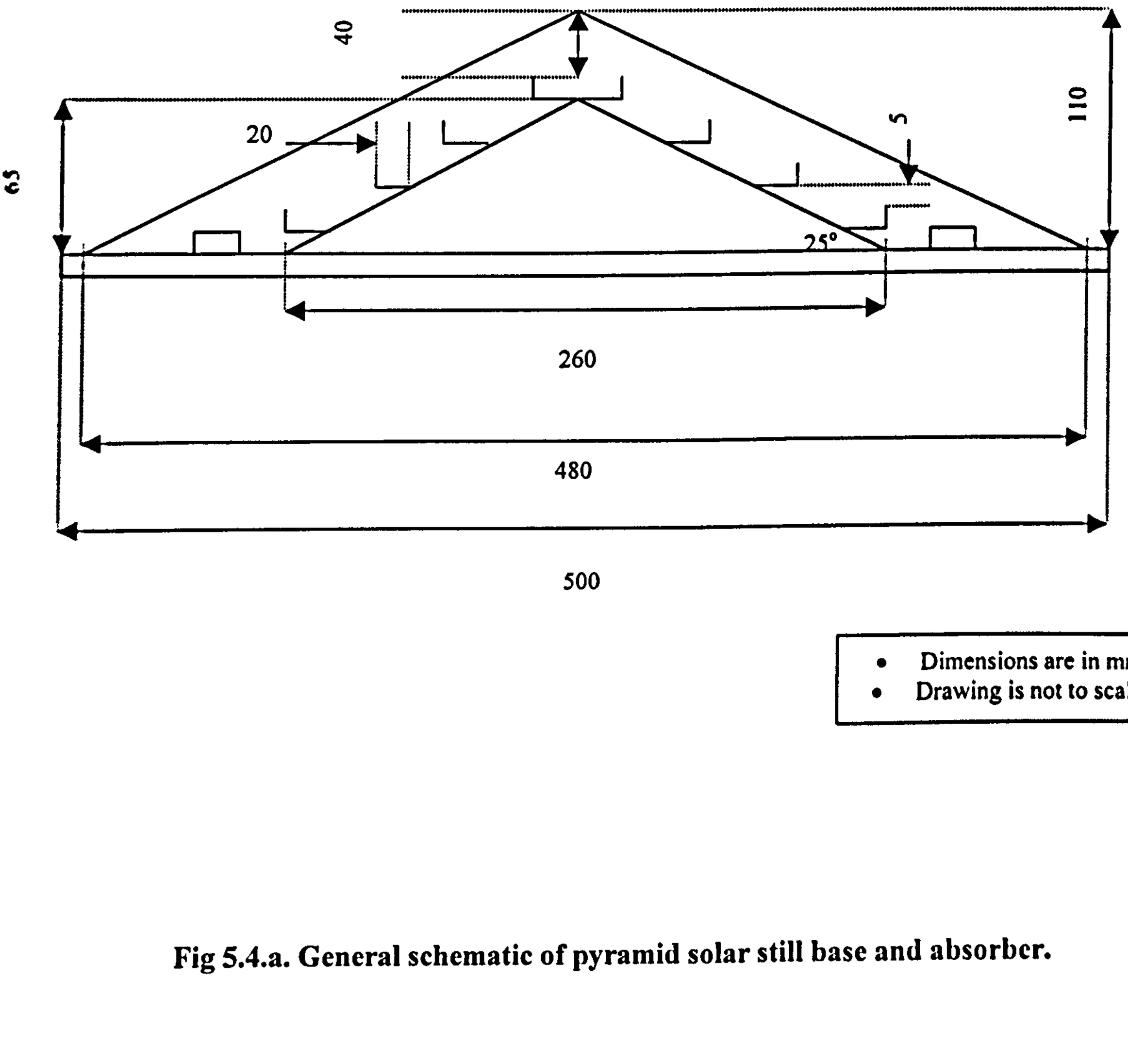

Fig 5.4.a. General schematic of pyramid solar still base and absorber.

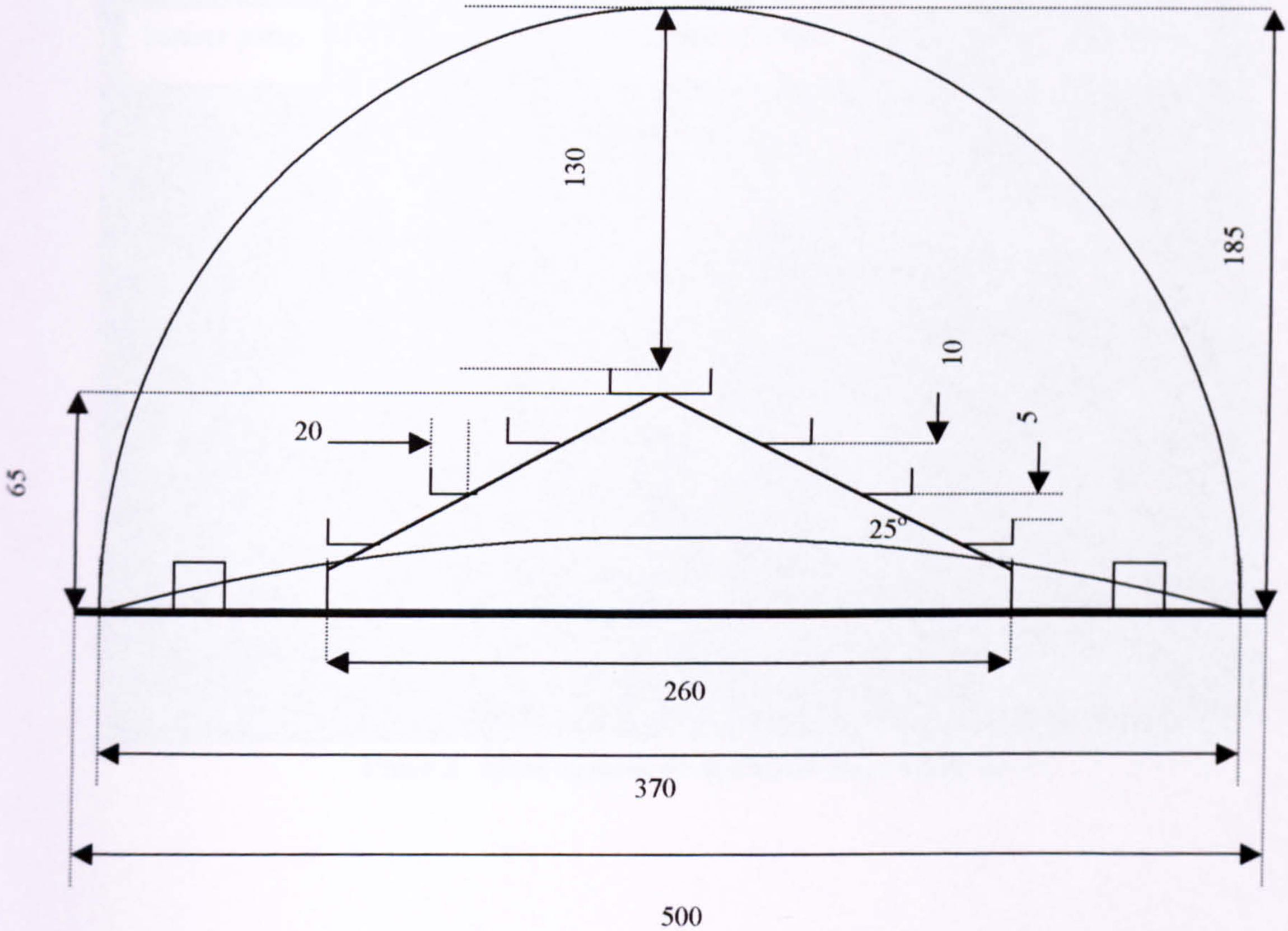

- Dimensions are in mm.
- Drawing is not to scale.

Fig 5.4.b. General schematic of dome solar still base and absorber.

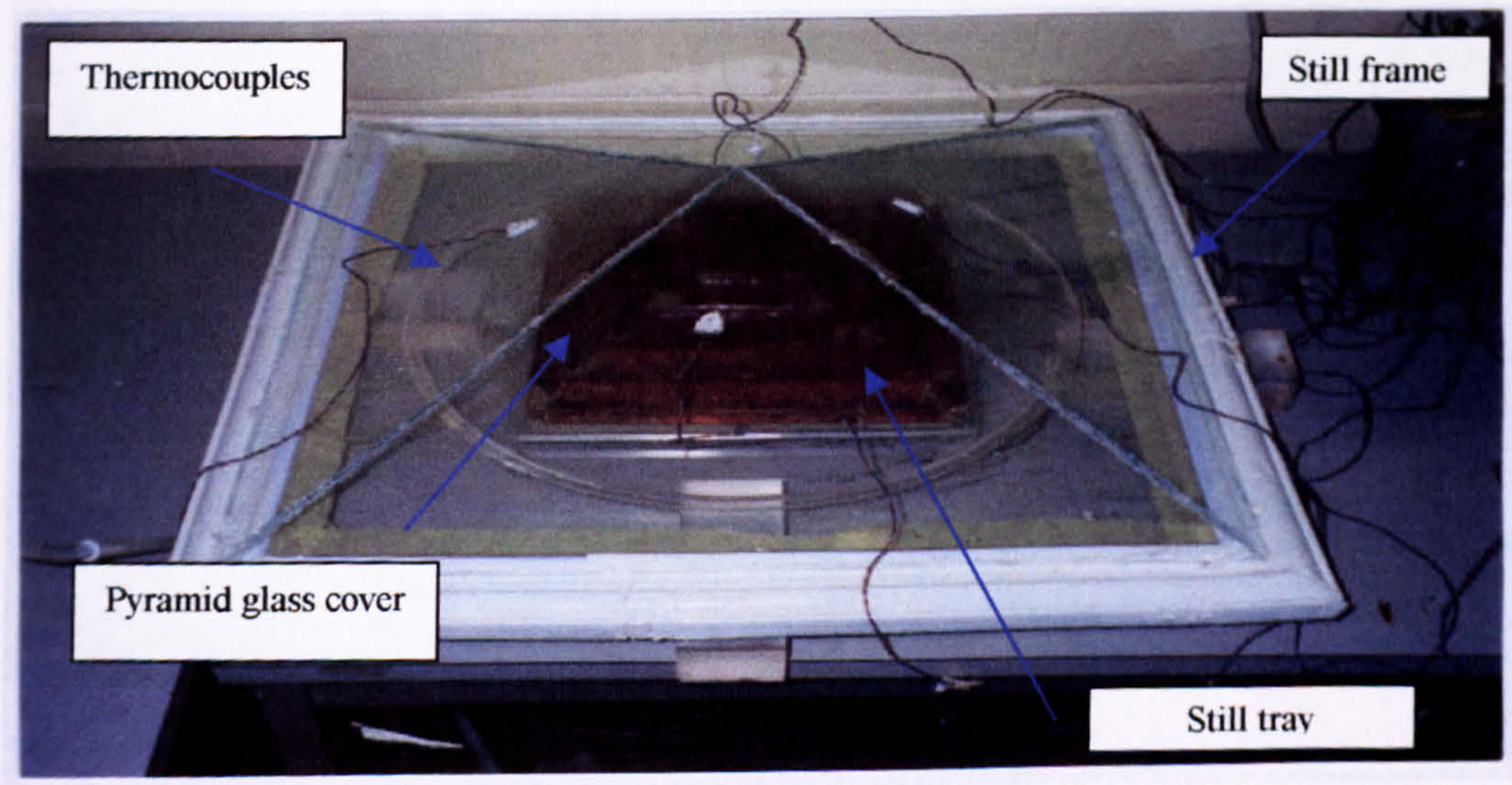

Plate 1. Pyramid solar still type.

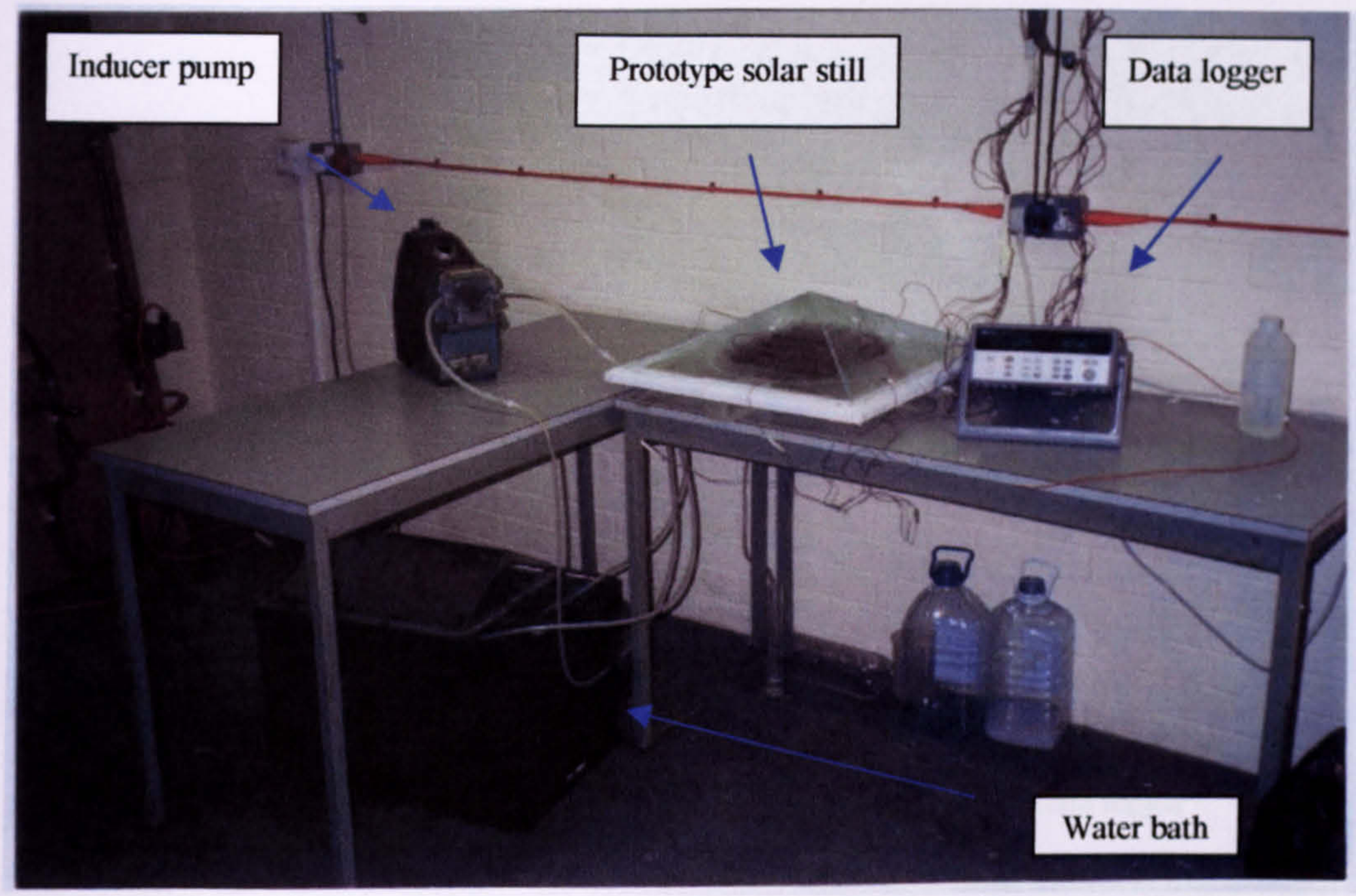

Plate 2. Flow system of pyramid solar still type.

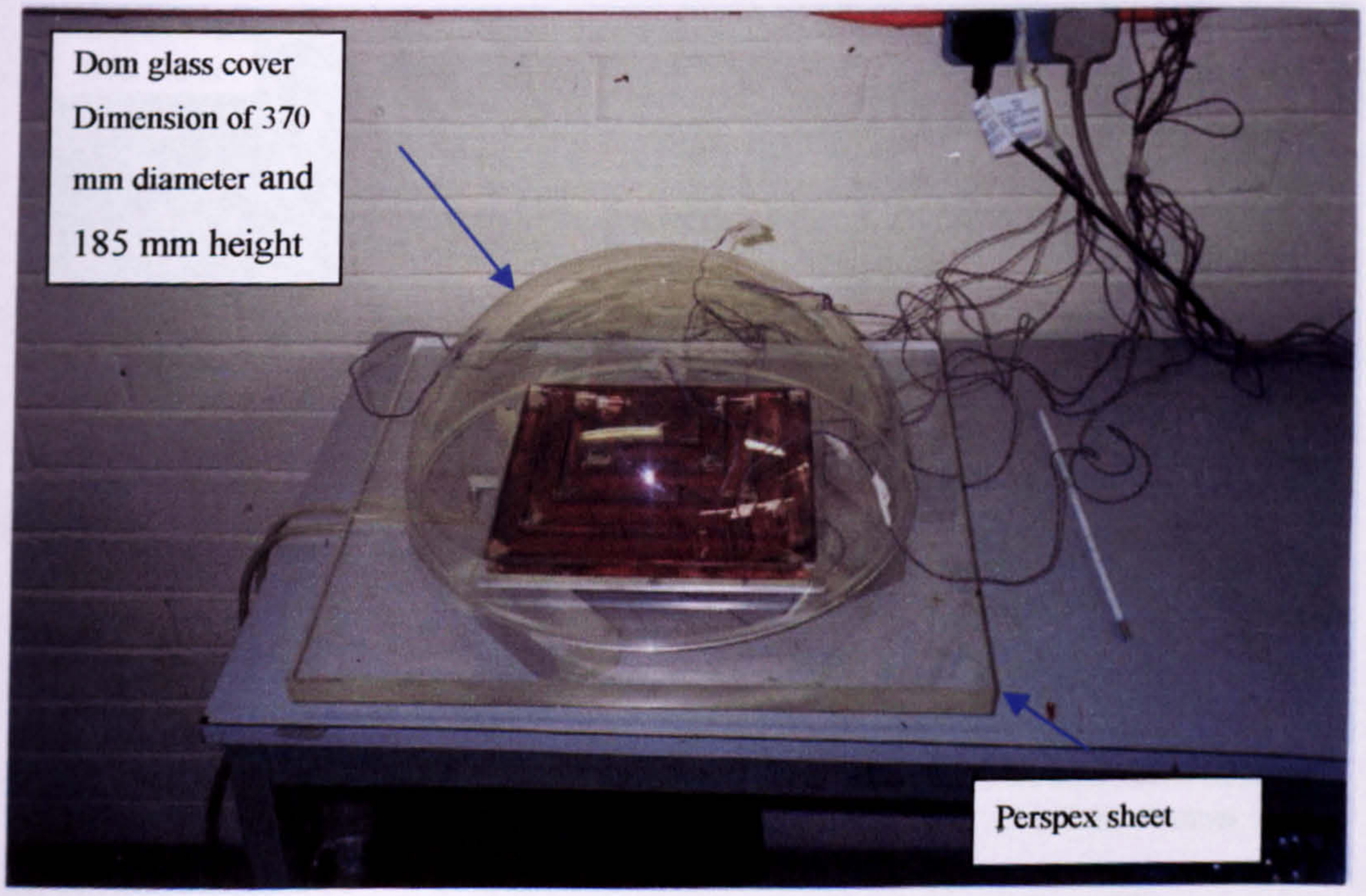

Plate 3. Dome solar still type.

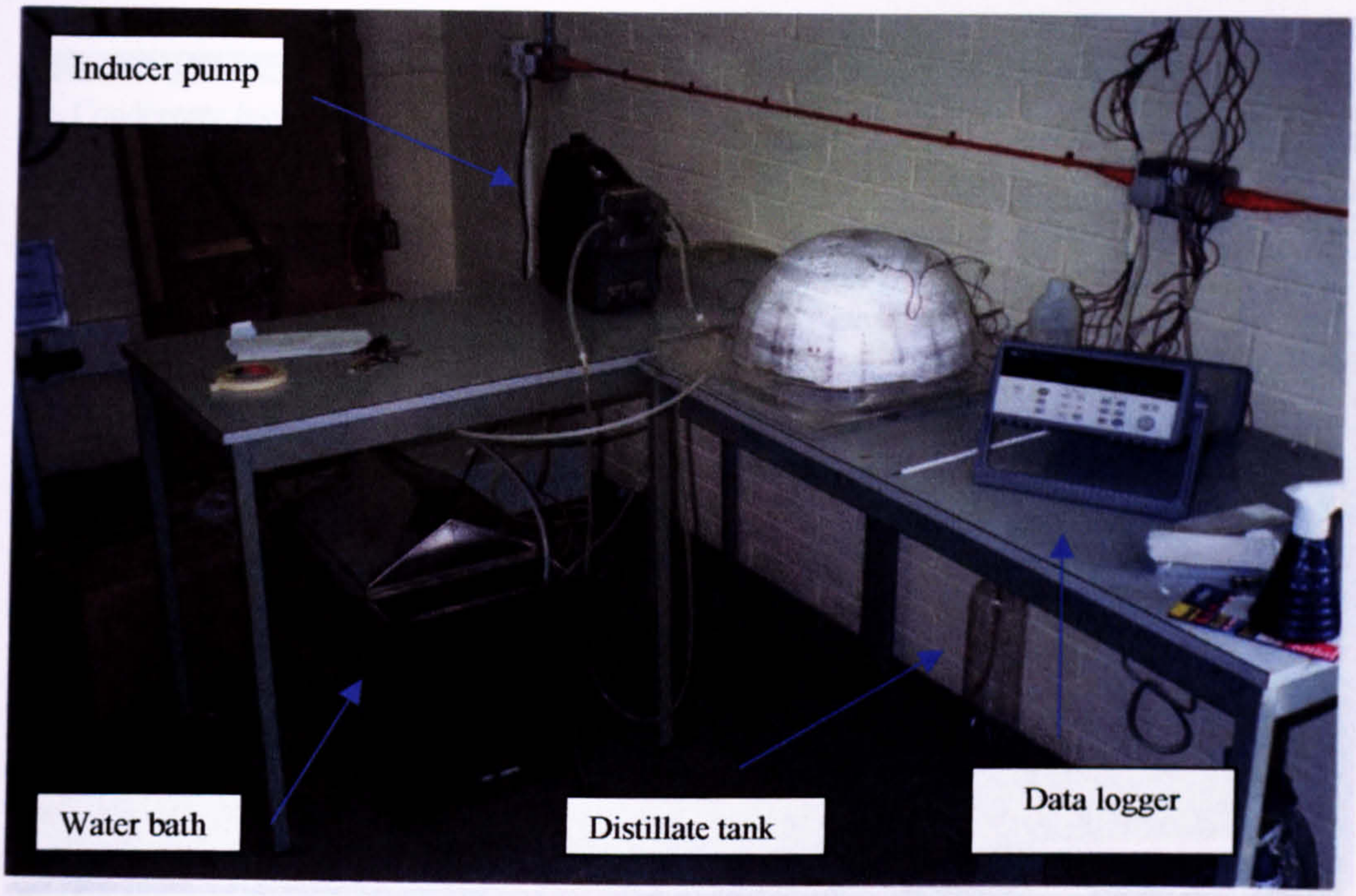

Plate 4. Flow system of dome solar still type.

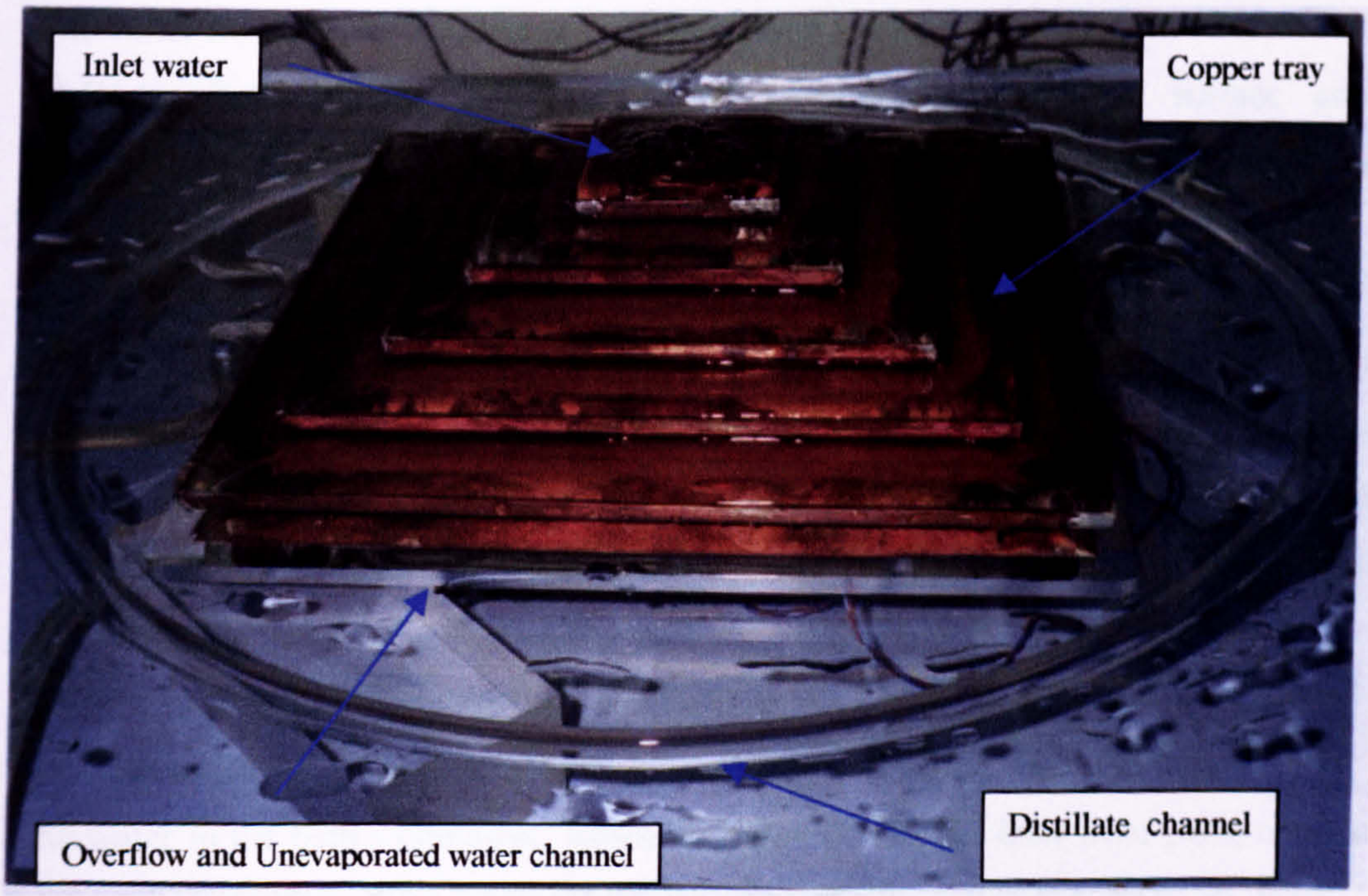

Plate 5. The pyramid absorber of tilted tray solar still.

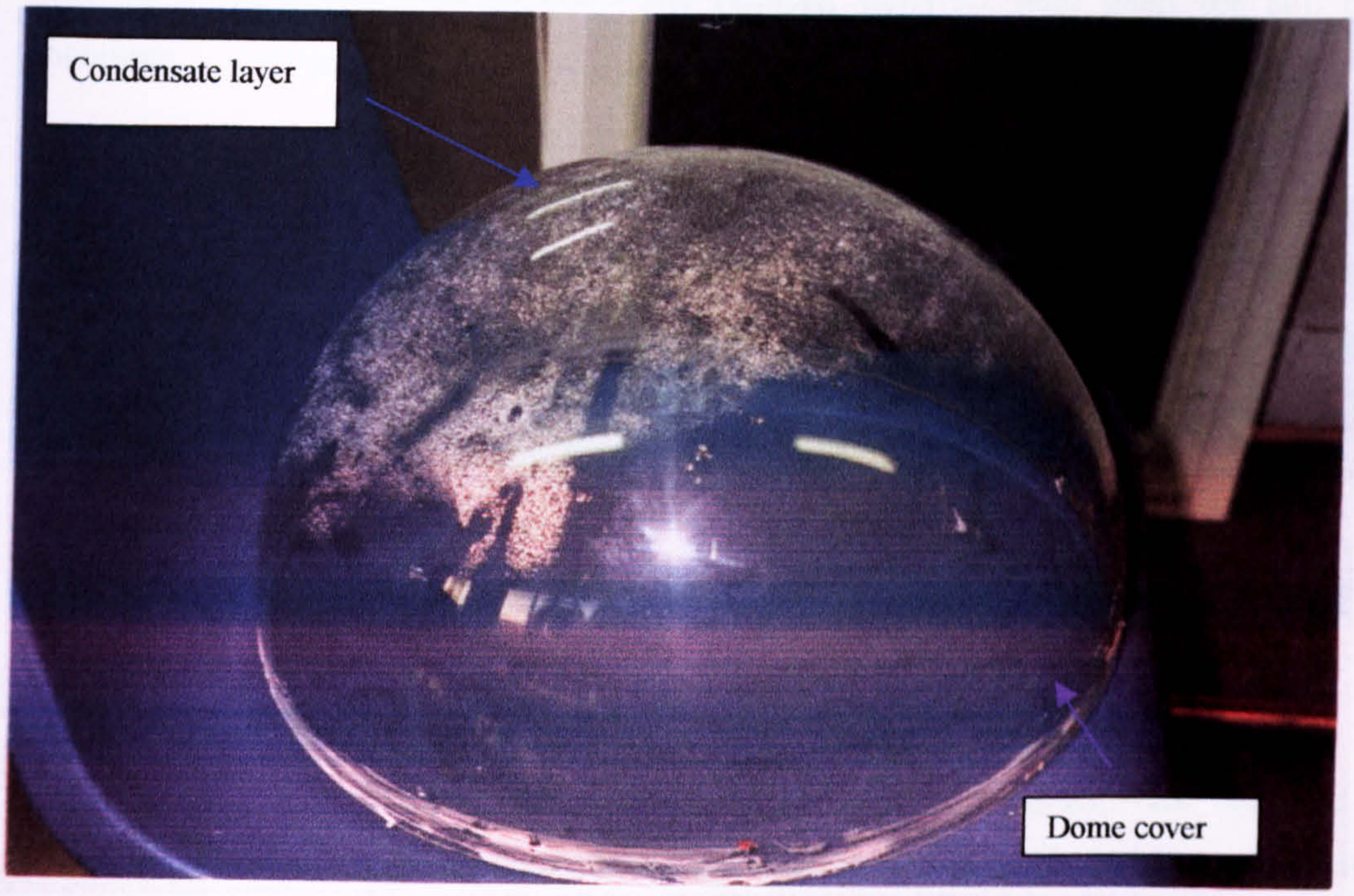

Plate 6. Dome solar still cover (Dropwise)

5.5 Water Flow System

The water flow system consists of two main parts:

(a) Water bath, of 50 litres maximum capacity with a water surface area of (500x 400 mm^2). This is the inlet water main reservoir. The main water reservoir is connected with water recirculation pump.

(b) An adjustable water flow inducer pump controlling the water flow rate to a very low rate of 0-10 kg/ hr. This was necessary to maintain constant water temperature throughout the experiment, reduce spatter and for keeping the water as long as possible on the trays. The water is fed to the still through a plastic pipe of 5 mm inner diameter.

5.6 Controlling The Inlet Water Temperature

The water in the bath's container, which was provided by the inlet water, was used in the evaporation process. The volumetric capacity of the container was 50 liters. The temperature of the water was adjusted by a thermostat. The still level was kept higher

than the level of the bath to allow the rejected water to flow from the still bath's container.

The constant temperature preheated water was transported to the still from the water bath by 5 mm plastic pipe connecting the bath to the inducer pump. The flow was adjusted to a constant rate in the inducer pump, which in turn was connected to the solar still by 5 mm plastic pipe. The overflow and non-vaporized water in the still was collected from underneath the lower tray and returned via brine channels back to the water bath to be reheated and pumped again to the still.

5.7 Instrumentation

(a) Temperature measurements

The temperatures of the tray and glass cover at various positions were recorded and stored by a data logger (Acquisition/Switch Unit, model HP 34970A) by twelve individually channels. This data logger has many features such as, 6.5-digit multimeter accuracy, reading rates up to 600 reading per second on a single channel and scan rates up to 250 channels per second, direct measurement of thermocouples, and interval scanning with storage of up 50,000 time-stamped readings. Still temperatures were measured in various positions of the still using E type thermocouples with temperature a range of -200°C – 1000 °C, and measurement accuracy of +/- 1 °C – 1.7 °C.

These measurements were vital in order to provide a full description of the still performance during the experiment. Four metal-sheathed thermocouples from Comark Electronics were fixed on the inner surface of the four-sided still tray. Furthermore, four self-adhesive patch thermocouples were attached at the four sides of outer surfaces of the glass cover to measure the cover temperatures. The inlet and the outlet water temperatures were also measured by means of sheathed thermocouples. One patch thermocouple was attached in a shaded location somewhere underneath the inclined support board, to measure the ambient temperature. All these thermocouples were connected to the HP34970A data logger, which recorded the temperature every fifteen minutes. The thermocouples data logger readings were calibrated against a mercury thermometer with an accuracy range of +/- 0.2°C.

(b) Spirit level, to fix the still on the horizontal level.

(c) Stopwatch to measure the experiment duration.

(d) Electronic balance to weigh the distilled water produced every 15 minutes.

(e) Mercury thermometer, to verify the selected inlet water temperature in the water bath.

5.8 Experimental Procedure

All tests on the two types of solar still were conducted under laboratory conditions, by varying the input water temperature between 40, 50, 60, and 70 °C. Moreover, the cavity between cover and water were also varied between 20,40, and 80 mm.

The following steps were taken in all the experiment:

- The Data Acquisition/Switch Unit was configured and its initial logging time was set and subsequently it was connected to the various sensors.
- Sufficient quantities of the hot water were prepared in readiness to be fed into the still.
- The inducer pump adjusted the required flow rate.
- The weight of distillate produced was determined every 15 minutes.
- Overflow and unvaporized water was periodically returned to the water bath via the plastic pipe.
- The Data Acquisition/Switch Unit was converted to a readable form.

5.9 Experimental Strategy

While the indoor experimental setup made it possible to study the influence of the two design shapes on the still productivity, it was decided to concentrate on:

- The inlet water temperatures.
- Different spacing between glass cover and water surface.
- Comparing the shape factor of the cover.

5.10 Preliminary Test

This section describe the indoor experiments that were conducted under control laboratory condition. Two main parameters were examined in this preliminary test; the first was the inlet preheated test and the second test was to investigate the optimum spacing between glass cover and water surface.

5.10.1 Experimental Setup

Model 1 (d) and (p) were laid on a horizontal cabinet in the thermodynamics laboratory at the University of Hertfordshire. The thermocouples were connected to a data acquisition/ switch unit. The data acquisition device was already calibrated, and the interval scanning data was predetermined at fifteen minutes. The still water inlet, ambient, cover, tray, and water outlet temperatures were monitored continuously in this experiment.

In these experiment, the water bath, which contains the inlet water, was used to heat the water in the still instead of solar radiation. Hence, water vapour forming due to increased inlet hot water temperature. Several parameters were also investigated in these preliminary tests including inlet water temperature, and the still cavity volume. In these experiments the following instruments were setup; the heat adjustable water bath for obtaining the required water inlet temperature; inducers pump for adjusting the required flow rate, and three plastic ring bases of various height for obtaining the optional cavity volume required between the still absorber and the still cover.

5.10.2 Experimental Results

Figure 5.5 (a, b) shows the variation of productivity for both still types and different inlet water temperatures. It can be seen that the average hourly output of both still are maximum when inlet water temperature was 70 °C. It can also be noticed that the minimum output of the two types is recorded when the inlet water temperature, 40 °C, is at its lowest value. The variation in productivity for the different inlet water temperatures is attributed to the amount of evaporation in the still. A high water temperature enhances the evaporation rate more than the low water temperature. Consequently, the condensate rate increases.

The second test was conducted to examine the optimum spacing between glass cover and water surface. To optimize the still design parameters, three different spacing (d_f) were tested. These were 20, 40, and 80 mm respectively. Comparison of the condensate volume resulting from the three designs is shown in Fig 5.6. (a, b). In these tests, the cavity is measured from the edge of the first tray to the inner apex of the pyramid cover. Still design with the closest distances between cover and water surface produced the highest yield. This is attributed to a decreased air thermal capacity for the shortest cavity distance still as clearly indicated in the literature (Garg, 1978).

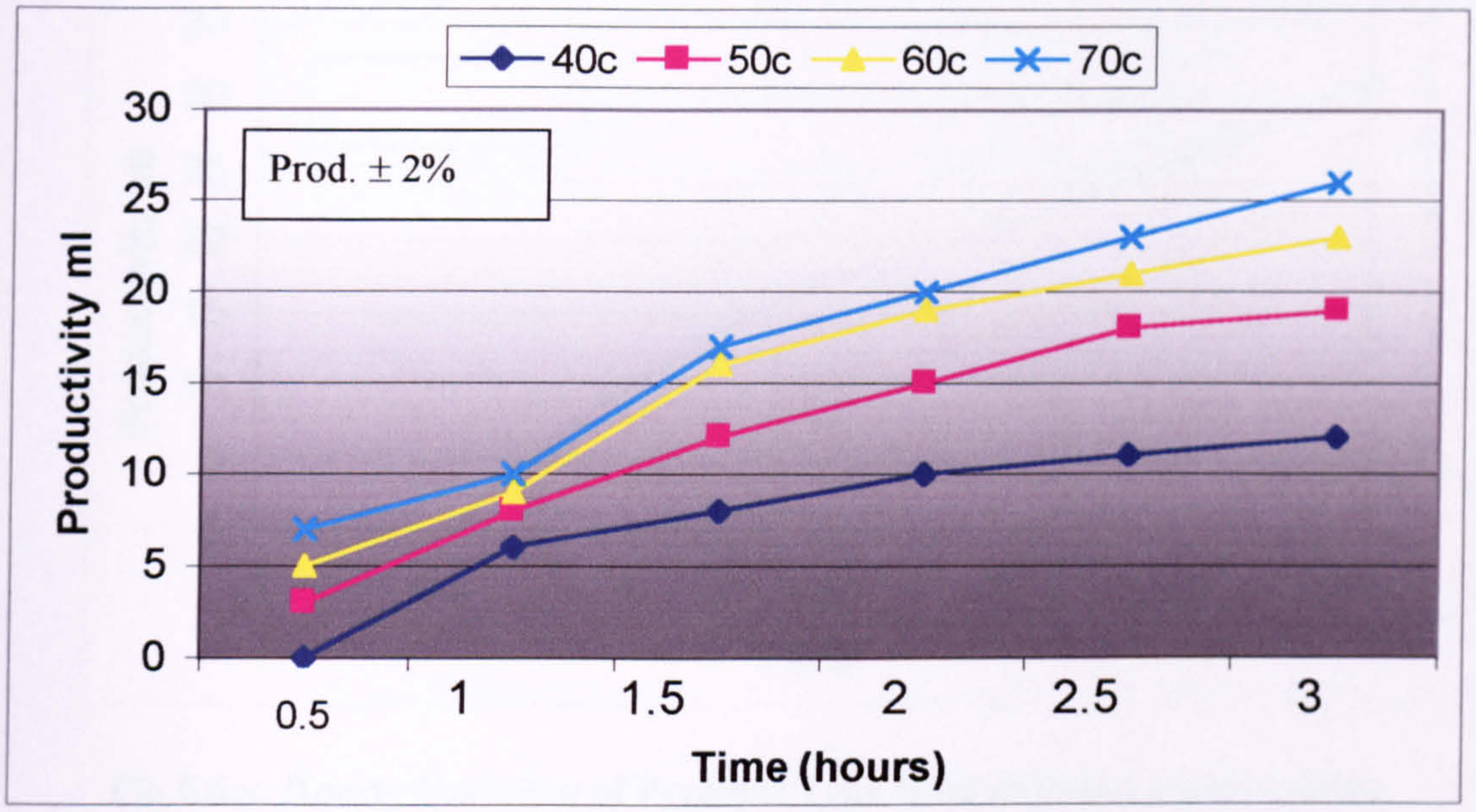

Fig 5.5.a. The hourly productivity of pyramid type with different inlet water temperature.

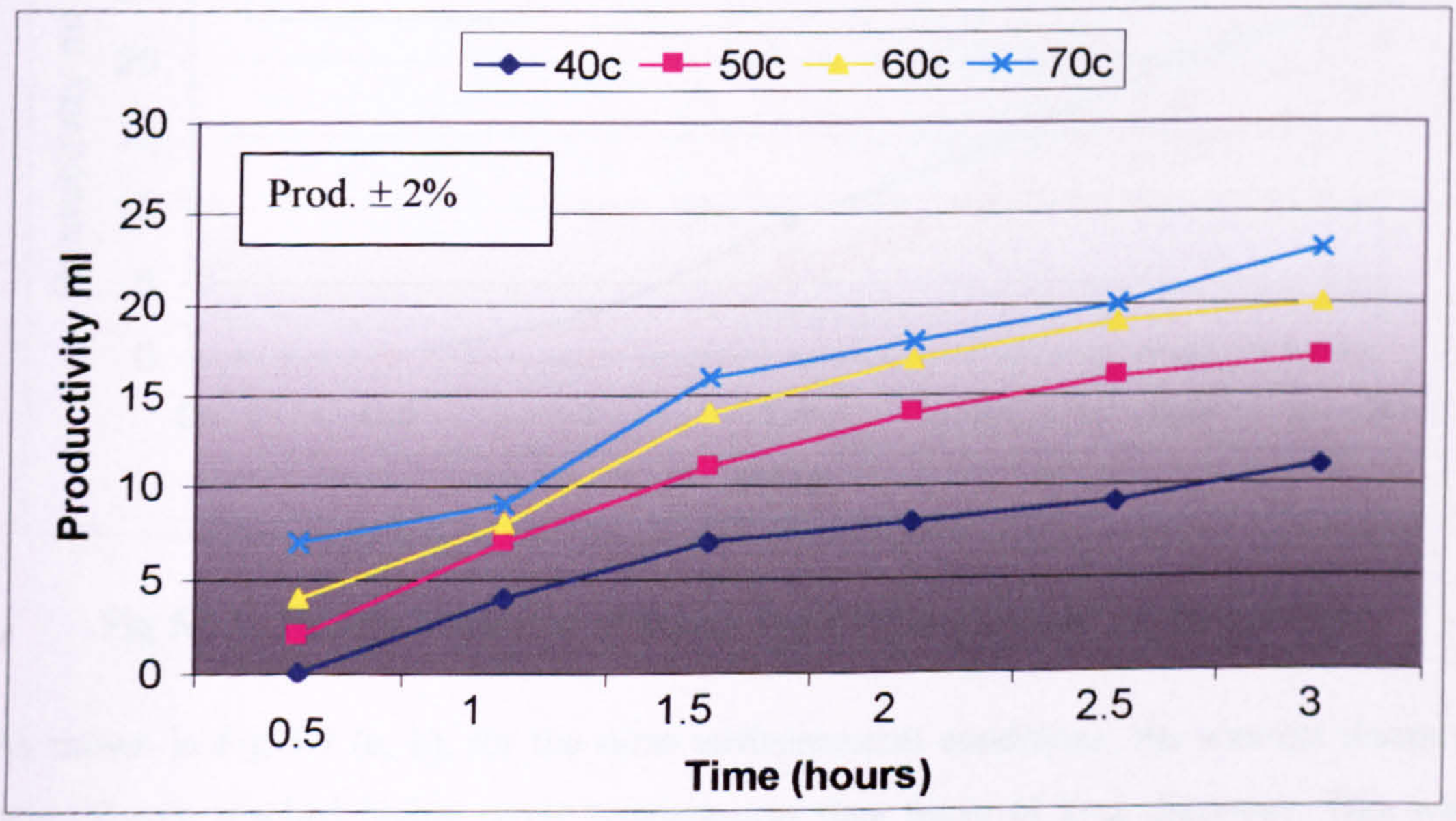

Fig 5.5.b. The hourly productivity of dome type with different inlet water temperature.

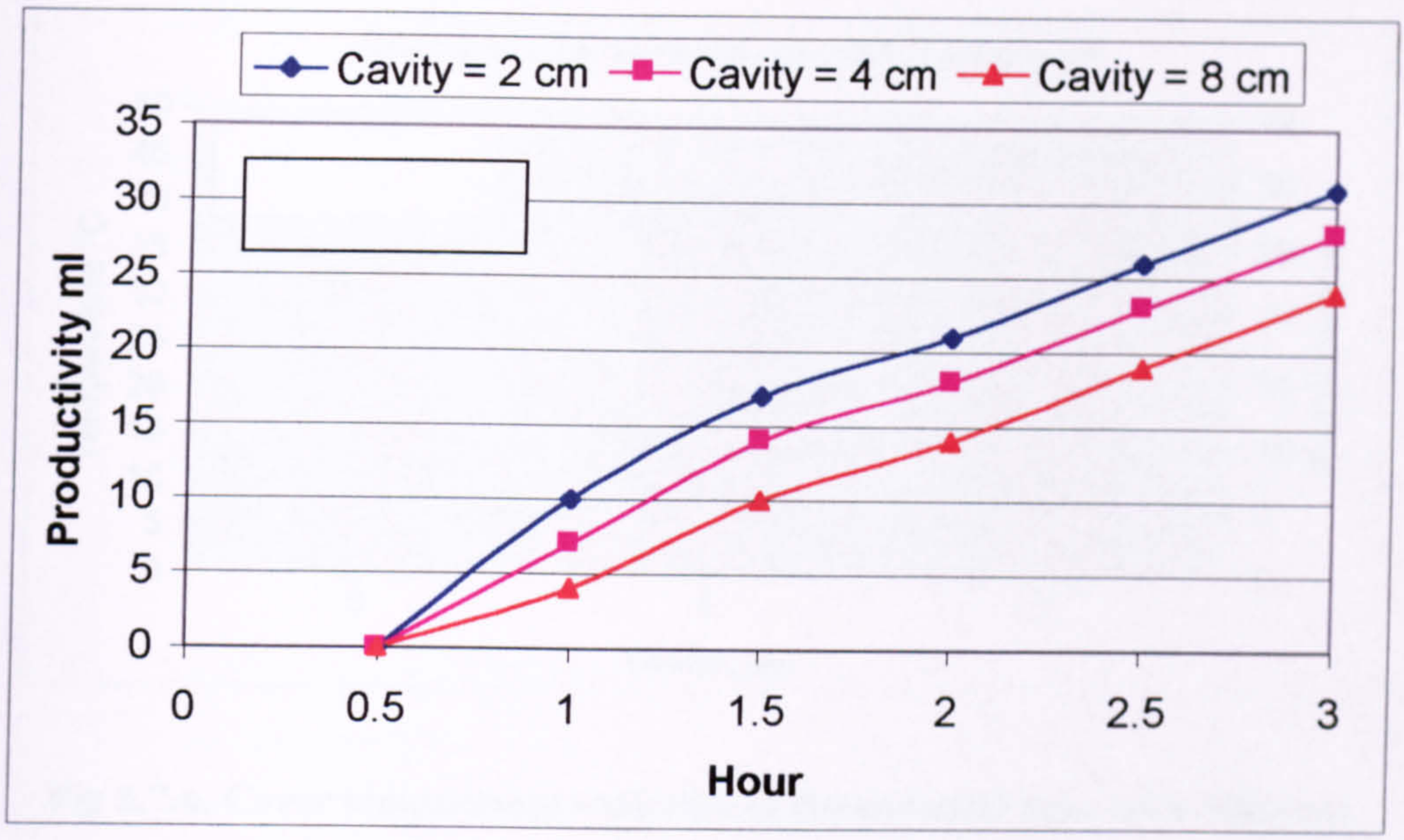

Fig 5.6.a. Hourly Variation of Pyramid Type With different cavity volume.

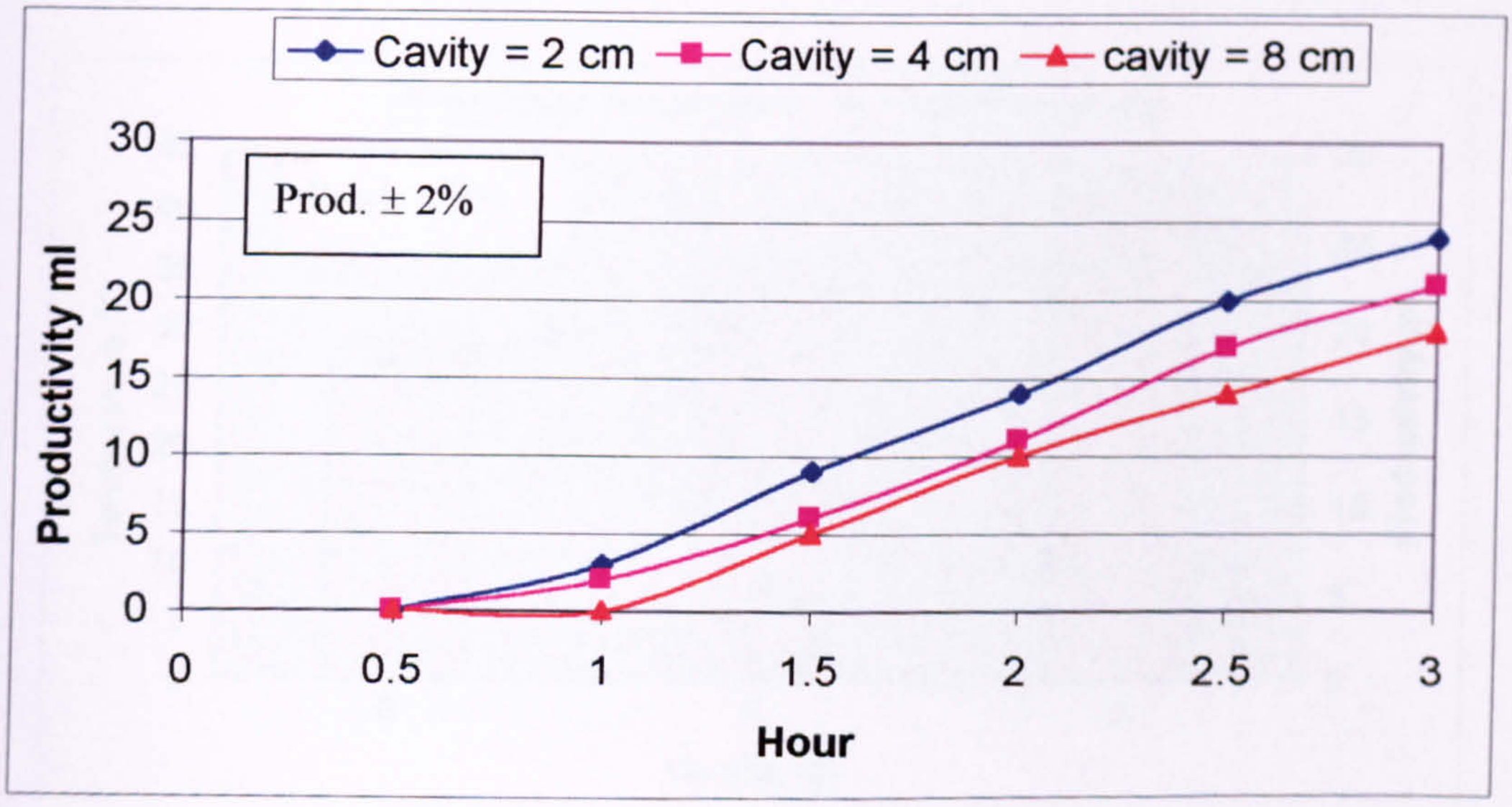

Fig 5.6.b. Hourly Variation of Dome Type With different cavity volume.

As shown in Fig 5.7 (a, b), for the same environmental conditions, the shortest distance type 20 mm reached higher cover temperatures than those of long distances. This was most likely caused by the longer distance traveled by the vapour in the case of larger cavity. In such case, the air humidity increase over a longer time. This also affects the still productivity as demonstrated in Fig 5.7 (a, b).

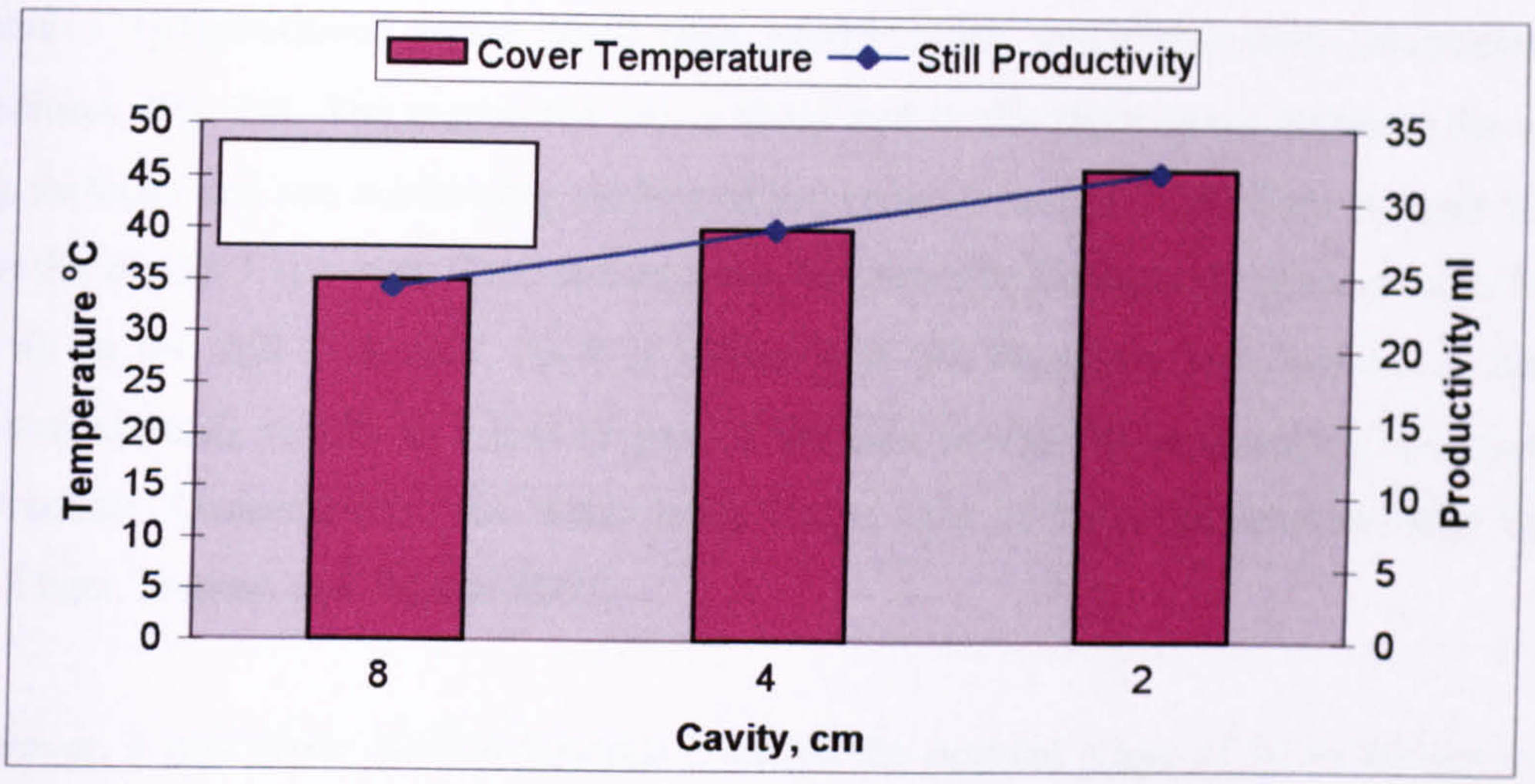

Fig 5.7.a. Cover temperature variation of the pyramid type with different cavity volume.

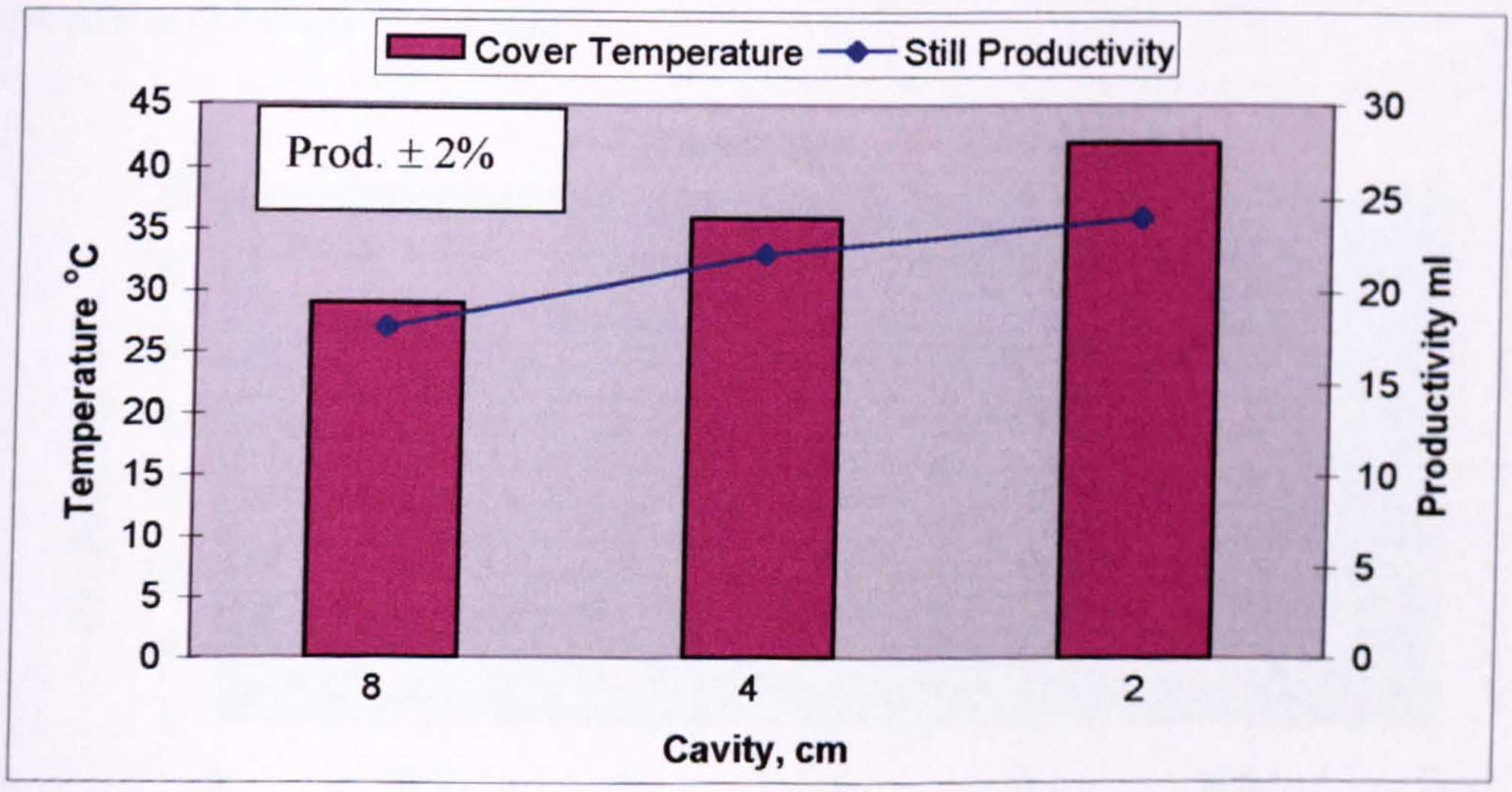

Fig 5.7.b. Cover temperature variation of the dome type with different cavity volume.

5.11 Comparison of The Dome & Pyramid Still

The geometry of the still cover is an important factor when considering a solar still, as it directly effects the amount of incident solar energy collected, stops the raising vapour and finally works as a condenser surface. In this work it was found from indoor tests that

model 1 (p) produced better yield than model 1 (d) under the same environmental condition, Fig. 5.8. The reason for this is likely due to the large space between the water tray surfaces and the condensing surface of the cover in model 1 (d). This is much higher than the model 1 (p) case. This distance can dramatically increase the thermal capacity of the air in the still enclosure. As it is indicated in the literature, any increase in the air thermal capacity results in a loss of part of the heat energy for evaporation by means of convection. Consequently, the water takes longer time to be evaporated in large cavity (Al-Thani, Nasser, and Sayigh 2000).

However, a tray cover surface distance is within the optimal range of 30 to 40 mm in the model 1 (p), as recommended in the literature (Achiloc, Zhraev and Akhtamov 1973). Also the model 1 (d) still cover has shown some disadvantages as compared with the model 1 (p) cover shaped, such as most of the condensate layer is concentrated on the top of the inner surface of the cover. There the angle is very high as can be shown in Plate 3, thus, the droplet could grow in size till its weight overcomes the surface tension and it eventually drops down in the tray.

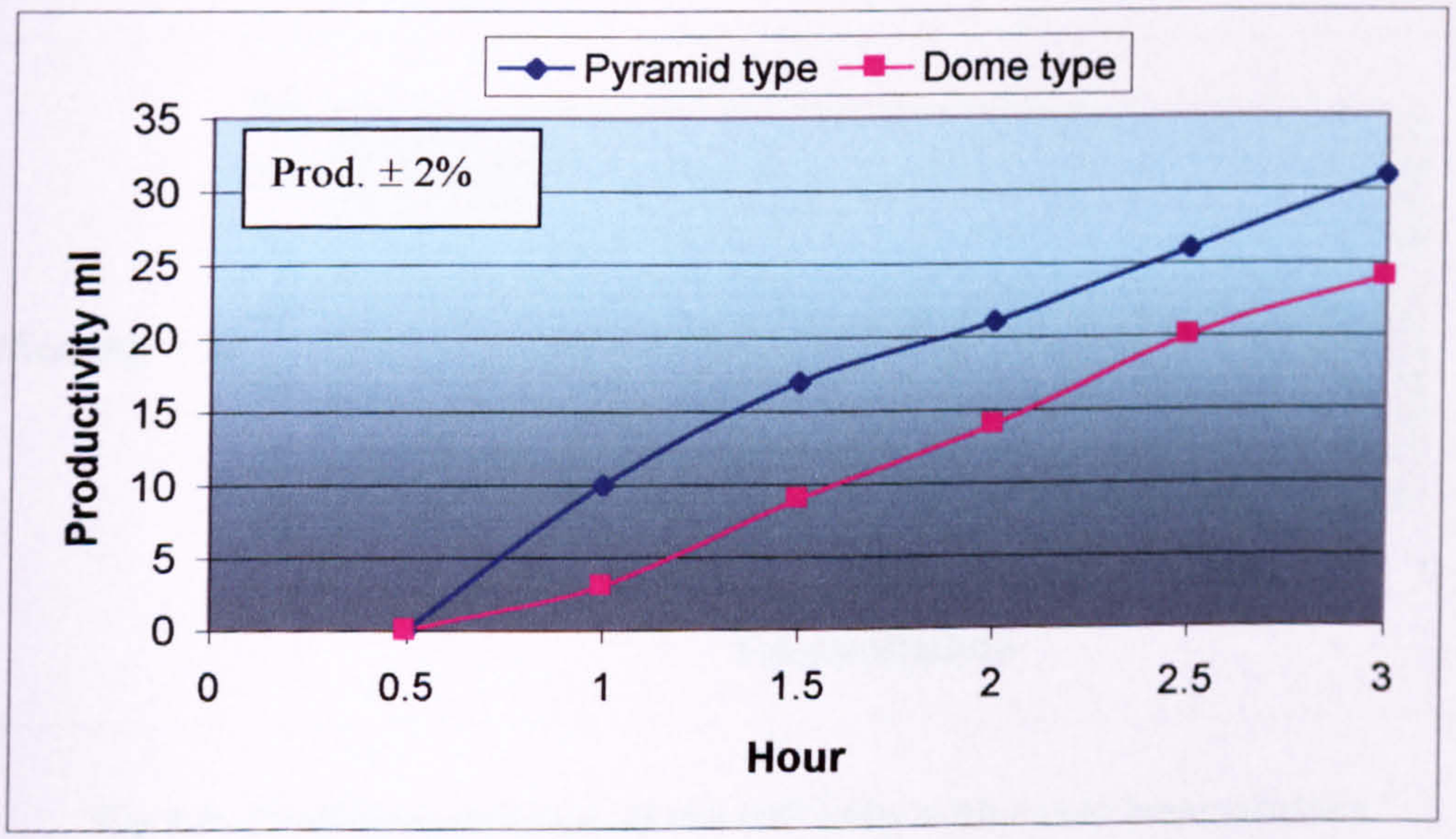

Fig 5.8. Comparison of Pyramid and Dome Type under optimum conditions.

On the other hand, in model 1 (p) shaped cover, as shown in Plate 4, the condensate layer was distributed over the whole cover surface and the thickness of the condensate was very thin as compared with the dome shaped cover. Therefore, the loss from backdrop is minimized. It was also observed that condensate film drained faster into the collecting

channel. Cooper 1969, mentioned in his studies that the size and the condensate affects the cover transmittance, by the increasing the reflection of incident solar rays

The transmittance of the glass cover is also an important factor in the predicted performance of the daily efficiency of the solar still due to its direct effect on the incident solar energy. It has been studied by many authors including Norton *et al.* (1988). From the predicted numerical calculations, which are shown in Fig 5.9, it can be seen that the still efficiency is a strong function of the cover transmittance. It decreases from 57.2 to 38.4 when the transmittance decreases from 0.95 to 0.70. The real experimental value of the transmittance of the solar still cover with condensation on it, in the form of thin film or dropwise, is a variable quantity and depends on the distribution of the drops and their size or the thickness of the film of condensate on the cover. *"It is essential that the condensing water vapour should form a thin film, which is invariably formed on the glass surface and acting like a small reflector. The appearance of such a surface is silvery white and the reflection losses may be as high as 40 per cent of the total incident solar radiation"* (Daniels and Duffie, 1955).

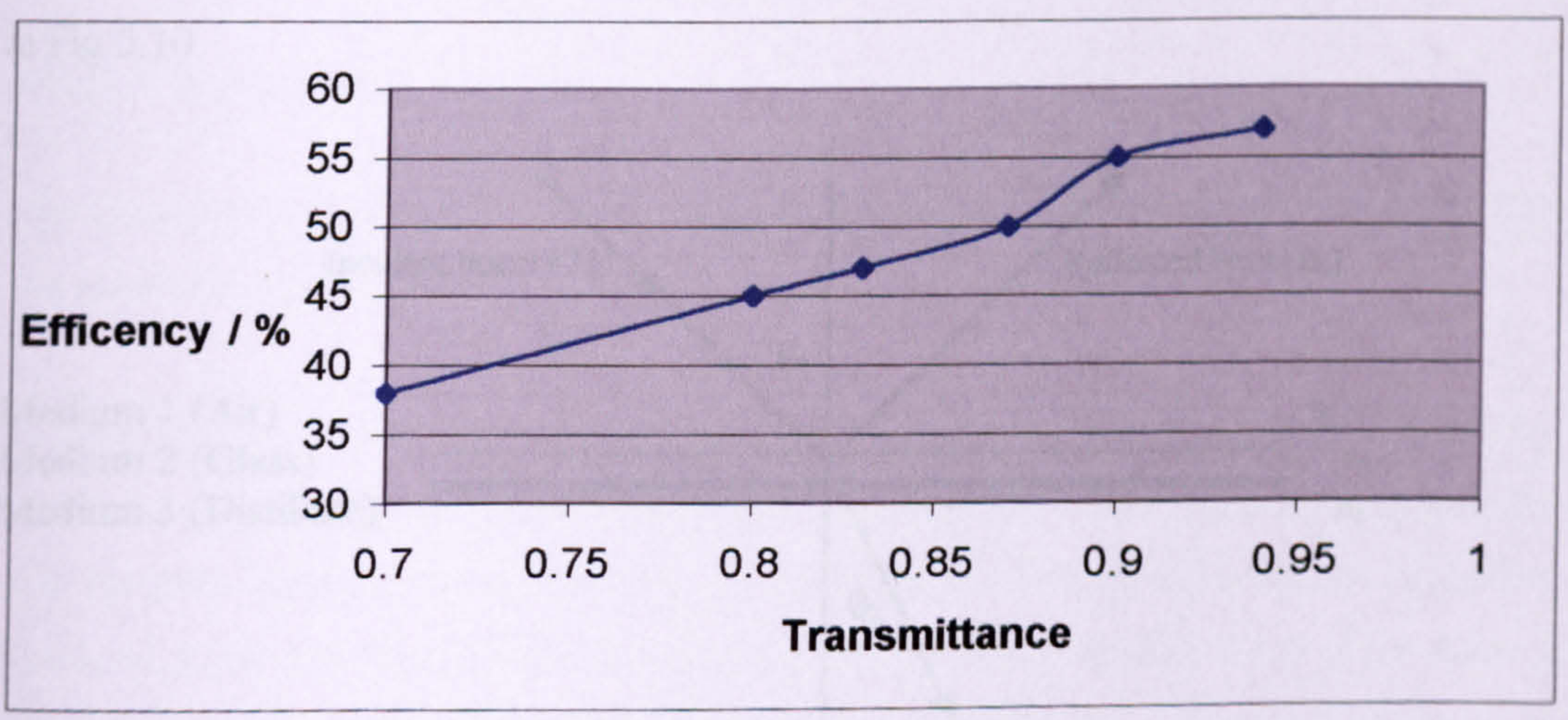

Fig 5.9. Predicted variation of the still daily with cover transmttance (Norton, 1988).

Transparent covers in various shapes are used to reduce heat and vapour losses from the solar still. Consequently, an understanding of the process and laws that govern the transmission of radiation though a transparent medium is important for the design of solar still. Materials for this type of application should be able to transmit solar radiation at all

angles of incidence, have dimensional stability, and have long-term durability under exposure to the sun and the weather.

For smooth surfaces Fresnel, in (Kreith, 1978), has derived expressions for the reflection of unpolarized radiation on passing from a medium 1 with a refractive index, n_1, to medium 2 with refractive index, n_2.

$$r_I = \frac{\sin^2(\theta_2 - \theta_1)}{\sin^2(\theta_2 + \theta_1)} \qquad (5.1)$$

$$r_{II} = \frac{\tan^2(\theta_2 - \theta_1)}{\tan^2(\theta_2 + \theta_1)} \qquad (5.2)$$

$$r = \frac{I_r}{I_i} = \frac{1}{2}[r_I + r_{II}] \qquad (5.3)$$

where I_i and I_r are incident and reflected beam; θ_1 and θ_2 are the angles of incidence; n_1, n_2, and n_3 are the refraction medium of air, glass, and distillate of respectively, as shown in Fig 5.10.

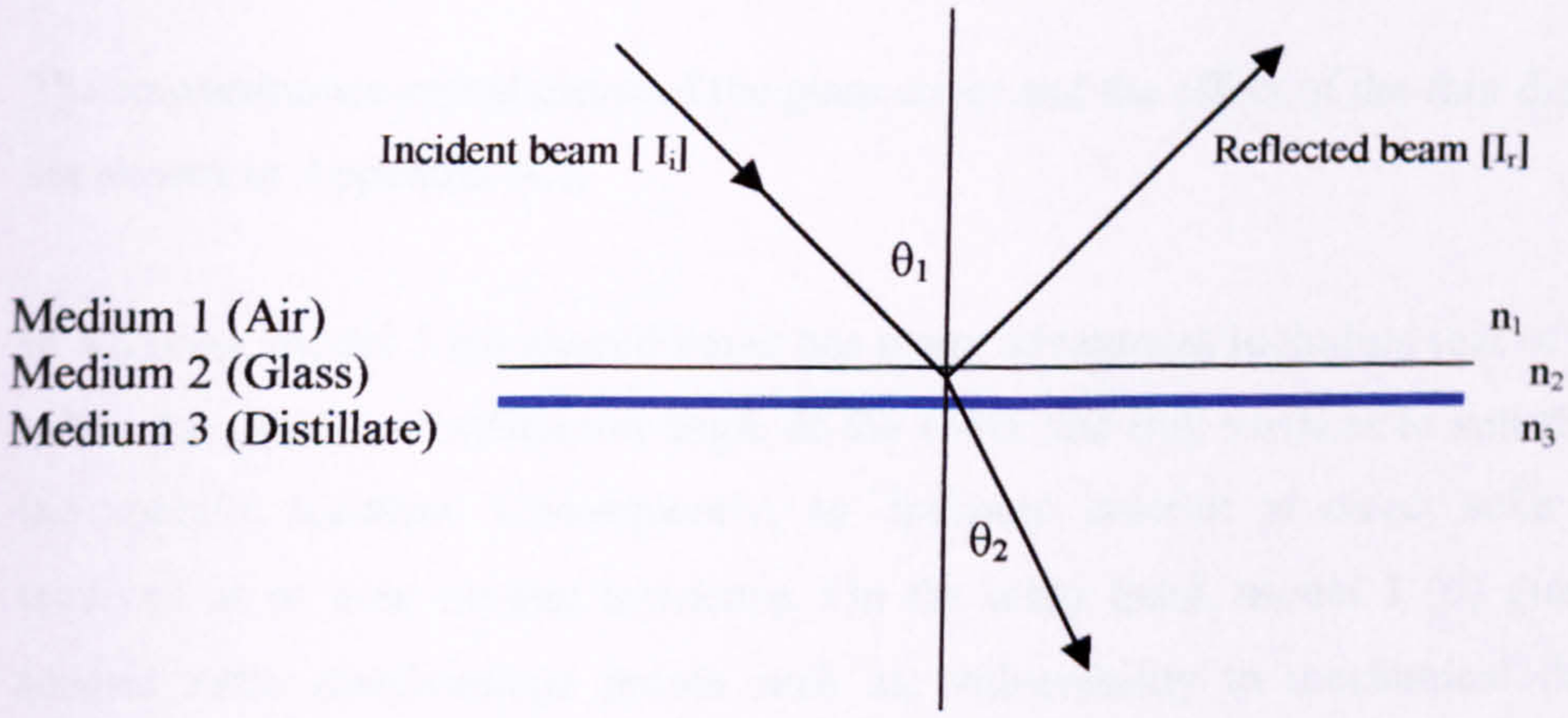

Fig 5.10. Diagram showing incident, reflected, and refracted beams of light and incidence and refraction angles for a transparent medium.

Equation 5.1. represents the perpendicular component of unpolarized radiation, r_I, and equation 5.2 represent the parallel component of unpolarized radiation, r_{II}. Equation 5.3,

then, gives the reflection of unpolarized radiation as the average of two components. The angles θ_1 and θ_2 are related to the indices of refraction by Snell's law,

$$\frac{n_1}{n_2} = \frac{\sin\theta_2}{\sin\theta_1} \qquad (5.4)$$

For radiation at normal incidence, both θ_1 and θ_2 are 0 (zero), and equations 5.3 and 5.4 can be combined to yield

$$r(0) = \frac{I_r}{I_i}\left[\frac{(n-1)}{(n+1)}\right]^2 \qquad (5.5)$$

In solar still applications, the transmission of radiation is through a distillate film so there are two interfaces per cover to cause reflection losses. Therefore the transmittance of cover can be calculated by the following equation:

$$\tau_{rN} = \frac{1}{2}\left[\frac{1-r_I}{1+(2N-1)r_I} + \frac{1-r_{II}}{1+(2N-1)r_{II}}\right] \qquad (5.6)$$

where N is the medium number.

The transmittance calculations of the glass cover and the effect of the thin distillate film are shown in Appendix (C).

In addition, model 1 (p) shaped cover has many advantages including that of the ability to select the optimum inclination angle of the cover and tray surfaces to suit the latitude of the specific location. Consequently, an optimum amount of direct solar radiation is received at or near normal incidence. On the other hand, model 1 (d) glass cover has several extra disadvantage points such as; vulnerability to mechanical damage, high weight, and the requirement of specialist skills for installation into the still, particularity in large-scale units. The observation of all laboratory based tests made prior to deciding the design parameters of prototype, which was selected for large-scale field experiments. It was concluded that model 1 (p) is highly appropriate for the field experiments. Therefore the large-scale pyramid type, which will be referred later as model 2 (p), was manufactured and tested under actual climatic conditions of Qatar..

5.12 Outdoor Experimental Work

5.12.1 Solar Desalination System

It can be seen from Fig 5.11 that the system is divided into five parts. The still (part 1) is fed by typical seawater from the main reservoir (part 2). The input flow rate is controlled by stop coke valve (part 3). The distillate is collected in a distillate bottle (part 4) located below the still and finally; the excess and unevaporated brine drained away of the still (part 5).

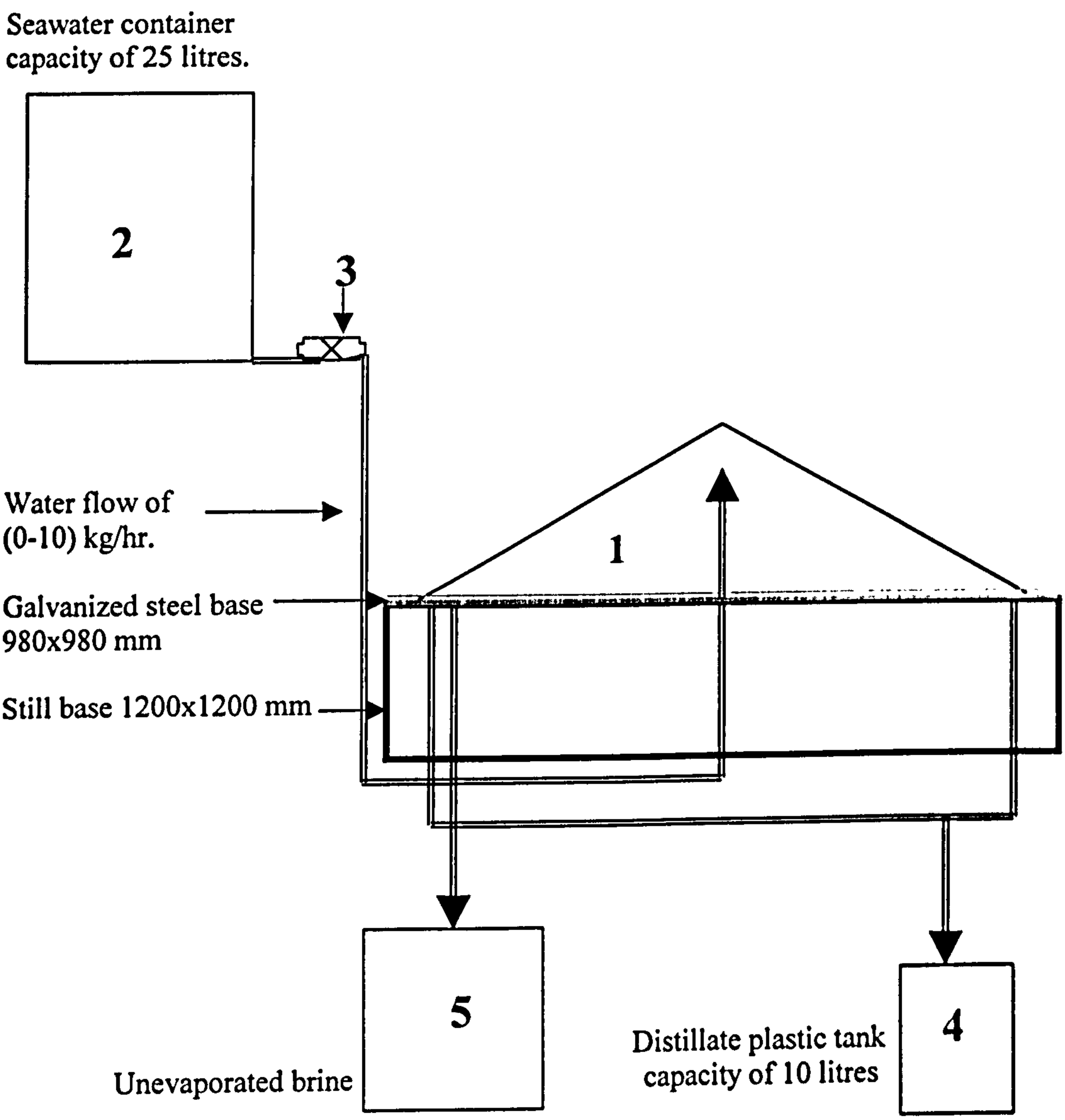

Fig 5.11. Block diagram of the out door solar still system.
(1) The still, (2) Seawater Reservoir, (3) Control Valve, (4) Distillate Bottle, and (5) Reject Brine Water.

5.13 Construction and Materials

A cross- section of the model 2 (p) solar still is depicted schematically in Fig 5.12. It comprises of the following main parts; an aluminium frames, wooden base, still tray (absorber), glass cover, filling and draining pipes, the distillate collection runner, the brine and distillate water channel, and the insulating layer. The still was manufactured in Qatar during the period of February - March 2000. A sheet of 2 mm thick of galvanized steel with square base dimensions of 980x 980 mm has been used to construct the pyramidal absorber trays.

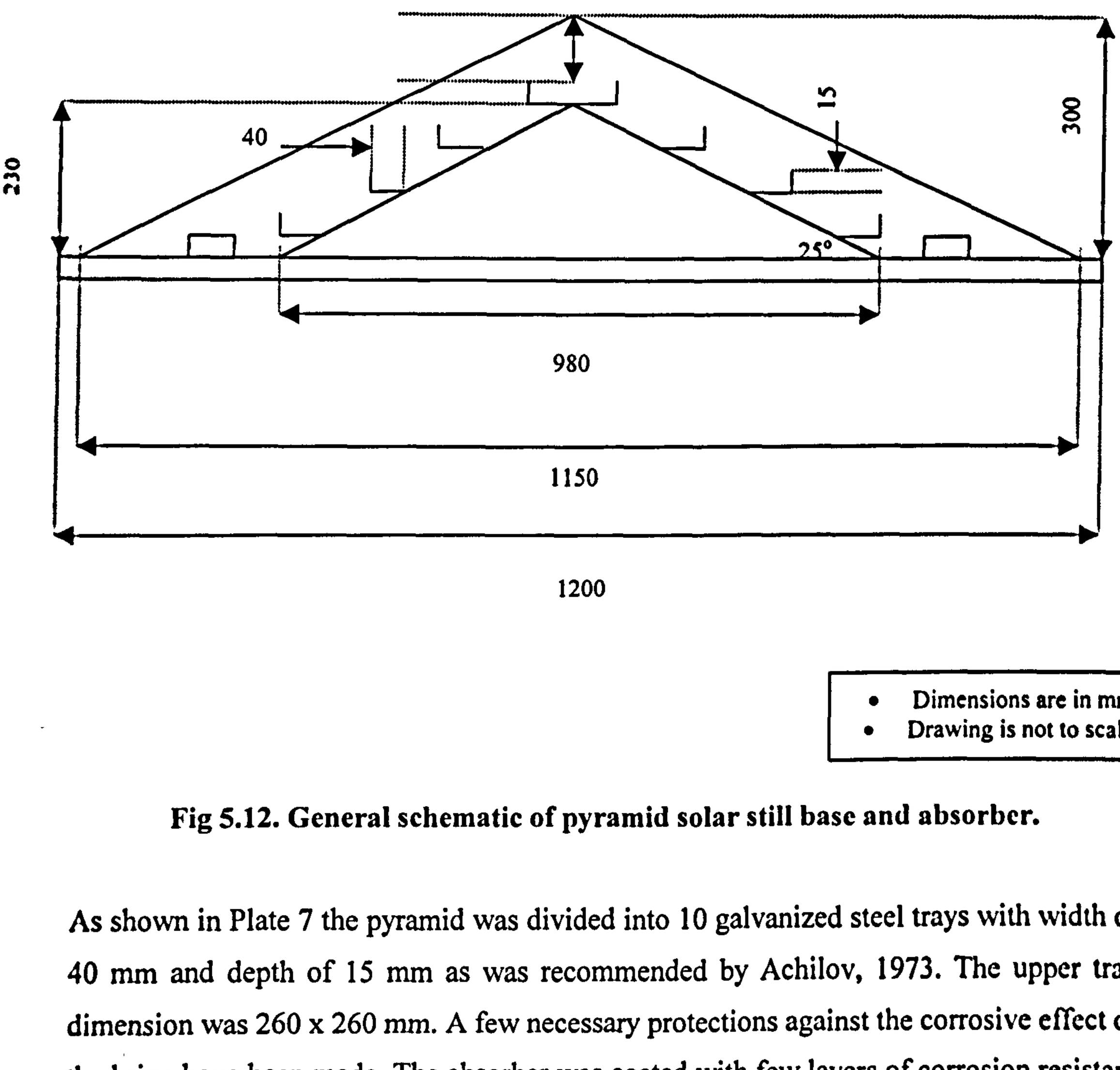

Fig 5.12. General schematic of pyramid solar still base and absorber.

As shown in Plate 7 the pyramid was divided into 10 galvanized steel trays with width of 40 mm and depth of 15 mm as was recommended by Achilov, 1973. The upper tray dimension was 260 x 260 mm. A few necessary protections against the corrosive effect of the brine have been made. The absorber was coated with few layers of corrosion resistant paint with a final coat of black non-gloss paint to maximize the solar radiation absorption and minimize any reflection. The upper tray of the absorber contains a narrow trough in the center to feed the still by inlet seawater. A drainage outlet was also positioned in the

lowest tray base of the still to drain brine and excess saline water to the outlet channel, which is connected to 10 mm diameter outlet through the still. The pyramid absorber is covered by 4 mm thick ordinary treated window glass, four triangular glass sheets 1150 x 630 mm were joined together by silicon glue to form a glass pyramid shape with square base dimensions of 1150 x 1150 mm, as shown in Plate 8.

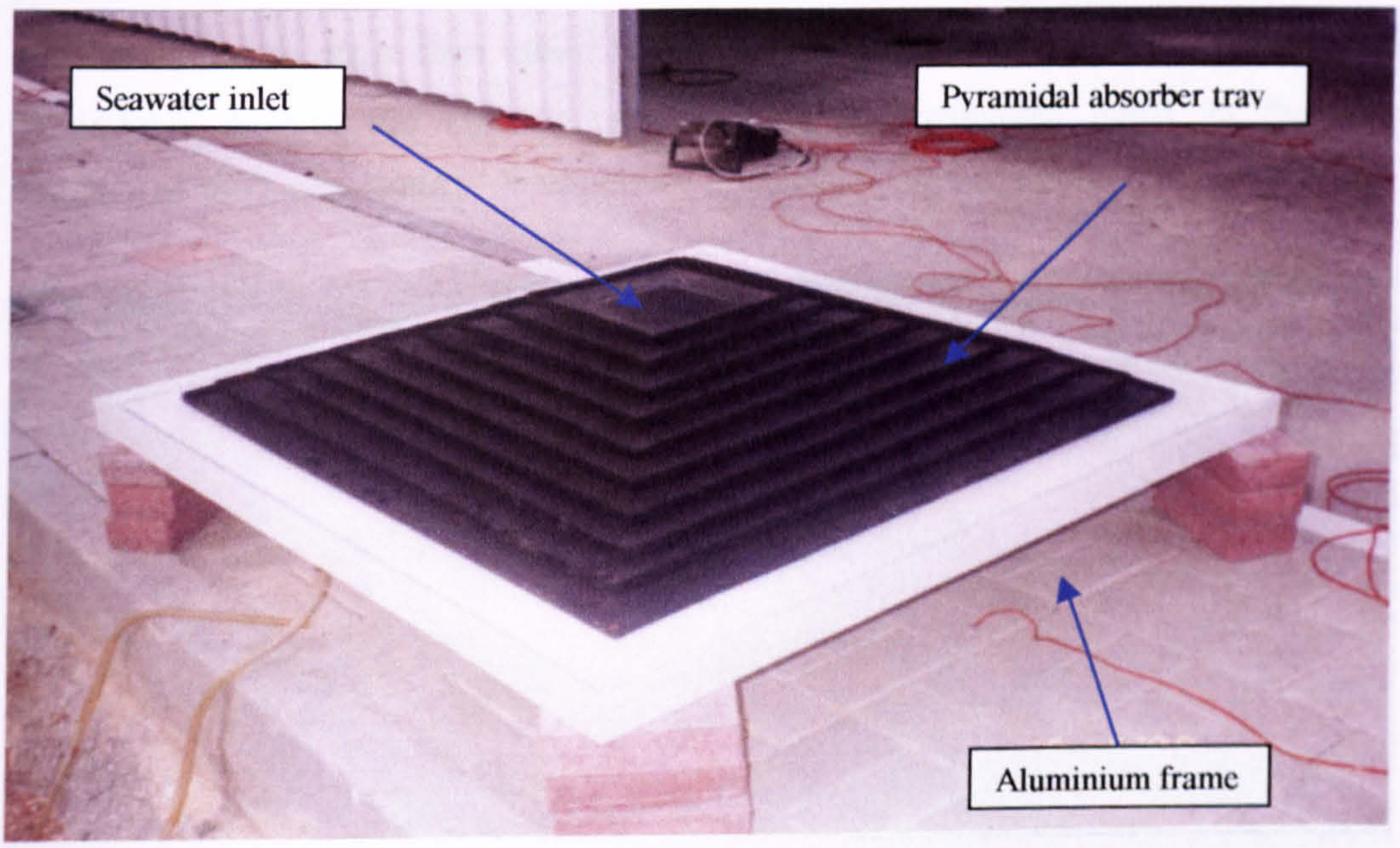

Plate 7. General overview of pyramid tilted tray solar still absorber (Qatar).

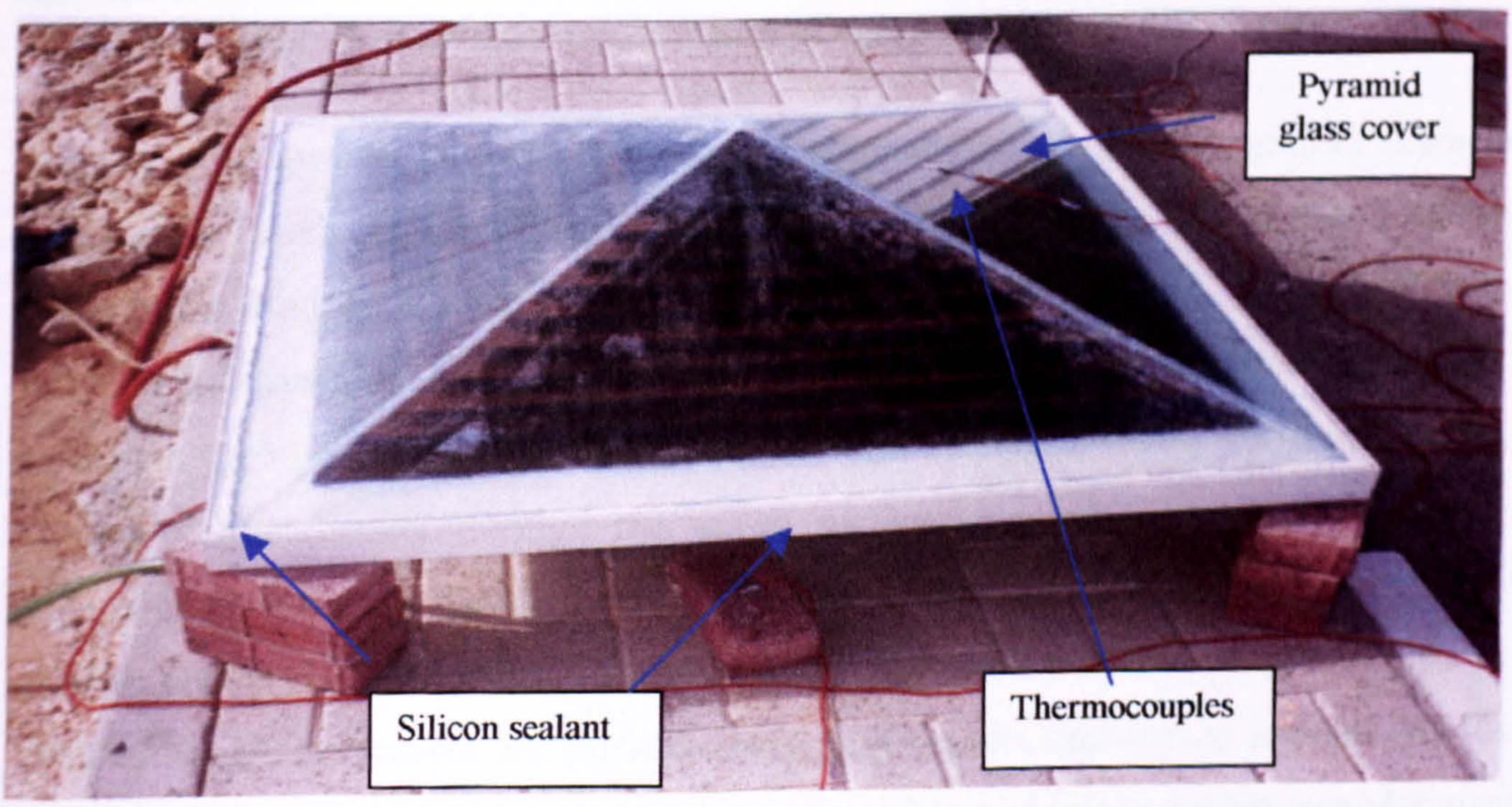

Plate 8. A glass cover of pyramid tilted tray solar still (Qatar).

The pyramid glass cover was fitted on aluminium frame with dimensions of 1200 x 1200 x 200 mm as shown in Plate 9. A sponge rubber gasket was fitted between each two sections to ensure there are no gaps between the glass base and the aluminum frame. Two distilled collection channels were connected to 10 mm diameter outlet (holes) through the aluminium frame. The pyramid absorber and cover were sloped at angle of 25° equal to the latitude of Qatar to receive an optimum amount of solar radiation. The optimum angle of cover change between the year seasons. However, every month has a different optimum angle than other. So for maximum annual collection, receiver should be oriented toward the equator with a slope approximately equal to the latitude (Duffie and Bechman, 1980).

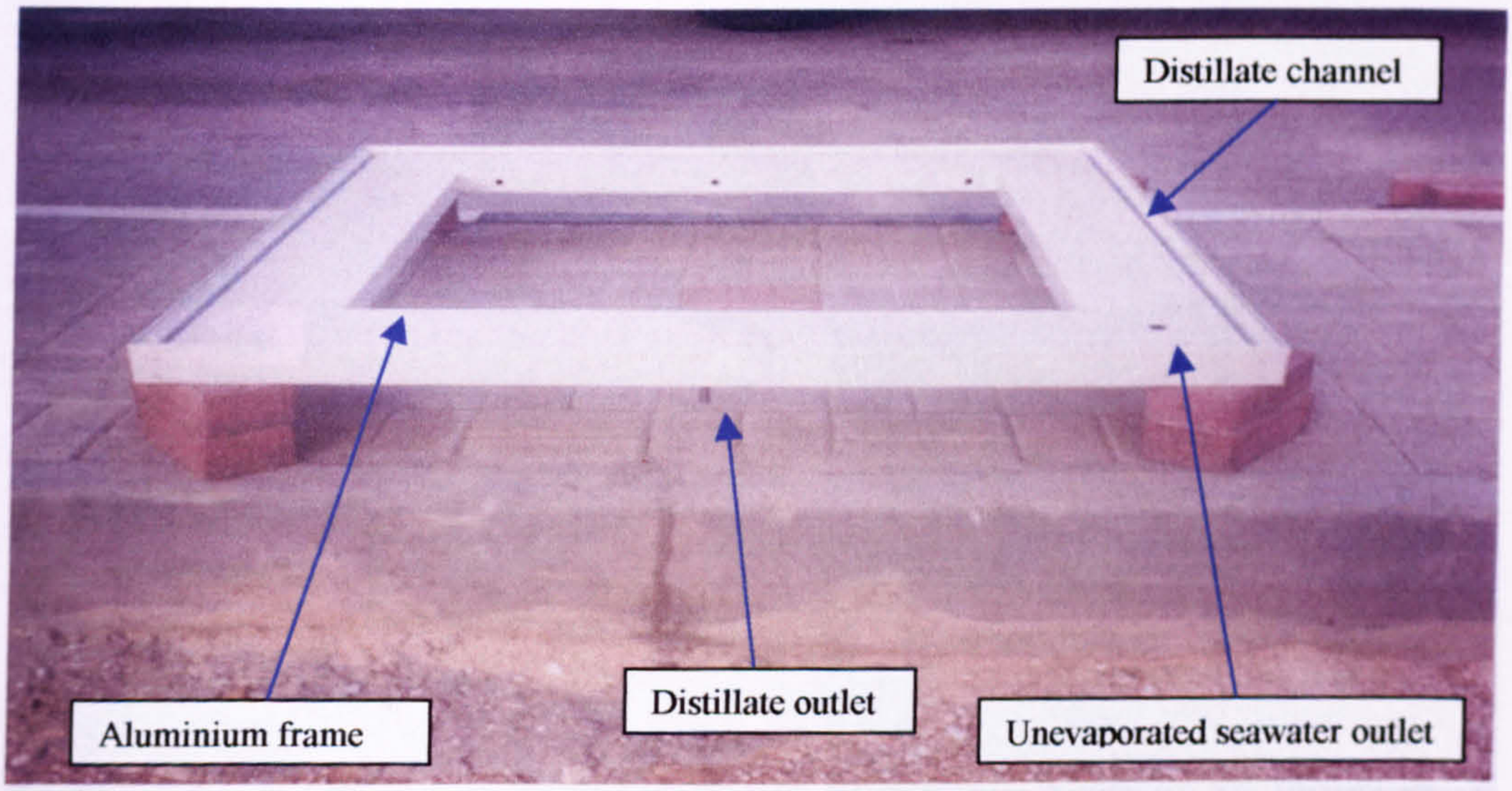

Plate 9. The aluminum frame of tilted tray solar still (Qatar).

A sheet of 50 mm thickness glass wool is positioned underneath the pyramid absorber to insulate the lower surface of the tray as shown in Plate 10. The absorber and aluminum frame were fixed on a sheet of painted 20 mm thickness plywood, which represent the still base as shown in Plate 11. The glass cover was held about 70 mm above the water surface in the upper tray of pyramid absorber. The aluminum frame has 20 mm wide and 20 mm depth channel through the upper surface; Fig 5.13. The outer part of the aluminum channel was used for fixing the glass cover and the inner channel space was used to collect the condensate from glass cover and convey it through plastic pipe to the distilled bottle. To prevent any possible leakage of vapour, and also to prevent any loss of the condensate from the glass cover and aluminum frame, a silicon rubber was also used.

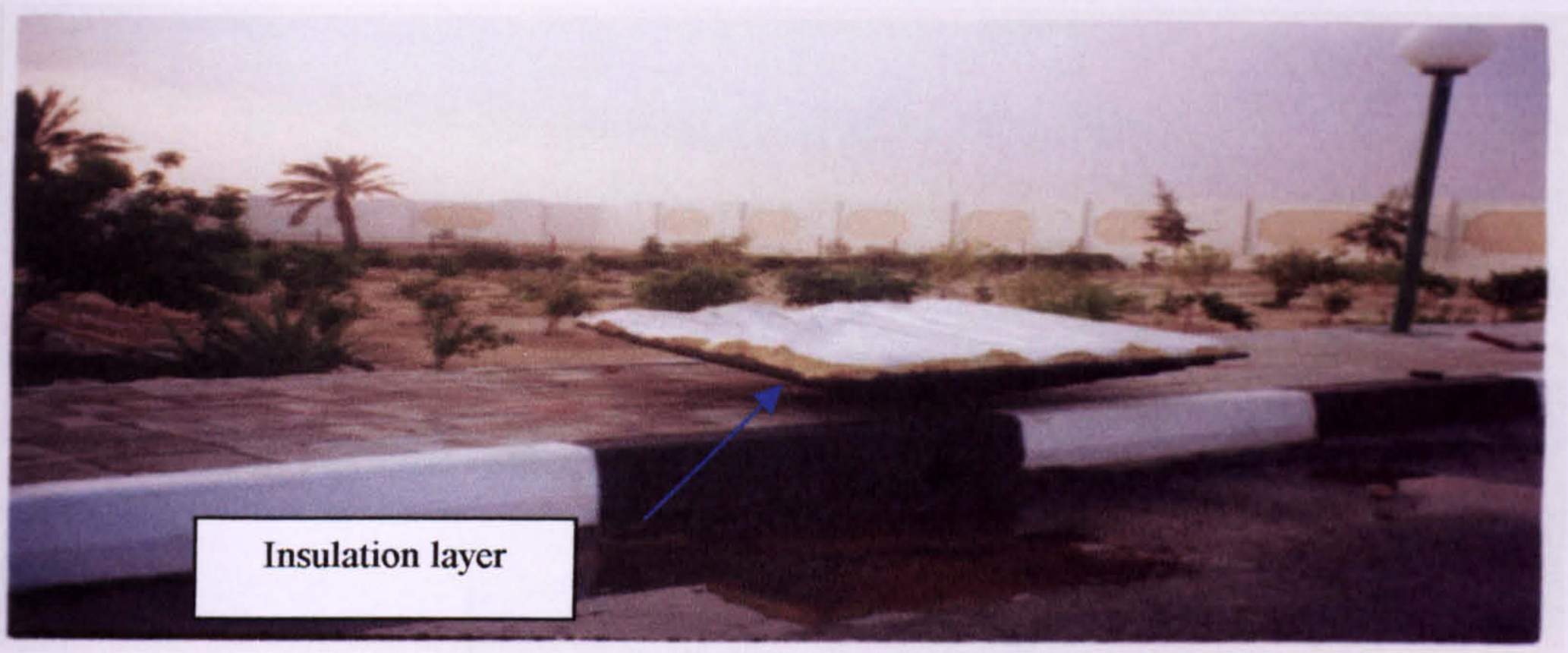

Plate 10. The insulation layer attached with the pyramidal absorber (Qatar).

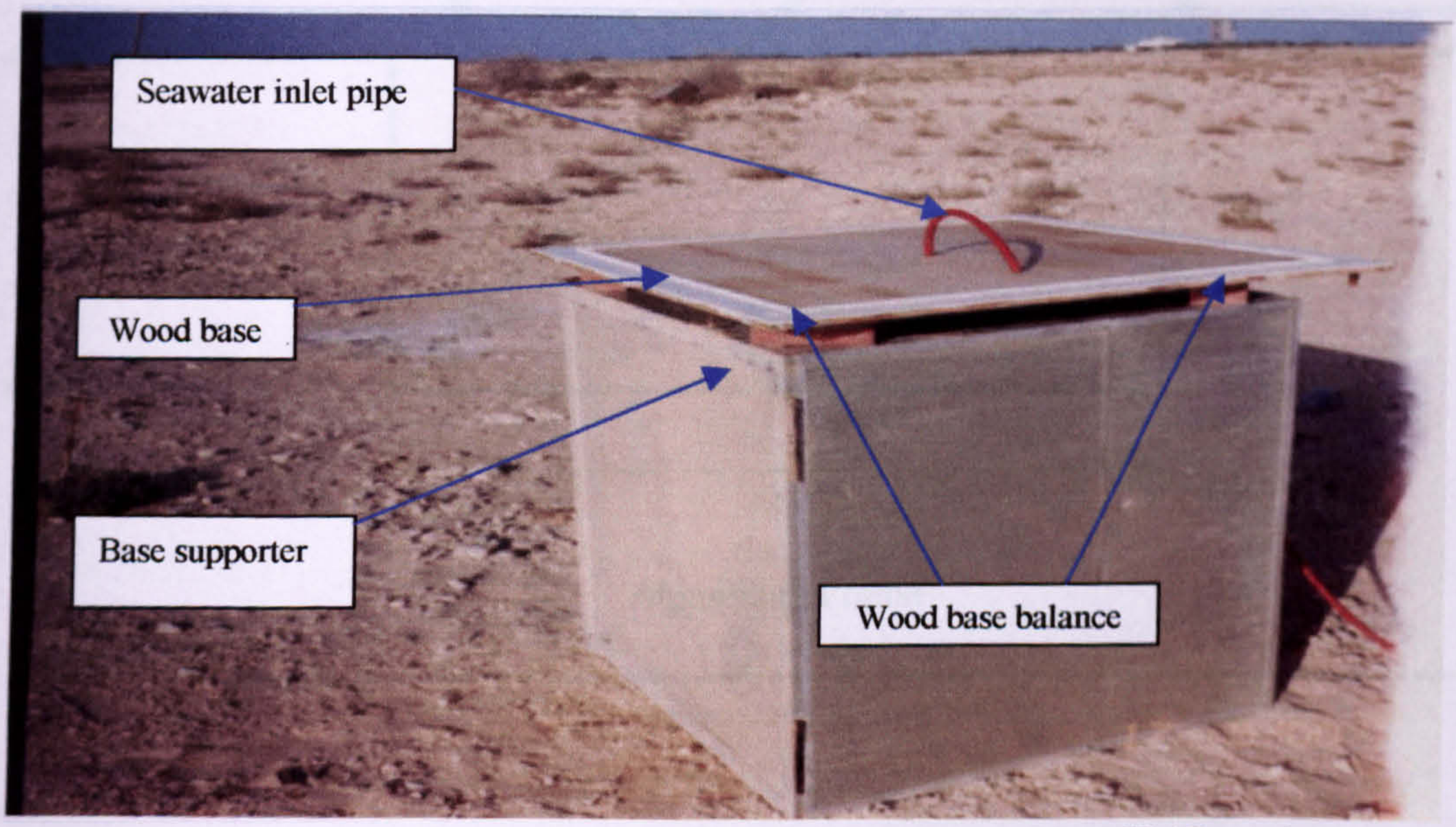

Plate 11. The plywood base for the tilted tray solar still (Qatar).

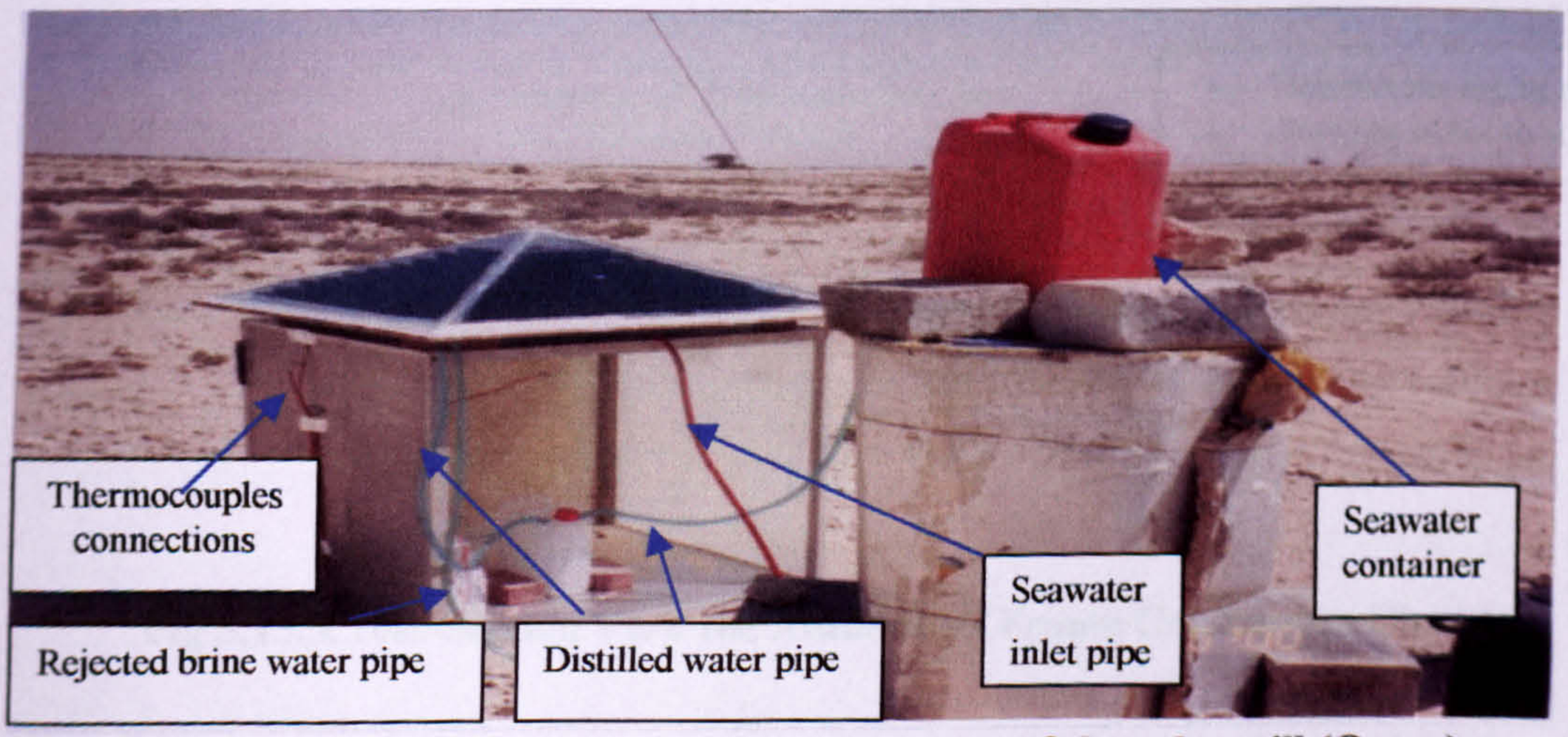

Plate 12. General overview on the main parts of the solar still (Qatar).

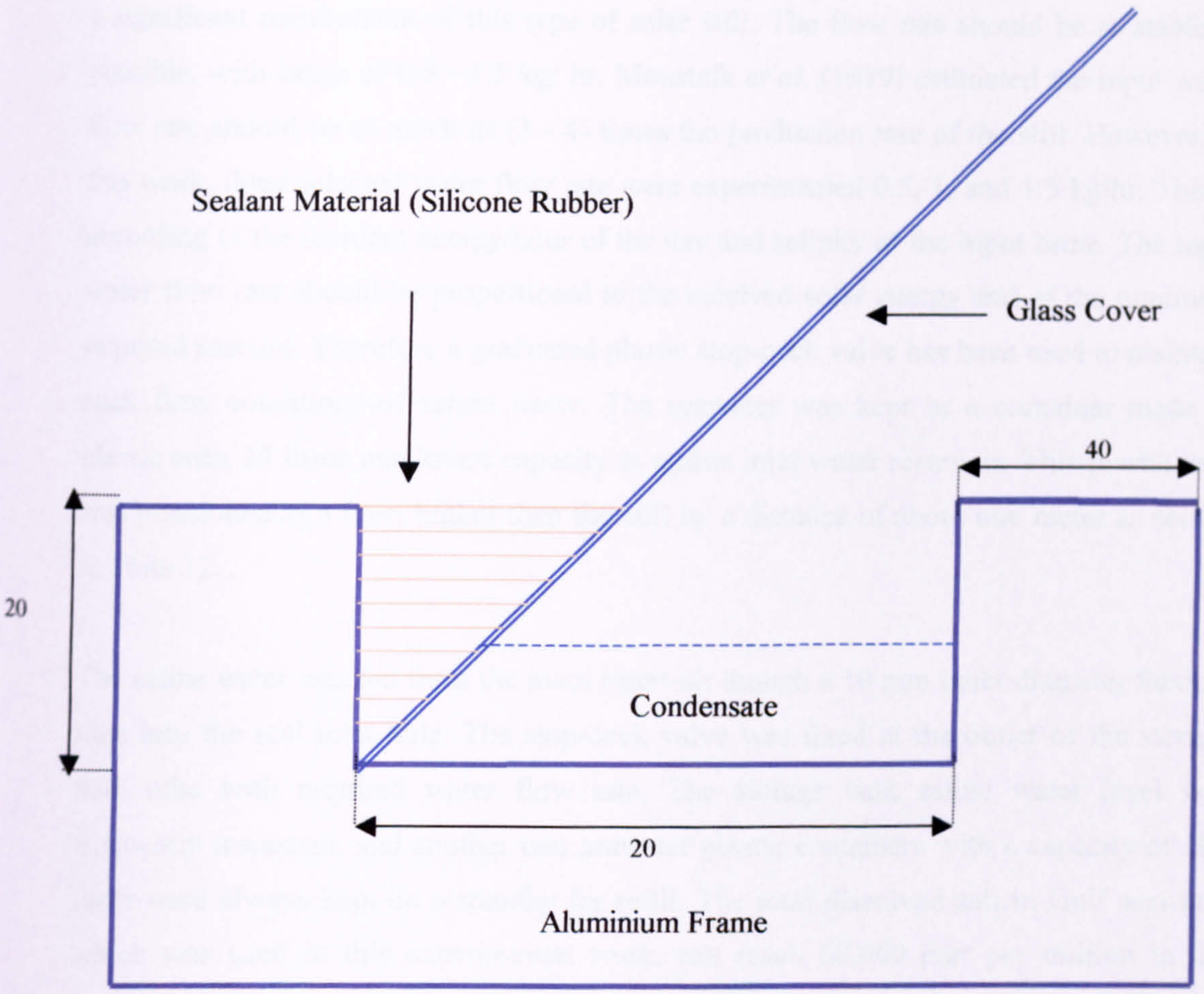

- Dimensions are in mm.
- Drawing is not to scale.

Fig 5.13. Cross-Section View the Aluminium Frame Condensate Channel.

5.14 Water Flow System

Continual and controllable saline water flow rate through the absorber trays is a significant requirement of this type of solar still. The flow rate should be as stable as possible, with range of 0.5 - 1.5 kg/ hr, Moustafa *et al.* (1979) estimated the input water flow rate should be as much as (3 - 4) times the production rate of the still. However, in this work, three selected water flow rate were experimented 0.5, 1, and 1.5 kg/hr. This is according to the incident energy/hour of the day and salinity of the input brine. The input water flow rate should be proportional to the received solar energy and of the minimum required amount. Therefore a graduated plastic stop-cock valve has been used to maintain such flow conditions of saline water. The seawater was kept in a container made of plastic with 25 litres maximum capacity as amine inlet water reservoir. This plastic tank was positioned at a level higher than the still by a distance of about one meter as shown in Plate 12.

The saline water was fed from the main reservoir though a 10 mm inner diameter flexible tube into the still inlet hole. The stop-cock valve was fixed at the outlet of the storage tank tube with required water flow rate. The storage tank saline water level was frequently inspected, and another two seawater plastic containers with a capacity of 100 litres were always kept on a standby for refill. The total dissolved salt in Gulf seawater which was used in this experimental work, can reach 60,000 part per million in the summer, which is considered as the highest salt concentration seawater in the world. This high salt concentration in the inlet seawater can considerably reduce the evaporation rate in the solar still. Moreover, it can increase the prospect of scale layer on the absorber surface, which minimizes the absorbed amount of solar radiation and maximize the reflection and diffusion of solar radiation from the absorber to the sky.

5.15 Instrumentation

To assess the performance of the still, various parameters are measured including absorber and cover temperatures, solar radiation, and wind speed. These parameters were vital to provide a full description of the still performance throughout the experiments. These parameters were sampled and printed out by means of multi-channel data logger unit. The Hydra data logger unit Fluke, model 2625A is a multi-channel data logger unit able to measure AC and DC voltages, resistance, frequency, and temperature via thermocouples. It features 21 input channels, 8 digital input/output lines, a Totalized

input, four alarm output lines, and 6.5-digit multi-meter accuracy. The data acquisition unit is portable for outdoor tests and can be AC or DC powered. The Hydra data logger (Model 2625A) combines data logging memory with features of the data acquisition unit. This data logger was connected with printer using sheet-paper style as shown in Plate 13, which is able to print the output data over 30 minutes frequently. Wind speed was measured manually by portable air flow meter that was positioned at various locations around the still. The solar radiation was measured by solar meter dome type, which is positioned near the still and connected by thermocouple to the data logger.

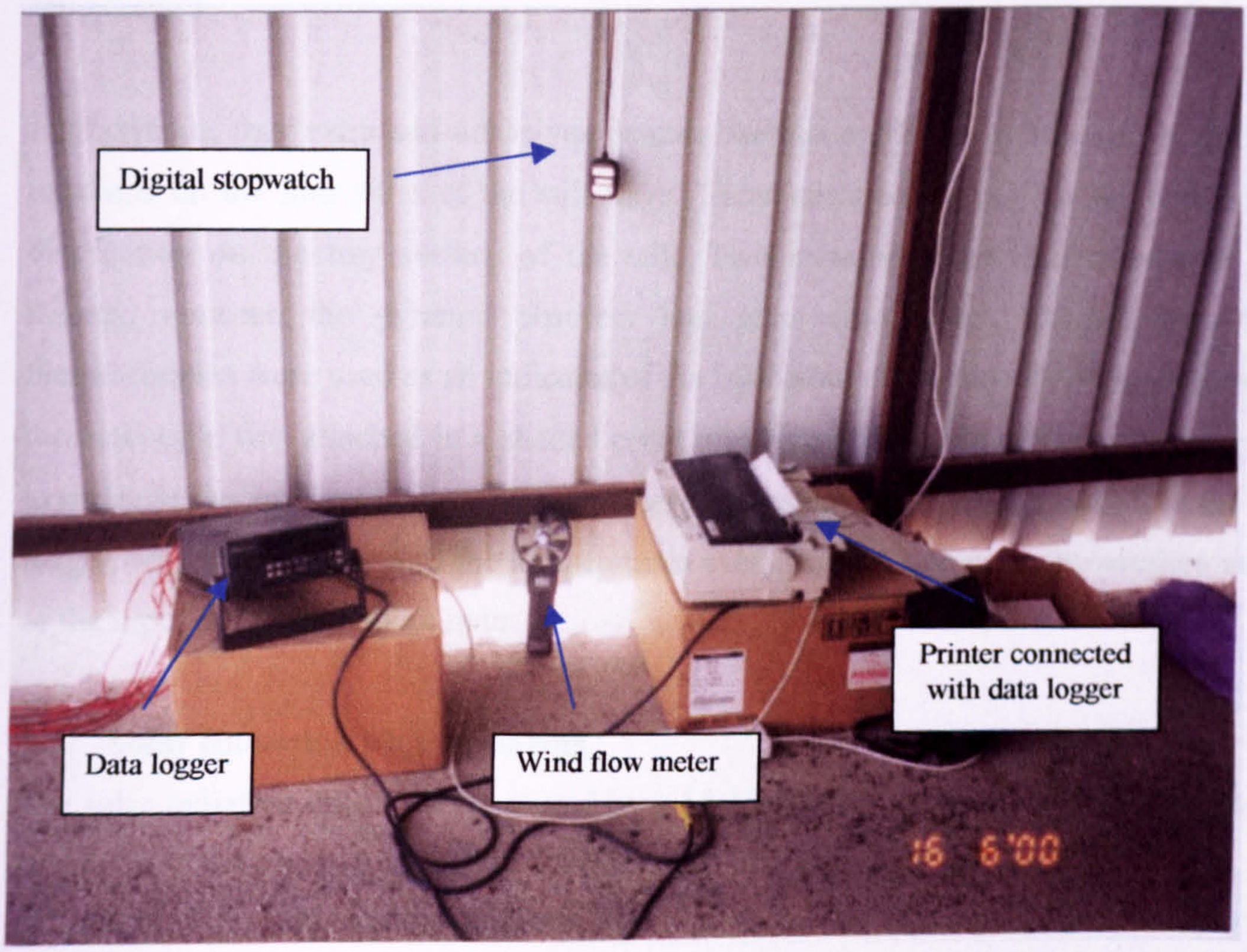

Plate 13. The data logger and other instruments used in the experiment (Qatar).

5.16 Temperature Measurements

The temperature of the tray, glass cover, ambient, inlet and outlet water were measured in this work. All temperatures were measured using K-type thermocouples suitable for operating up to 250 °C, which is sufficient for this type of experiment. A copper-constantan thermocouples K-type from Cmark Electronics Limited were connected to a Hydra date logger Fluke, model 2625A. The thermocouples were calibrated using iced

and boiling water, excellent measurement accuracy was obtained. The maximum difference obtained between the thermocouples and the mercury in glass thermometer was about 0.4 °C.

In this work fourteen channels were used and their input was in the form of voltages from the dome shape solarimeter and the thermocouples. Four self-adhesive patch thermocouples are attached at west, east, north and south sides of glass cover outer surface to measure the cover temperatures. Another two patches thermocouples were immersed on upper and lower tray to measure the inlet and outlet saline water temperature.

Furthermore, four extra self-adhesives patches thermocouples were attached at different locations on the four sides of the still trays. These are used to monitor the temperature distribution on the tray surface of the still. Two metal-sheathed thermocouples were inserted between the pyramid absorber and glass wool sheet. Output from these thermocouples were used as an indicator of the insulation efficiency. Finally, one patched thermocouple was attached in a shaded point underneath the main saline water reservoir to measure the ambient temperature. All these thermocouples were connected to the data logger, which is set to record the temperatures every minute, and print the average values of the input data over half an hour.

5.17 Solar Radiation Measurements

The solar radiation data were measured by a Middeltopn instruments solarimeter, model No. S/ 1433AA as shown in Plate 14. The Kipp and Zonen dome shape solarimeter was calibrated at the Mechanical Engineering Department Laboratory of Qatar University. The electrical output signal, produced by a copper constantan thermopile, was proportional to the difference in temperature between the black and white areas, since the black areas absorb most short wave radiation and the white areas does not. A glass cover limits the solarimeter to incident wavelength of 0.35 to 2.5 microns. This includes involves visible to the near infrared wavelengths. The time constant stated by the manufacturer of the dome solarimeter is 5 seconds.

The calibration factor of the dome solarimeter is 12.677 mV/kWm^{-2} and accuracy within 1.5%. A calibration curve was obtained and is depicted in Fig 5.14. The solarimeter was

used to measure both the instantaneous values of total direct and diffuse solar radiation. This was fixed somewhere beside the solar still and connected to the data logger. The solarimeter measures the solar irradiance every minute and print the average irradiance values for every half hour throughout the experiment running time.

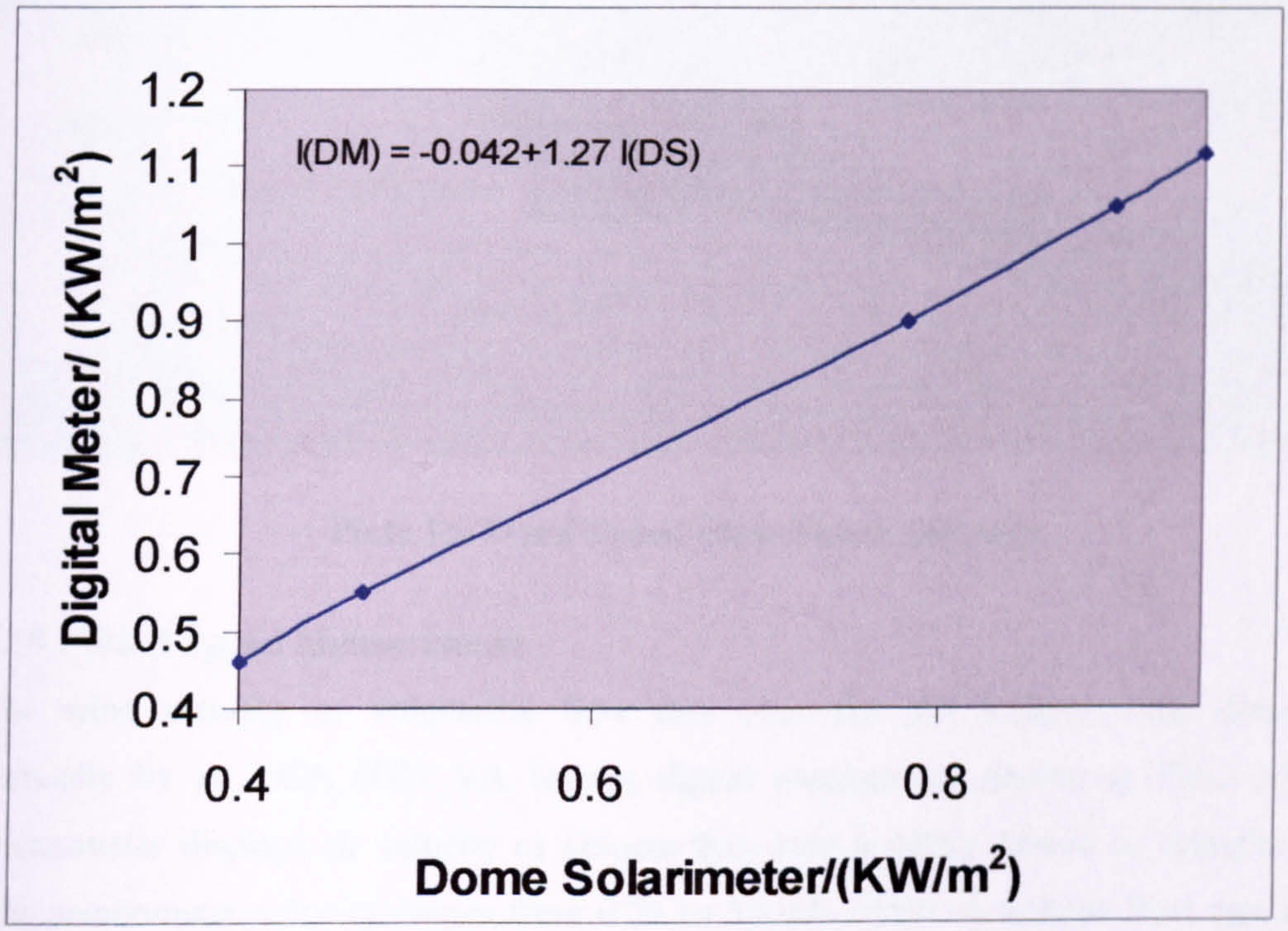

Fig 5.14. Dome Solarimeter calibration curve.

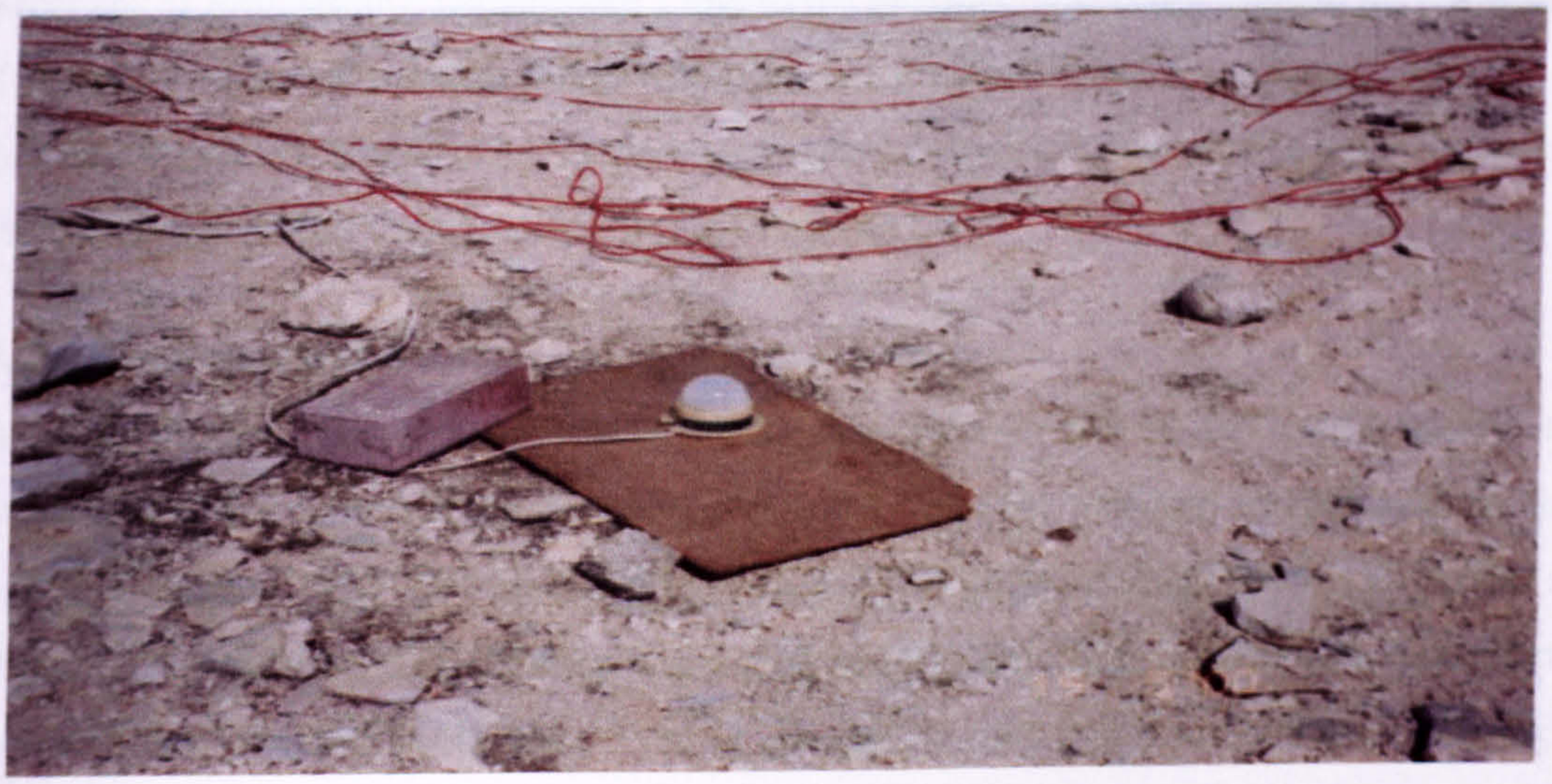

Plate 14. The dome solarimeter (Qatar).

Plate 15. Wind Speed Flow Meter. (Qatar).

5.18 Wind Speed Measurement

The wind velocity or volumetric flow rate over the still location was determined manually by an LCA 6000 VA battery digital anemometer shown in Plate 15. The anemometer displays air velocity or volume flow rate in either Metric or Imperial units. The anemometer velocity ranges from 0.25 to 30 m/s whilst its volume flow rate ranges between 0.002 to 3000 m^3/s with duct cross sectional areas programmable within the range of 0.008 to 90.00 m^2. The digital anemometer measurement was calibrated at the Mechanical Engineering Department Laboratory of Qatar University against an electronic TSI model 1650 air velocity meter using the wind tunnel in the aerodynamic laboratory of the Mechanical Engineering Department. Wind velocity was recorded manually every thirty minutes during the course of the experimental test.

5.19 Distillate Measurements

A white plastic tank with capacity of 10 kg was used to collect the hourly amount of condensate. To minimize the revapourisation by reducing distillate temperature in the bottle, a piece of cloth was used to cover the distillate bottle during the tests as shown in Plate16. The accumulated distillate was hourly measured to estimate the hourly distillate production of the still during the course of the experiments. The nocturnal yield was kept in the distilled bottle to be measured either after the solar still distilled water production

gradually decreased to a minimum, which is usually take three to four hours after the sun set, or to be measured before the beginning of the next day.

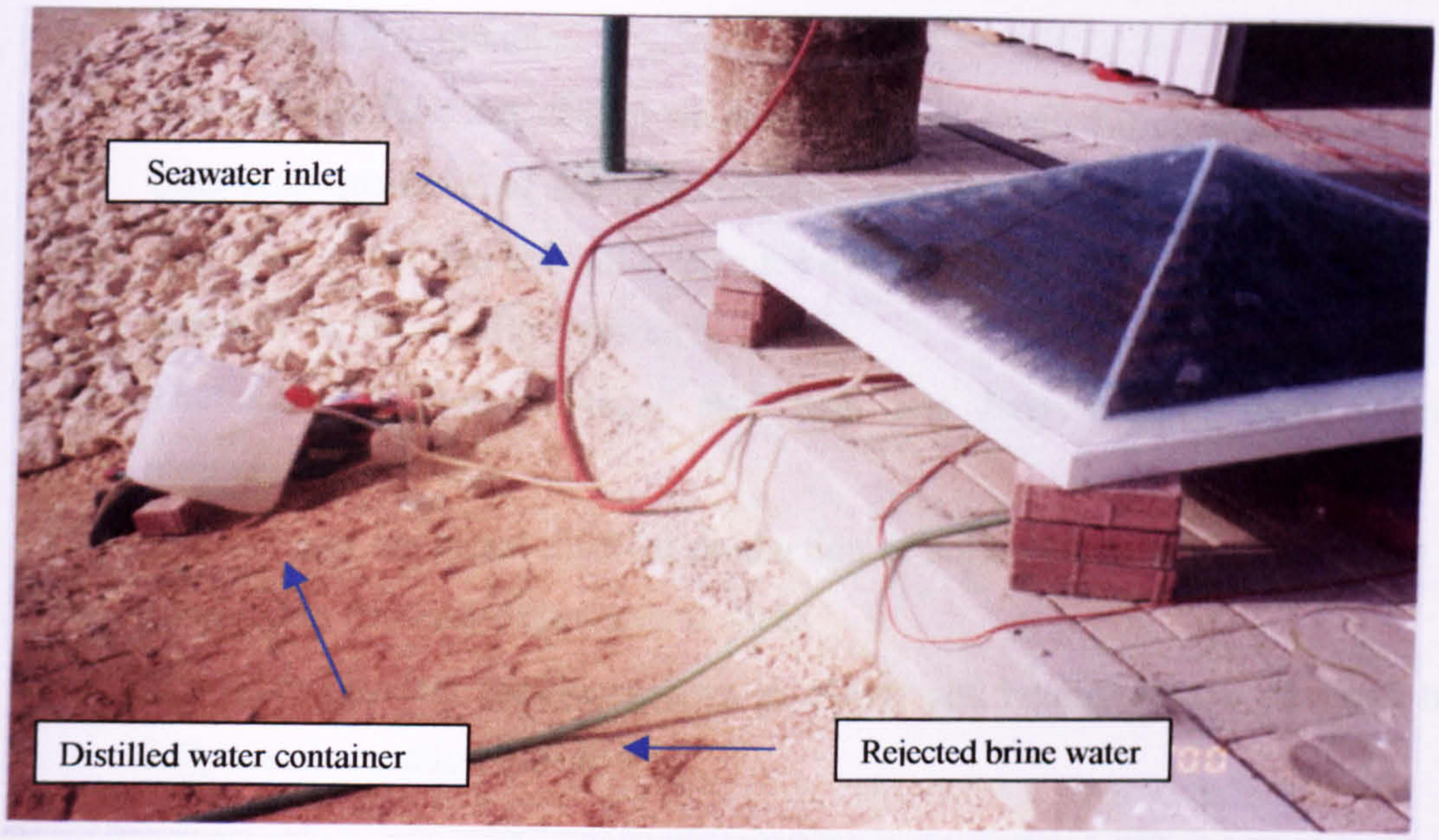

Plate 16. Distillate storage tank system. (Qatar).

A scientific measuring tube capacity of 2 litres, graduated by 2ml was used to collect the amount of condensate once every hour from the start of the operation, which usually starts at 6 a.m to the chosen end of testing at 6 p.m. These measurements and local weather conditions were also recorded in separate daily test sheet.

5.20 Other Instruments

(a) Digital stopwatch to measure the distilled production time.

(b) Spirit level to fix the horizontal level of the still base.

(c) Mercury thermometer.

5.21 Experimental Procedure

The experiments of solar still were conducted under outdoor environmental conditions of Qatar. The outdoor experimental setup made it possible to study the climatic influence of the developed design shape of still on the productivity. The following steps were undertaken throughout the experimental period: -

- The data-logger unit was configured and its initial interval logging time was set and then connected to the various sensors.
- The data logger was connected with a printer and set to print out the measured data every thirty minutes.
- The required flow rate of feed water was adjusted by graduated stop-cock valve.
- Sufficient quantities of seawater container were prepared.
- The wind speed was manually recorded every 30 minutes by using digital air flow meter, with the aid of a stopwatch.
- The outlet distillate produced each hour was determined by using scientific measuring test tube.
- The day and nocturnal distilled production of solar still have been collected and recorded in the daily experimental sheet.
- The other climatic conditions such as clarity and humidity were obtained from daily weather station broadcast.

5.22 Experimental Strategy

The main aim of this outdoor experimental work was to undertake a fundamental investigator into the optimal design features of the developed absorber surface and the still cover geometry under local climatic conditions of Qatar, which may effect the solar still performance and ultimately reduce the cost of distilled water production. The first step taken to achieve this aim was to study and analyze the two indoor tested stills. The optimum productivity still, which was model 1 (p), was selected and tested in a bigger scale and outdoor environment. The next section covers all the outdoor experimental work and presents the main results.

5.23 Input Flow Water Rate Performance Test

5.23.1 Experimental Setup

The input water flow rate was controlled manually by means of a graduated stop-cock valve. The saline water was supplied to the top of the still by a plastic pipe at three different flow rate 0.5, 1, and 1.5 kg/hr. As outdoor environmental conditions vary with time, it was difficult to change the flow rate according to these conditions, particularly in unsettled weather. Hence, in the present work, the flow rate was manually set daily. This flow rate was sufficient to keep the trays (absorber) full in the clear days. In the still, the

water flows from the upper tray to the lowest tray. The distillate was collected at the base through a plastic pipe and stored in the distillate receiver, which usually located in shadow or covered area, to reduce the re-evaporation. The over flow and unevaporated brine water was directly rejected by a plastic pipe to outside the still. These tests were conducted during the period of May-June 2000.

5.23.2 Experimental Results

Tests were conducted to measure the still productivity variation with three different input water flow rates. It can be seen from Fig 5.15, that the stills productivity decreases as the flow rate increases under almost identical climatic conditions. It also can be noticed that, when the highest flow rate adopted (1.5 kg/hr) the still's productivity was as low as 6.8 kg/day. However, the still's productivity was increased to 7.8 kg/day when a low water flow rate of 0.5 kg/hr was adoptable. It was noticed that the cover and absorber temperature were increased when the still was operated on lowest flow rate. This is most likely caused by the fact that at lower flow rate; the irradiance and ambient temperature heat gain is maximized. Moreover, the saline water in the trays gain a significant amount of a heat by conduction while passing through the still trays. At highest flow rate the inlet saline water loses considerable amount of heat; consequently, its evaporation rate is lower.

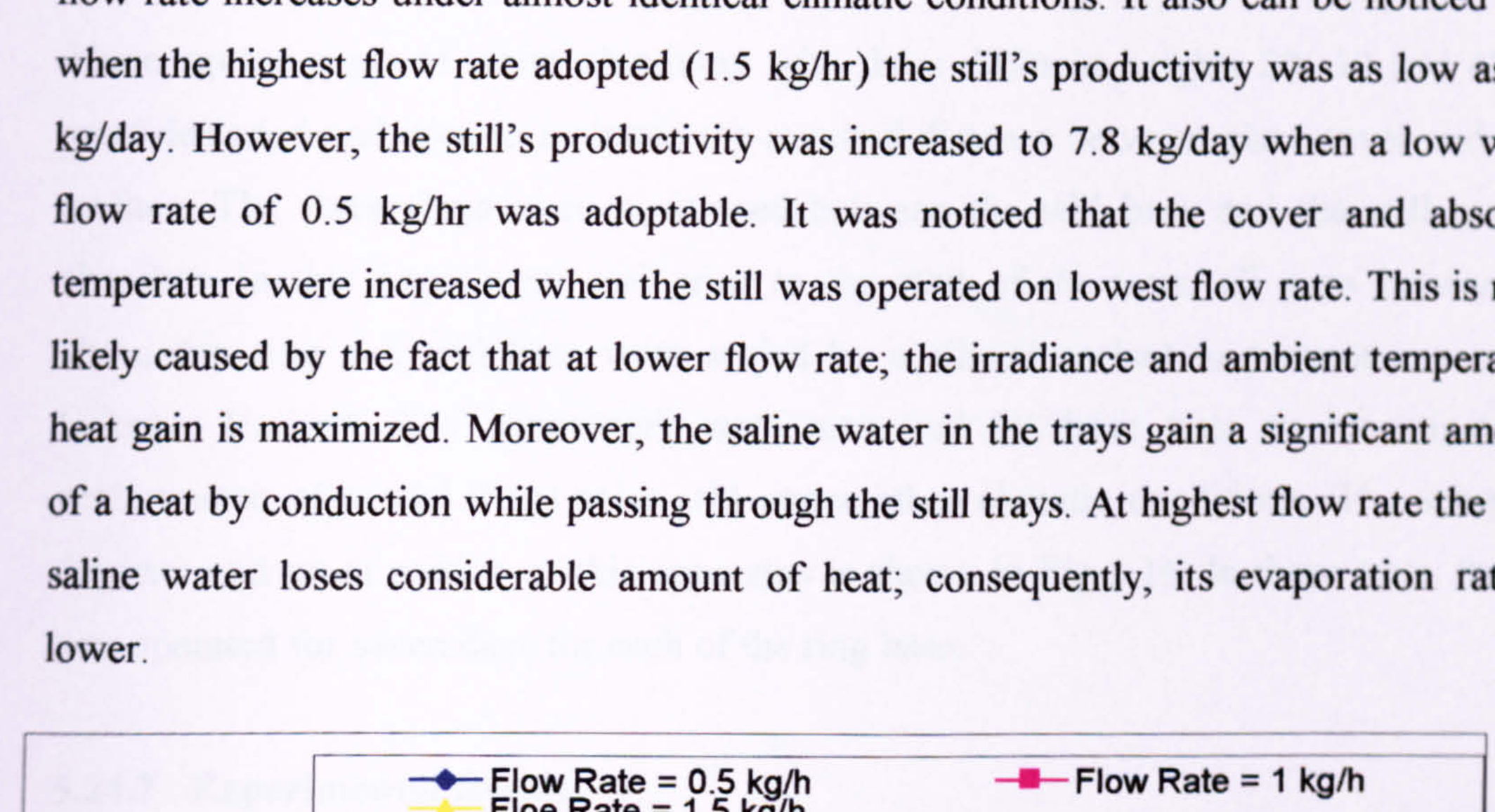

Fig 5.15. Hourly Variation of Accumulated Yield with Different Inlet Flow Rate.
(All yield values in kg/hr are within −/+ 3%)

5.24 Solar Still Performance With Cavity Variation

5.24.1 Experiment Setup

The pyramid-tilted tray solar still was tested to determine the optimized design parameters. It was shown in the preliminary test that for the case of 20 mm cavity there was a possibility of some water drops spilling or overflowing on the inner surface of cover, which may contaminate the distillated water. Hence in model 2 (p) experiments, the minimum cavity was selected to be 30 mm. Three different clearance distances between the glass cover and water surface have been tested, these were 30, 40, and 50 mm. All were tested under identical climatic conditions.

Three square rings of white aluminum with three different heights 20, 30 and 40 mm were designed and used to maintain the required distance between glass cover and water surface. The three rings were positioned between the still base and the still pyramid absorber. In this experiment and prior to the start of the tests, all gaps between the aluminum ring and still base were sealed by a silicon sealant to prevent any vapour leakage. Various data parameters were measured in these tests to investigate the performance of model 2 (p) solar still under other climatic conditions. The schematic diagram and cross section of this apparatus is shown in Fig 5.16. In these tests, the still was operated for seven days for each of the ring base.

5.24.2 Experimental Result

Comparison of the yield from the stills with three gaps shows that the smallest gap produces the highest yield as compared with the other two gaps, Fig 5.17. This can be attributed to the total volume of the cavity between the water surface and glass cover being small. Hence, the air thermal capacity was reduced and the still productivity was increased as a consequence. Moreover, it was found that distillate producing time started earlier. Furthermore, the vapour takes shorter distance to reach the condensing surface (glass cover). It was also noticed that for the same climatic conditions, the temperature of the cover of the small gap still was higher than that of the larger gap still. That was likely due to the large quantity of vapour forming and condensing on the inner surface of the still cover. On the other hand, for case of larger cavities such as 40 and 50 mm the performance of still slightly decreased. Moreover, the cover temperature has taken much longer time to gradually increase. This phenomenon can be attributed to that condensate

formed in a longer time with such large cavity, which increases the air thermal capacity in the still.

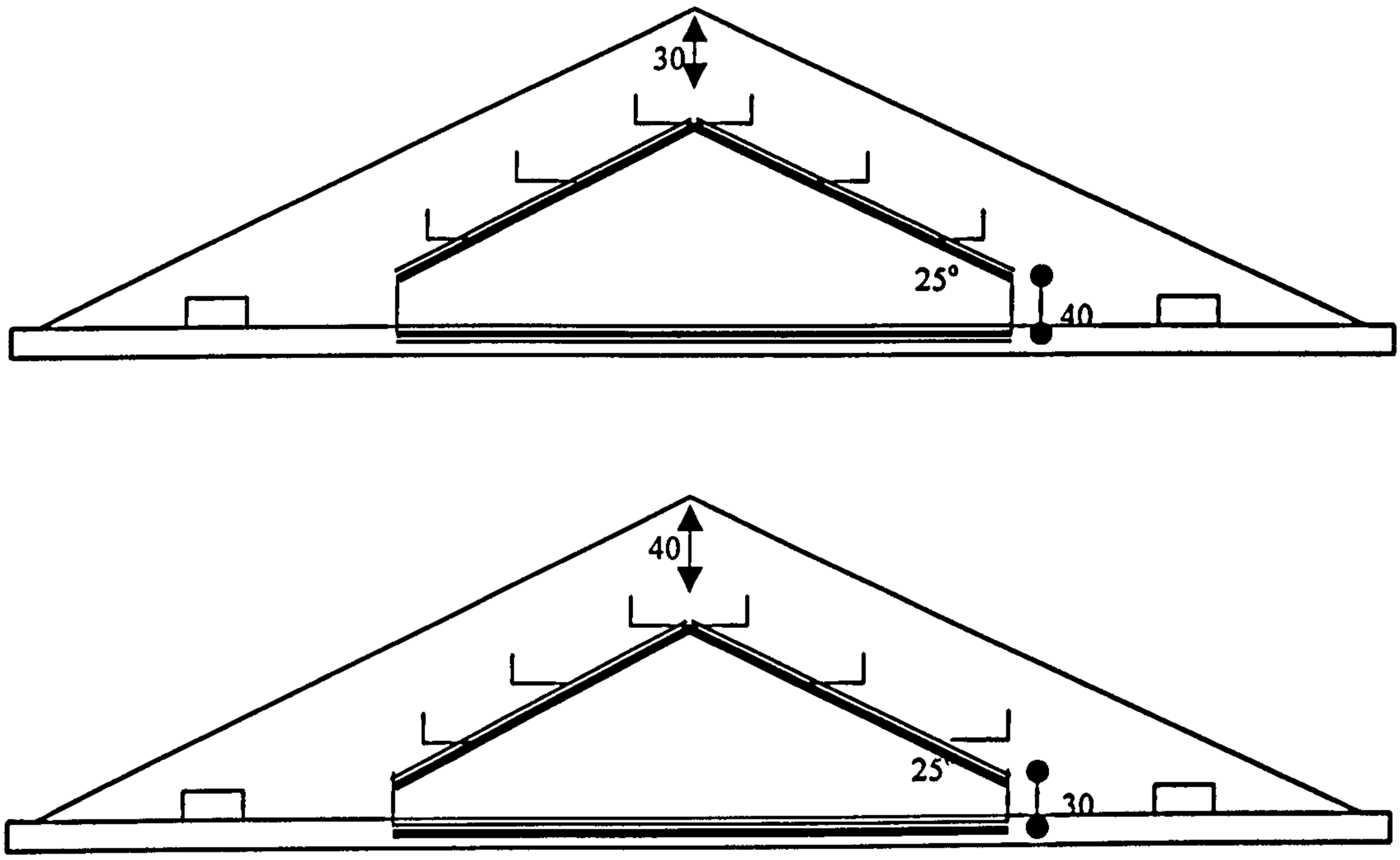

- Dimensions are in mm.
- Drawing is not to scale.

Fig 5.16. The Cavity Variation of Pyramid Tilted Tray Solar Still

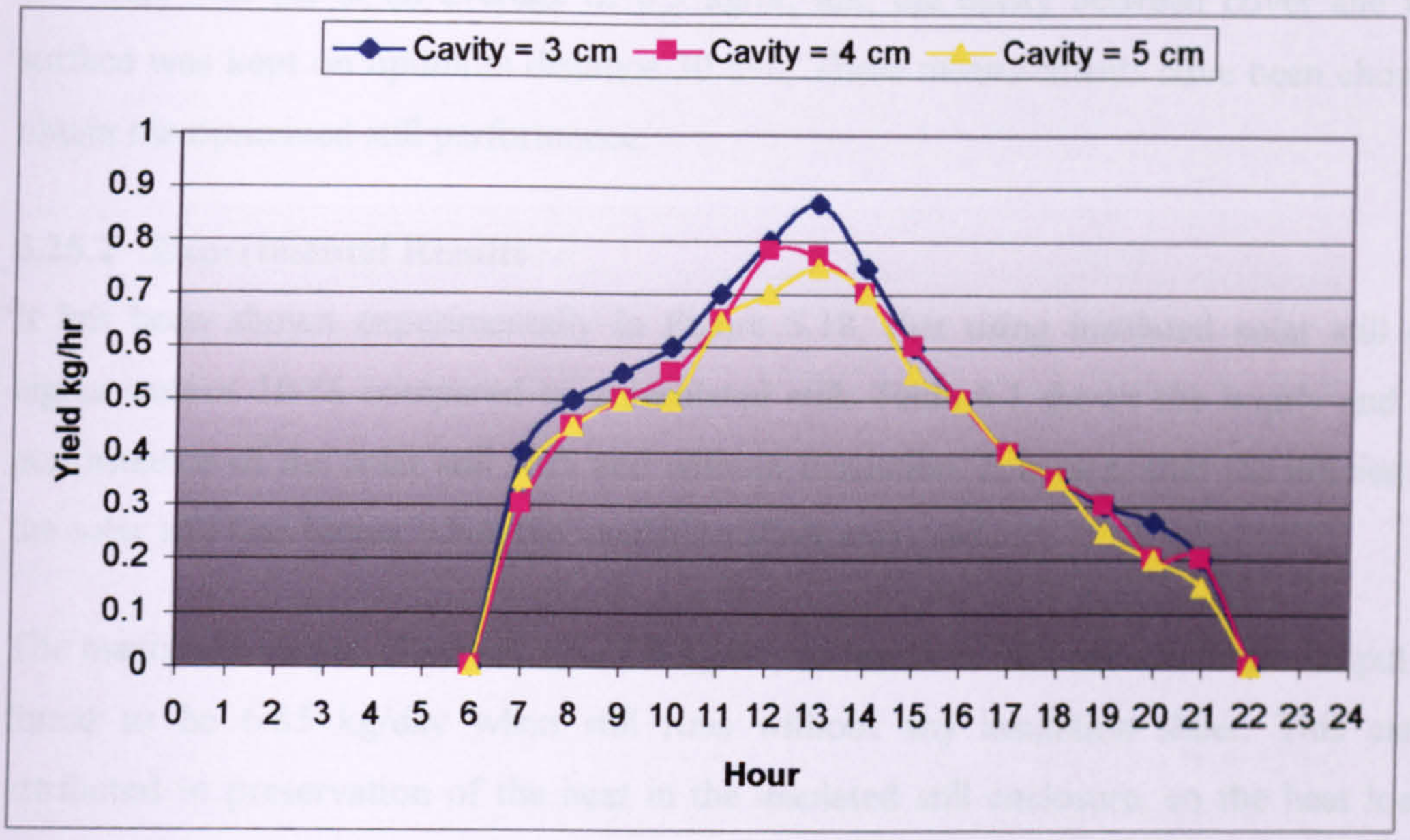

Fig 5.17. Hourly Variation of Accumulated Yield With Different Cavity Size.
(All yield values in kg/hr are within −/+ 3%)

5.25 Comparison of The Still Performance With and Without The Insulation.

5.25.1 Experimental Setup

The effect of climatic parameters and insulation on the still output was determined in these experiments. Model 2 (p) solar still has been tested with and without the insulation; these experiments were undertaken in the months of May and June of 2000. The solar still was tested without insulation and the pyramid absorber was positioned directly on the wooden base. In the insulated solar still experiments, which were undertaken on similar clear days in June 2000, a sheet of glass wool of a dimension of 1000 x 1000 x 50 mm was used as an insulation layer. The glass wool sheet considered as one of the lowest thermal conductivity materials 0.039 W/m.°C, can withstand high temperature particularly, when the still gets dry. Also the glass wool sheet was easy to fabricate to cover all the inner base of the still absorber area, as show on Plate 7.

Strong water-prove tape (plaster) was used to joint the insulation sheet with the still absorber. All still absorber edges were also covered by tape to prevent any air leakage. Hourly values of output-distilled water, solar radiation on horizontal surface, ambient air temperature, and average wind speed were recorded during these tests. The input water

flow rate was set at an average of 0.5 kg/hr, and the cavity between cover and water surface was kept on optimum distance 30 mm. These measurements have been chosen to obtain the optimized still performance.

5.25.2 Experimental Results

It has been shown experimentally in Figure 5.18, that using insulated solar still gives higher output 10 % compared to uninsulated still. Table 5.1 shows the hourly and daily performance of the solar still with and without insulation. It is clear that the efficiency of the solar still was higher when the insulation sheet was used.

The maximum output observed was 7.8 kg/day in insulated still and minimum output was found to be 6.85 kg/day when still runs without any insulation sheet. This can be attributed to preservation of the heat in the insulated still enclosure, so the heat loss by conductivity was minimized. Furthermore, as the ambient temperature drops at night, Table 5.1, also indicates that nocturnal production of insulated still is significantly higher.

In addition, it has been observed that still saline water temperature been greatly increased in the insulated still. Figures 5.19. (a, b) shows the variations of the ambient (T_a), water (T_w), and cover temperatures (T_g) together with the solar still yield (Y) with time.

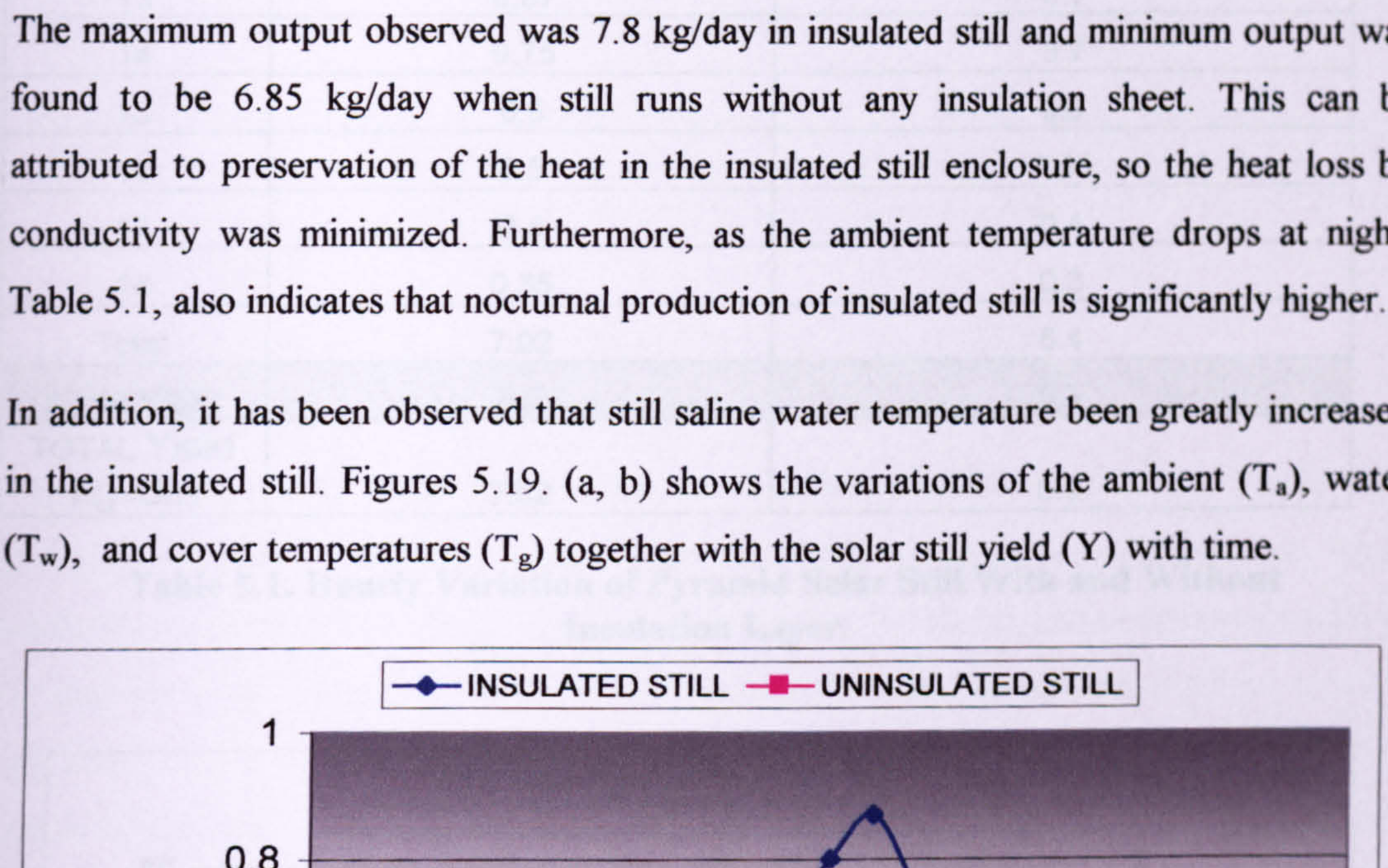

Fig 5.18. Effect of Insulation on the Solar Still Productivity.
(All yield values in kg/hr are within −/+ 3%)

Insulation Test		
Hour	INSULATED STILL	UNINSULATED STILL
6	0	0
7	0.4	0.35
8	0.5	0.45
9	0.55	0.5
10	0.6	0.6
11	0.7	0.65
12	0.8	0.7
13	0.87	0.7
14	0.75	0.7
15	0.6	0.6
16	0.5	0.45
17	0.4	0.4
18	0.35	0.3
Total	7.02	6.4
Night Yield	**0.8**	**0.5**
TOTAL Yield Kg /day	7.82	6.9

Table 5.1. Hourly Variation of Pyramid Solar Still With and Without Insulation Layer.

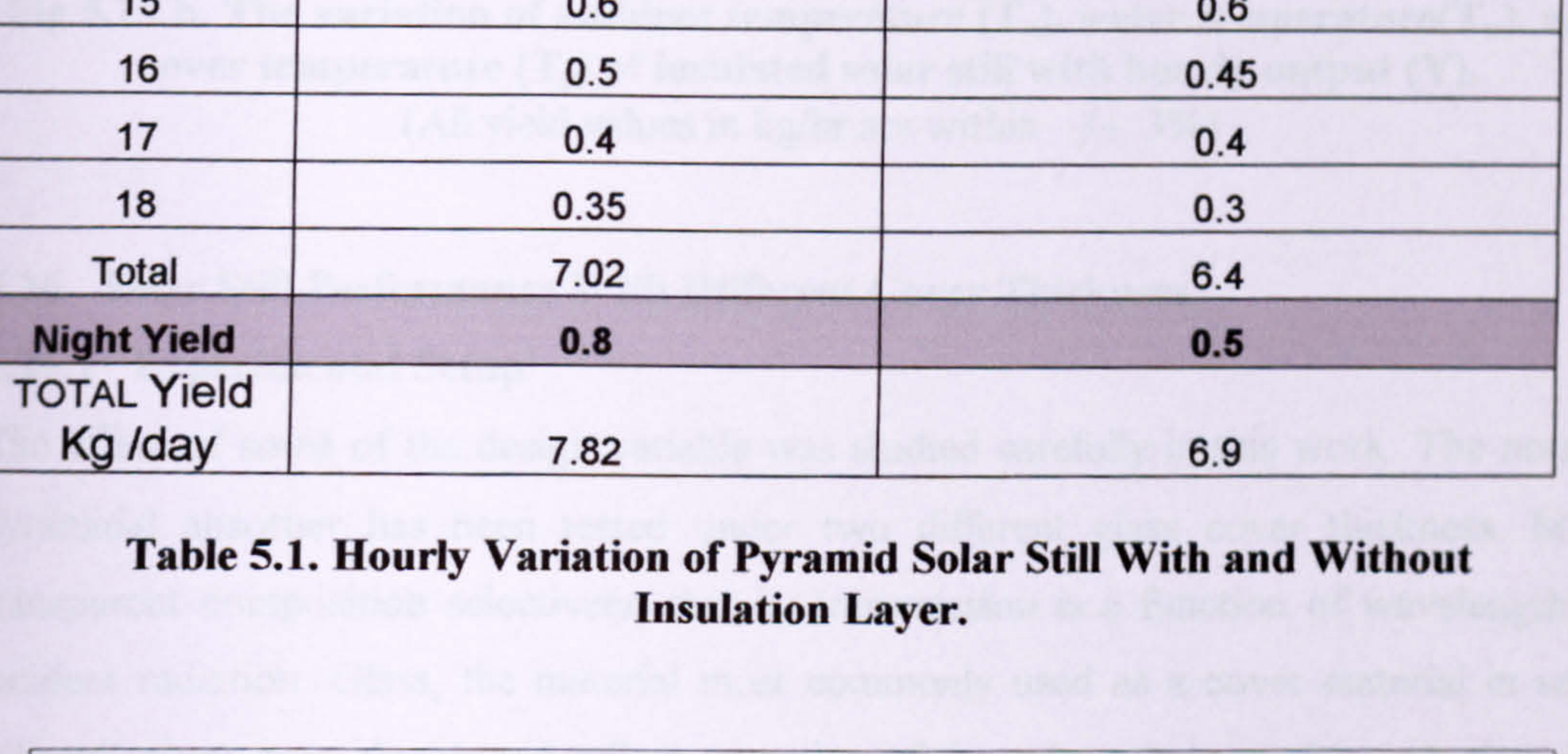

Fig 5.19.a. The variation of ambient temperature (T_a), water temperature (T_w), and cover temperature (T_g) of non-insulated solar still with hourly output (Y).

(All yield values in kg/hr are within –/+ 3%)

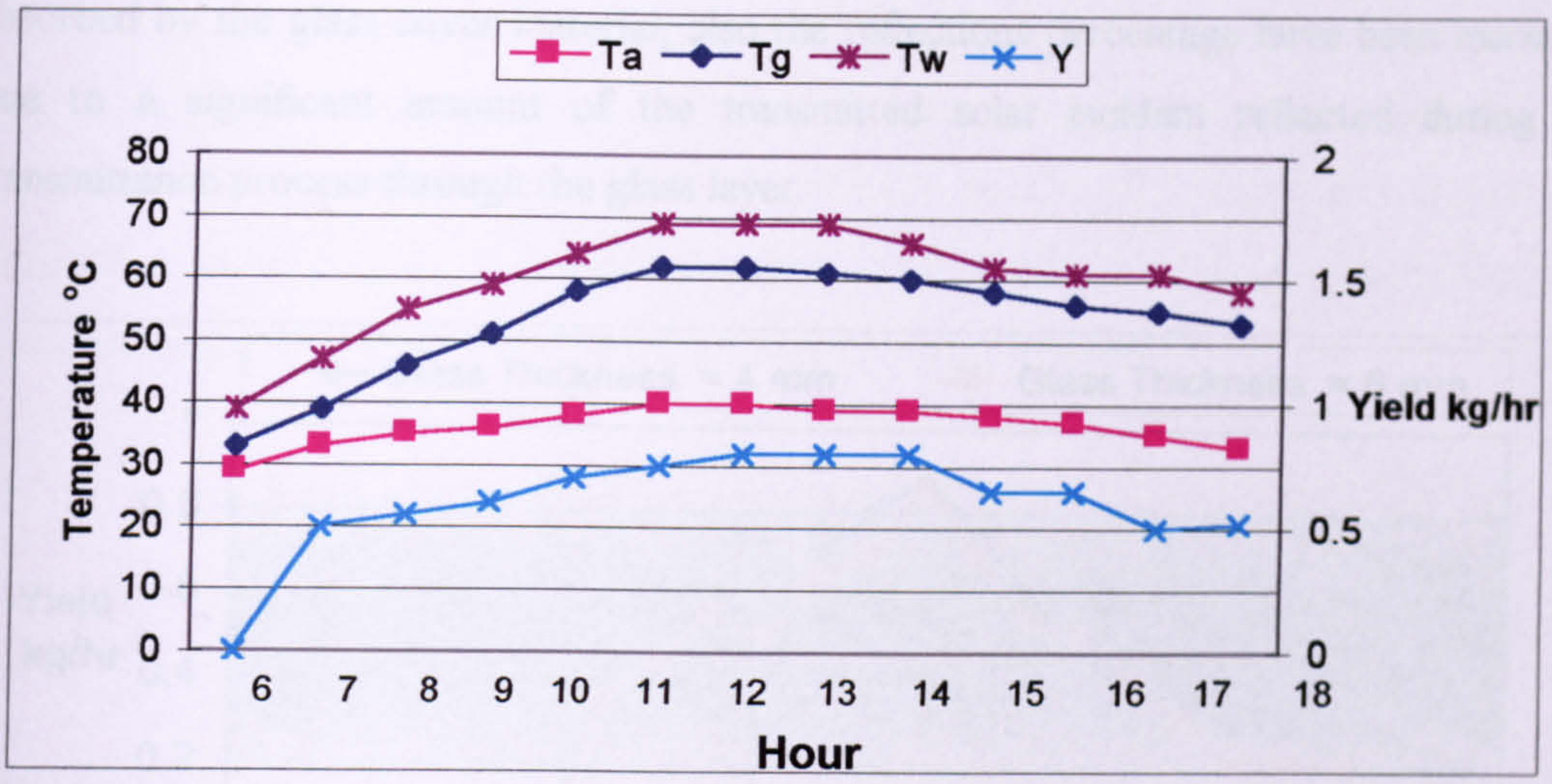

Fig 5.19.b. The variation of ambient temperature (T_a), water temperature(T_w), and cover temperature (T_g) of insulated solar still with hourly output (Y).
(All yield values in kg/hr are within −/+ 3%)

5.26 Solar Still Performance With Different Cover Thickness

5.26.1 Experimental Setup

The effect of some of the design variable was studied carefully in this work. The normal pyramidal absorber has been tested under two different glass cover thickness. Most transparent composition selectively; that is, transmission is a function of wavelength of incident radiation. Glass, the material most commonly used as a cover material in solar still collectors, may absorb and reflect a portion of the solar spectrum although glass has some advantages compared to other material like plastic film, such as glass is self supporting, glass was generally long wavelength, infrared absorbency, making it opaque to thermal radiation from the absorber. Finally, monolithic glass exhibits exceptional resistance to long duration weather processes particularly to the desert weather in Qatar. Therefore 4 and 6 mm soda-lime glass (window glass) sheet were tested as still cover under outdoor climatic condition over a period of six days in each case.

5.26.2 Experimental Results

Many parameters can control and determine the efficiency of the glass cover. Cover thickness is one of the important parameter that can have direct effect on the value of the transmission radiation, which may be absorbed through the cover. It can be seen from Fig 5.20, that the thinner glass gave the highest yield. This is attributed to the fact that when thicker glass cover employed a fundamental solar radiation amount has been

absorbed by the glass cover material, also the reflections percentage have been increased due to a significant amount of the transmitted solar incident reflected during the transmittance process through the glass layer.

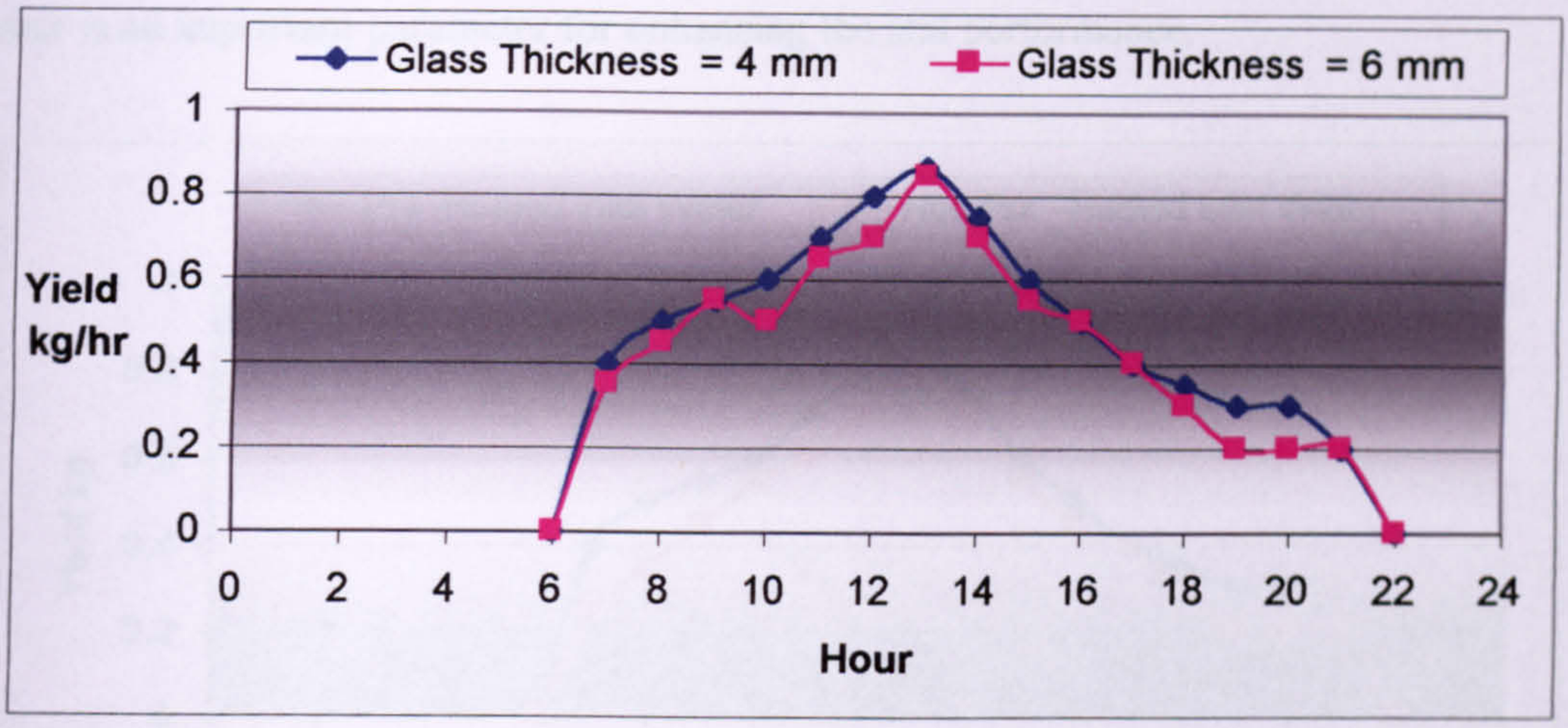

Fig 5.20. The hourly productivity of different glass cover thickness.
(All yield values in kg/hr are within −/+ 3%)

5.27 Solar Still Performance With Different Inlet Temperatures

5.27.1 Experimental Setup

The final test was carried out to examine the effect of preheated inlet water temperature on the still productivity. The still inlet water temperature was selected manually by means of a water bath in the indoor laboratory test. However, in the outdoor environmental conditions the inlet water temperature is difficult to control. Hence in this test, only two types of operation inlet water temperatures have been adopted; firstly, when the main seawater storage tank was exposed directly to sun and other climatic conditions. Secondly, when the main seawater storage tank has been covered by opaque cloth to maintain two different inlet water temperatures. Each test was conducted for a period of 12 days during May and June 2000.

5.27.2 Experimental Result

The effect of two different inlet water temperatures on the still productivity have been observed and summarised in Fig 5.21. The highest yield 7.8 kg/day was found when storage tank was uncovered. The inlet water temperature was observed around 5 °C higher than covered one. The variation in the still productivity may due to the different

amount of evaporation and condensation forming in the still. The inlet water temperature slightly decreases when main storage tank has been covered. When storage tank was uncovered the tank container gained a significant amount of heat from the sun and transmitted directly to the seawater by means of conduction. Thus, preheating the inlet water is an important parameter for enhancing the still performance.

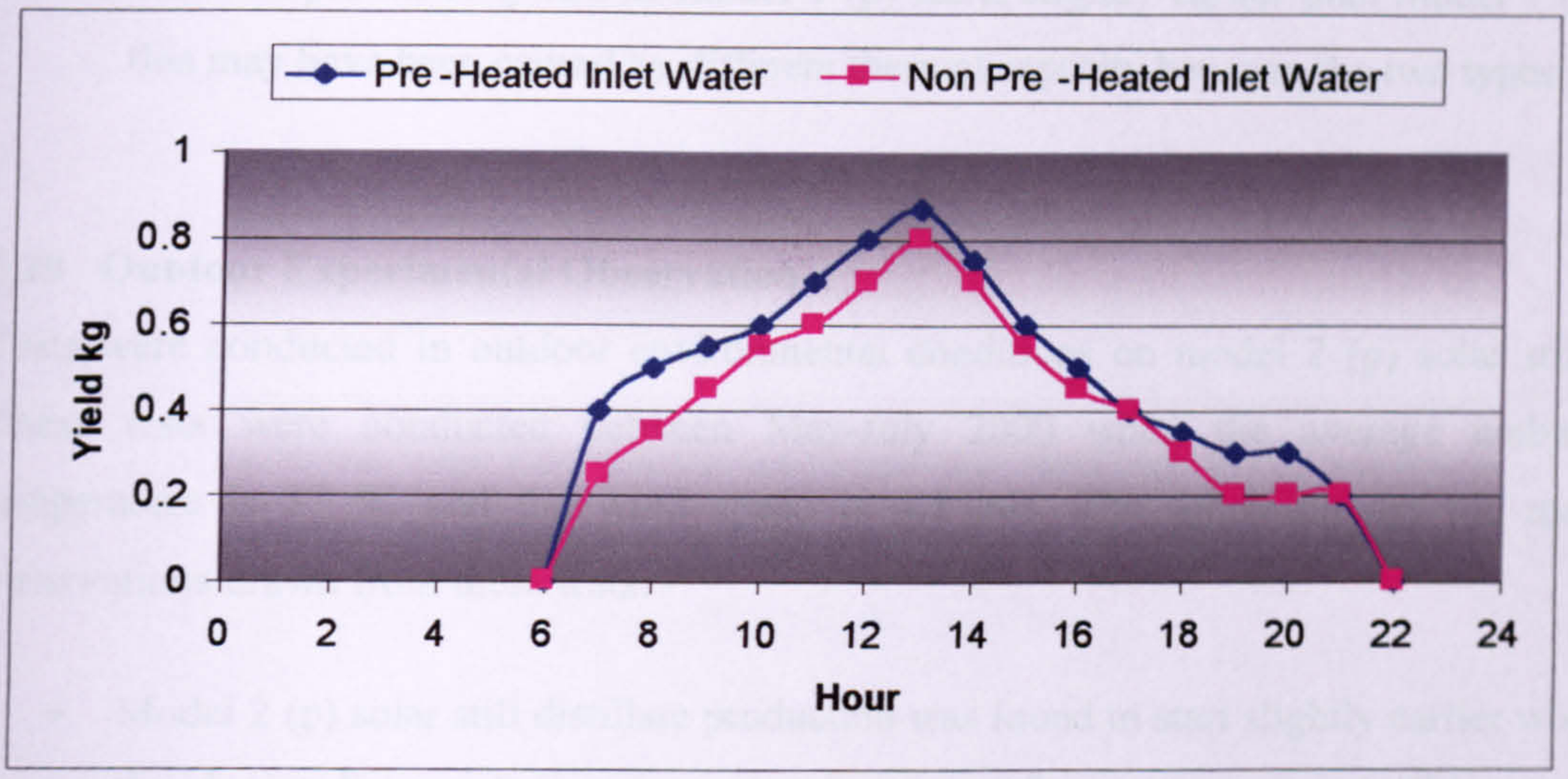

Fig 5.21. Hourly productivity with different inlet water temperature.
(All yield values in kg/hr are within −/+ 3%)

5.28 Indoor Experimental Observation

- As the inlet water temperature increased from 40 °C to 70 °C in the primary tests, both model 1 (d) and (p) solar stills showed a dramatic increase in the distilled water production. This suggests that the evaporation process increases with higher inlet pre heating water temperature.
- Some heat was lost as the water was transferred from the water bath to the top of the still.
- It was noticed that a certain quantity of the condensed water was lost because the trough, which collected the produced water, was not deep enough.
- It has been shown that the higher the tray temperature the higher is the still performance.
- In the laboratory test it has been found that the model 1 (p) shaped cover produces a higher yield than model 1 (d) shaped cover.

- In model 1 (d) solar still case, most of the condensate layer is concentrated on the top of the inner surface of the cover, which increases the distillate drops fall back to the still trays. Moreover, when the distillate drops concentrated in the small area in the inner surface of the cover the drops size starts to increase which also enhances the drops fall back again to the trays still.
- The still productivity rate in model 1 (p) starts slightly earlier than model 1 (d); this may have been caused by different thermal capacity between the two types.

5.29 Outdoor Experimental Observation

Tests were conducted in outdoor environmental conditions on model 2 (p) solar stills. These tests were conducted between May-July 2000 when the average ambient temperature is 37 °C and the wind speed is 4.3 m/s. The following are the main observations drawn from these tests: -

- Model 2 (p) solar still distillate production was found to start slightly earlier when the closest distance between cover and water surface was employed. This can be attributed to a decrease in the air thermal capacity in the still enclosure of a smaller volume.
- The lower inlet water flow rate yielded more distillate than higher inlet flow rate under similar outdoor environmental condition. This was attributed to the fact that exposed water surface take much longer time gaining sun radiation and absorber heat.
- The distillate yield was found higher in model 2 (p) solar still type when insulation layer was employed. The difference was caused by the heat losses from the still basin by conduction through ground and convection by air has been minimized.
- The 6 mm glass cover, used in the cover test, may have decreased the solar radiation reaching the plate by reflecting more solar radiation and absorb more radiation than the other covers.
- The temperature of water in the storage tank was reported to be about 2-5 °C higher than the air ambient temperature during the experiment; this indicates that there was a continuous heat gain from the sun radiation.

- The temperature of the water in the covered storage tank dropped by 4-6 °C below the ambient temperature.
- Pre heating inlet water enhances the still productivity rate, particularly in daytime.
- It has been found that the sealing of the solar still has greatly affected water production by increasing vapour leakage. This conclusion agreed well with those reported in the literature survey.
- The West, East and South sides of the still cover attained highest temperature during the day. However, the North side cover reached the lowest temperature. This phenomenon can be attributed to the sun declination during this period of time and experimental latitude.
- The corrosions started to appear three to four days after the first test took place. The inspection indicated that the unpainted inlet steel pipe that is welded with the upper tray is the main source of this corrosion. After treating this pipe by black waterproof paint the corrosion diapered for the rest tests.

5.30 Comparison Between Experimental Results and Theoretical Prediction

Comparison of the outdoor experimental results with the theoretical ones obtained from the numerical calculations and model reported in chapter four are summarised hereafter. As can be seen from Fig 5.22 – 5.26, the numerical and the corresponding experimental results are quite similar. Various experimental parameters such as, ambient, glass, water temperature, isolation, yield and insulation effect were compared with those predicted by the theoretical model. Theoretical tests were performed similarly on the day no.15 (15^{th} of January) and 166 (15^{th} of June) in order to obtain the average yield and climatic parameters for the whole year. Based on these two date, the predicated performance of the solar still was determined.

(a) Ambient Temperature (T_a)

It is impossible to predicate variation of ambient temperature (T_a). However, the theory can predicate the expected temperature based on recorded values over the previous 10 to 20 years. This was investigated in chapter two. The comparison with met records theory suggests that the model for hourly variation of temperature predicted T_a to be maximum around mid-day, Fig 5.22.

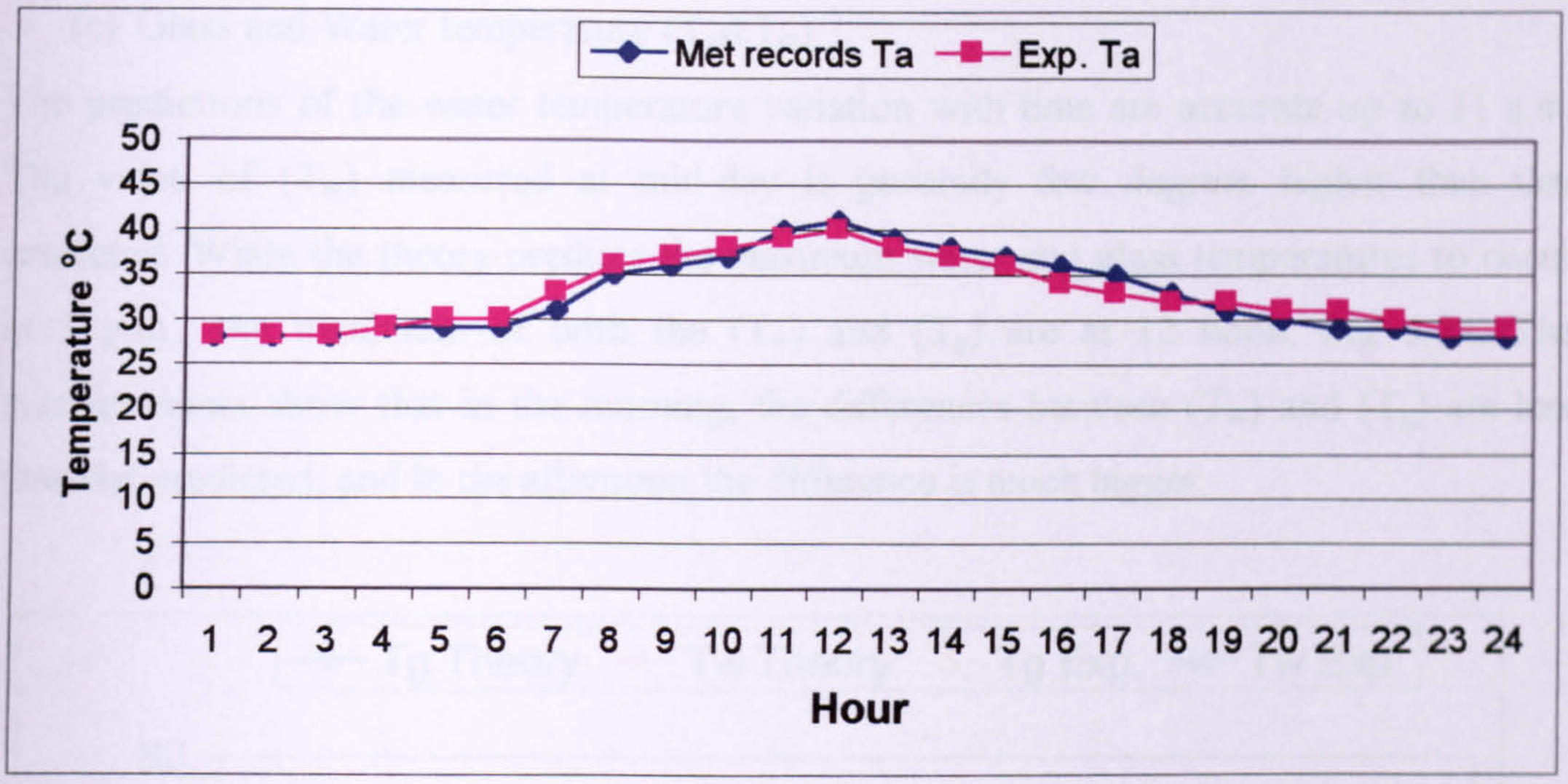

Fig 5.22. Hourly variation of ambient temperature for day No.166

(b) Solar Radiation (H_s)

The comparison between theoretically predicted and measured solar radiation (H_s) variation indicates that model employed for modeling solar radiation is satisfactory. However, as is clear from all test cases and in particular in Fig 5.23.

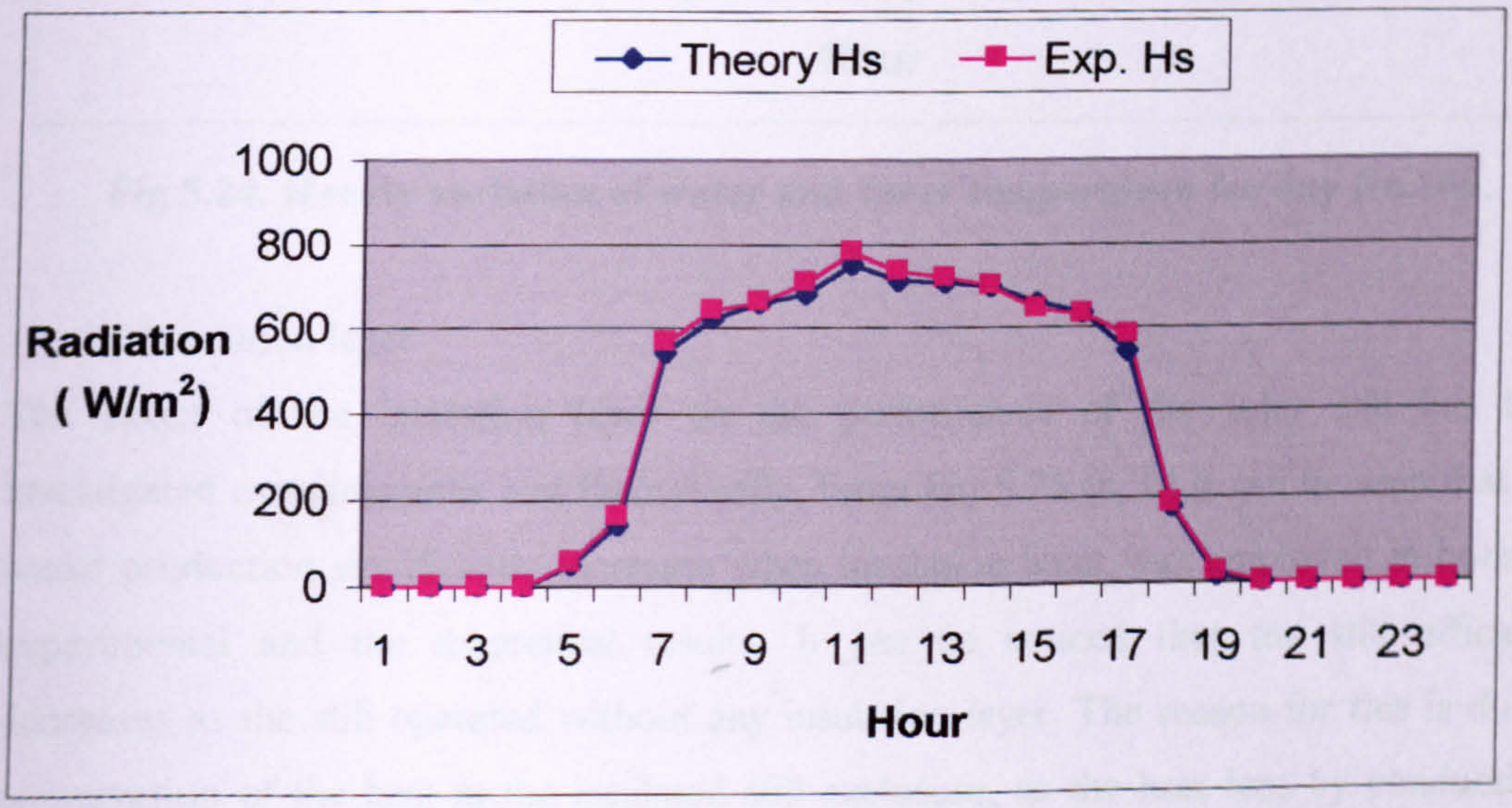

Fig 5.23. Hourly variation of insolation for day No.166.

(c) Glass and Water temperature (T_g&T_w)

The predictions of the water temperature variation with time are accurate up to 11 a.m. The value of (T_w) measured at mid-day is generally few degrees higher than that predicted. While the theory predicts the maximum water and glass temperatures to occur at 1 p.m., the maximum of both the (T_w) and (T_g) are at 12 noon, Fig 5.24. The measurements show that in the morning, the differences between (T_w) and (T_g) are less than the predicted, and in the afternoon the difference is much bigger.

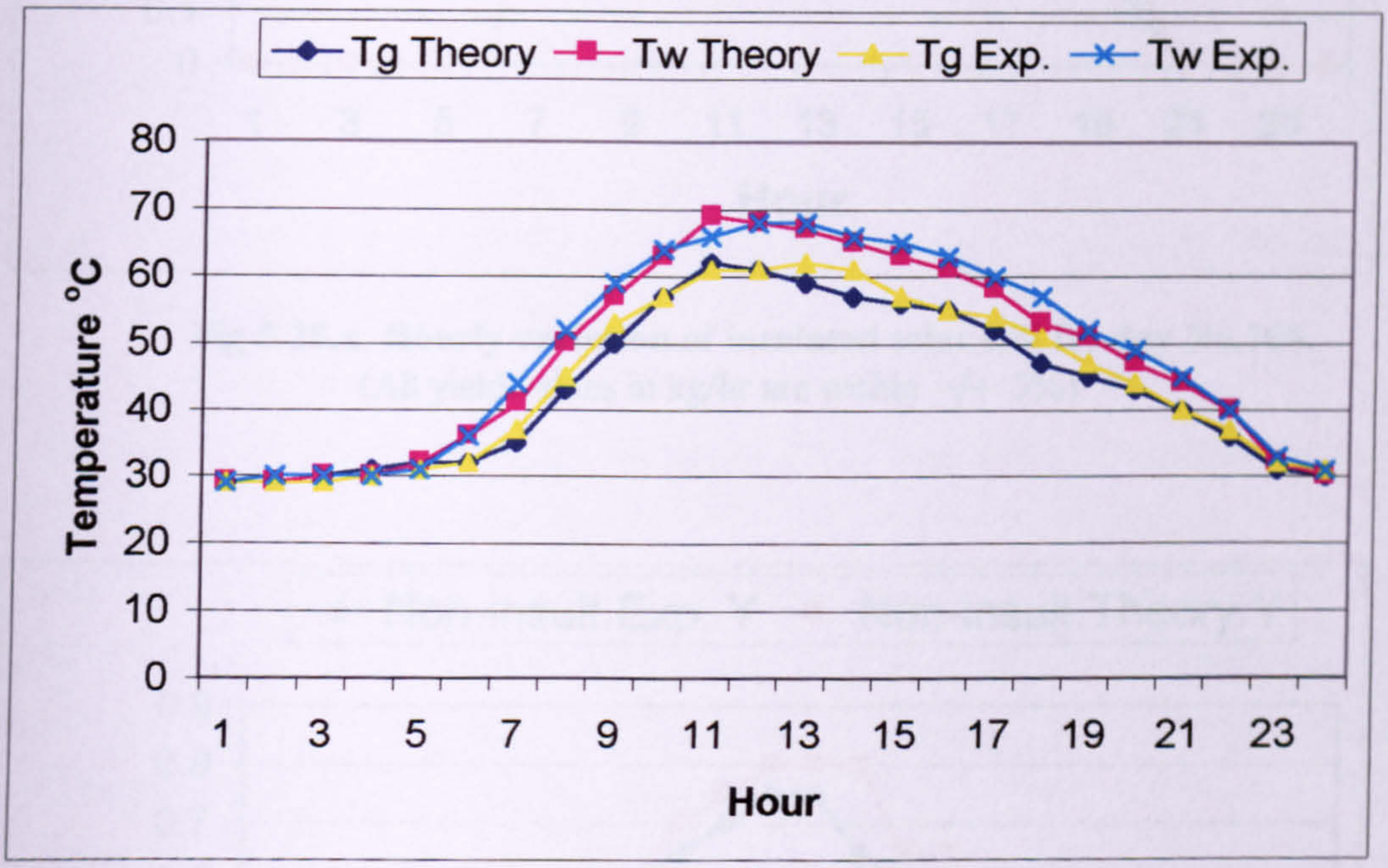

Fig 5.24. Hourly variation of water and cover temperature for day No.166.

(d) Insulation layer

The effect of the insulation layer on the performance of the solar still has been investigated experimentally and theoretically. From Fig 5.25 (a, b) it can be seen that still water production significantly increases when insulation layer was employed in both the experimental and the theoretical results. It can be noticed that the still efficiency decreases as the still operated without any insulation layer. The reason for this is due to preservation of the heat in the insulated still enclosure, so the heat loss by conductivity was minimized.

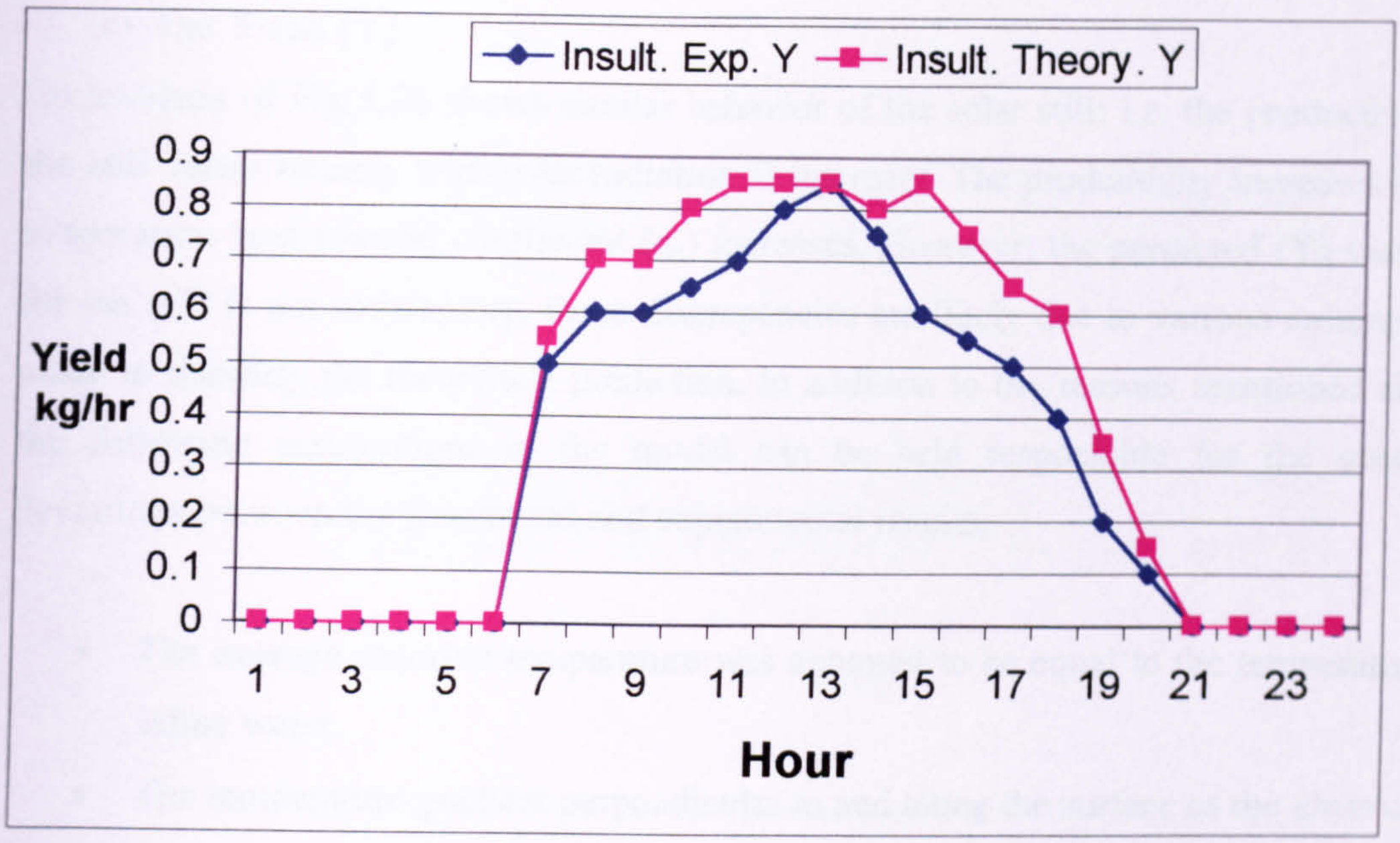

Fig 5.25.a. Hourly variation of insulated solar still for day No.166.
(All yield values in kg/hr are within –/+ 3%).

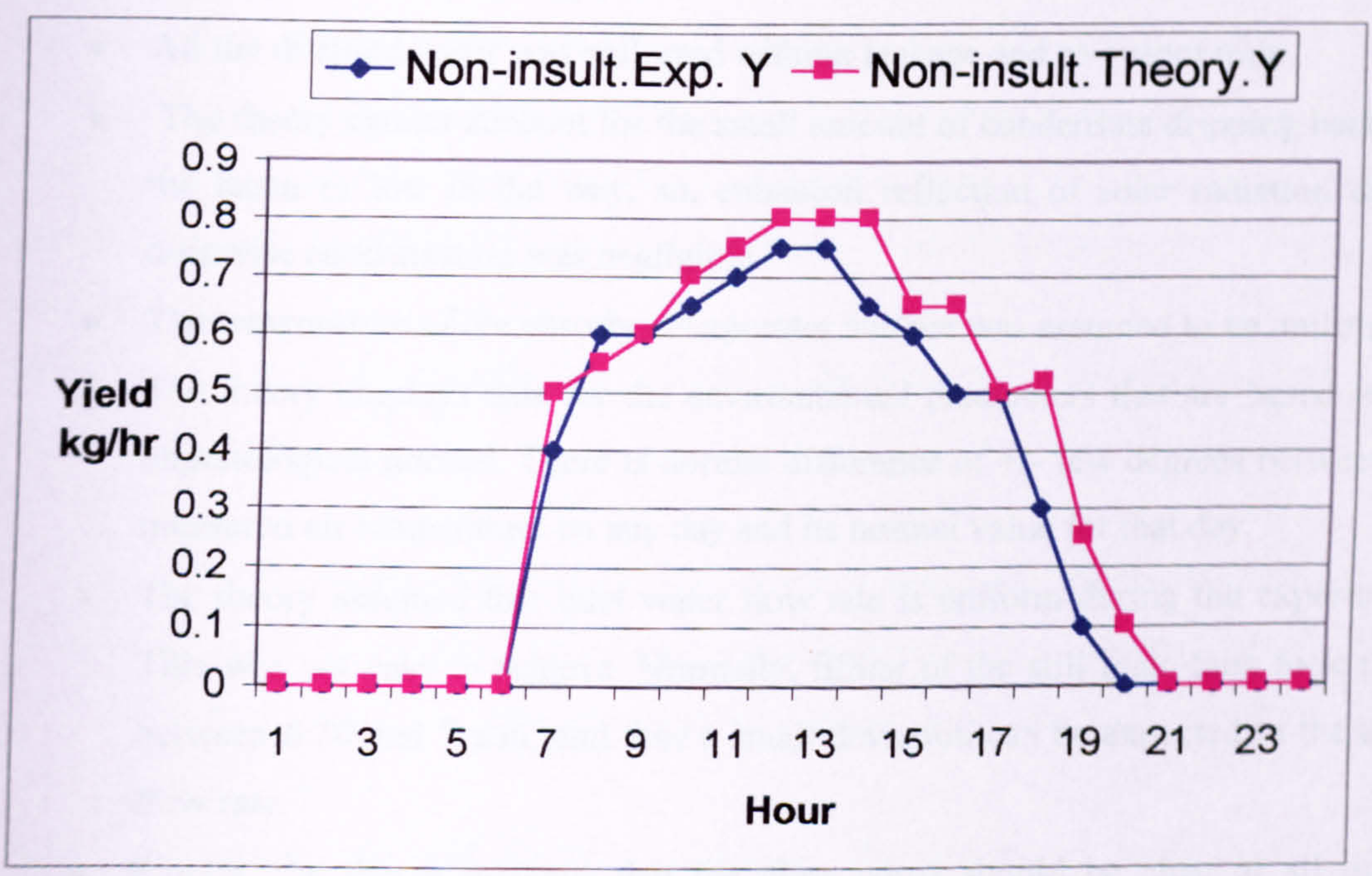

Fig 5.25.b. Hourly variation of non-insulated solar still for day No.163.
(All yield values in kg/hr are within –/+ 3%).

(e) The Yield. [Y]

Comparison of Fig 5.26 shows similar behavior of the solar still; i.e. the productivity of the still varies linearly with solar radiation H intensity. The productivity increases as the evaporation heat transfer coefficient (q_e) increases. However, the predicted (Y) variation for the still is not satisfactory, these discrepancies are likely due to various assumptions made to simplify the theoretical prediction. In addition to the reasons mentioned above, the following assumptions in the model can be held responsible for the observed deviations between the theoretical and experimental results:

- The average absorber temperature was assumed to be equal to the temperature of saline water.
- The temperature gradient perpendicular to and along the surface of the glass cover was assumed to be negligible.
- It was assumed that there was no vapour leakage from the still.
- The condensation film on the glass cover was uniform and has small heat capacity, which can be neglected.
- All the distilled water was collected without leakage and re-evaporation.
- The theory cannot account for the small amount of condensate dripping back into the basin or lost in the way, so, enhanced reflection of solar radiation due to dropwise condensation was negligible.
- The temperature of the absorber/evaporator surface was assumed to be uniform.
- The theory employs data for the environmental parameters that are based on the climatological normal. There is normal difference of +/- few degrees between the measured air temperature on any day and its normal value for that day.
- The theory assumed that inlet water flow rate is uniform during the experiment. This was not easy to achieve. Normally, filling of the still main tank took place between 6:30 and 7 a.m. and thus a small deviation can be expected in the input flow rate.
- Finally, the theory assumes that the glass cover should be clear at all times. However, in the outdoor experiments, it has been found that fine dust layer on the glass cover was always appear particularly in windy days.

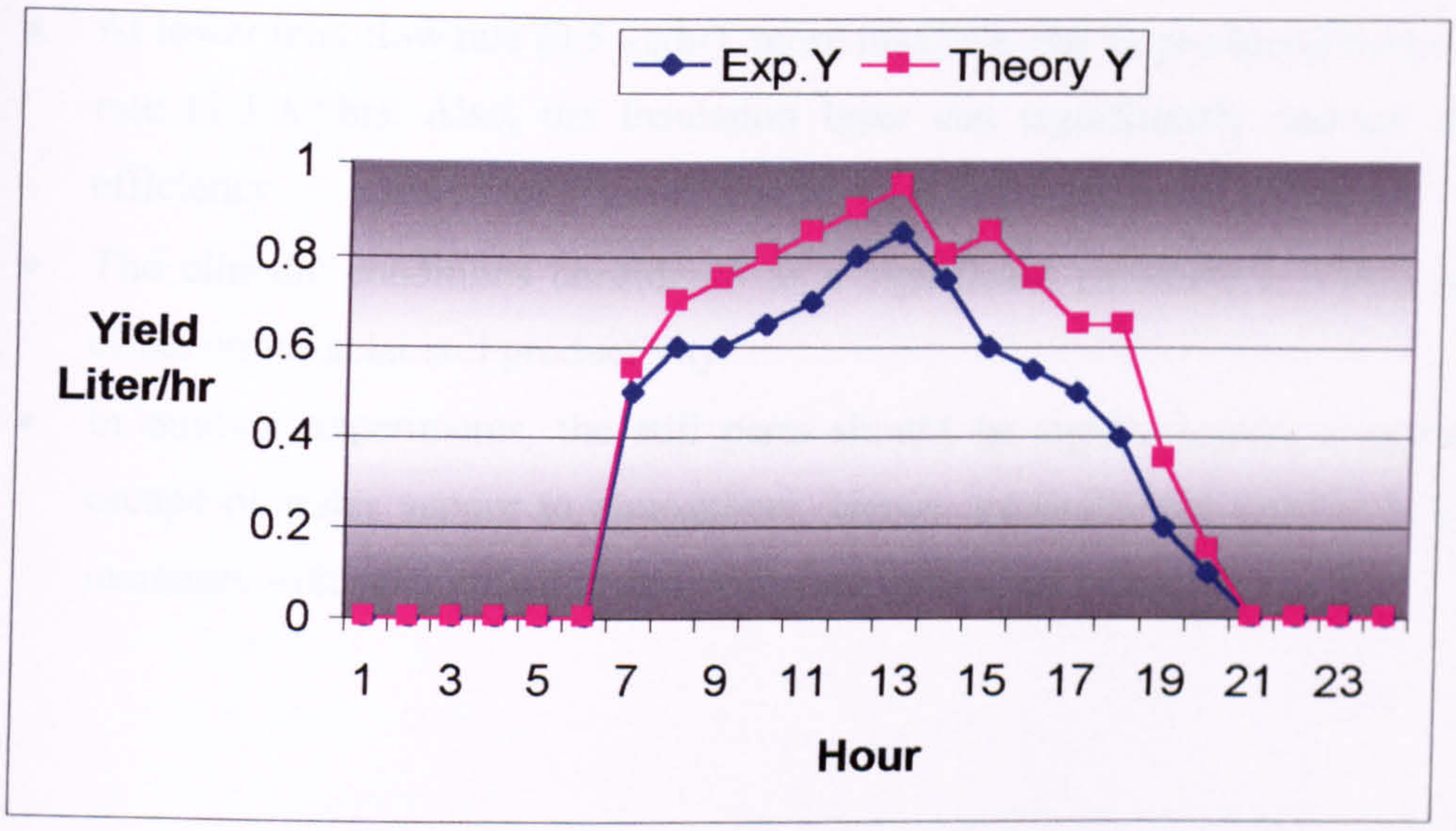

Fig 5.26. Hourly variation of instantaneous yield for day No.166.
(All yield values in kg/hr are within –/+ 3%)

5.31 Conclusions and Recommendations

In operating the experimental still, many parameters must be controlled before starting the experiment. The input flow rate must be reduced and kept as uniform as possible. Any bubbles or sudden increase in the flow rate can cause salt water drops accumulation on the inner surface cover and contaminate the distilled water. Still should be kept wet by seawater feeding to inhibit the creation of a salt layer on the trays surface, affecting the performance.

For a better use and longer effective operations, the following precautions shall be taken into consideration:

- For the indoor solar still tests, pyramid cover is more suitable than dome cover.
- The cover dimensions, still construction material, insulation layer and sealant material should be carefully selected, which may dramatically impair still performance.
- To increase the still distillate production, the still should be covered with a thinner glass cover.
- Inlet flow rate should be fixed along the test to avoid contamination caused by the spilling or overflowing inlet seawater on the condensate layer. The 30 mm cavity between cover and water surface is sufficient to eliminate this incidence.

- At lower inlet flow rate (0.5 kg/hr), more distillate can be produced than at higher rate (1.5 kg/hr). Also, the insulation layer can significantly increase the still efficiency.
- The climatic conditions considered as a significant parameters, which have an effect on the solar still productivity.
- In outdoor experiments, the still parts should be tightly sealed to prevent the escape of water vapour to atmosphere. Hence, generally the produced distillate increases with solar radiation and decreases with wind velocity.

CHAPTER SIX

ECONOMICAL COMPARISON

6.1 Introduction

The demand for a constant, economical supply of water is relentlessly increasing all over the world, and supply often falls short of the present requirements. In Qatar, this problem will become more arduous to remedy in the future. One obvious solution to the problem of inadequate water availability is desalination of seawater. Over 98% of the total fresh water produced in Qatar originates from water desalination plants. This solution consists of distilling seawater by a variety of processes, with the result that adequate quantities of fresh water are produced that are suitable for the selected final use. One drawback of this solution is the exorbitant cost involved. A desalination plant requires a substantial capital investment for the construction and additional investment in the running and maintenance costs. In spite of this, however, there are many desalination plants in use throughout the world. The initial cost is fully compensated for by the advantages in terms of quantity of fresh water provided, so necessary for all living beings.

Having a reliable and constant supply of drinking water is of paramount importance in the provision of a decent life style and adequate health for any population. This consideration, coupled to the growth in industrialization and the growing requests for desalination water for irrigation purposes, confirms the necessity for securing increased quantities of desalination water in areas of adverse climatic and geological conditions. In Qatar, desalination is an excellent solution to the problem, provided that there are sufficient quantities of fresh water to meet the needs of the inhabitants. The primary consideration for attempting to develop a desalination technology is to minimize the cost of eliminating the salt content in the water without incurring deleterious environment effect.

The potable water demands in arid countries, such as Qatar, are in part fulfilled by desalted water, however, accessibility to remote areas with desalted water is very limited and uneconomical. As a consequence of this and in lands receiving high incident solar radiation, solar desalination can be seriously considered as mean to satisfy the water needs, particularly, in small remote villages. These villages depend only on ground water, which has a high salt concentration, include Al-Shamal, Al-Amariah, Am-Taqah...etc. Solar desalination methods offer an economically viable

method of harvesting and storing solar energy to supply fresh water or heat to several types of desalination systems.

In this chapter, the overall cost of water produced from various desalting systems has been reviewed. Moreover, economical analysis of various water desalination processes was undertaken with respect to several criteria; namely specific energy consumption, capital cost, operational and maintenance costs. These processes were investigated in detail through a value analysis. The investment costs were subsequently calculated for the processes identified as being the most appropriate for Qatar applications. Furthermore, the cost comparison was limited to those processes, which could be commercially viable in Qatar. A preliminary study of the overall arrangements followed this and an assessment of such systems for use in future water desalination plant projects in Qatar was also investigated.

6.2 Capital and Water Cost of Water Desalination Processes

The major costs of distillate water production from seawater, like those of almost any other production process, can be classified into three main categories: (a) energy consumption costs, (b) capital costs, and (c) operation and maintenance costs. Moreover, when considering various technical aspects, costs have to be scrupulously evaluated, Fig 6.1. These considerations play determining role in process selection. A complete desalination facility can include a power plant, administrative offices, stores, intake and outfall systems, maintenance facilities, firefighting equipment, workshops, …etc. Therefore, the total cost of the desalting equipment can be a small part of the total cost involved (Morin, 1993; Wangnick, 1996 and Wade, 1993).

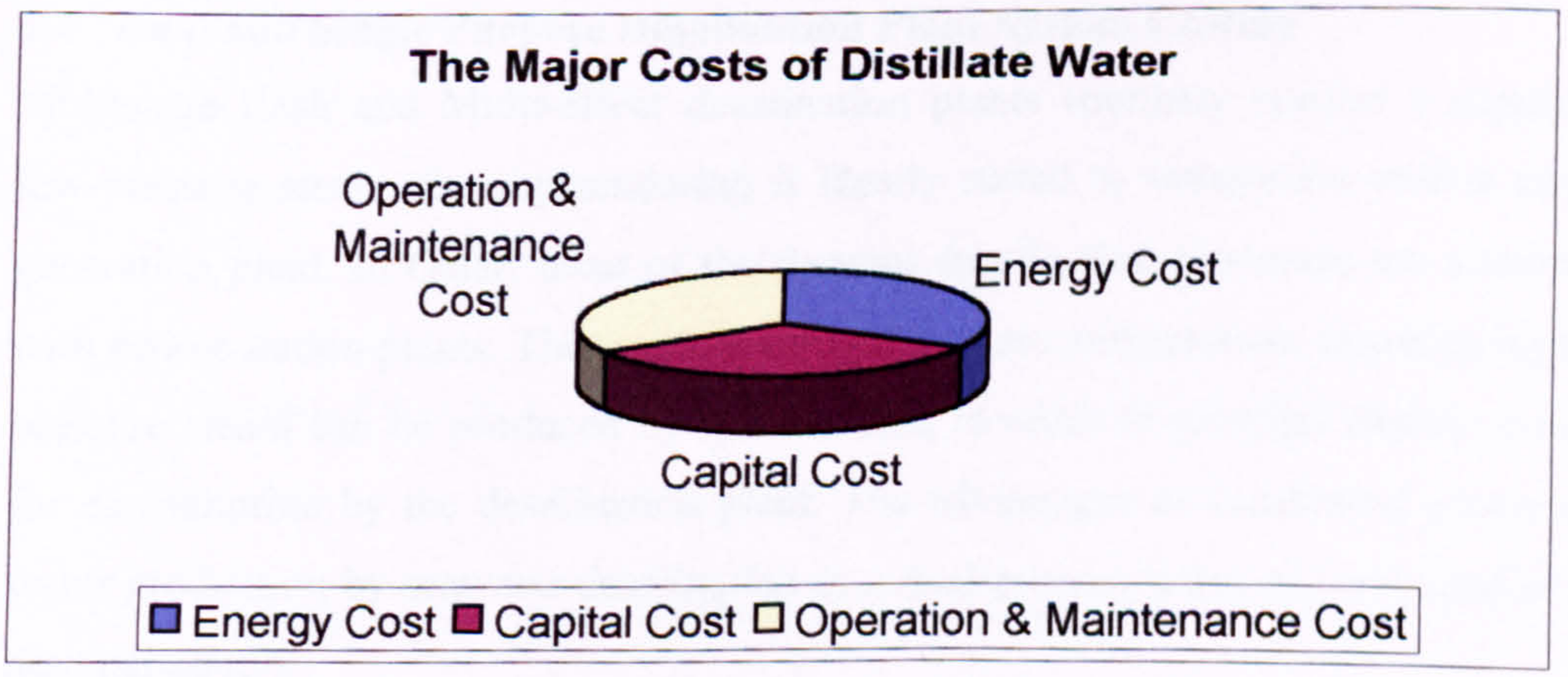

Fig 6.1. The Major Costs of Distillate Water Production (Wade, 1993).

The fuel costs can significantly change the economics of any such venture. It can influence the selection of the process itself due to its effect on the final product (water) cost. As a means of establishing the optimum desalting process, a complete economic analysis is essential and must therefore, include any associated costs. In any analysis, it is important to correlate the desalination process to the desired product water quality, quantity, site-specific conditions, and energy costs. The responsiveness of the overall cost of desalted water to each independent design parameter requires evaluation. Parameters, which have the potential to alter the costs, are capacity, process, feed water salinity, feed water quality, location, design energy, materials, intake and reject system. Some of these parameters are known to influence the water cost significantly. A single consideration can dramatically influence optimization. Some parameters ascent only a minor impact and be disregarded without modifying the result of an optimization. These parameters will be discussed for each process in distillates in the following sections.

6.3 Energy Consumption Costs

In simple terms, the major part of the capital and operational costs is associated with heat transfer surfaces and the production of steam. These costs account for more than 50 % of the total cost of producing the water. Operational costs are even higher as they include manpower, chemicals, and maintenance costs. In this study a comparison between the principle water desalination processes have been discussed. Moreover, the effects of various parameters, which influence the cost of water production, have also been evaluated (Tempereley,1995).

6.4 Dual and Single Purpose Desalination Plant System Costing

Multistage flash and Multi-effect desalination plants routinely require a supply of low-pressure steam; thereby rendering it ideally suited to integration with a power generation plant. In Qatar, most of the thermal desalination processes are combined with power station plants. The result is a cogeneration configuration, in which higher-pressure steam can be produced by gas turbines, in order to generate electric power, for consumption by the desalination plant. The advantages of combining power and water production by seawater desalination in a dual-purpose plant are reviewed in the next paragraph.

In fact, the gas turbine plant can provide power and eliminate the most expensive part of water desalination plant operation costs, by providing continuous steam as a by-product. The heat input section of the evaporation plant serves as the condenser or heat rejection unit of the turbine plant, therefore the condensate requires less heating prior to re-use, by an amount dependent on the difference between the new elevated temperature and the standard temperature of the power-only unit. Other advantages accrue from the sharing of common services, supervision, and organization. From the literature survey, it has been shown that the advantage of a dual-purpose plant ranges between 20% and 60% saving in water cost dependent upon the scale of operation and method of cost allocation, as shown in Table 6.1

Costs		Single Purpose MSF Plant	Dual Purpose MSF Plant
Plant Energy Consumption	Fuel Oil	0.37	0.2
	Electricity	0.07	0.07
	Subtotal	0.44	0.27
Capital Charges		0.29	0.3
Operation & Maintenance		0.09	0.09
Total Water Cost		0.81	0.65

Table 6.1 Overall Cost Comparison between Single and Dual Purpose Desalination Plant in $/ cu.m (Hanbury, Hodgkiess and Morris, 1992).

The most important differences between single and dual-purpose desalination plants is the variation in efficiencies with which they utilize the fuel employed in their

operation. In single purpose desalination, the heat source originating from the oil/gas-fired boiler with no electricity generation. In a dual purpose desalination plant heat is received from the waste gases of the gas turbines which made to generate electricity concurrently. Whereas, all practical fuels are capable of producing heat at high temperatures, and power generation systems attain their highest efficiency when operating at the maximum practicable temperature, typically using steam at 540°C, the greater number of desalination plant operations are confined to temperatures less than 120°C (El-Dessouky, 1985).

The utilization of fuel to produce high temperature energy to exclusively operate a single purpose desalination process, which is only capable of capitalizing on this energy after it has been substantially degraded, is, therefore, expensive and not generally cost effective. Therefore, the exploitation of this type of system must be confined to infrequent applications on a relatively small scale when the circumstances dictate it as necessary expedient. This reflects the present status of single purpose desalination plants which have only been constructed in isolated areas where there is insufficient demand for additional power to that already available and relatively small amount of water is required, or where a small stand by source of water production is required for infrequent operation at a low electricity load characteristic (Clelland, 1981).

6.5 RO Energy Costing

In the reverse osmosis process, the electrical energy constitute the largest factor in the operation cost of the plant. The energy requirements of the RO process can be divided into four main sections; pretreatment system, high-pressure pump, second stage pump, and the product distribution pump. The largest load is consumed by the high-pressure pump, which feeds the first stage membranes. The electricity required to power the plant is usually supplied directly or, generated by heavy fuel operated diesel generators with a nominal generator capacity of 2760 kVA, particularly in remote areas. Normally, one generator is designed to carry the full load of the plant whereas the second is necessary during the start-up of the large drives and serves during operation as a stand-by capacity (Porteous, 1988).

The high-pressure pump consumes between 5.3 and 7.9 kWh/m^3 of water production. The source water supply and the pretreatment systems use between 0.3 and 1 kWh/m^3. The total consumption normally ranges between 8-11 kWh/m^3 for a seawater RO system and 2-3 kWh/m^3 for a brackish water RO system. These figures can be reduced if energy is recovered from the reject brine system. Large seawater RO plants with energy recovery required 0.5-0.3 the energy required by the MSF plants. The typical energy consumption of the RO process as compared with RO process employing recovery system is shown in Table 6.2.

Costs		RO with no Recovery	RO with Recovery
Energy Consumption	Fuel Oil	0	0
	Electricity	0.18	0.12
	Subtotal	0.18	0.12
Capital Charges		0.23	0.24
Operation & Maintenance		0.32	0.32
Total Water Cost		0.73	0.68

Table 6.2. Overall cost comparison between recovery and non recovery system reverse osmosis desalination plant in $/cu.m (Hanbury, Hodgkiess and Morris, 1992).

6.6 Solar Energy Requirement

Solar energy can generally be converted into useful energy such as heat, using a solar still, and solar collectors, or as electricity, with photovoltaic cells. As described in Chapter three, several methods of utilizing solar energy have been used to produce fresh water. The direct method can only utilize solar energy whenever it is available, and their ability to collect solar radiation is inefficient. However, in an indirect collection system, solar energy is collected by more efficient solar collectors, in the form of hot water or steam. It should be noted however, that although solar energy constitutes a free energy source it is only available for approximately half of the day.

This implies that the process operates for only half the time available unless some accumulation tank is used. The accumulation tank, which is generally costly, can be located adjacent to back-up boiler or supply of electricity from the grid in order to operate the system during periods of low insolation and at night-time. In all solar energy desalination systems an optimum performance ratio has to be calculated based on the cost of the solar energy collectors, accumulation tank, and of the desalination plant.

The energy required for various desalination processes, as obtained from a survey of manufacturers data, is presented in Table 6.3. It can be seen that the process with the smallest energy requirement is RO combined with energy recovery system. However, this is only a viable proposition for very large systems due to the high cost of the energy-recovery turbine. The next lowest in terms of energy requirement is the RO system without energy recovery, and MED method. It can also be seen that the MSF desalination process has the most excessive energy consumption. In spit of solar still considered as the highest energy consumption process, it must be remembered, however, that the consumed energy is free (Porteous, 1988 and Soteris,1996).

Process	Heat Input (kJ/kg of product)	Mechanical Power Input (k Wh/m^3 of production)	Prime Energy Consumption (kJ/kg of production)
MSF	294	3.7	338.4
MED	123	2.2	149.4
RO with Recovery	0	7.9	94.8
RO with no Recovery	0	12	144
Solar Still	2330	0.3	2333.6

Table 6.3. Energy Consumption of Desalination Processes (Soteris, 1996).

6.7 Desalination Plant Capital Cost

The capital costs of the potential water desalination plants have been assessed in a number of different ways. As plant designed for different locations and duties can differ significantly both in the technical complexity and in the commercial conditions

under which they are constructed, there are some considerable variations in the capital costs caused by considerations such as the capacity, size, feed water source...etc. The capital costs have been expressed in terms of expenditure per unit capacity in U.S. Dollars per cubic meter of water produced per day (El-Dessouky, Ettouney, and Al-Roume, 1999).

As portrayed in Table 6.4 (a, b), the estimation of capital costs between MSF and MED for medium-size desalination plants capacity (9000 m^3/day) at Dukhan city in western coast of Qatar are reviewed. The capital cost estimation identifies the MSF distillers as being about 15% higher than the MED distiller plants, in terms of the cost of the evaporator unit with auxiliaries and erection. Boiler costs will be approximately the same for either type of plant, as a comparable steam flow is required for both. Other equipment costs are higher for the MSF than for the MED due to the complexity of the plant system. It was also estimated that the unit water cost for the MED plant is 17% lower than the equivalent MSF scheme due to a reduced quantity of seawater throughout.

Item	FOB	Shipping and Delivery	Erection	Total
Evaporators, pumps and auxiliary equipment	10,186	1,222	2,015	13,424
Boilers	388	47	70	504
Pipe work and valves	1,798	216	323	2,337
Electrical equipment	707	85	127	919
Instrumentation	579	69	104	753
Seawater intake pumps and screens	663	80	119	862
Miscellaneous plant	221	27	40	287
Spare part	708	85	0	793
Product system	205	25	37	267
Electrical supply system	332	40	60	432
Civil Works	0	0	0	2,381
Sub Total	15,787	1,895	2,895	22,958
Project sub Total				24,565
10% Engineering and Contingencies				2,456
Total Project Cost				27,021

Table 6.4.a. Estimated Capital Costs-MSF Desalination Plant Capacity of 9000 m^3/day at Dukhan City (U.S.$ x1 000) (Mockler, 1987).

Item	FOB	Shipping and Delivery	Erection	Total
Evaporators, pumps and auxiliary equipment	8,953	1,074	1,720	11,747
Boilers	388	47	70	504
Pipework and valves	1,578	189	284	2,051
Electrical equipment	601	72	108	782
Instrumentation	492	59	89	640
Seawater intake pumps and screens	630	75	113	818
Miscellaneous plant	187	22	34	243
Spare part	602	72	0	674
Product system	205	25	37	267
Electrical supply system	303	36	55	394
Civil Works	0	0	0	2,038
Sub Total	13,940	1,671	2,509	20,159
Project sub Total				21,570
10% Engineering and Contingencies				2,157
Total Project Cost				23,727

Table 6.4.b, Estimated Capital Costs-MED Desalination Plant Capacity of 9000 m^3/day at Dukhan City (U.S.$x1000) (Mockler, 1987).

Moreover, the lower operation temperature of the MED reduces the threat of corrosion and scaling. Consequently, the maintenance costs in the MED is 10% lower than a comparable MSF desalination plant. The study excludes the RO process from this project due to in fact that RO is insufficient for highly saline feed water such as that found in the Gulf Sea. Moreover, the high cost of the seawater type membrane and the functional brevity, all contribute to the inflated maintenance costs of the plant (Mockler, 1987).

A comparison of the costs of the desalination equipment and seawater treatment, as obtained from a survey of manufactures data, is shown in Table 6.5 (Soteris, 1996). The least expensive of the systems considered is the solar still, 900-1000 $/$m^3$/day. This comprises of a direct collection system, which is very easy to construct and operate. The disadvantage of this process is its appreciably low yield, which implies that large areas of flat ground are required. It is questionable whether such processes

can be viable unless cheap, desert-like, remote villages are used to locate such process.

Item	MSF	MED	RO	Solar Still
Scale of application	Medium-Large	Small-Medium	Small-Large	Small
Seawater treatment	Scale inhibiter Anti foam Chemical	Scale inhibiter	Sterilizer Coagulant Acid Dexidiser	None
Equipment price U.S.$/m^3 of water production.	5000-12000	4000-11000	1000-6000 Membrane replacement every 3-4 years	900-1000

Table 6.5. *Comparison of Desalination Processes Capacity* (Soteris, 1996).

The capital costs are likely to be quoted for only seawater desalination processes. However, in the RO case, the capital costs rely on supplied water quality. Consequently, the capital costs can be varied form brackish and seawater with range between 1000-2000 \$/m^3/day to 2000-4000 \$/m^3/day respectively. It must be stressed that these figures maybe realistic for large plant without any water intake or civil works problems, however, the installed cost of small to medium-sized seawater plants tend to be in the range from 3000-6000 \$/m^3/day. Although, MED is the only process that approaches the RO plant in terms of estimated capital cost, the installation cost of small-to medium-sized plants can vary between 4,000-11,000 \$/m^3/day. The MSF plant is encumbered by the largest installation cost compared to the other desalination processes; this cost can be in the range of 5,000-12,000 \$/m^3/day medium-and large-size plant.

6.8 Operation and Maintenance Cost

The bulk of the feed water comprises of a variety of suspended solids and dissolved materials. Typical component include sand, silt, clay, mud, natural organics, dissolved chemicals, debris, microorganisms, corrosion products, carryover from treatment systems, products from anti-scale inhibitors, and dissolved salts. These can precipitate inside a desalination plant resulting in the manifestation of innumerable maintenance

problems. The areas most predisposed towards deposition are the heat exchangers; which profoundly influence the evaporation ratio of the plant. The overall operating costs of a desalination plant consist of a variety of constituents, which includes Plant Construction costs, Fuel, Manpower, Chemicals, Spare parts…etc. The constituent that represents the biggest proportion of overall operating costs is nearly always the capital charge, usually accounting for 30-40% of the ultimate water cost. The relative amounts and actual values differ between with variations in feed water sources.

Item	MSF	MED	RO	Solar Still
Steam	60-78%	60-80%	0	0
Manpower	15%	13%	30%	50%
Chemicals & Materials	5%	4%	20%	0%
Power	2%	3%	50%	50%
Total	82-100%	80-100%	100%	100%

Table 6.6. Comparison of Desalination processes and Operating Costs (Khan, 1986).

A number of the actual and estimated operating costs for water desalination plants are presented in Table 6.6. The average cost contribution distribution of MED, MSF, RO, *SD are illustrated in the Fig 6.2- 6.5. It can be observed* that the operating costs for the varying types of seawater desalination plants vary quite *dramatically. The most* noticeable differences in the figures occurs between the dual purpose MSF and the RO system combined with a recovery plant. MSF would appear to be more expensive to install, yet cheaper to operate. Seawater reverse osmosis on the other hand is cheaper to install, however, it is more expensive to operate merely due to the excessive cost of membrane replacement.

The operational and maintenance costs of MSF and MED desalination plants are quite different. The prime fuel consumption is considerably elevated in the MSF 338.4 kJ/kg of product, compared to 149.4 kJ/kg of product in MED desalination plant. What is more the MSF process requires the addition of a wide range of chemicals,

such as; Scale inhibiter, pH control, Sodium sulphite, and Anti-foam. Whereas, only scale inhibiter is routinely required in the MED system, therefore the chemical cost component is reduced. The solar still does not rely on the application of additives or chemicals and is the largest free energy consumption process. However, the projected productivity is very low compared with the other processes (Khan, 1986).

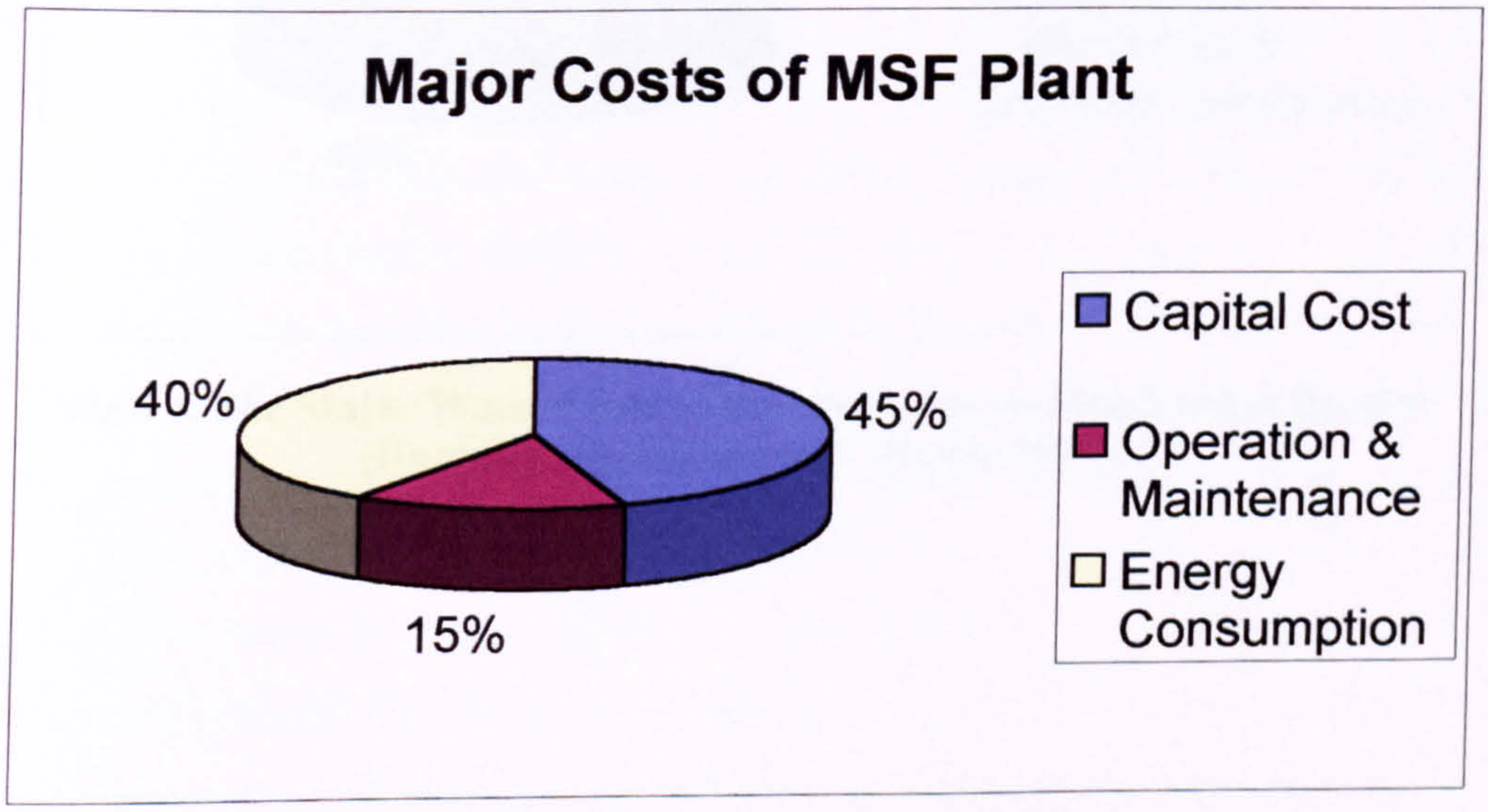

Fig 6.2. The Major Water Costs of Multistage Flash Desalination System (Hanbury, Hodgkiess and Morris, 1992).

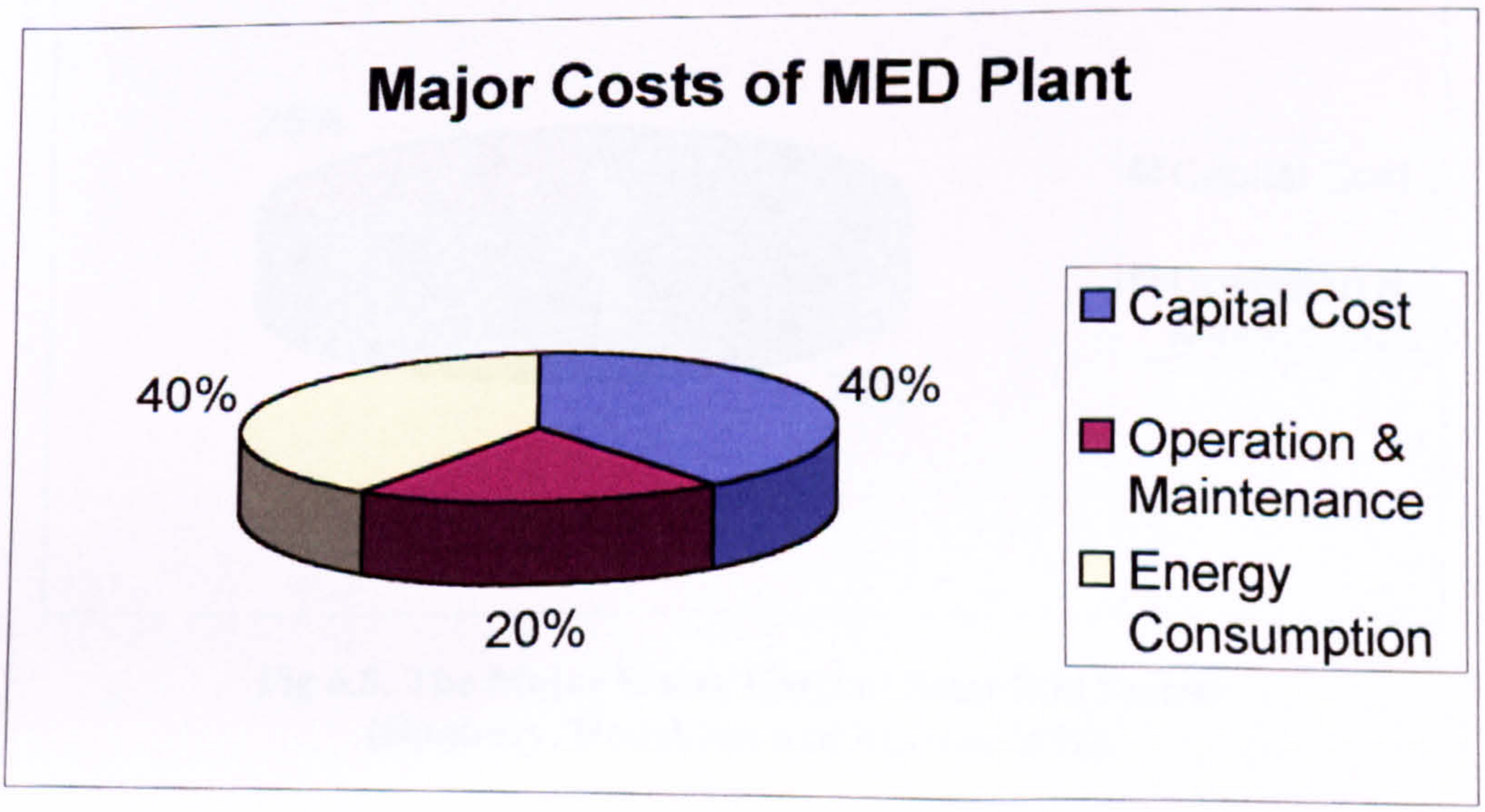

Fig 6.3. The Major Water Costs of Multi Effect Desalination System (Hanbury, Hodgkiess and Morris, 1992).

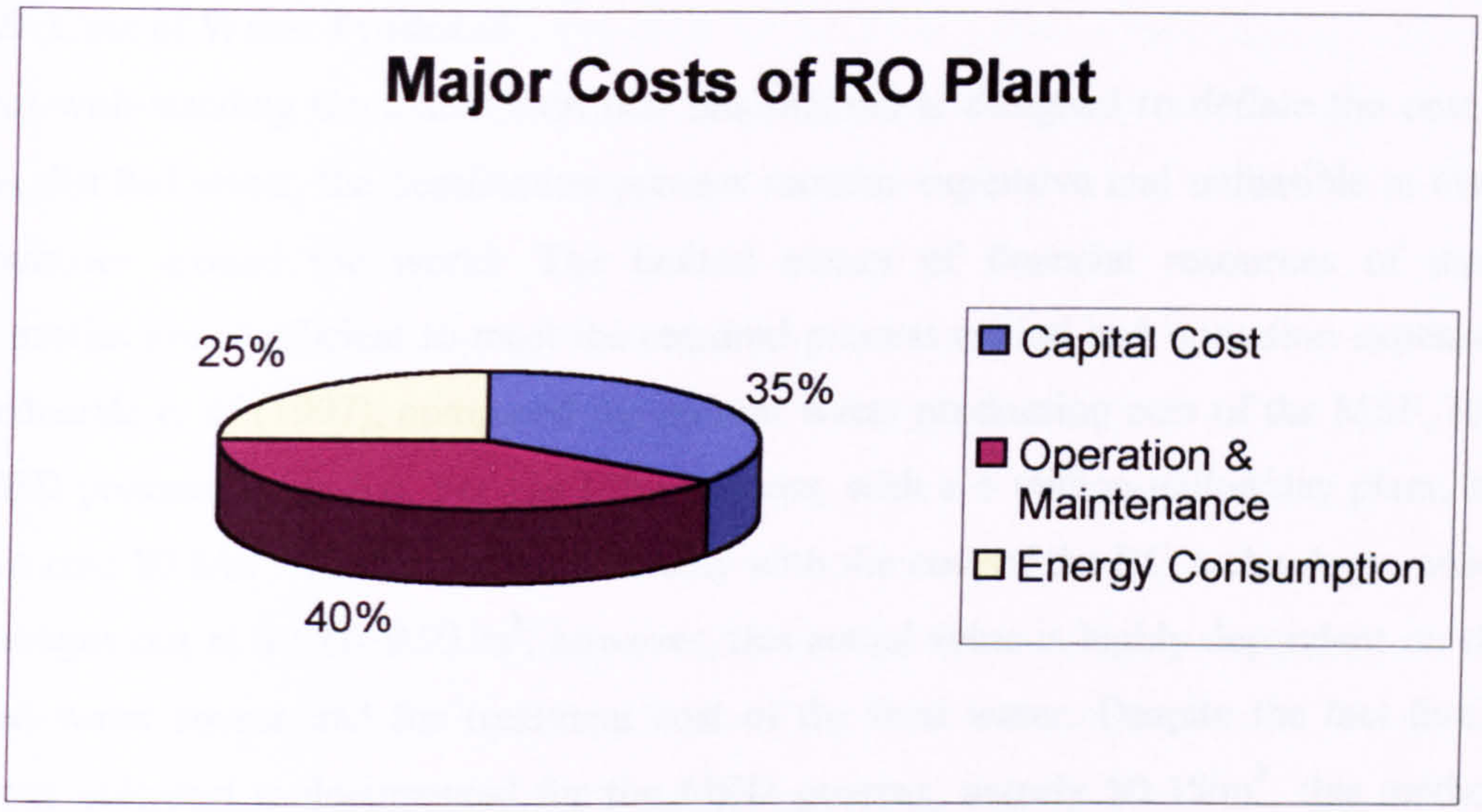

Fig 6.4. The Major Water Costs of Reverse Osmosis Desalination System (Hanbury, Hodgkiess and Morris, 1992).

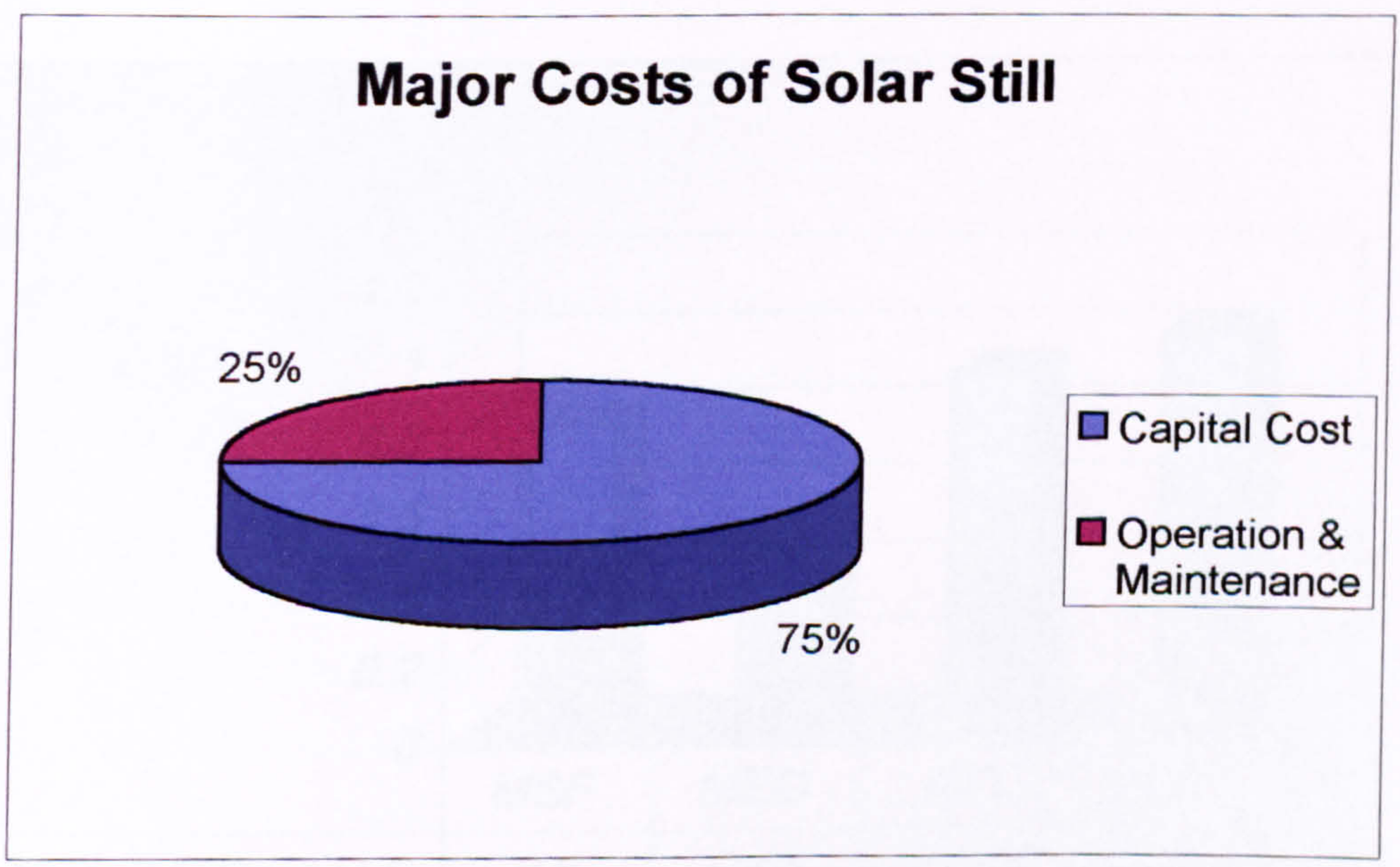

Fig 6.5. The Major Water Costs of Solar Still System (Hanbury, Hodgkiess and Morris, 1992).

6.9 Cost of Water Produced

Not-with-standing the assumption that this method is designed to deflate the cost of the distilled water, the desalination process remains expensive and unfeasible in many countries around the world. The limited means of financial resources of many countries are insufficient to meet the required process capital and operation expenses. Bednarski *et al* (1997), compared the current water production cost of the MSF, RO, MED processes, Fig 6.6. For the MSF process, with a 6 million-gallon/day plant, the unit cost \$0.8/m^3. This compares favorably with the cost of the RO technology, which averages out at \$0.72- 0.93/m^3, however, this actual value is highly dependent on the feed water source and the treatment cost of the feed water. Despite the fact that a lower unit cost is documented for the MED process, namely \$0.45/m^3, this method has only been embraced by the desalination industry to a very limited scale. The lower unit cost in the MED process is primarily a reflection of the higher thermal performance ratio. Field data on the MED system published by de Gunzbourg and Larger show consistent results, where an existing MED system is reported to attain thermal performance ratios of 12 when compared to MSF, which failed to exceed 9.

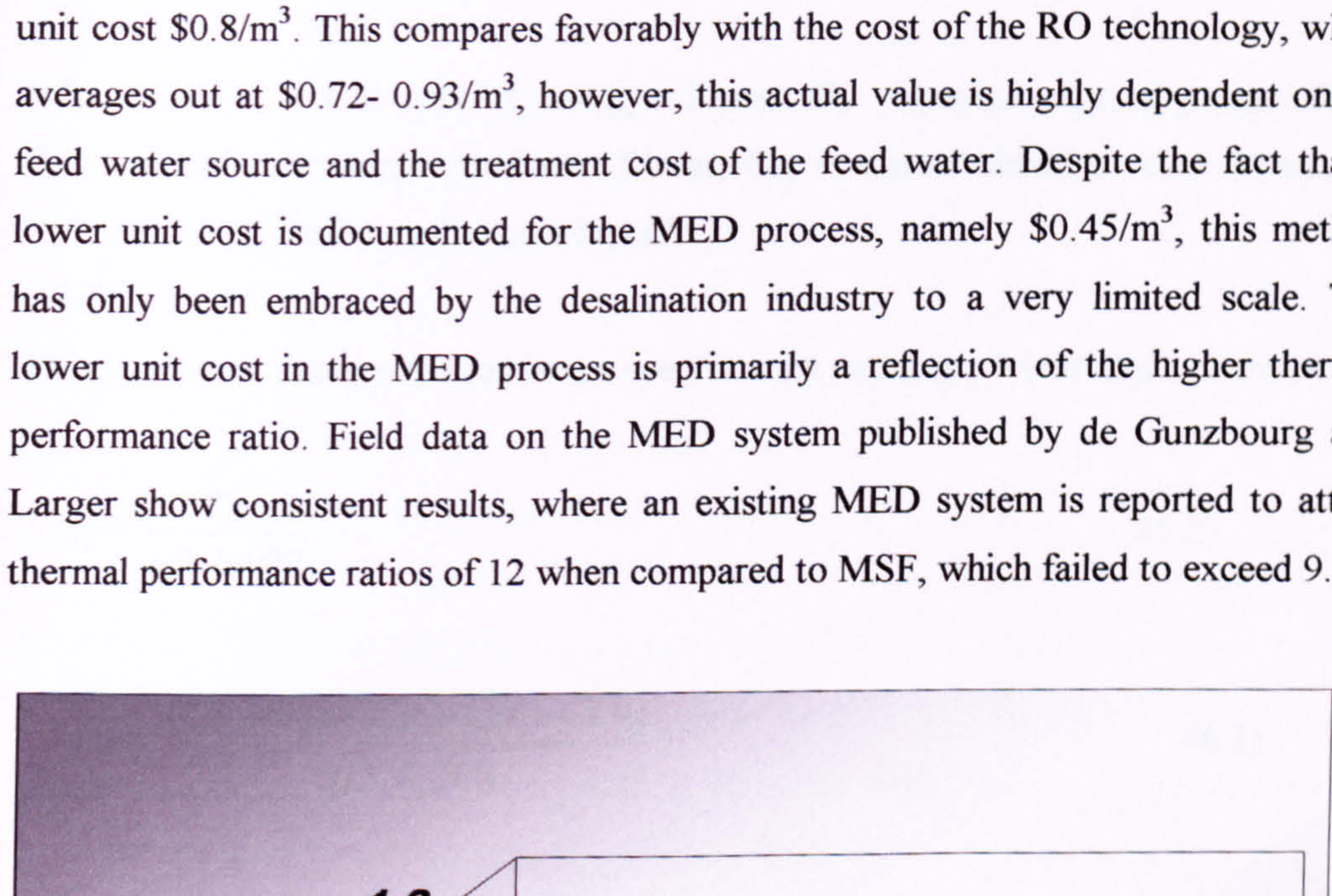

Fig 6.6. Average Cost of Water Produced by several Water Desalination Processes (Bednarski, 1997).

Many theoretical approaches have been proposed in order to represent the optimum performance ratio and rite the pre-eminent value as the result of the minimum cost function (Malik, 1981).

The water cost function, C_r, can be written as:

$$C_r = C_e + C_p + C_o + C_{ch} + C_c \qquad (6.1)$$

Where C_e = annual cost of energy \$/year, C_p = annual cost of power \$/year, C_o = annual operation capital cost \$/year, C_{ch} = annual chemical cost \$/year, and C_c = annual amortised capital cost \$/year.

This function can be converted into a specific cost assuming 8,000 hours per year.

$$C = \frac{Cr}{qD\ \ 8{,}000} \qquad (6.2)$$

$$Cr = \frac{(Ce + Cp + Cc + Co + Cch)}{qD\ \ 8{,}000} \qquad (6.3)$$

Where q = mass flow per hour, D = tube diameter.

The optimal performance ratio is then obtained by the partial differentiation

$$\frac{\partial c}{\partial R} = 0 \qquad (6.4)$$

As it is evident, the cost function depends on several parameters which can vary from plant to plant or, simply from time to time. Listed below are the principle variables, which influence this cost function:

- Cost of fuel
- Cost of labour
- Cost of chemicals
- Annual interest rate
- Flashing range

- Distillate production
- Brine recycle concentration ratio
- Cost of tube bundle
- Cost of shell material

The annual cost of water produced by a solar still is highly dependent on the following major factors:

1. The total fixed costs as an annual percentage of initial capital investment;
2. Cost of supplying saline water to the distiller; and
3. Operating labour and maintenance costs.

The sum of these expenses divided by the annual distilled water, plus the collected condensate could be the cost of distilled water. It can be seen from Fig 6.6, the average water cost by using solar still is the highest among other processes. However, the volume 225 m^3/day and lower, the cost of fresh water from solar stills remains the lowest. For instance existing desalination plants, with capacities of 1 million gallon/day, supply fresh water at approximately 1 \$/m^3. Currently, plants of even greater capacities are being designed with the view to reducing this cost to less than 0.5 \$/m^3. Solar stills in their current form are incapable of competing with these large desalination plants. On the contrary, for water requirements less than 225 m^3/day the MSF or MED desalination plants cannot compete in economic terms with solar stills. However, the only competition might be offered by the RO plant, but the cost of water in this case would depend on the salinity of the available source water and also the availability of electric power (Malik, 1981).

The following equations relate the annual cost of water production by solar still for 4.5 m^3 to the above factors.

$$C = \frac{10 \times I\ [AP + MR + TI] + 4.5\ LW}{Yd\ Ad + Yr + Ar} + S \qquad (6.5)$$

Where C = cost of water $ per 4.5 m^3, I = total capital investment $, AP = annual interest and depreciation, MR = annual maintenance and repair, labour and materials costs, TI = annual taxes and insurance charge, L = annual operating labour cost, W = operating labour wages, $/man-hours, Yd = annual unit yield of distilled water (1000 liters/m^2 of total solar still area), Yr = annual unit yield of condensate (1000 liters /m^2 of total solar still area), Ad = area of distiller on which distillate yield is based (m^2), Ar = area of distiller on which condensate collection is based (m^2), and S = total cost of salt water supply.

As every system requires some maintenance, the annual cost should also be considered. In this system, maintenance must be performed routinely and in the case of a breakdown to ensure: (a) continuous water supply into the still, (b) replacement of broken glass covers during maintenance, (c) cleaning of solar still. The annual cost has been assigned to be 10% of the first annual cost. Therefore, the annual cost of the system is given by:

$$\text{Annual cost} = \text{First annual cost} + \text{Annual maintenance cost} + \text{Annual salvage value} \quad (6.6)$$

$$\text{Product Cost per Litre} = \frac{Annual\ \ Cost}{Yield} \quad (6.7)$$

$$\text{Annual Cost per } m^2 = \frac{Annual\ \ Cost}{Area\ \ of\ \ Still} \quad (6.8)$$

6.10 Project Pre-study

The aim of this section of the study is to optimize the basic design parameters and evaluated the choices prior to the selection of a particular desalting method. In order to carry out an informed decision regarding the most appropriate process for seawater desalination, both technical and economical characteristics of various desalting processes require investigation. Consequently, a number of steps and regulations are necessary to plan and install a desalination plant.

6.10.1 Demand Forecast

Initially it is imperative to identify future desalination water demand for the area in question. The corresponding daily average distilled/groundwater consumption in

Qatar was around 25 million m^3 in 1973 for domestic and agriculture purposes, this has drammatically risen to 120 million m^3/year in 2000. Numerous studies predict that water demand will continue to increase in the future. Calculations based on the industrial and economical factors and the average rate of annual water consumption of 2.4 m^3 per person per day combined with a 2.93% increase in the population number by year, show that the total water demand will increase to 160 million m^3/year until the year 2003.

The growth of national demand for fresh water in Qatar is likely to be around 5-6% per annum over the next ten years. With this fact in mind, the government decided to install the second expansion phase RAF-B2, for Ras Abufontas (B) power and desalination plant, which was expected to contribute in the region of 27 million gallons of desalinated water daily. This expansion project will be commissioned by Alstom Power Company at an estimated cost of 270 million US-Dollars. In addition, the government has plans to install the forth power and water desalination plant in Ras Laffan Industrial Area over the next few years, which is expected to substantially reduce the continuing fresh water deficit. This project is scheduled to be completed and fully operational by at the middle of the year 2004, the capacity of phase one should attains 750 MW of Power and produce over 30 million gallons water daily. The second phase will probably take place by the end of 2007, thereby doubling the total expected production (Qatar Electricity & Water Co, 2000).

6.10.2 Plant Rating

Subsequent to the estimation of the potential future demand for desalination water, the next step is to determine the installed capacity required. This should equate to or exceed the maximum demand. There should be enough margin to take care of unplanned shortages and output reductions due to periodic cyclical maintenance of the plant. Typically, the install capacity is calculated to exceed by about 25% more than the maximum demand. Consequently, identifying and selecting the most economical desalination process depends on the fresh water quantity required per day. The end use of water produced and therefore its final quality can also determine which process is chosen. Based on industrial, agricultural, or domestic use, product water quality requirements may vary from nil to 1,000 ppm of salt. MSF, MED, and SD processes

produce the purest water with salinity ranging from 2-50 ppm. However, the RO process routinely produces concentration range from 350-500 ppm, depending on the specifications of the feed water source and the membranes used (Khan, 1986; Borsani, Superina and Sommariva, 1995).

6.10.3 Feed Water Quality

Three of the most crucial feed water characteristics, which significantly influence the selection of the desalting process are: composition, reliability and temperature. Feed water composition is a vital consideration for some processes. The RO process is sensitive to qualitative variations in inlet water, but whereas it is well-equipped to operate using brackish water, it would constitute a less appropriate choice for, a seawater feed source, which can be regarded as a living, changing, and complex medium. However, alternative desalting processes such as the MSF, MED, and SD are readily available to desalinate water from a few ppm to over 50,000 ppm. The most important advantage of these processes is their ability to treat saline waters with a high salt content. Indeed, these processes do not significantly vary in the amount of energy required to desalting either low or high concentration feed waters; a factor which renders them ideally suited to desalting seawater and other high salinity waters.

The reliability of feed water quantity is an important factor, since different processes have different feed water requirements. Feed water requirements can vary from a few hundred gallons/day as in the RO and SD processes, to millions of gallons/day when required by the MSF or MED processes. Moreover, ambient temperature of the feed water can affect the process selection or, the design of a particular process. It can effect the heat economy of distilled water processes. In a situation with a low inlet temperature a higher amount of energy is required to raise the feed water temperature, yet alternatively when inlet water of a higher temperature is used it may downgrade the plant productivity since the feed is used in condensation processes. However, higher inlet water temperature (over 30 °C) can destroy or reduce the effective life time of the RO membranes (Mockler, 1987).

6.10.4 Availability of Energy

Most desalination processes require energy of various types. These energy impute can significantly effect the capital and operating costs. The types and availability of

energy should be thoroughly evaluated to select the most economical process for the situation. This is a very important factor as a major proportion of the operational costs of running a desalination plant is the highest after that of energy. If fresh water is only required, then RO, SD, and single purpose MSF/MED systems would be the recommended choice. However, when both electricity and water are required the integrated power and desalination plant provides a relatively economical choice, since the dual purpose system in the MSF and MED processes can benefit in terms of savings in fuel and common facilities, therefore, the economics can change quite significantly (Khan, 1986; Borsani, Superina and Sommariva, 1995; and Wade, 1993).

6.10.5 Plant Location

When the demand for fresh water is less than 45 m^3 per day, as would be more likely in small remote villages, it is highly uneconomical to install pipelines to supply fresh water to that region. At times fresh water is supplied by tankers at cost as high as 7 $ per 4.5 m^3. However, when employing a solar desalination system, water could be supplied at less than half of this price (United Nations, 1970).

In Qatar, more than 1,200 tankers still supply fresh water for the consumers, and over 40% are used for remote areas. In such situation, a desalination plant should be sited as close as possible to the feed water source. For instance, the new desalination plant which has been constructed at Dukhan city was recommended by the consulting company to be located in a costal area instead of inland, therefore, affording a significant capital cost saving approximately 10% in favour of the costal sitting. This expedient avoided the cost of excessive pumping and pipeline construction from the feed water source to the plant.

The plant location should, where feasible, be adjacent to the energy source and usually in close proximity to the big cities or industrial areas where the demand is high. Thus, costly investment in lengthy distribution systems is minimized and the pumping requirements are similarly reduced. However, the presence and operation of a desalination plant can result in several types of environmental pollutions such as, air, noise, and water pollution. Therefore, when possible it should be located at a reasonable distance from the populated areas. This problem has been identified in the

Rus- Abufontas power and desalination plants A and B, where the distance is less than few meters between the plants and nearest populated area.

For those plants located adjacent to the coastal areas, disposal does not create a serious problem, since reject lines can be channeled directly into the sea. This reduces the temperature and salinity of reject brine by rapid mixing with the receiving water. These reject lines should be located as far away as possible from the intake area. However, this reject brine has the known potential to damage the marine life, since it has an altered temperature and pH and contains a high salinity, and many dissolved chemicals which are used in the different desalination possesses. Therefore, a neutralization step has to be made to prior to disposed of the reject brine to minimize any adverse environmental impact.

Moreover, for plants located inland such as the RO process which are routinely adopted for desalting brackish water, the situation is quite different. The salinity of reject brine from RO can be very high compared with intake brackish water. So, the reject lines should be collected in big ponds and there are usually located a substantial distance away from the plant wells. Since, feed water salinity can change over a period of time, which has been documented to reduce the efficiency of the plant.

Ultimately, since Qatar is located in the Arabian Gulf, which is considered one of the busiest seas in the world in terms of export oil-tankers, the threat of oil pollution is never far from reality. In 1995, Sharqa, UAE, the power and desalination plants were temporarily forced to shutdown for three weeks due to an oil-tanker sink. Therefore, a suitable location should be selected as the lowest area to be effective, yet not one which is in imminent danger of contamination should there be an oil pollution incident. In Qatar, a statistical survey has identified that the western coastal region has suffered the least with oil pollution, however, the three main power and desalination plants are located on the eastern coastal areas of Qatar, being located adjacent to the areas of demand (Temperley, 1995. and Khan, 1986).

6.11 Conclusion

The demand for a steady, economical supply of water is *relentlessly increasing* all around the world, and supply often does not equal the present needs. This problem

will become more recalcitrant in the future. One obvious solution to the problem of insufficient water availability throughout the world would definitely be desalting. This consists of distilling saline water by various processes, with the result that large quantities of water are produced that are tailored for the final use. One drawback of this solution is the high cost involved. A desalination plant requires an initial disbursement for its construction and additional operation/maintenance costs. The main reason for attempting to develop a desalination technology is to reduce the cost of eliminating the salt content in the water without incurring environmental problems. Various types of water desalination processes have been discussed from technical and economical view point with respect to energy consumption, capital cost, operation costs, and maintenance costs.

Despite the cost of operation, the RO process can be seen as the ideal choice to desalt brackish water when fresh water only required. However, the RO membranes are extremely sensitive to high inlet salinity water like seawater. In view of its efficiency and cost advantages, it is expected that the MED technology will attract increasing interest over the coming future as an alternative to MSF process. The MSF technology is considered very developed, it has a less complex mechanical design, less stringent control requirements and the effect of scale on the performance is less than that of the MED type.

It can be concluded that each specific desalination process has its advantages and disadvantages. However, some processes are viable in certain situations. The range of applicability is determined primarily by the demand for electricity and the volume of fresh water. Although the cost of solar desalination is assumed to be 20% higher than the other desalination processes, it is still the most economic choice for a small-sized (45 m^3/day or less) plant. On the basis of this investigation, it has been found that the solar desalination for small-scale plants is a more viable proposition for to use in remote areas, where the fresh water transportation cost is comparatively high and water consumption is low. In addition, solar stills are relatively easy to install and maintain and can be fabricated with locally available material.

The selection of a desalting process is often based on a cost study and is usually carried out by estimating fixed or, capital costs of materials, equipments, and

installation requirements, in additional to the operation and maintenance costs. Energy cycle selection and design optimization are performed to determine which desalting plant will produce the desired quantity and quality of desalted water at the lowest overall cost. Since electricity consumption ratio is parallel with fresh water demand in Qatar, the co-generating system seems to be an economic option to generate electricity and produce fresh water as a by-product. Moreover, the pre-study relating to the installation of new desalination plants in Qatar identifies the most important parameters that require consideration prior to the selection of suitable and economic process.

CHAPTER SEVEN

CONCLUSIONS AND RECOMMENDATIONS

7.1 Conclusion

Despite the fact that Qatar is well endowed with non-renewable fossil fuels such as oil and gas, it is also receives abundant supplies of renewable energy, in particular solar energy. However, Qatar lacks of fresh water resources. Solar desalination can be an excellent technique to provide fresh water continuously and without any deleterious effects on the environment. For all practical purposes, Qatar can be regarded as one of the founder members of the Organisation of Petroleum Exporting Countries (OPEC), and has long been regarded as a typical oil-producing state of the Gulf. However, it must be stressed that in contrast to many of the other members of OPEC, Qatar's oil reserves are comparatively expected to deplete over the next twenty years when the natural gas replace the energy niche occupied by oil in the future (Al-Thani, 1996).

The current estimated water production from desalination plants in Qatar is over 98% of the total fresh water. As a direct result of the continuing population growth and an escalating demand for the fresh water, this percentage is expected to approach 100% in the next few years. The benefits of solar energy can be seen in its renewable, safe, free, and low maintenance qualities, which is ideally suited to any solar desalination process. The cost of potable water produced for the more remote areas of Qatar from solar energy driven desalination plants can be substantially less than the cost of the same water produced from desalination plants powered conventional energy sources. The employment of renewable energy sources in desalination plants will conserve fossil fuels, reduce pollution of the environment, and in addition to being a free, continuous, clean source of energy, is simple and uncomplicated to operate and maintain. As the cost of fresh water escalates, the relative cost of capitalizing on solar energy decreases, and it becomes economic to pursue particularly on remote localities.

The study of water resources in relation to the climate of Qatar has identified a dramatic deficit of fresh water and an abundant amount of solar radiation prevailing in the region. A tilted tray solar still system is the recommended type of still because it is found that it produced higher rate of water and has relatively low maintenance requirement. The optimization of the design was executed using a pyramid absorber and two different shapes of covers, dome and pyramid. Various parameters have been studied in both model 1 (d) and (p) designs; the variation in the output to performance

ratio was then compared with the large design, model 2 (p), which was carried out under the prevailing climatic conditions of Qatar.

The analysis of eighteen years data of global radiation and ambient temperature for Qatar provides sufficient information to enable prediction, on a monthly basis, the performance of the solar still. However, the accuracy is still not reliable enough for studying the effect of climatic changes on the daily still performance trends. The variation in the ambient temperature has been observed to exert two effects, firstly on the heat losses from the inlet storage tank and secondly, and most importantly, the effect on the efficiency of the solar still. Alternatively, an hourly temperature model can be produced from the long-term temperature data. This would be a more acceptable and efficient alternative for the predication of the daily still performance.

(a) Laboratory Test

Initial results from laboratory tests indicated that a pyramidal shape is the more appropriate shape for a solar still than a dome shape. The model 2 (p) solar still has been studied, both theoretically and experimentally in this work, and the effects of experimental and design parameters on the performance of the still elucidated.

As the inlet water temperature increases from 40 °C - 70 °C, the production of fresh water increases from zero to 1.5 litre/hour, which suggest that the evaporation process increase with higher tray temperature.

The pyramid shaped covers produced a higher output than the dome shaped covers. The productivity decreased from 0.35-0.5 litre/hour, than dome cover, implying that pyramid covers shape more suitable to collect more distillate.

(b) Outdoor Test and Theoretical Comparison

The lower inlet water flow rate yielded more distillate than the higher inlet flow rate under similar outdoor environmental conditions. This is concurred with the theoretical results. Therefore, reducing the input flow rate is a recommended expedient. The effects of the insulation layer on the performance of the solar still have been investigated experimentally and theoretically. It has been demonstrated that the still

water production significantly increases when an insulation layer was included in both experimentally and theoretically derived result.

The distillate yield was observed to be greater in the pyramid solar still type when the insulation layer was utilized. The difference was caused by the heat loses from the still basin by conduction through the ground and by convection to the air as these have been minimized. The thickness of the glass cover was a probable cause of decreased solar radiation reaching the plate as result of increased reflectance and absorbance of solar radiation, by this type of glass.

The result of the comparison of the three different spaces between the glass cover and water surface in the pyramid type, shows a significantly more distilled water produced when the cover and water surface were in the closest position, that is when the gap between the two surfaces is minimum.

From the comparison between experimental and theoretical results, it was found that ambient temperature is difficult to predict. However, the theory can predict the expected temperature based on recorded values over the previous 10 to 20 years. Moreover, the correlation between theoretically predicted and measured of solar energy variation confirms that the model employed for modelling solar radiation is reliable.

There is a linear relationship between yield and the evaporation heat transfer, whereby an increase in the evaporation heat transfer coefficient (q_e) results in a concomitant increase in the yield. However, the predicted yield (Y) variation for the still shows poor correlation with the actual value, such discrepancies probably reflect the influence of various assumptions which have been made to simplify the theoretical prediction, such as the average absorber temperature was assumed to be equal to the temperature of saline water, the temperature gradient perpendicular to and along the surface of the glass cover was assumed to be negligible, and no leakage or revaporation was assumed.

When considering the routing maintenance, it is recommended that the still absorber should always be protected from the sun when the still is not operating. Moreover, the technical and manufacturing tolerances of the still such as cover dimensions, still

construction materials, insulation layer and trays dimensions are very essential which may significantly impair the solar still performance.

It was demonstrated that the climatic conditions constitute significant parameters, which can exert a profound effect on solar still productivity. Under variable desert conditions, cover shape and angle can be extremely effective in protecting against dust accumulation, which can affect the transmittance of the glass cover. The presence of such a dust layer could reduce the distilled water production and also maximize the maintenance work time.

An important consideration when embarking on practical experiment was identified as the inlet flow rate should be stabilized before commencing the test to prevent any distillate contamination, which maybe caused by spilling or overflowing of inlet seawater into the condensate channel. Therefore, in model 2 solar still, 30 mm cavity between cover surfaces has been recognized as an optimum distance between the top tray surface and the glass cover.

Practical field experiments demonstrated that distillate production increases with solar radiation and decreases with wind velocity, as a consequence of which the still parts should be tightly sealed.

(c) Economical Comparison

On the basis of this investigation, it has been demonstrated that solar powered desalination on a small-scale is more viable to use in remote areas, where the value of the land, necessary for solar stills installation is relatively low. Moreover, the cost of water transportation to such areas is comparatively high and the rate of water consumption is relatively low. In addition, solar stills are easy to install and maintain and can be fabricated from locally available materials. Therefore in conclusion the establishment of solar energy in Qatar should be encouraged, promoted, invested, implemented, and manifested in the form of projects, particularly for small remote villages.

The selection of a desalting process is often based on cost studies and is usually performed by estimating fixed or capital costs of materials, equipment, and installation requirements, in addition to the operational and maintenance costs. A pre-

study for the installation new of desalination plants identifies the most important parameters to select the suitable and economics process.

The MED process is a more applicable and economic option for a medium-sized plant. Unlike the MSF plant, the performance ratio from MED plant is more rigidly linked to and cannot exceed a limit determined by a number of inherent properties of the plant. However, the technology is currently available for a larger-sized plant.

The reverse osmosis process is the most highly developed process. Many experts consider that the MSF plant will be superadded by the RO process in the near future. This reflects the influence of the lower energy costs, approximately 50% less than MSF process. However, the reverse osmosis of seawater was recently implemented and found more applicable in terms of cost for small-and medium-sized plants operating with brackish water.

The multistage flash process has many attractive features, which distinguish it from other desalination methods. The performance ratio of an MSF plant is not directly connected to the number of stages, as is the case for MED processes, so that in the event of tubes are fouling, there is a choice between decreasing the product output or increasing the steam consumption. The scale prevention precautions are less hazardous in the MSF plant than in the MED, more especially when an acid treatment system is adopted. Since its well known since the late 1950s, a wealth of field experience has been amassed in the process technology, design procedure, construction practice, and operational techniques of MSF.

In the light of above, the author strongly considers that a dual propose MSF system will endure as the principle desalination process, especially in Qatar. This is as a result of the following considerations:

1. The conservative nature of desalination client, most of desalination clients prefer to employ a similar desalination system for new plants.
2. The product is a strategic life-supporting element;
3. Process reliability;
4. Extensive experience in construction and operation;

5. Limited experience held on a small database, and unknown risks with new technologies.
6. The parallel rapid consumption of electricity and water in Qatar.

7.2 Recommendations for planning a New Desalination Plant in Qatar

- A well organized preliminary study to investigate the potential benefits of any new desalination plant should be carried out before the commencement of any project. The pre-study should encompass many important factors such as: water demand, feed water characteristics, availability of energy, and plant location.

- The pilot study should estimate the needs for electricity, thereby selecting a dual purpose desalination plant in such a case could significantly minimize the energy costs required for the desalination process.

- The important limitations and restrictions of any desalination process should be well documented prior to selecting the desalination process.

- Besides considering various technical aspects, costs and plant life cycle have to be carefully evaluated. Process economics can play an important role in the effectiveness of the selection process.

7.3 Future Work

Most of the initial targets of this research have been successfully fulfilled. From the discussion in Chapter 4, 5 and 6, some recommendations are proposed in respect of further research and development:

1. The theoretical and experimental results of the pyramidal tilted try solar still are combined together to form the basis for the design of a full-scale solar still ideally suited for remote areas in the future studies.

2. Further research is needed to evaluate the physical properties of the still constructional materials, the still performance, and their deterioration over time of continuous running the still outdoors.

3. Investigation of the environmental impact of the current desalination plants in Qatar.

4. A more detailed economical analysis should be executed to investigate the potential of supplying fresh water for small isolated communities in Qatar through the use of solar stills.

5. Further experimental studies to enhance the development of the pyramid solar still design should ultimately lead to quite rewarding commercial opportunities for this technology, with the possibility of economic profitability in remote areas.

6. A substantial study shall be undertaken to evaluating the production cost of fresh water produced by the single purpose MED or reverse osmosis process and the cost of water produced as a by-product in the dual purpose co-generating system.

REFERENCES

Achilov. B. M, Zhuraev. T. D, and Akhtamov. R., "Test on a portable solar still" (1973), Geliotekhnika, Vol.9, No.6.

Akhtamor.R.A, "Study of Regenerative Inclined Stepped Solar still" (1978), Solar Energy, Vol.14, No.4.UK

AlKA Mihclic and Boganic, "Investigation of solar Desalination" (1996). Renewable Energy, Vol.7, No.3 pp271-277.

Al-Saleh. H. " Future of the oil industry" (1985), OAPEC Journal, Vol.11, No.3

Al-Sulaiman. F and Ismail. B, "Estimation of monthly average daily and hourly solar radiation impinging on a sloped surface using the isotropic sky model for Dhran, Saudi Arabia" (1997). Renewable Energy, Vol.11. No. 2. pp 257-262. UK.

Al-Thani. F, Nasser. S, and Sayigh. A. A. (a) "A Comparison Of Two Developed Designs Of Tilted Tray Solar Still" (2000), World Renewable Energy Congress VI, UK.

Al-Thani. F, Nasser. S, and Sayigh. A. A. (b) "A controlled laboratory test on pyramid shaped tilted tray solar still." (2000), World Renewable Energy Congress VI, UK.

Al-Thani. H. N. "Project Management in the oil and gas industry" (1996), PhD, thesis. University of Wales, UK.

Angstrom. A., "On the computation of Global Radiation from records of sunshine" (1956), Arkiv, Geophsih, Vol.3. pp.551.

Bednarski. J, Minamide. M, and Morin. O " Test program to evaluate and enhance seawater distillation process for the metropolatian water district of southern California" (1997), Proceedings of the IDA world Congress on Desalination and Water Sciences, Vol. 1, Madrid, Spain pp 227-241.

Borsani. R, Superina. R, and Sommariva. C. " MSF Desalination, the myth of the largest unit some technical and economical evaluation" (1995), Abu Dhabi I.D.A. Conference .UAE.

Chambers. S. " Economics: Effect of water/power ratios and the role of dual process dual purpose plants" (1967), Nuclear Desalination. The British Nuclear Energy Society. UK.

Clelland. D. W. "Single and Dual Purpose Desalination Plants" (1967), Nuclear Desalination. The British Nuclear Energy Society. UK.

Cooper. P. And Read.W, "Design Philosophy and Operating Experience for Australian Solar Stills" (1973), Solar Energy, Vol.16, UK.

Cooper. P. I " The maximum efficiency of single-effect solar stills" (1972), Solar Energy Vol.18, pp.205-217.

Cooper. P. I. " Solar Distillation Solar Energy Progress in Australian and New Zealand" (1969), Publication of the Australian and New Zealand Section of the solar Society, Vol.8, No.45.

Cooper.p, "The Maximum Efficiency of Single-Effect Solar stills" (1972), Solar Energy, vol.15, UK.

Cooper.p. and Appleyard.J, "The Construction and Performance of a Three Effect, wick type, tilted Solar Still" (1987), sun at work, Vol.12, No.4.

Daniels. F and Duffie. J, "Solar Energy Research", (1955), The University of Wisconsin Press, Madison.USA.

Darwish. M. A " on the thermodynamics of dual purpose powered desalination planrs" (1987), Desalination, Vol. 64. Part 1 and II.
Delhi, India.

Desalination Studies. Technical Report. Alexandria University, Technology center, Vol.1. (2000), Egypt.

Dhiman. N, "Evaluation of optimum thickness of bottom insulation for a conventional solar still" (1990), Desalination, Vol.78, pp201-208.

Dickson. A. " The Potential for Renewable Energy, Particularly Solar Power" (1997), Renewable Energy Conference in Dubai, UAE.

Duffie, John A, "*Solar engineering of thermal processes*" (1980). A Wiley-Interscience publication. USA.

Duffie.J .A and Beckman.W. A. "*Solar energy Thermal Processes*" (1974), Wiley Inter Science, New York.

Dunkle.R, "Solar Water Distillation; The Roof Type Still and Multiple Effect Diffusion Still" (1961), International Development in Heat Transfer, ASME.

El-Dessouky. H, Ettouney. H, and Alroumi. Y. " Multi-stage flash desalination: present and future outlook" (1999) Chemical Engineering Journal, Vol.73, pp 173-190. UK.

Ernani Sartori. "Solar Still versus solar Evaporator: Comparative Study Between Their Thermal Behaviors" (1996), Solar Energy, Vol.56, No.2, UK.

Garg, H.P, *Advancess in Solar Energy*, Technology, (1987), D.Reidel Publishing Company. Holland.

Garg. H.P. " Effect of climatic parameterizes on the performance of single sloped solar still" (1974), Allahabad Conference, pp-30-34. India.

Glueckstren. P. "Design and operation of medium-and small-size desalination plants in remote areas, New perspective for improved reliability, durability and lower costs" (1999), Desalination, Vol.122, pp 123-140.

Gocht. W and Sommerfeld. A " Decentralized desalination of brackish water by a directly coupled reverse-osmosis-photovoltaic-system, A pilot plant study in Jordan" (1998), Renewable Energy, Vol.14, Nos.1-4, pp 287-292. UK.

Gopinthan. K. K and Alfonso Soler " Effect of sunshine and solar declination on the computation of monthly mean daily diffuse solar radiation" (1996), Renewable Energy, Vol.7, No.1, pp 89-93.UK.

Hamed. O. A, Eisa. E. I, and Abdulla. W.E "Overview of solar desalination" (1993), Desalination, pp 563-579.

Hanbury. W. T, Hodgkiess.T, and Morris. R "*Desalination Technology* 1992" (1992) Porthan Ltd., Glasgow, UK.

Harpreet S.Kwatra, "Performance of a Solar Still; Predicted Effect of Enhanced Evaporation Area on Yield and Evaporation Temperature" (1996), Solar Energy vol.56, no.3, UK.

Hasnain. S. M. and Al-Ajlan. S " Coupling of PV-Powered R.O Brackish water desalination plant with solar stills" (1998), Renewable Energy, Vol. 14, Nos. 1-4, pp, 281-286. UK.

Helal. A. M, Medani. M. S, Soliman. M. A, and Flow.J.R " A trdiagonal matrix model for multistage flash desalination plants" (1986), Comput Chem. Eng. Vol.10. pp 324-327.

Herold. D, Hostmann. V, Neskaskis. A, and Plettner. L " Small scale photovoltaic desalination for rural water supply- Demonstration plant in gran canria" (1998), Renewable Energy, Vol.14, Nos.1-4, pp 293-298. UK

Hirschmann. J. R and Roefler. S. K " Thermal inertia of solar stills and its influence on performance" (1970), Solar Energy Congress, Melbourne.

Howe. E and Tliemat. B, "Review Paper Twenty Years of Work on Solar Distillation at the University of California" (1973), University of California, Berkely. USA.

Idso. S., "A set of equation for full spectrum and 8-14 um and 10.5 – 12.5 um thermal radiation from cloudless skies" (1981). Water resources Research, Vol. 17, No.2, pp.295-304, April 1981.

Khan. A. H, *Desalination Processes and Multistage Flash Distillation Practice.* (1986), Elsevier, USA.

Klabi, A. "Weather Analysis and Forecasting Services" (1990). Ministry of Communication and Transport. Department of Meteorology, Doha-Qatar.

Kreider. J and Kreith. F " *Solar Energy Handbook*" (1980), McGraw Hill.

Kreith. F "Principles of Solar Engineering" (1978), Hemisphere Publishing Corporation. USA.

Lessley. R. L, Lindemuth. T. E, and Lam. E.Y. " Technical and economic assessment of solar distillation for large production of fresh water" (1977) Technical Development Project, California. USA.

Lof. G. O., Eibling. J. A, and Blomer. J. W " Energy balance in solar distillation" Am. Institution of Chemical Engineering, Vol. 7.

Malik. M.A.S, *Solar Distillation*, (1980), Indian Institute of Technology. New Delhi, India.

Matthias Rommel, "Solar Thermally Driven Desalination Systems With Corrosion-Free Collectors" (1996), Renewable Energy, vol.14, nos.1-4, UK.

Mawer. P. "Paper 4. WRA Conference on Desalination as a Supplementary Water Resource". (1966) UK.

Mealey. A. Y, "Solar still performance" (1991). Desalination Conference, Vol.2, Solar Processes.

Memotechnique, "Desalinating Seawater" (1999), Planete Technical Section-No.31, February SIDEM, France.

Menguy. G, Chassagne. G, Sfeir. A, and Saab. J " Experimental study and optimization of solar still" (1976), Heliotechnique, p 46.

Ministry of Communication & Transport, Long Period (1962-98) *Climate Report*, 1999. Department of Meteorology, Doha-Qatar.

Ministry of Water & Electricity, *The Annual Report*, (1998). The State of Qatar.

Mockler.P.J " *Dukan Potable Water Supply Supplementary Report*" (1987), Ewbank Preece Power and Water Ltd, UK.

Morse. R. N. and Read.W .R. W. "A traditional basis for the engineering development of solar still, (1968), Solar Energy, Vol.12, No.1, pp 5-17.

Moustafa. S "Direct use of solar energy for water desalination" (1979). Solar Energy.UK.

Moustafe. S. M. A, Brusewitz. G. H, and Farmer. D.M, "Direct use of solar energy for water desalination" (1979), Solar Energy, Vol. 22, No.2, pp141-148.

Mowla. D and Karim. G, "Mathematical modeling of solar stills in Iran" (1995), Solar Energy, Vol.55, No.5, pp.389-393.

Naresh K. Dhiman, "Evaluation of Optimum Thickness of Bottom Insulation for a conventional Solar Still" (1990), Desalination, vol.78, Netherlands.

Nijegor Odov. N. and Jain. P, "Optimum slope of north-south aligned absorber plate from the north to the south poles" (1997), Renewable Energy, Vol.11, No.1, pp 207-118.

Norton. E."The Evaluation of Surface Geometry Modification to Improve the Directional Selectivity of Solar Energy Collectors",(1988), Solar Enrgy, New York, pp. (37-44).

Porta. M, "Extreme Operating Conditions in Shallow Solar Stills" (1997). Solar Energy, vol.61, No.4, UK.

Porteous.A. "*Desalination Technology, Developments and Practice*" (1988), Applied Science Publishers, UK.

Qatar General Electricity & Water Corporation, "Kahramaa" (2001). Monthly Periodical, Doha -Qatar

Rajka Bundia and Veijko Filipan, "Investigation of Solar Desalination" (1996), Renewable Energy, Vol.7, No.3, UK.

Riffat.S.B, "Solar Absorption System For Water Desalination" (1995), Renewable Energy, Vol.6, No.2, UK.

Sabbagh.j, Sayigh.A and Elsalam.E, "Estimation of the Total Solar Radiation From meteorological" (1977), Solar Energy, Vol.19, pp 307-311. UK.

Sambo. A. S, "Empirical models for the correlation of Global solar radiation with meteorological data for Northe, Nigeria" (1986). Solar and Wind Technology. Vol.3, No.2, pp 89-93.

Sanjay Kumar and G.N.Tiwari, "Estimation of Convective Mass transfer in Solar Distillation Systems" (1996), Solar Energy, Vol.57, No.6, UK.

Sayigh. A. A. and El-Salam, "Optimum design of a single slope solar still in Riyadh" (1977), Saudi Arabia, Revue'd Heliotechniqu, Vol.1, No.40.

Selcuk. M. K " Design and performance evaluation of a multiple effect, tilted solar distillation unit" (1964), Solar Energy, Vol.23, pp 23-30.

Silver. R. S. " The physics of desalination by Multi-stage flash Distillation" (1967), Nuclear Desalination. The British Nuclear Energy Society. UK.

Sosna and Barbara, *Momentum* (1984). Orlando, Florida University of Arizona USA. Hk.

Soteris Kalogirou, (a) "Survey of solar desalination systems and system Selection" (1997), Renewable Energy, Vol.22, No 1-4.UK

Soteris Kalogirou, (b) "Economic analysis of a solar assisted desalination system" (1997), Renewable Energy. Vol. 12. No.4, UK.

Spiegler. K. S. and Laird. A. D. K. "*Principles of Desalination*" (1980). Academic Press. New York.

Spiegler. K. S., *Salt-Water Purification.* (1981). Second Edition Plenum press. London.

Tanaka. K, Umehara. T, and Watanabe. K " Improvements of the performance of the tilted tray wick type solar stills" (1983), ISES Congress, Australia.

Tiwari. G and Kuma. A, "Desalination" (1988). Vol.69, pp 309-319.UK

Tiwari. G, Thomas. J, and Khan. E, "Optimization of glass cover inclination for maximum yield in a solar still". (1994), Heat Recovery Systems and CHP, Vol.114, No.4 pp447-455.

Tiwari. G. N. and Yaday. Y. P., "Desalination" (1986), Vol.67, pp191-202.

Tiwari. N. and Lawrence., "New heat and mass transfer relations for a solar still" (1991). Energy Conversion Management 31,201-203.

Tiwari_G, "Optimization of glass cover inclination for maximum yield in a solar still" (1994), Heat recovery systems & CHP, Vol.69.Netherland.

Tleimat. B. W. and Howe. E. D, "Nocturnal production of solar distillers" (1986) University of California, Sea water Conversion Laboratory Report, Vol.66-7, and No. 105.

Wade. N. M, "Technical and economic evaluation of distillation and reverse osmosis desalination processes" (1993), Desalination. Vol.93, pp343-363.

Yousef. A. G. Abdalla, "Solar radiation over Doha (QATAR)" (1987), Solar Energy, Vol.5.UK

Zuhairy. A. and Sayigh A. A., "Simulation and Modeling of Solar Radiation in Saudi Arabia".(1995), Renewable Energy.Vol.6, no.2, UK.

United Nation, "Strategic Approaches to Freshwater Management Report" (1970), Sustainable Development, New York. USA

APPENDICES

APPENDIX -A

AUTO CAD SOLAR STILLS

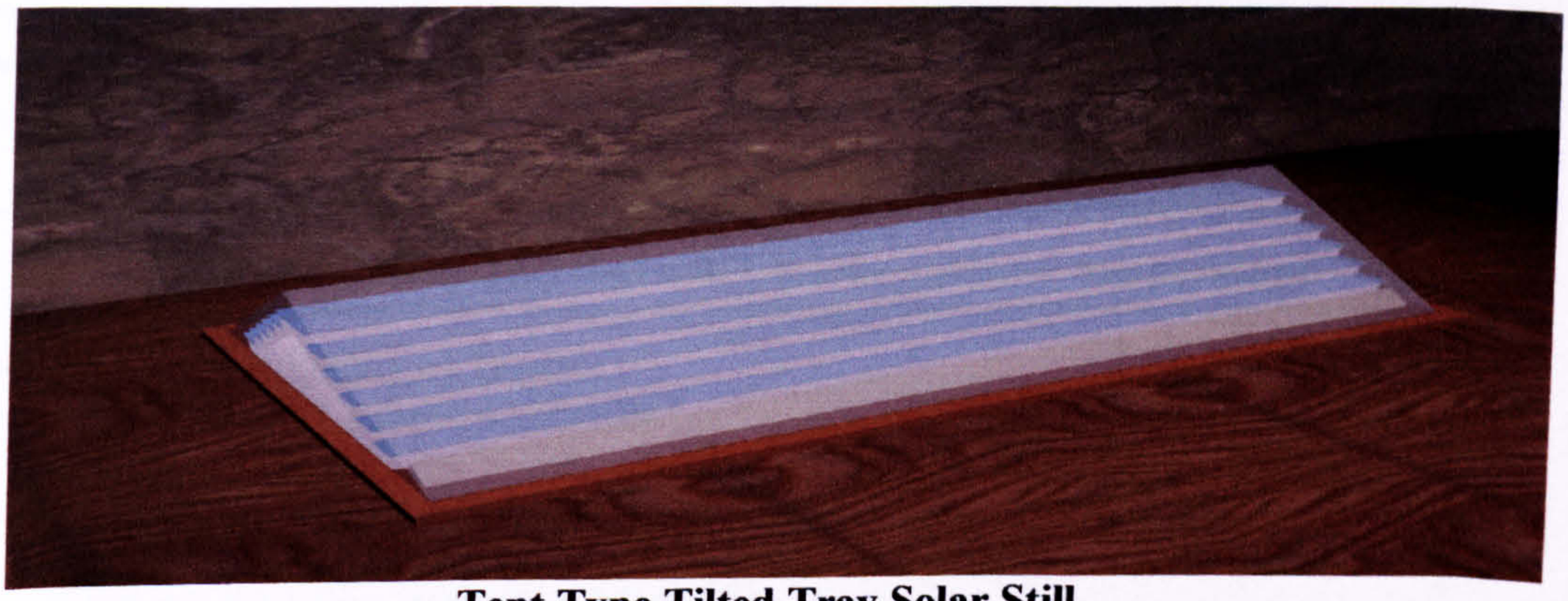

Tent Type Tilted Tray Solar Still

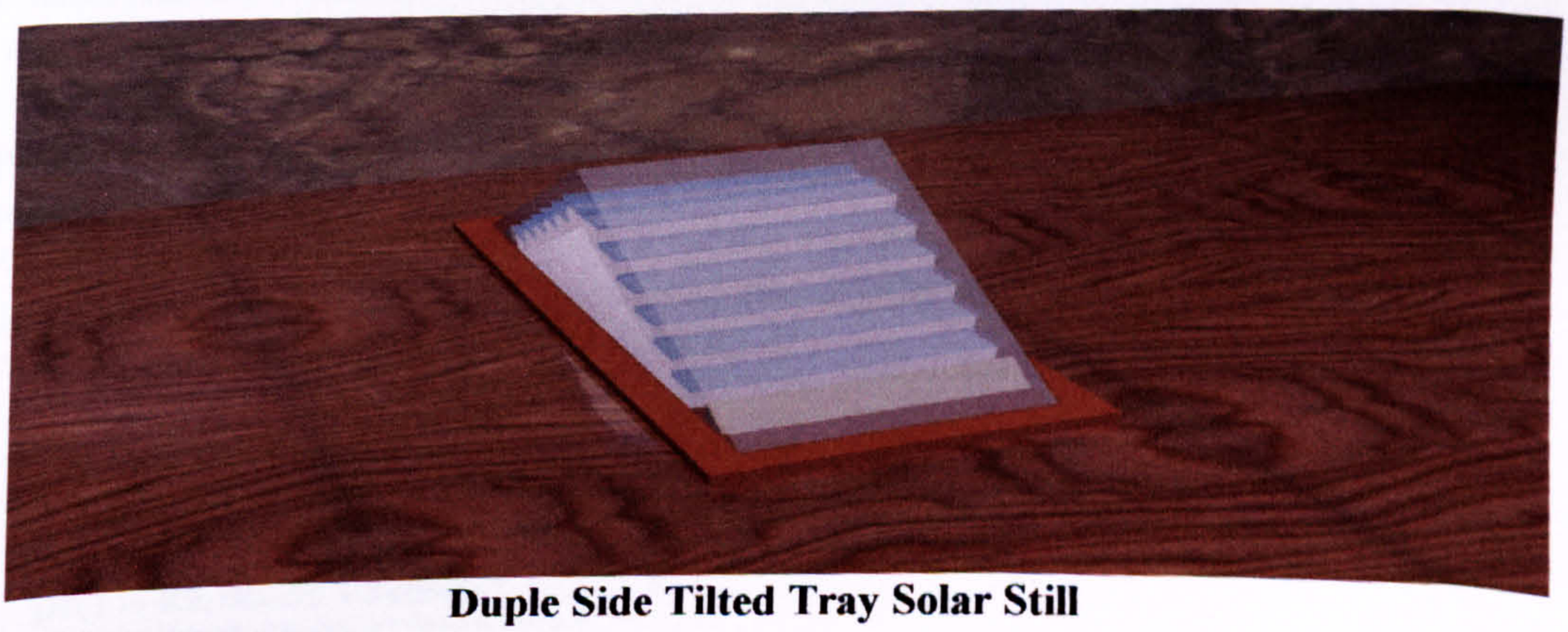

Duple Side Tilted Tray Solar Still

Dome Shape Tilted Tray Solar Still

APPENDIX -B

Computer Programme Declaration

```
""""""""""""""""""""""""""""""""""""""""""""""""""""""""""""""""""""""""""""""""""""""""""""""""""""""""""""""""""""""""""""""""""""""""""
**********************************************************************'
*******
  """"""""""""""""""""""""""""""""""Declaration Area For the program""""""""""""""""""""""""""
""""""""""""""""""""""""""""""""""""""""""""""""""""""""""""""""""""""""""""""""""""""""""""""""""""""""""""""""""""""""""""""""""""""""""
"""""""""""""""""""""""""Declaring Ta() that will hold the ambiant temperature"""
""""""""""""""""""""""""""""""""""""""""""""""""""""""""""""""""""""""""""""""""""""""""""""""""""""""""""""""""""""""""""""""""""""""""""
Public ta(0 To 100000) As Double
Public Const Pi = 3.14159265358979
'
'declaring S_Boltz as Steve boltzman constant
'
Public Const S_boltz = 5.67051 * 10 ^ -8
""""""""""""""""""""""""""""""""""""""""""""""""""""""""""""""""""""""""""""""""""""""""""""""""""""""""""""""""""""""""""""""""""""""
 'Here the min and the max are the begining and ending time respectevely"
""""""""""""""""""""""""""""""""""""""""""""""""""""""""""""""""""""""""""""""""""""""""""""""""""""""""""""""""""""""""""""""""""""""
Public min As Integer
Public max As Integer
""""""""""""""""""""""""""""""""""""""""""""""""""""""""""""""""""""""""""""""""""""""""""""""""""""""""""""""""""""
'Here interval is the increment time fro Tg,tw, as interval"
 'and for ta,irr as interval2 which is interval/2"
""""""""""""""""""""""""""""""""""""""""""""""""""""""""""""""""""""""""""""""""""""""""""""""""""""""""""""""""""""
Public interval As Double
Public Flag As Integer
"""""""""""""""""""""""""""""""""""""""""""""""""""""""""""" '
   'Irr() is Radiation intensity"
"""""""""""""""""""""""""""""""""""""""""""""""""""""""""""" '
Public Irr(0 To 100000) As Double
$$$$$$$$$$$$$$$$$$$$$$$$$$$$$$$$$$$$$$$$$$$$$$$$$$$$$$$$$$$$$$$$$$$$$$$$$$$$$$$$$$$$$$$$$$$$$$$$$$$$$$$$$$$$$$$$$$$$$$$$$$$$$$$$$$$$$$$$'
$                                                          '
 'declaring Solar data as the No of the day of the year N_day$
$                                                          '
$$$$$$$$$$$$$$$$$$$$$$$$$$$$$$$$$$$$$$$$$$$$$$$$$$$$$$$$$$$$$$$$$$$$$$$$$$$$$$$$$$$$$$$$$$$$$$$$$$$$$$$$$$$$$$$$$$$$$$$$$$$$$$$$$$$$$$$'
Public Total_rad As Double
Public N_day As Integer
١٥٧ ='
&&&&&&&&&&&&&&&&&&&&&&&&&&&&&&&&&&&&&&&&&&&&&&&&'
&&&&&&&&&
'Declaring the Tg() And Tw() as the temperature of&
'glass and water respectively&
```

```
&&&&&&&&&&&&&&&&&&&&&&&&&&&&&&&&&&&&&&&&&&&&&&'
&&&&&&&&&
Public Tg(0 To 100000) As Double
Public Tw(0 To 100000) As Double
'
'declaring V_speed as Wind spead and T_ground as ground
'temperature
'
Public T_ground As Double
Public V_speed As Double
&&&&&&&&&&&&&&&&&&&&&&&&&&&&&&&&&&&&&&&&&&&&&&&'
&&&&&&&&&&&&&&&&&&&&&&&&&&&&&&&
&                                    '
'Declaring the thermal capacity of the water and the glass respectivly&
'as Mw and Mg&
&                                    '
&&&&&&&&&&&&&&&&&&&&&&&&&&&&&&&&&&&&&&&&&&&&&&&&'
&&&&&&&&&&&&&&&&&&&&&&&&&&&&&&&
Public Mw As Double
Public Mg As Double
""""""""""""""""""""""""""""""""""""""""""""""""""""""""""""""""""""""""""""""""
'Declare the water and glass emessivity as public""
""""""""""""""""""""""""""""""""""""""""""""""""""""""""""""""""""""""""""""""""
Public W_emis As Double
Public G_emis As Double
""""""""""""""""""""""""""""""""""""""""""""""""""""""""""""""""""""""""""""""""""""""""""""""
'Declaring the Overall heat transfere coefficient from basin"
'to the ground, through the insulation"
""""""""""""""""""""""""""""""""""""""""""""""""""""""""""""""""""""""""""""""""""""""""""""""
Public U_basin As Double
""""""""""""""""""""""""""""""""""""""""""""""""""""""""""""""""""""""""""""""""""""""""""""""""""""
'Declaring the radiation capacity of watar and glas respectively"
""""""""""""""""""""""""""""""""""""""""""""""""""""""""""""""""""""""""""""""""""""""""""""""""""""
Public taw_w As Double
Public taw_g As Double
Sub Initial()

""""""""""""""""""""""""""""""""""""""""""""""""""""""""""""""""""""""""""""""""""""""""""""""""""""""""
""""""""""""""""""""""""""""""The value of the most constant are""""""""""""""""""""
           """"""""""""""""""""""""""""entered here""""""""""""""""""""
""""""""""""""""""""""""""""""""""""""""""""""""""""""""""""""""""""""""""""""""""""""""""""""""""""""""
""""""""""""""""""""""""""""""""""""""""""""""""""""""""""""""""""""""""""""""""""""""""""""""""""""""""
'The value of min,max,interval which declared before is entered here"
'min - begining time, max - ending time, interval - increment time"
"""""""""""""""""""""""""""""""""""""""""""""""""""""""""""""""""""""""""""""""""""""""""""""""""""""" '
min = 0: max = 24: interval = 0.005

""""""""""""""""""""""""""""""""""""""""""""""""""""""""""""""""""""""""""""""""""""""""""""""""""""""""
'N-day, the number of the solar day of the year
'Total_rad, the total radiation rec
```

```
'N_day = 157        'june_6
'Total_rad = 671.9

"""""""""""""""""""""""The value of Water and glass emmisivity"""""""""""""""""""""""
W_emis = 0.96: G_emis = 0.94

"""""""""""""""""""""""""""""""""The value of thermal capacity of water and glass
"""""""""""""""""""""""""""""""""are entered here; in J/(kg C(
'Mw = 668000
Mg = 9240

    """""""""""""""""""""" 'The value of overall heat transfer coefficient from
  """""""""""""""""""""""The basin to the ground is entered here in W /(m2 C.(
'U_basin = 8.6

  """""""""""""""""""""" 'The value of the average wind speed,and the average ground temp
at N_day
        """""""""""""""""""""" 'are entered here where V_speed  in m/s, T_ground in C
'V_speed = 2.73: T_ground = 35

  """""""""""""""""""" 'the value of radiation capacity of water and glass
        """""""""""""""""""" 'entered here
  taw_w = 0.95: taw_g = 0.0475

  End Sub

    'This subroutine is using sine cosine series Knowing a s fourier curve
  'fitting.
  '
  'it's good for periodical data
  '
  'you have to submit , initial value, maximum, new interval,the points.
  '


  Sub curve_fit(xin, xfinal, interval, Ti(), Length(&
  mean_temp = 0:  Lo& = 3:

  Length& = (xfinal - xin) / interval

  ReDim m(Lo&), N(Lo&), absl(Lo&), Epsay(Lo(&


  For i = 0 To 23
  mean_temp = mean_temp + Ti(i(
  Next i
  mean_temp = mean_temp / 24
```

```
For i = 1 To Lo&
Mr = 0
Nr = 0
For j = 0 To 23
Mo = Ti(j) * Cos(j * i * 2 * Pi / 24(
No = Ti(j) * Sin(j * i * 2 * Pi / 24(
Mr = Mr + Mo
Nr = Nr + No
Next j
N(i) = Nr / 12
m(i) = Mr / 12
absl(i) = Sqr(m(i) ^ 2 + N(i) ^ 2(
If m(i) < 0 And N(i) < 0 Then GoTo 100
If m(i) < 0 And N(i) > 0 Then GoTo 100
If m(i) > 0 And N(i) < 0 Then GoTo 300
Epsay(i) = Atn(N(i) / m(i((
GoTo 200
١٠٠Epsay(i) = Atn(N(i) / m(i)) + Pi
GoTo 200
٣٠٠Epsay(i) = Atn(N(i) / m(i)) + (2 * Pi(
٢٠٠Next i

ReDim Ti(Length(&
For k = 0 To Length&
Ti(k) = o
For i = 1 To Lo&
Ti(k) = Ti(k) + absl(i) * Cos(k * interval * i * 2 * Pi / 24 - Epsay(i((
Next i
Ti(k) = mean_temp + Ti(k(
Next k

End Sub

unction h_ca(v(
 'v here is the wind speed "V_speed"

h_ca = 5.7 + 3.8 * v

End Function

Function h_cw(Twat, Tglass(
 'tw ----water temperature
 'tg------Glass temperature
tt# = Abs((Twat - Tglass) + (S_Pr(Twat) - S_Pr(Tglass)) * (Tglass + 273.15) / (268.9
* 10 ^ 3 - S_Pr(Twat(((
h_cw = 0.884 * (tt#) ^ (1 / 3(

End Function

Function h_eff(Twat, Tglass(
```

```
'tw ----water temperature
'tg------Glass temperature

h_eff = 8.14 * 10 ^ -3 * h_cw(Twat, Tglass(
End Function

Function q_ca(Tglass, tamb(
'ta here is the ambient temperature
'tg here is the glass temperature

q_ca = h_ca(V_speed) * (Tglass - tamb(

End Function

Function q_cw(Twat, Tglass(
'tw ----water temperature
'tg------Glass temperature

q_cw = h_cw(Twat, Tglass) * (Twat - Tglass(
End Function

Function q_ew(Twat, Tglass(
'tw ----water temperature
'tg------Glass temperature

q_ew = h_eff(Twat, Tglass) * (S_Pr(Twat) - S_Pr(Tglass((
End Function


Function q_ins(Twat(
'tw ----water temperature
'tgr------deep ground temperature

q_ins = U_basin * (Twat - T_ground(
End Function

Function q_ra(Tglass, tamb(
'tg ----- glass temperature
'ta ----- ambiant temperature

tsky = tamb - 12
q_ra = G_emis * S_boltz * ((Tglass + 273.15) ^ 4 - (tsky + 273.15) ^ 4(
End Function


Function q_rw(Twat, Tglass(
'tw ----water temperature
'tg------Glass temperature

q_rw = W_emis * S_boltz * ((Twat + 273.15) ^ 4 - (Tglass + 273.15) ^ 4(
```

```
End Function

Function S_Pr(t) As Double

'here Saturated Pressure in Pascal

S_Pr = 102.941029311713 * t - 0.107063299386969 * t ^ 2 + 2.96134887902872E-
02 * t ^ 3 + 5.9870103828835 4E-04 * t ^ 4

End Function
```

```
'////////////////////////////////////////////////////////////////////
   'Rk4 Advances A Solution Vector Y(N) Of A Set Of Ordinary Diff.
   'Eqs. Over A Single Small Interval H Using Fourth-order Runge-kutta
   'Method.
'////////////////////////////////////////////////////////////////////
Sub Rk4(Y(), Dydx(), N, X, H, Yout(()
ReDim Yt(N), Dyt(N), Dym(N), Yout(N(
Hh# = H * 0.5
H6# = H / 6
Xh = X + Hh#
For i = 1 To N
Yt(i) = Y(i) + Hh# * Dydx(i) * 3600
Next i
   Flag = 2
   Call Derivs(Xh, Yt(), Dyt(), N(
   For i = 1 To N
   Yt(i) = Y(i) + Hh# * Dyt(i) * 3600
   Next i
   Call Derivs(Xh, Yt(), Dym(), N(
   For i = 1 To N
   Yt(i) = Y(i) + H * Dym(i) * 3600
   Dym(i) = Dyt(i) + Dym(i(
   Next i
   Flag = 0
   Call Derivs(X + H, Yt(), Dyt(), N(
   For i = 1 To N
   Yout(i) = Y(i) + H6# * (Dydx(i) + Dyt(i) + 2# * Dym(i)) * 3600
   Next i
   End Sub

   'The sub derivs is used by RKDE, DERK, RK4, RK5
   Sub Derivs(X, Yz(), Dyz(), N(
   t& = (X / interval) + 0.1
   If Flag > 1 Then
   ll& = t& - 1
   ambt = (ta(t&) + ta(ll&)) / 2
   Hs = (Irr(t&) + Irr(ll&)) / 2
   Else
```

```
ambt = ta(t(&
Hs = Irr(t(&
End If

Dyz(1) = (taw_g * Hs + (q_rw(Yz(2), Yz(1)) + q_cw(Yz(2), Yz(1)) + q_ew(Yz(2),
Yz(1))) - q_ra(Yz(1), ambt) - q_ca(Yz(1), ambt)) / Mg
Dyz(2) = (taw_w * Hs - (q_rw(Yz(2), Yz(1)) + q_cw(Yz(2), Yz(1)) + q_ew(Yz(2),
Yz(1))) - q_ins(Yz(2))) / Mw

End Sub
```

```
Function Acos(X(
Acos = 1.5707963267949 - Asin(X(
End Function
Function Asin(X(
If Abs(X) > 1# Then MsgBox ("Error: Abs(X)>1 In Asin(X) "): End
If X = 1# Then
Asin = 1.5707963267949
ElseIf X = -1# Then
Asin = -1.5707963267949
Else
Asin = Atn(X / Sqr(1# - X * X((
End If
End Function
```

```
Sub Solar_I(S_int(), Inc, N%, ss(
 'here ss is the total day solar irradiant in mWhat.hr/Cm2
 'in order to change it to J/m2 we have to multiply it by 36000
ss = ss * 36000
L& = 24 / Inc
ReDim S_int(L& + 1(

For i& = 0 To L&

c = 360 / 364 * (N% - 81) * Pi / 180
equation_of_time = (9.87 * Sin(2 * c) - 7.53 * Cos(c) - 1.5 * Sin(c)) / 60

 'changing local time to solar time
S_time = (i& * Inc) + (26.66667) / 60 + equation_of_time


S_angle = (S_time - 12) * 15 * Pi / 180
Latitude = 25.25
D_angle = 23.45 * Sin(2 * Pi * (284 + N%) / 365(
Sunset_angle = Acos(-Tan(Latitude * Pi / 180) * Tan(D_angle * Pi / 180((
a = 0.409 + 0.5016 * Sin(Sunset_angle - 60 * Pi / 180(
B = 0.6609 - 0.4767 * Sin(Sunset_angle - 60 * Pi / 180(
```

```
Rt = Pi / 24 * (a + B * Cos(S_angle)) * (Cos(S_angle) - Cos(Sunset_angle)) /
(Sin(Sunset_angle) - Sunset_angle * Cos(Sunset_angle((
If Rt < 0 Then
Rt = 0
End If
S_int(i&) = (Rt * ss) / 3600

Next i&

End Sub
```

APPENDIX –C

CALCULATION OF THE GLASS COVER TRANSMITTANCE

The reflectance of two surfaces of glass and water at normal incidence can be calculated from the following example. The average index of refraction of the glass and water for the solar spectrum are 1.526 and 1.33 respectively.

The glass reflection at normal incidence,

$$r(0) = \frac{I_r}{I_i}\left[\frac{(n-1)}{(n+1)}\right]^2$$

$$r(0) = \left[\frac{0.526}{2.526}\right]^2 = 0.0434$$

The water reflection at normal incidence,

$$r(0) = \left[\frac{0.33}{2.33}\right]^2 = 0.02005$$

The transmittance of glass cover at normal incidence,

$$\tau_{rN} = \frac{1}{2}\left[\frac{1-r_I}{1+(2N-1)r_I} + \frac{1-r_{II}}{1+(2N-1)r_{II}}\right]$$

$$\tau_{r(0)} = \frac{1-0.0434}{1+3(0.0434)} = 0.85$$

The transmittance of water at normal incidence,

$$\tau_{r(0)} = \frac{1-0.02005}{1+3(0.02005)} = 0.92$$